Neogene evolution of the Pacific - Australia plate boundary zone in NE Marlborough, South Island, New Zealand.

Dougal B. Townsend

A thesis

submitted to the Victoria University of Wellington

in fulfilment of the requirements for

the degree of

Doctor of Philosophy

in Geology

Victoria University of Wellington

2001

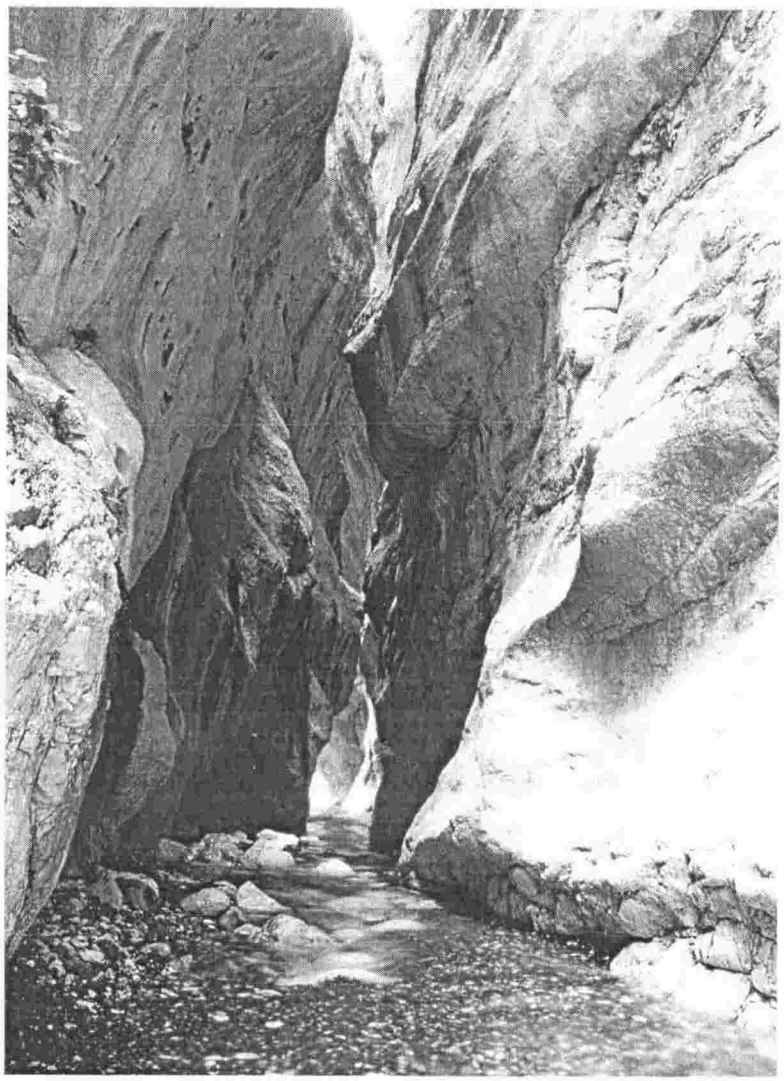

Frontispiece: Sawcut Gorge, Isolation Creek, cut into Palaeocene Amuri Formation limestone.

Neogene evolution of the Pacific - Australia plate boundary zone in NE Marlborough, South Island, New Zealand

ABSTRACT

Six new palaeomagnetic localities in NE Marlborough, sampled from Late Cretaceous - Early Tertiary Amuri Formation and Middle Miocene Waima Formation, all yield clockwise declination anomalies of 100 - 150°. Similarity in the magnitude of all new declination anomalies and integration of these results with previous data implies that clockwise vertical-axis rotation of this magnitude affected the entire palaeomagnetically sampled part of NE Marlborough (an area of ~700 sq. km) after ~18 Ma. Previous palaeomagnetic sampling constrains this rotation to have occurred before ~7 Ma. The regional nature of this rotation implies that crustal-scale vertical-axis rotations were a fundamental process in the Miocene evolution of the Pacific - Australia plate boundary in NE South Island.

The Flags Creek Fault System (FCFS) is a fold-and-thrust belt that formed in marine conditions above a subduction complex that developed as the Pacific - Australia plate boundary propagated through Marlborough in the Early Miocene. Thin-skinned fault offset accommodated at least 20 km of horizontal shortening across a leading-edge imbricate fan. Mesoscopic structures in the deformed belt indicate thrust vergence to the southeast. The palaeomagnetically-determined regional clockwise vertical axis rotation of ~100° must be undone in order to evaluate this direction in the contemporary geographic framework of the thrust belt. Therefore the original transport direction of the thrust sheets in the FCFS was to the NE, in accordance with NE-SW plate motion vector between the Pacific and Australian plates during the Early Miocene.

The two new palaeomagnetic localities that are within ~3 km of the active dextral strike-slip Kekerengu Fault have the highest clockwise declination anomalies (up to 150°). Detailed structural mapping suggests that the eastern ends of the FCFS are similarly clockwise-rotated, by an extra 45° relative to the regional average, to become south-vergent in proximity to the Kekerengu Fault. This structural evidence implies the presence of a zone of Plio-Pleistocene dextral shear and vertical-axis rotation within 2-3 km of the Kekerengu Fault. Local clockwise vertical-axis rotations of up to 50° are

inferred to have accrued in this zone, and to have been superimposed on the older, regional, ~100° Miocene clockwise vertical-axis rotation.

The Late Quaternary stratigraphy of fluvial terraces in NE Marlborough has been revised by the measurement of five new optically stimulated luminescence (OSL) dates on loess. This new stratigraphy suggests that the latest aggradation surface in the Awatere Valley (the Starborough-1 terrace) is, at least locally, ~9 ka old, several thousand years younger than the previous 16 ka thermoluminescence age for the same site. This new surface abandonment age implies that terrace-building events in NE Marlborough lasted well after the last glacial maximum (~17 ka). The timing of terrace aggradation in this peri-glacial region is compared with oxygen isotope data. Downstream transport of glacially derived sediment at the time of maximum deglaciation/warming is concluded to be the primary influence on the aggradation of major fill terraces in coastal NE Marlborough. This interpretation is generally applicable to peri-glacial central New Zealand.

Patterns of contemporary uplift and directions of landscape tilting have been analysed by assessing the rates of stream incision and by the evolution of drainage networks over a wide tract of NE Marlborough that includes the termination of the dextral strike-slip Clarence Fault. Relative elevations of differentially aged terraces suggests an increase in rates of incision over the last ~10 ka. Uplift is highest in the area immediately surrounding the fault tip and is generally high where Torlesse basement rocks are exposed. Independently derived directions of Late Quaternary tilting of the landscape display a similar pattern of relative uplift in a broad dome to the north and west of the fault tip. This pattern of uplift suggests dissipation of strike-slip motion at the Clarence Fault tip into a dome-shaped fold accommodating: 1) crustal thickening (uplift) and 2) up to 44° of vertical-axis rotation of a ~40 km^2 crustal block, relative to more inland domains, into which the fault terminates. The distribution of incision rates is compared with the pattern of crustal thickening predicted by elastic models of strike-slip fault tips. The observed pattern and spatial extent of uplift generally conforms with the distribution of thickening predicted by the models, although the rate of incision/uplift over the last ~120 ka has been variable. These differences may be due to variability in the strike-slip rate of the Clarence Fault, superimposition of the regional uplift rate or to interaction with nearby fault structures not accounted for in the models.

Acknowledgments

I wish to thank Geoff Rait, Andy Roberts, Dick Walcott, Bernard Spörli, Jamie Schulmeister, Anna Pulford & Charlotte Morgan for their input and discussion of ideas during the time that this thesis was in preparation.

An extra special thanks to Gillian Turner & Gary Wilson for all their time and long hours supervising laboratory equipment during palaeomagnetic experiments and for their help with analysis and interpretation of the data.

Thanks to John Patterson, Eric Broughton, Brian Daniels, Andrew Sutton, Stewart Bush, David Winchester, Stephen Eagar, Mike Hannah, Olav Lian, Ningsheng Wang & Uwe Rieser for their technical support during research. This thesis would not have been possible without their expertise.

Thanks to Adrian, Tony and, recently, Ruth, for their tolerance and sense of humour that made the writing of this thesis more enjoyable. Thanks to Adrian also for his help setting up the initial EDM survey. Thanks to Liz Palmer for the (albeit brief) company during fieldwork.

Thankyou to Gill Ruthven, School of Earth Sciences librarian, for all of your advice on the final presentation of this thesis.

Thankyou to all the landowners who kindly allowed me free access to their property: the Chaffeys (Kekerengu), Jock & Nick Clouston (Black Hill Station), Jack Chekley (Tinline Downs), Ellie & Leigh (Matiawa Station), Lester Murray (Wharanui), Bruce Murray (Waima Hills), Geoff and Mary Bewick (Te Rapa Station), Dave Parsons (Boar Gully), Rob Peter (Waima River Valley), David and Lauren Bewick (Blue Mountain Station), Mark & Nicky Roberton (Blue Mountain Station) and to the Forgans (The Rock) and also to all the staff at The Store, Kekerengu, who supplied me with café-style coffee during fieldwork!

Many thanks to my supervisor, Tim Little, for his vision and support. His exhaustive knowledge of Marlborough and of tectonics in general greatly helped with the production of this thesis. Thanks also for the time taken to proof-read the many draft chapters.

Thanks to my parents, Heather & Ian and to the rest of my family, Jackie, Andrew and Guy, who kept me generally in good spirits over the years and helped me keep things in perspective.

Thanks to Louise, for your constant support and for never giving up. Thanks for enduring the blistering Marlborough heat and helping with the two final EDM surveys. Thanks for putting up with all the odd hours and allowing me to work when needed. Thanks for distracting me when I needed to take a break. Thanks.

Contents

CHAPTER 2: MECHANISM, TIMING AND TECTONIC SIGNIFICANCE OF VERTICAL-AXIS FAULT BLOCK ROTATIONS WITHIN THE NORTHERN PART OF THE MARLBOROUGH FAULT SYSTEM, NEW ZEALAND **PAGE**

CHAPTER 3: EVOLUTION AND TECTONIC SIGNIFICANCE OF THE FLAGS CREEK FAULT SYSTEM, MARLBOROUGH, NEW ZEALAND PAGE

CHAPTER 4: LATE QUATERNARY ALLUVIAL TERRACES OF EASTERN MARLBOROUGH AND THEIR CORRELATION WITHIN CENTRAL NEW ZEALAND **PAGE**

CHAPTER 5: NEOTECTONIC PATTERNS OF UPLIFT AT THE TERMINATION OF THE STRIKE-SLIP CLARENCE FAULT, NE MARLBOROUGH, NEW ZEALAND **PAGE**

List of figures:

CHAPTER 1: INTRODUCTION **PAGE**

CHAPTER 2: MECHANISM, TIMING AND TECTONIC SIGNIFICANCE OF VERTICAL-AXIS FAULT BLOCK ROTATIONS WITHIN THE NORTHERN PART OF THE MARLBOROUGH FAULT SYSTEM, NEW ZEALAND **PAGE**

CHAPTER 3: EVOLUTION AND TECTONIC SIGNIFICANCE OF THE FLAGS CREEK FAULT SYSTEM, MARLBOROUGH, NEW ZEALAND **PAGE**

CHAPTER 4: LATE QUATERNARY FLUVIAL TERRACES OF EASTERN MARLBOROUGH AND THEIR CORRELATION WITHIN CENTRAL NEW ZEALAND **PAGE**

CHAPTER 5: NEOTECTONIC PATTERNS OF UPLIFT AT THE TERMINATION OF THE STRIKE-SLIP CLARENCE FAULT, MARLBOROUGH, NEW ZEALAND **PAGE**

Chapter 1: Introduction

This thesis is concerned with the tectonic evolution of the Pacific – Australia plate boundary that propagated through NZ in the Early Miocene and, in particular, how ongoing crustal deformation has been accommodated in NE Marlborough since that major tectonic event took place. Deformation associated with the Early Miocene initiation of subduction of Pacific Plate beneath the east coast of NZ (Fig. 1.1) was achieved by crustal shortening in extensive fold and thrust belts that developed along the length of the margin above the incipient subduction-trench system. Importantly for Marlborough tectonics, this subduction front did not propagate southwards of the region that is today the Chatham Rise (Fig 1.1).

This work documents a changing style of deformation from dip-slip reverse and thin-skinned crustal shortening in the Early Miocene to transcurrent dextral strike-slip deformation today.

The thesis is formatted such that each chapter is an independent paper intended for separate publication describing a different aspect of how deformation has been accommodated in this transitional segment of the Pacific-Australia plate boundary zone.

In Chapter 2, new palaeomagnetic data are presented for large-magnitude clockwise vertical-axis tectonic rotations affecting parts of the Hikurangi margin since the Middle Miocene (Fig. 1.1). Basement terranes in NE Marlborough contain a distinct NE-SW striking, steeply-dipping structural fabric. In proximity to the Alpine Fault, this fabric makes a spectacular > 90°change in strike, a change which distinguishes the New Zealand Orocline. New and existing palaeomagnetic data from Marlborough suggest that this NE strike was attained in the period 18 – 8 Ma and was accompanied by 100° of regional clockwise vertical axis rotation of Marlborough. Thus the orocline is interpreted as Middle Miocene in age.

On a smaller scale, in NE Marlborough, the Flags Creek Fault System is also spectacularly folded and, in part, lies at a high angle to the NE-SW striking structural fabric of Marlborough (Fig. 1.2 a). The Flags Creek Fault System (FCFS) formed above a subduction trench in the Early Miocene as part of the early thin-skinned tectonic

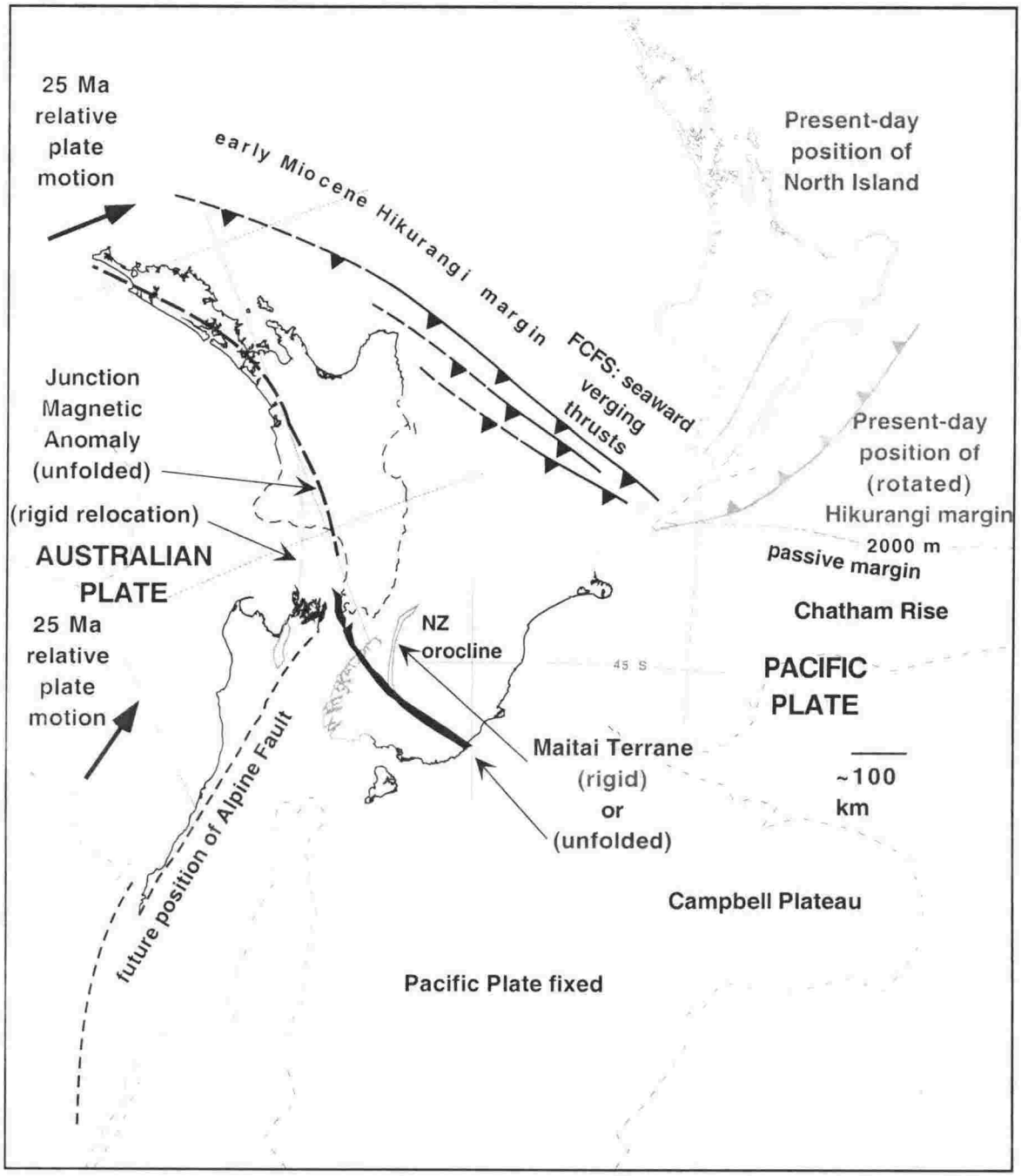

Figure 1.1. A reconstruction for the New Zealand region at 25 Ma, based on Sutherland [1995, 1999], with rigidly relocated coastline for reference shown in black; the present-day North Island and Hikurangi margin are also shown (in grey) to emphasise the rotation of the southern part of the Hikurangi margin since the Early Miocene. The Maitai Terrane/Junction Magnetic Anomaly is a steeply dipping basement terrane that can be used as a strain marker for measuring offset along the Alpine Fault. The long-wavelength sigmoidal shape of the Maitai Terrane is here inferred to be pre-Miocene in age, whereas its tighter folding in a zone near the Alpine Fault is consistent with ~100° clockwise vertical axis rotation of Torlesse Terrane basement [Little & Roberts, 1997], >90° clockwise rotation of the Early Miocene Flags Creek Faults System (FCFS) [Chapter 3] and a 100° "regional" clockwise rotation of 60 - 17 Ma rocks in Marlborough [Walcott et al. 1981; Vickery, 1994; Chapter 2].

deformation episode (e.g., Fig. 1.1). Today, the FCFS is conspicuously arcuate in map view, with folding that defines the NNE-trending, gently plunging Ben More anticline (Fig. 1.2 b). Previous palaeomagnetic sampling in Marlborough has mostly been from coastal sites, on the eastern limb of the Ben More anticline, where 60 – 18 Ma old rocks have been clockwise rotated by ~100°. This research addresses the question of whether the axis of the large fold structure functions as a boundary of crustal-scale vertical-axis tectonic rotations, suggested by Little & Roberts [1997], but a hypothesis which had not been tested. New palaeomagnetic data from the western part of the arcuate Ben More massif suggests that there has been a similar amount of clockwise vertical axis rotation during the period 18 – 8 Ma on both limbs of the fold, thereby discounting the Ben More anticline as a vertical-axis rotation boundary and demonstrating that the large post-Miocene vertical-axis rotations are both regional in nature and not related to the Ben More anticline.

Two of the new palaeomagnetic localities and several of the existing ones that are close to active strike-slip faults, such as the Kekerengu Fault, exhibit clockwise declination anomalies that are significantly greater than the regional 100°, with some being as large as 150°. The "extra" rotation at these localities, also borne out by structural mapping, is ascribed to distributed dextral shear in a zone parallel to the active faults and to have accrued since Pliocene inception of the strike-slip faults.

Younger rocks document a different pattern of vertical-axis rotations than those recorded by adjacent, older rocks. Some parts of NE Marlborough, especially the lower Awatere Valley (the Awatere Block [Roberts, 1992]; Fig. 1.3), are continuing to rotate, whereas others are not, resulting in a complicated distribution of vertical-axis rotations in space and time. This younger, spatially variable rotation is, in part, attributed to onshore termination of the dextral strike-slip Clarence Fault and is revisited in Chapters 5 & 6.

In Chapter 3 , the direction, timing and amount of transport of the large thrust sheets within the arcuate FCFS (Fig. 1.2 b) is investigated. These faults probably formed in response to contraction within the accretionary wedge of the Early Miocene subduction complex. Some parts of the fault system were locally uplifted and subject to syntectonic erosion and deposition, providing a syntectonic source for the Great Marlborough Conglomerate, which an extremely poorly sorted olistostromal unit that

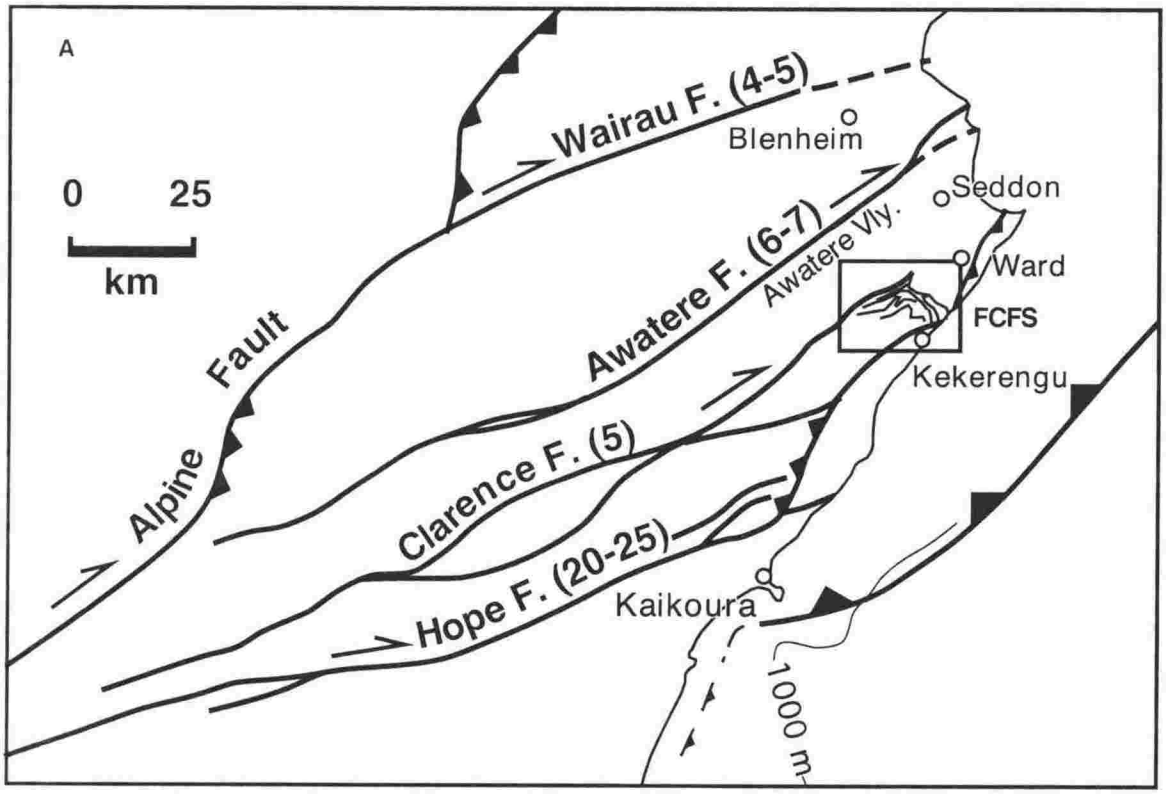

Figure 1.2A. The NE-striking structural fabric of Marlborough and the active Marlborough Fault System (MFS), with approximate rates of strike-slip offset shown in brackets (mm a^{-1}) [after Little & Roberts, 1997; Van Dissen & Nicol, 1999]. The Flags Creek Fault System is conspicuously folded in map view.

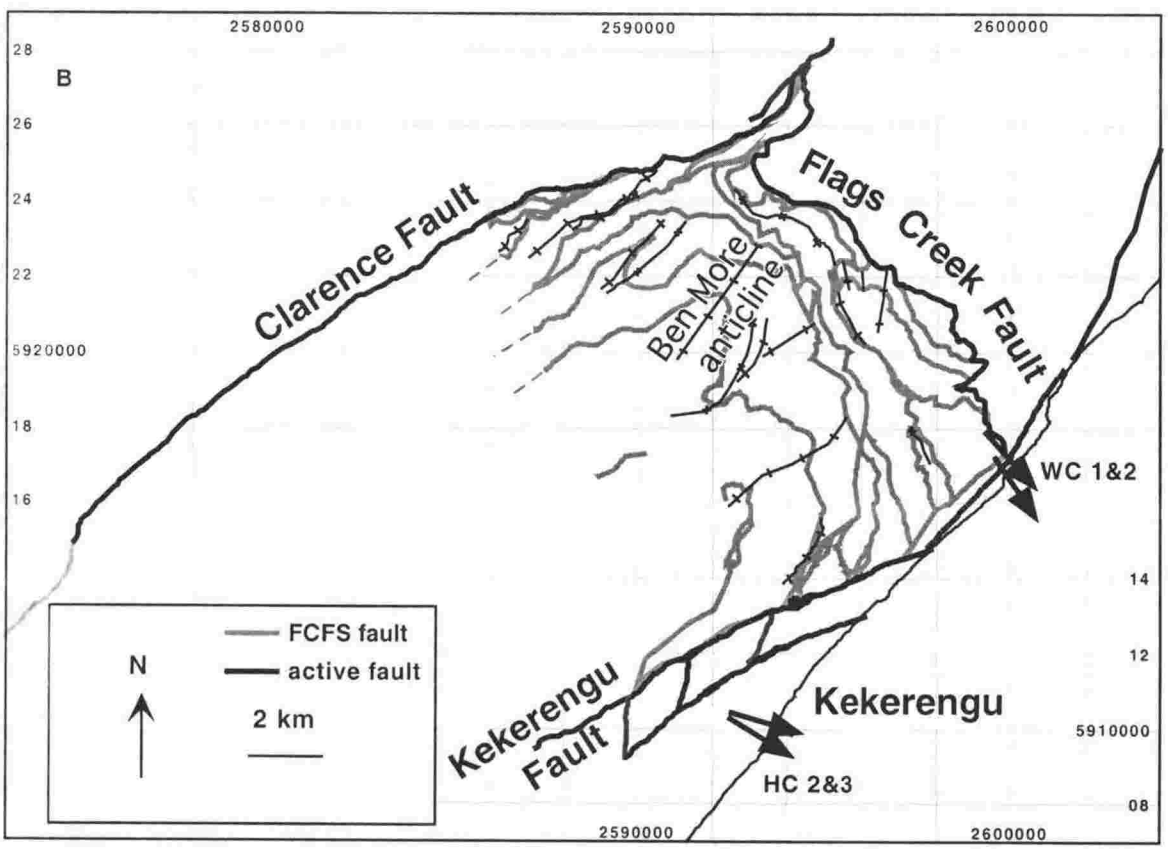

Figure 1.2B. Closer view of the Flags Creek Fault System (FCFS). Previous palaeomagnetic sample localities WC 1&2 and HC 2&3 [Vickery, 1994] are shown to emphasise the generally sparse data and complete lack of sample localities from around the FCFS.

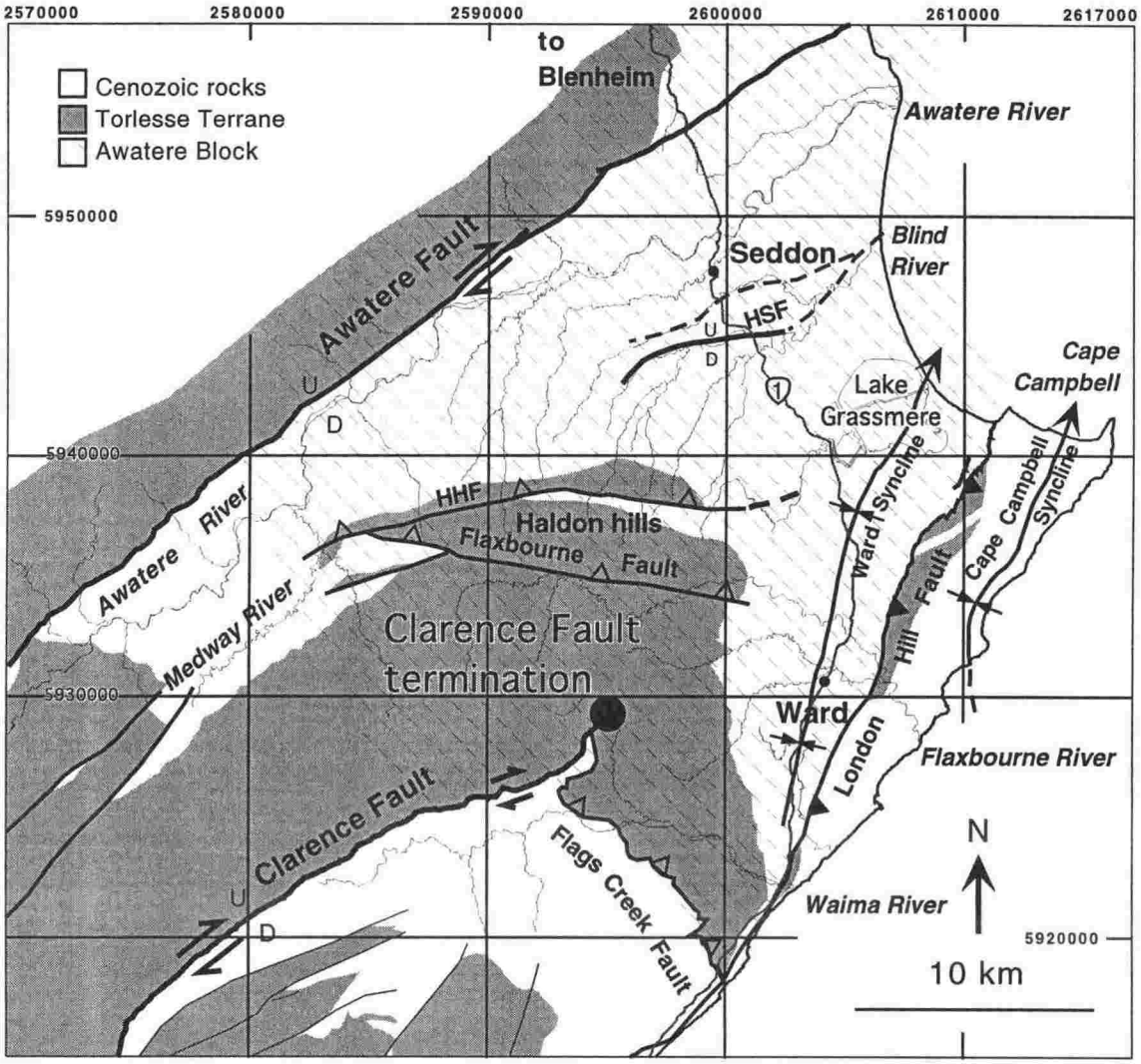

Figure 1.3. Simplified geological map of the Awatere - Ward area emphasising the distribution of Mid - Late Cretaceous Torlesse Terrane (shown in grey), after Russel [1959] and Lensen [1962]. Active structures include the Awatere, London Hill and Clarence faults, the latter of which terminates near the centre of the study area. Other faults that may be active are the Hog Swamp Fault (HSF) and the Haldon Hills (HHF) and Flaxbourne faults. The Ward and Cape Campbell synclines are also actively being deformed [Townsend, 1996].

has an Aquitanian – Burdigalian (Otaian – Altonian; ~24 – 16 Ma) age. Rare kinematic slip indicators on the fault surfaces and abundant mesoscopic structures adjacent to the larger faults, such as small-scale faults, minor shear zones, asymmetric folds, stylolitic cleavage and fractures indicate a consistently SE-directed transport direction across the majority of the Flags Creek Fault System, in present-day coordinates. This direction, parallel to the continental margin trend, is anomalous with respect to the NE-SW direction of contraction implied by Early Miocene plate boundary reconstructions (e.g., Fig. 1.1). When corrected for the regional clockwise vertical-axis rotation, however (documented in Chapter 2), these SE-vergent directions become NE-vergent, perpendicular to the continental margin, reflecting the Early Miocene contraction direction within the nascent plate boundary zone.

The regional pattern of SE-directed thrust transport is complicated by later overprinting of the Early Miocene tectonic fabrics by younger reactivation of the (now-rotated) fault structures. These relationships provide important new data on the evolution of the Pacific-Australia plate boundary zone. Deformation has changed from primarily thin-skinned thrusting in the Early Miocene, through an interval of large magnitude, regional clockwise vertical-axis rotation (100°), to the current regime of dextral strike-slip faulting.

An analysis of Late Quaternary deformation across a large tract of NE Marlborough is also presented. The Late Quaternary stratigraphic framework of NE Marlborough is revised in Chapter 4, to aid in the accurate determination of rates of Late Quaternary deformation. This revision is focused particularly on the Awatere River valley (Fig. 1.3), where Late Quaternary fluvial terraces are spectacularly preserved. These terraces have been mapped on the basis of aerial photogrammetry and, using the refined stratigraphy, have been correlated with coeval surfaces external to the Awatere Valley. Five new optically stimulated luminescence (OSL) ages on loess have enabled refinement of the morphostratigraphic sequence of NE Marlborough [Eden, 1989]. Dating of the Starborough-1 terrace, the latest aggradation surface in the Awatere Valley, at ~9 ka suggests that, at least locally, this aggradation event lasted several thousand years longer than previously interpreted [Little et al., 1998]. Older terraces returned ages of ~60, ~80, ~100 and ~120 ka, which correlate with warming peaks in the oxygen isotope ratio [Martinson et al., 1997]. A model of terrace aggradation at the

time of peak deglaciation is presented in Chapter 4, whereby outwash of glacial/colluvial debris and terrace formation is lagged with respect to sediment availability. This model differs from previous models of timing of aggradation, which assume that terrace-forming events are related to outwash of glacially derived material during the time of maximum glacial extent [e.g., Penck & Bruckner, 1909]. Steady tectonic uplift and relatively soft bedrock are necessary preconditions for the model presented here.

Spatial termination along strike of the active dextral strike-slip Clarence Fault near the Marlborough coast offers a globally important opportunity to study how strain is distributed into the tip region of a major transcurrent fault. In Chapter 5, the rate of stream incision over the last ~120 ka into fluvial terraces correlated in Chapter 4 is investigated. Rates of uplift in this inland region, including the tip area of the Clarence Fault, are inferred from these rates of stream incision and a spatial pattern of incision/uplift rates is resolved in relation to the fault tip. These inferred uplift rates are partially "calibrated" by reference to nearby coastal sites for which the rate of uplift of marine terraces has been documented previously [Ota et al., 1996; Townsend, 1996].

Directions of landscape tilting are assessed independently by the study of drainage networks and stream piracy patterns. Abandonment of stream channels in favour of topographically lower courses suggest uplift or "doming" of an area that lies to the north of the Clarence Fault termination. This area is the Haldon Hills (Fig. 1.3), where Torlesse terrane basement is exposed. The distribution of uplift/tilting inferred from older terraces is similar to that inferred from younger surfaces, suggesting that uplift patterns have not substantially changed over the last ~120 ka.

Models of 3-D elastic strain predict areas of differential uplift and subsidence in the vicinity of a strike-slip fault tip [ten Brink et al., 1996]. The distribution of uplift inferred from patterns of differential stream incision is compared with the pattern of uplift predicted by the 3-D model of elastic strain. The area of fastest uplift predicted by the elastic model coincides approximately with the area observed to have the highest rate of incision/uplift in NE Marlborough. This suggests that strain modelled elastically in the vicinity of a strike-slip fault tip is preserved by finite deformation, such as uplift of terrace surfaces, in a way that can be predicted. Vertical-axis rigid block rotation of the area into which the fault terminates is also inferred to be a mechanism by which tip

stresses are distributed, resulting in local convergence (and divergence) along the boundaries of the rotating blocks (e.g., the Awatere Block; Fig. 1.3).

In Chapter 6, the Neogene tectonics of the coastal area between the mouth of the Awatere River and Cape Campbell (Fig. 1.3) is investigated. This paper was written and published during early Ph.D. research and is referred to hereafter as Townsend & Little [1998]. The field research was conducted as part of a B.Sc. (Hons) project by the author [Townsend, 1996]. This work included a kinematic analysis of populations of mesoscopic faults that crop out along the coastal cliffs and a study of the London Hill Fault, about which little was previously known. The direction of principal horizontal shortening strain (PHS) calculated from these fault slip data suggest a change in the direction of contraction from the north of the coastal region, where the PHS direction trends ~090°, to the southern region, where the PHS direction trends ~154°. East of the London Hill Fault, in the Cape Campbell syncline, the direction of PHS is again oriented NW-SE and parallel to the regional geodetic shortening direction of 110° [Bibby, 1981] (Fig. 1.3). This changing pattern of infinitesimal strain is interpreted as representing a clockwise rotation of the "Awatere Block", bounded to the east by the London Hill Fault. Palaeomagnetic evidence also argues that the London Hill Fault is a major crustal discontinuity, separating the rapidly rotating Awatere Block to the west, from the Cape Campbell Block, to the east, which exhibits a smaller finite vertical axis rotation than parts of the Awatere Block.

Chapter 2: Mechanism, timing and tectonic significance of vertical-axis fault block rotations within the northern part of the Marlborough Fault System, New Zealand.

ABSTRACT

Twelve new palaeomagnetic localities have been sampled over a ~25 × 15 km area from Late Cretaceous – Early Tertiary Amuri Formation limestone and Middle Miocene Waima Formation siltstone from eastern Marlborough, totalling more than 260 samples. Of these new samples, approximately one third are interpreted as producing reliable tectonic results, which consistently display clockwise declination anomalies of between 100 and 150°. Early-Middle Miocene rocks are rotated as much as Palaeogene rocks, suggesting that regional clockwise vertical-axis rotation of a large part of the NE South Island occurred after 18 Ma. Palaeomagnetic samples from across a folded Early Miocene thrust belt, the Flags Creek Fault System, exhibit similar declination anomalies on either limb of the fold (the Ben More anticline), suggesting that this fold did not form as a result of differential vertical axis rotation between the limbs, as has been hypothesised. The regional nature of this rotation implies that vertical-axis rotations were a fundamental deformation process in the evolution of the Early Miocene Pacific – Australia plate boundary in NE South Island.

Basement rocks of NE Marlborough, the Middle Cretaceous Torlesse terrane, contain a steeply-dipping, dominantly NE-SW -striking structural fabric that delineates one limb of the New Zealand orocline. Tertiary rocks overlying the Torlesse terrane in Marlborough have been regionally clockwise-rotated, relative to the Pacific Plate, by at least 100° since the early Middle Miocene (18 Ma). This paper argues that the present-day NE-SW -oriented structural fabric of Marlborough is a consequence of the regional ~100° clockwise vertical-axis rotation of originally NW-SE -striking basement rocks, a rotation that is also recorded throughout the palaeomagnetically sampled parts of NE Marlborough. The timing of this rotation is constrained by new palaeomagnetic and structural evidence to have occurred since the early Middle Miocene. This rotation is interpreted to have developed in a zone of distributed dextral shear adjacent to the incipient Alpine Fault. Dextral strike-slip faulting is the dominant deformation process in NE Marlborough today. The two new palaeomagnetic localities that are within ~3 km of the active, dextral strike-slip Kekerengu Fault have locally anomalous clockwise declination anomalies of up to 150°. New structural mapping undertaken in NE Marlborough suggests that early Miocene transport directions of large-scale thrust sheets of the Flags Creek Fault System (FCFS) are similarly clockwise-rotated in proximity to the Kekerengu Fault by up to 45° (i. e., from SE-verging over the majority of the FCFS to S-verging near the Kekerengu Fault). This structural evidence implies the presence of a zone of Plio-Pleistocene distributed dextral shear and vertical-axis rotation within 2 – 3 km of the Kekerengu Fault. Local clockwise vertical-axis rotations of up to 50° are interpreted to have accrued in this zone, and to have been superimposed on the older, regional, ~100° Miocene clockwise vertical-axis rotation mentioned above.

INTRODUCTION

Vertical axis rotation of crustal blocks commonly occurs within zones of continental convergence or transform motion and has been widely documented in New Zealand by palaeomagnetic studies [e.g. Walcott et al., 1981; Mumme & Walcott, 1985; Roberts, 1992; Vickery, 1994; Vickery and Lamb, 1995; Wilson & McGuire, 1995; Little & Roberts, 1997]. However, despite the extent of palaeomagnetic sampling, the limit of crustal blocks which have undergone rotation, the position of their boundaries with unrotated regions and the timing of rotations are generally poorly known.

Numerous hypotheses have been presented to explain the mechanism by which motion in transcurrent plate-boundary zones is transferred between translation and vertical axis rotation [e.g. Lamb, 1987, 1988; McKenzie & Jackson, 1983; Roberts, 1995; Little & Roberts, 1997]. Kinematic models for fault-block rotation include slat or trellis systems, variously pinned at one or both ends and also the case of freely floating rigid blocks embedded within a continuously deforming substratum. Little & Roberts [1997] present the special case for Marlborough, New Zealand, where vertically dipping basement rocks are thought to have undergone crustal-scale kink-style folding about vertical axes.

The most obvious crustal scale geological feature of New Zealand is the change of basement strike through the central part of the New Zealand continent (Fig. 2.1). The origin of this bending is poorly understood, as is the timing of its formation [e.g. Walcott, 1978; Kamp, 1987; Little & Roberts, 1997]. The Maitai Terrane is a narrow (<5 km wide) zone of rocks that can be traced almost the entire length of New Zealand [e.g. Sutherland, 1996]. In the South Island, the Alpine Fault dextrally offsets the vertically-dipping Maitai Terrane marker by an apparent maximum distance of 450 km. Recent plate reconstructions [Sutherland, 1999] indicate as much as 800 km of total displacement between the Pacific and Australian plates since the Eocene (45 Ma). These reconstructions also suggest that basement rocks were originally linear in late Eocene times (Fig. 2.1, inset), but provenance studies of clastic rocks from the West Coast of the South Island suggest that the arcuate shape had been acquired some time prior to 4.5 Ma [Sutherland, 1996]. Thus, the timing of formation of the New Zealand Orocline is poorly constrained. If the plates are treated as rigid, removal of 800 km of dextral slip on the Alpine Fault results in a reconstruction with ~350 km of apparent sinistral offset of basement rocks before the development of the Pacific–Australia plate

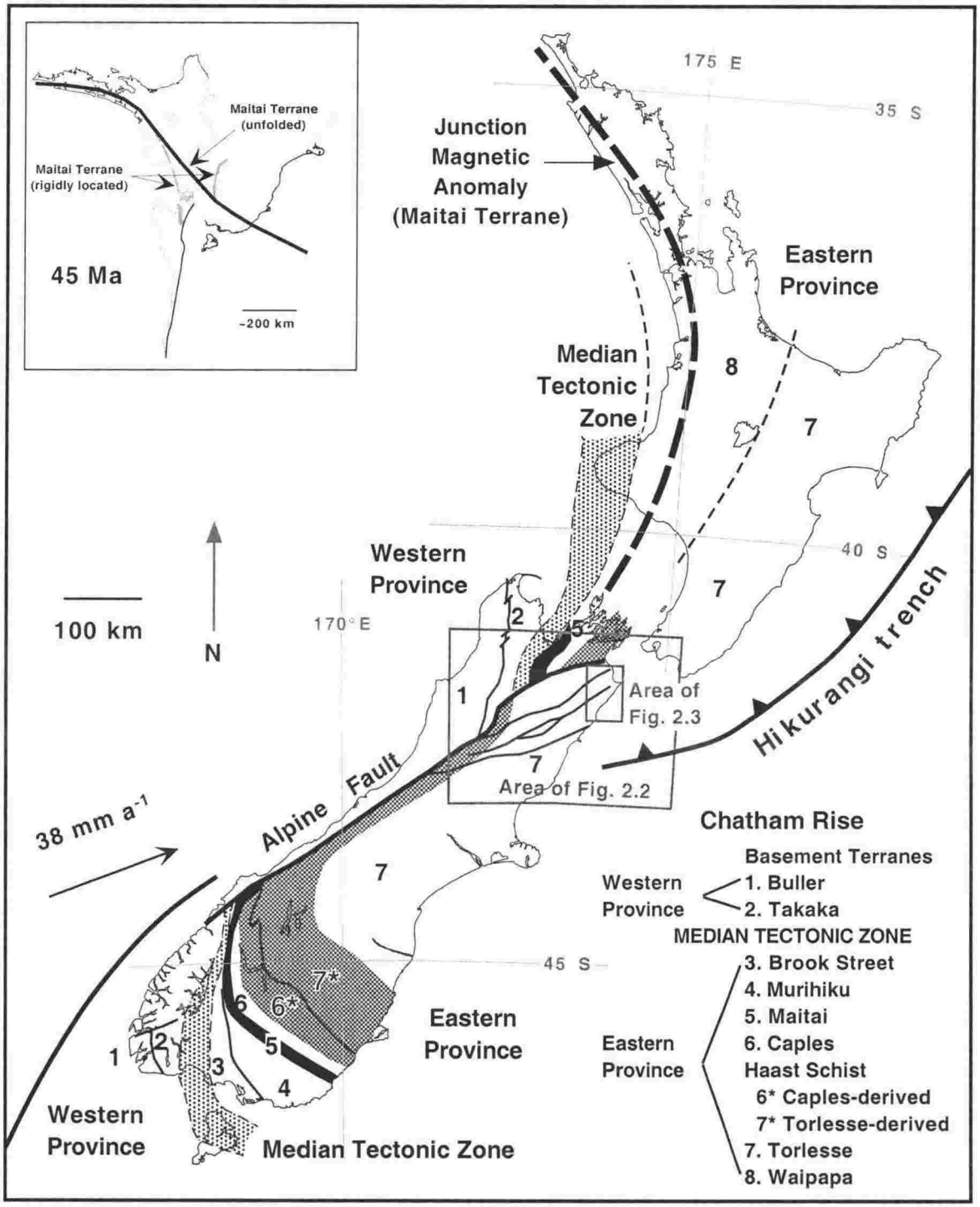

Figure 2.1. The tectonic setting of New Zealand showing prominent bending of basement terranes that produces the New Zealand Orocline; redrawn from Sutherland [1999]. Inset: relative position of the Maitai Terrane at 45 Ma (after Sutherland [1995]) with rigid plate relocation (shown in grey) and assuming that dextral shear within the evolving plate boundary has curved the originally NW-SE striking marker (shown in black).

boundary through New Zealand (Fig. 2.1, inset). Motion between rigid plates is not a viable theory, as Pliocene and younger deformation in the South Island, New Zealand, has been distributed over a zone that is several 100's of km wide [e.g. Walcott, 1998]. The gradual change in strike of basement rocks in the central part of New Zealand as one approaches the Alpine Fault also suggests that non-rigid deformation has occurred in a broad zone along the plate boundary. This style of deformation may have been favoured because of the steep dip of the basement rocks, that allowed crustal-scale folding about vertical axes in the lower part of the crust [e.g. Little & Roberts, 1997], while unconformably overlying strata, which had more gentle dips, would have been passively rotated about vertical axes as folding took place beneath. The driving mechanism behind this deformation is inferred to be the accommodation of strain that accumulated at the southern termination of the Hikurangi subduction margin. A pre-existing zone of weakness along what is now the Alpine Fault may have allowed the linking of fault segments within a shear– or fold- zone as the Early Miocene plate boundary propagated through New Zealand [Norris et al., 1990].

In this paper, new palaeomagnetic data are presented from a strongly clockwise-rotated part of the Marlborough region, in the northern part of the South Island, New Zealand (Fig. 2.1). I will argue that the New Zealand Orocline in this region formed rapidly in the middle-late Miocene, by the initiation of a dextral shear zone, originating at the southern termination of the Hikurangi subduction margin, that became the through-going Alpine Fault.

GEOLOGICAL SETTING OF NE MARLBOROUGH

Present tectonics of the Marlborough Fault System

In the central South Island, shortening between the Pacific and Australian plates is currently concentrated largely on the dextral-reverse Alpine Fault [Norris & Cooper, 1997]. In the NE of the South Island, this pattern changes to distributed deformation over a width of ~200 km on a series of 5 crustal-scale strike-slip faults that make up the plate boundary zone in Marlborough (Figs. 2.1 & 2.2). These faults are the Marlborough Fault System (MFS), which links subduction of the Pacific Plate beneath the Hikurangi margin to oblique dextral-reverse slip on the Alpine Fault. Faults of the MFS collectively accommodate 80 – 100% of the Pacific-Australia Plate motion [Holt

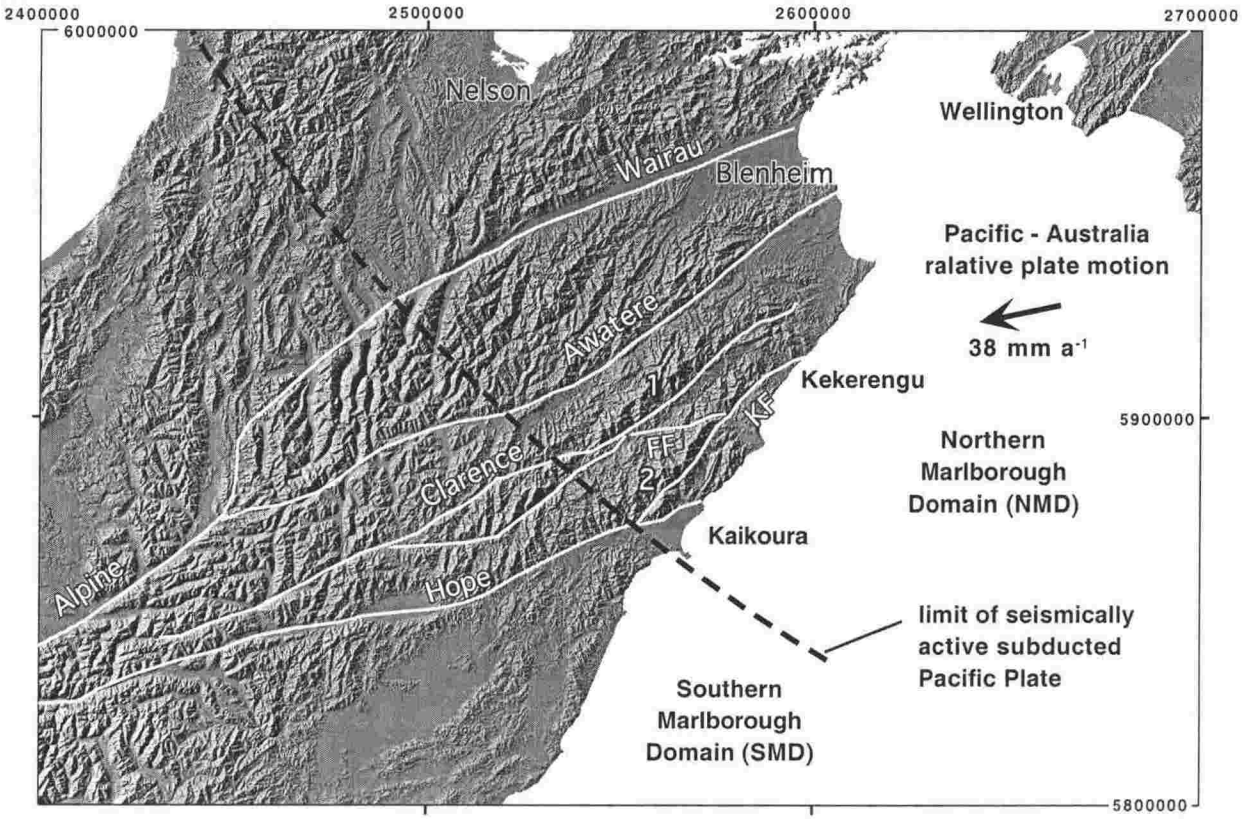

Figure 2.2. Northern South Island relief map generated from 1: 50 000 map series digital contours. Major valleys correspond to the position of the Marlborough faults (white lines), which change strike near the southern limit of the seismically active subducted Pacific Plate (dashed line). FF: Fidget Fault; KF: Kekerengu Fault; 1: Inland Kaikoura Range; 2: Seaward Kaikoura Range.

& Haines, 1995], which is approximately 38 mm a^{-1} in central New Zealand [DeMets et al., 1994].

The MFS has been divided into two domains on the basis of a change in mean fault strike near Kaikoura [e.g. Lamb & Bibby, 1989]. The boundary between the northern and southern domains trends NW-SE and coincides approximately with the southern limit of the subducted Pacific Plate [Lamb & Bibby, 1989] (Fig. 2.2). In the southern domain, the Marlborough faults strike ~075°, approximately parallel to the Pacific–Australia relative plate motion vector and deformation there is almost purely strike-slip. The northern domain faults strike ~055° and more obliquely to the relative plate motion vector. This region is underlain by seismically active, subducted Pacific Plate [Eberhart-Phillips & Reyners, 1997]. The misalignment of faults in the Northern Marlborough Domain (NMD) with current relative plate motion results in a large component of dip-slip motion on the faults and is responsible for uplift of the Kaikoura ranges [Van Dissen & Yeats, 1991]. Lamb & Bibby [1989] interpreted these faults to be

reactivated Early Miocene dip-slip faults that initiated with a NW-SE strike. A component of up-to-the-west dip slip on the NMD faults is suggested by inliers of Palaeogene rocks that are preserved in their footwalls, juxtaposed against Mesozoic rocks of the Torlesse Terrane on their NW sides. No correlative inliers of Palaeogene rocks exist on the footwalls of the Southern Marlborough Domain (SMD) faults. The tractional effects of the underlying, subducted Pacific Plate in the NMD may also play a large part in the crustal dynamics of this region [Eberhart-Phillips & Reyners, 1997]. If the interface between subducted Pacific Plate and overriding Australian Plate is locked beneath northern Marlborough, as suggested by Bibby [1981], then the orientation of structures accommodating deformation in that region almost certainly will not conform to typical patterns of strike-slip or reverse faulting observed in areas where there is no slab effect.

The northern part of the MFS is continuing to rotate today. Clockwise vertical axis rotations of up to 44° have been documented from rocks as young as Pliocene (~4 Ma) near the onshore termination of the Clarence Fault [Roberts, 1992]. The region undergoing contemporary vertical axis rotation is generally referred to as the Awatere Block [Roberts, 1992] (Fig. 2.3). The extent of the Awatere Block has been defined by unrotated 6-7 Ma old rocks along its western boundary [Little & Roberts, 1997] and 3-4 Ma old rocks to the south near Kekerengu [Roberts, 1992; Vickery, 1994].

Miocene tectonics of New Zealand

The late Oligocene – early Miocene was a time of widespread tectonic change in New Zealand. Increased early Miocene clastic sedimentation suggests that an emergent landmass was present and the onset of andesitic volcanism in the north of New Zealand indicates that subduction of the Pacific Plate beneath the Australian Plate was well established by *c.* 21 Ma [e.g. Rait et al. 1991]. Tectonic inversion of older extensional basins by reverse faulting at this time has been documented from the West Coast of the South Island [Bishop & Buchanan, 1995], from Taranaki [King & Thrasher, 1992] and from Southland [Norris et al., 1990] (see Fig. 2.1), indicating a change from an extensional or passive tectonic regime to one of increasing convergence or transpression. Parts of a NW-SE -oriented Mesozoic subduction zone, which had ceased activity near the end of the Cretaceous [Bradshaw, 1989], were reactivated at this time, as activity migrated southward into New Zealand [Walcott, 1978]. Importantly, this

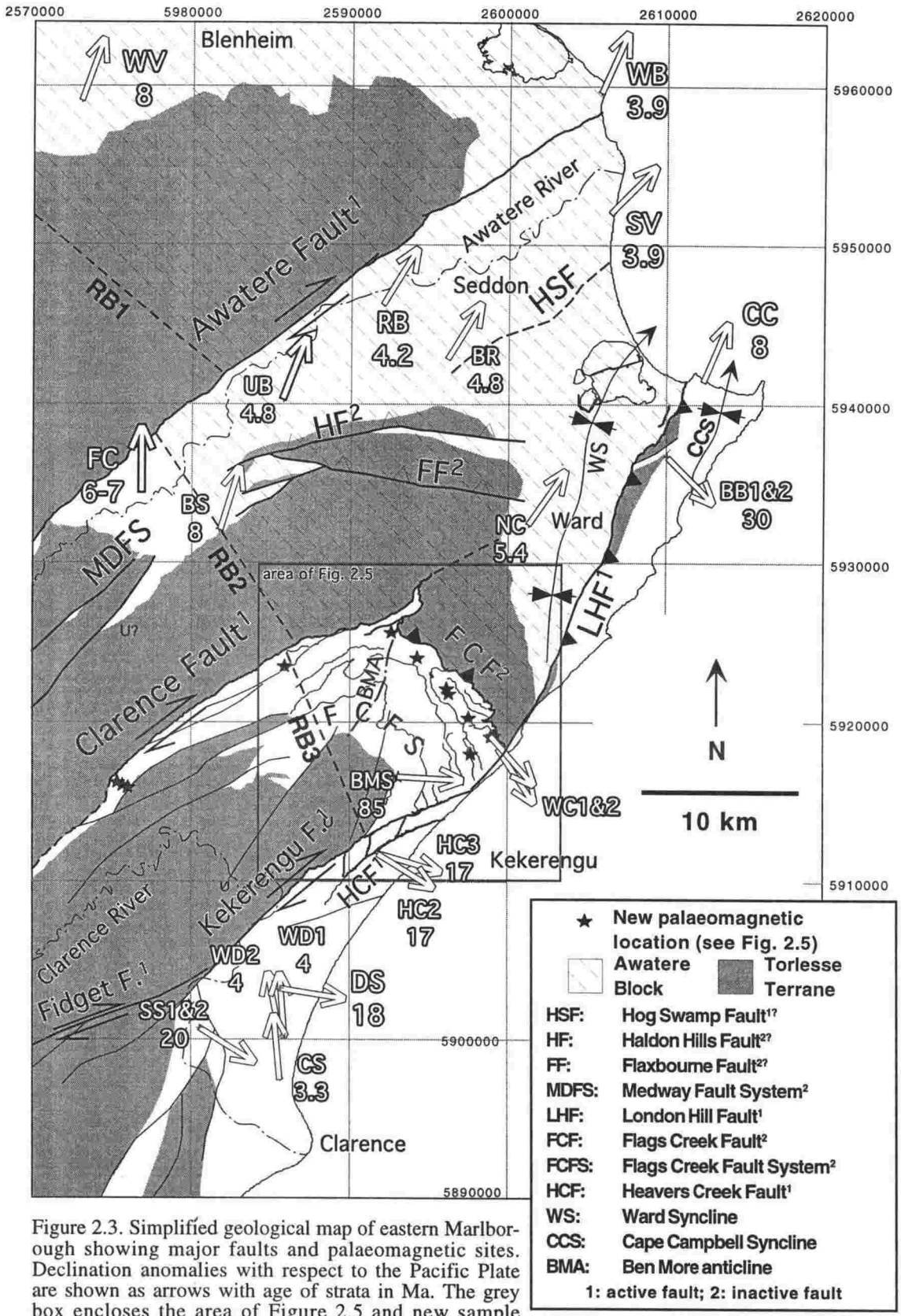

Figure 2.3. Simplified geological map of eastern Marlborough showing major faults and palaeomagnetic sites. Declination anomalies with respect to the Pacific Plate are shown as arrows with age of strata in Ma. The grey box encloses the area of Figure 2.5 and new sample locations. RB1, 2 & 3: rotation boundaries of Little & Roberts [1997]. See Table 2.3 for site abbreviations and Figure 2.1 for location. Palaeomagnetic data are compiled from Walcott et al. [1981]; Mumme & Walcott [1985]; Roberts [1992]; Vickery [1994]; Little & Roberts [1997].

early Miocene subduction front did not propagate eastwards of the area that is today the Chatham Rise, possibly due to thickened oceanic crust of the Hikurangi Plateau (part of the Pacific Plate) being too buoyant to subduct [Eberhart-Phillips & Reyners, 1997]. In the early Miocene, NW-SE -striking fold and thrust belts developed above the reactivated subduction zone. These are preserved onshore in Northland, Raukumara Peninsula, East Coast/Wairarapa and Marlborough (the Flags Creek Fault System; FCFS) [Prebble, 1976; Rait et al., 1991]. Stratigraphic and structural evidence in Marlborough indicate that the FCFS was active from ~24 to 18 Ma ago [Prebble, 1976; Vickery, 1994].

The buoyancy of Chatham Rise continental crust [Eberhart-Phillips & Reyners, 1997] (Fig. 2.1) is probably an important kinematic boundary condition in the development of the plate boundary through New Zealand. The western end of the Chatham Rise is interpreted to have formed a hinge-zone at the termination of the Miocene subduction zone, about which the overriding Australian Plate to the north has pivoted ~100° clockwise since the middle Miocene [Lamb & Bibby, 1989]. As this region has rotated clockwise, so has the Australia – Pacific relative plate motion vector, swinging from ~035° in the early Miocene to 078° today [DeMets et al., 1994; Sutherland, 1995], which has possibly enabled some of the clockwise-rotated structures in Marlborough to be reactivated, or to remain active for longer than they would have had they not been rotated (see below).

Previous palaeomagnetic studies in Marlborough

The earliest studies of vertical axis rotations including data from Marlborough are based on a sparse dataset and do not attempt to define spatial or temporal patterns of rotations within a regional context [Walcott et al., 1981; Mumme & Walcott, 1985]. Lamb and Bibby [1989] incorporated a detailed structural analysis of the Kekerengu area (Fig. 2.3) with palaeomagnetic data from one locality near Kekerengu and interpreted an >87° clockwise regional rotation of Marlborough, relative to the Pacific Plate, to have taken place since 18 Ma. Roberts [1992], however, sampled Late Miocene to Pliocene mudstone rocks of the Awatere and Wairau valleys over a narrow geographic interval and obtained consistent clockwise rotations of ~20 – 35°. Roberts [1992] interpreted these data to represent a contemporary "regional" clockwise rotation of 20°, that affects all rocks to the north of the Kekerengu Fault, with additional rotation

of parts of the lower Awatere Valley due to a second order rotation mechanism. These vertical axis rotations affect rocks as young as 4 Ma, though no rotation occurred between 8 and 4 Ma, attesting to a punctuated rotational history in Marlborough. The significance of the Clarence Fault termination was noted by Roberts [1995] as a means of imparting additional clockwise rotation to rocks of the Awatere Valley. Rigid-body rotation of a block that pivots about the Clarence Fault tip was proposed to explain the distribution of palaeomagnetic declination anomalies in that area.

Palaeomagnetic studies of early Tertiary rocks from Marlborough [Vickery, 1994; Vickery and Lamb, 1995] corroborated the interpretation of Lamb & Bibby [1989], that the entire Marlborough region has been affected by a regional clockwise rotation of 60 - 100°, which occurred between 18 and 8 Ma. In the model of Vickery and Lamb [1995], this regional rotation was followed by a further 4 Ma to present-day rotation of ~20°, affecting all rocks between the Wairau and Kekerengu faults, with the strongly rotated Lower Awatere Valley area identified by Roberts [1995] receiving an additional ~15° of clockwise rotation (Fig. 2.3). A further 30 – 40° of localised clockwise rotation adjacent to active faults was inferred from rocks that have clockwise declination anomalies as high as ~145° (Fig. 2.3, sites WC1&2, BB1&2) [Vickery, 1994]. The assumption that the entire area between the Wairau and Kekerengu faults is currently undergoing clockwise vertical axis rotation was disproved by Little and Roberts [1997], who obtained an unrotated site mean direction for 6 – 7 Ma old rocks from the middle Awatere Valley (Fig. 2.3, site FC). Little and Roberts [1997] also argued that, because the Torlesse bedrock of Marlborough acquired its steep dip prior to the onset of rotational deformation, changes in bedding strike can be used to define boundaries between blocks that have experienced different amounts of vertical axis rotation.

Stratigraphy of eastern Marlborough

Basement rocks of Marlborough are made up of siliciclastic Late Cretaceous Torlesse terrane that accumulated in a subduction trench off the coast of the Gondwana supercontinent. In the western Kekerengu region (Fig. 2.3), a short hiatus occurred in the Mid. Cretaceous (Motuan stage); in the east this period of non-deposition lasted a further ~10 Ma until the Mangaotanean [Crampton & Laird, 1997], resulting in Burnt Creek Formation conglomerate and mudstone being unconformably deposited on Torlesse rocks (Fig. 2.4). Paton Formation glauconite sandstone marks a period of

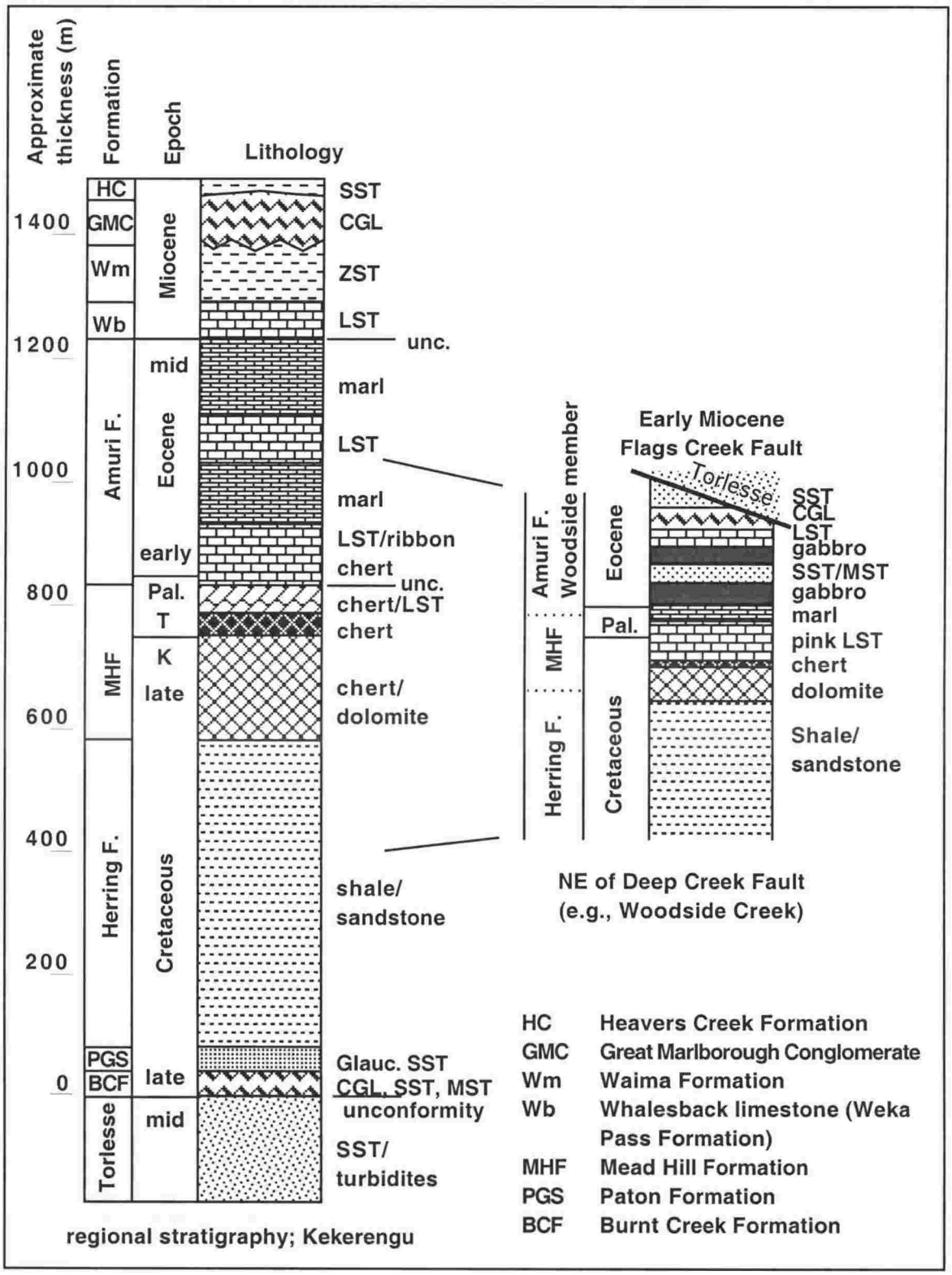

Figure 2.4. Generalised stratigraphic column for the Kekerengu area, emphasising the lithologic differences to the SW and NE of the Deep Creek Fault (see Figure 2.5). The thickness of the Mead Hill and Amuri formations on the regional column is from Strong et al. [1995].

lower sedimentation rates and the initiation of the "East Coast Basin" [Moore, 1988]. Late Cretaceous Herring Formation shale was deposited in this anoxic basin, which extended along the entire eastern margin of New Zealand [Moore, 1988]. Deposition of the siliceous Mead Hill Formation flint and calcareous Amuri Formation limestone and marls in the Late Cretaceous and early Tertiary [Strong, et al., 1995] attest to the development of a passive margin environment. The Woodside Member of the Amuri Formation is a <200m thick unit of siltstone and mudstone turbidites with interdigitating bodies of gabbro, but crops out solely to the NE of the Deep Creek Fault [Prebble, 1976] (Fig. 2.5). Gabbroic units of the Woodside Member exhibit chilled lower margins with the host mudstone becoming contact metamorphosed to a hard, recrystallised marble. Petrographic thin-sections of the host rock reveal the presence of a recrystallised calcite matrix, enveloping clastic/detrital grains of the original sedimentary rock. Chilled margins within the gabbro bodies are also prevalent, indicating several episodes of igneous intrusion. Upper contacts of the igneous bodies are not exposed, leaving open the possibility that these gabbroic sequences are flows rather than sills. Other igneous rocks in Marlborough include the extrusive Eocene-aged Grasseed Volcanics, outcropping 60 km to the SW of the FCFS, in the Clarence Valley [Reay, 1993] and the Early Miocene Cookson Volcanics (Fig. 2.5). If igneous rocks of the Woodside member of the Amuri Formation are extrusive, their Eocene age (constrained by the ~50 Ma host rock turbidites [Prebble, 1976]) makes the Grasseed Volcanics a possible lateral correlative. If the Woodside Member igneous rocks are intrusive, either Grasseed or Cookson volcanic rocks are likely candidates as temporal correlatives. Further petrographic and geochemical study is necessary to determine their affiliation with other volcanic rocks of Marlborough.

In Eastern Marlborough, middle Eocene marl is unconformably overlain by Early Miocene Weka Pass Formation [e.g., Strong et al., 1995], which is known locally as Whalesback limestone [Prebble, 1976]. An increase in clastic sedimentation during the latest Oligocene (Waitakian Stage [Vickery, 1994]), that marks the onset of the current subduction regime along the east coast of central New Zealand, also marks the development of the Flags Creek Fault System in Marlborough. Early Miocene olistostromal deposits in Marlborough (the Otaian to Altonian aged Great Marlborough Conglomerate [Prebble, 1976]) attest to the wide-scale deformation along this part of the plate boundary. Although this deformation episode was short-lived, lasting only

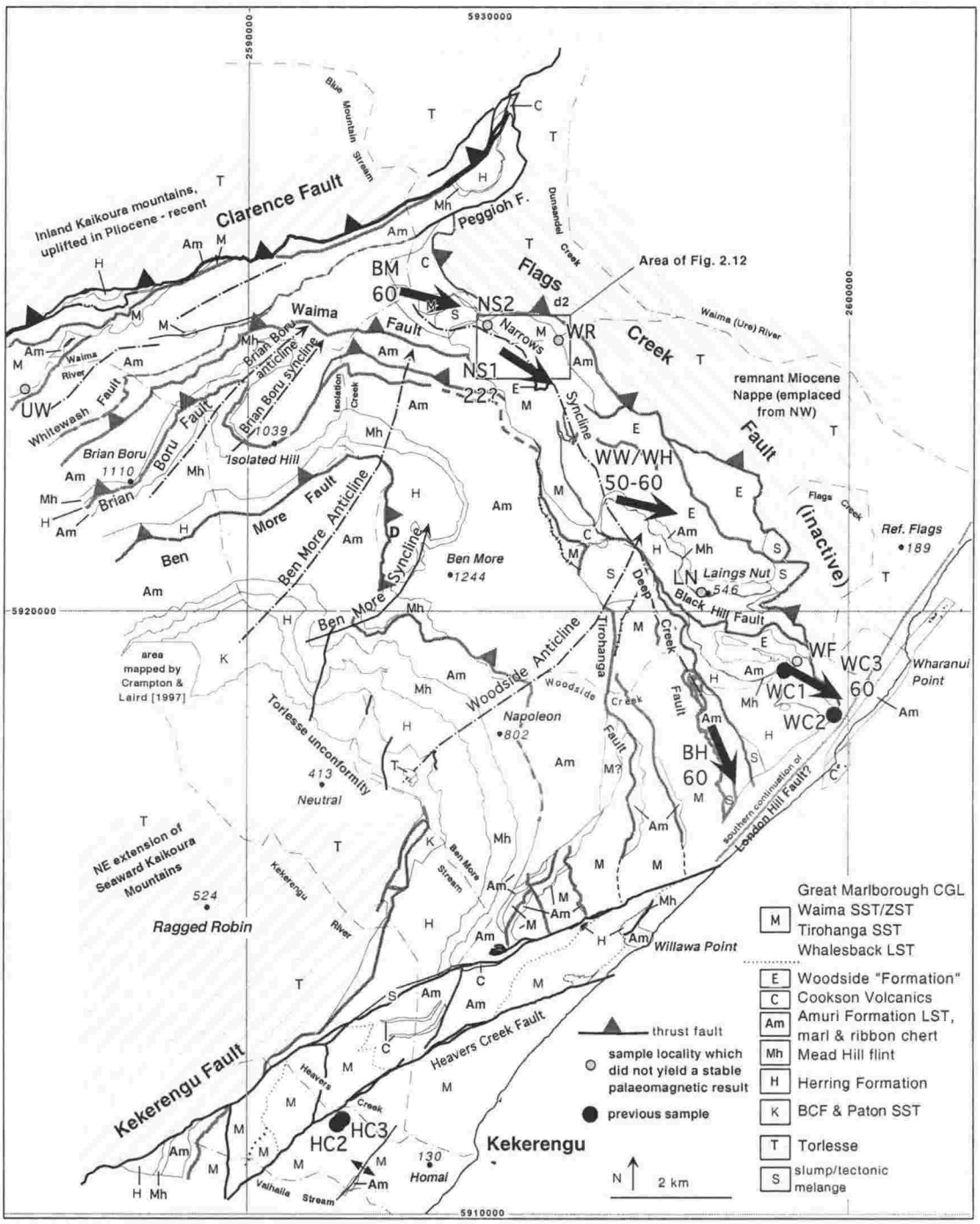

Figure 2.5. Detailed view of the Flags Creek Fault System and new palaeomagnetic localities; abbreviations are UW: Upper Waima River; BM: Blue Mountain Stream; NS1, NS2 & WR: Narrows syncline; WW: Waima Hills Amuri Formation Woodside member; WH Waima Hills Amuri Formation limestone; LN: Laings Nut; WC3: Woodside Creek and BH: Black Hill Station. Previous sample locations WC1 & 2: Woodside Creek and HC 1 & 2: Heavers Creek [Vickery, 1994].

about 5 Ma [Rait et al., 1991], rocks of this age are well represented in the Kekerengu area, with the transition from calcareous Whalesback limestone to Waima Formation siltstone (Otaian – Middle Altonian; Vickery [1994]) recording an increasingly terrigenous sedimentation sequence (Fig. 2.4). Thrust faulting and syntectonic erosion resulted in the localised formation of Early Miocene unconformities that truncate many of the older, overthrust units. Variably sorted lenses of Great Marlborough Conglomerate (GMC) are scoured into these units, resulting in buttress unconformities with varying angular relationships to the structurally deformed units below. In some areas (e.g., Valhalla Stream; Fig. 2.5), eastward tilting of Early Miocene siltstone and conglomerate facies rocks is implied by eastward thickening sequences. Eastward tilting of this region is also suggested by a basal post-Early Miocene unconformity exhuming Eocene Amuri Formation marl in the west, but only eroding as deeply as Whalesback limestone in the east [Chapter 3]. Syntectonic deposition and eastward dip-fanning in this region is also inferred from preliminary results of a shallow seismic reflection/refraction survey along the south bank of Heavers Creek (Fig. 2.3) [Henderson, in prep.]. As tectonic activity abated, these faulted, folded sequences were overlain by Middle Miocene sandstone and siltstone of the (Upper Lillburnian – Upper Waiauian [Vickery, 1994]) Heavers Creek Formation. Widespread syntectonic deposition in the Awatere basin, 10 km to the north of the FCFS, resumed in the early Late Miocene. Increasingly convergent relative plate motion at the end of the Miocene possibly resulted in thrust reactivation of the FCF and erosion of its Torlesse terrane hangingwall rocks [Chapter 3]. This period of activity waned in the Latest Miocene (Kapitean Stage) and deposition of fine-grained clastic rocks within the Awatere basin continued into the middle Pliocene [Roberts & Wilson, 1992].

THE USE OF PALAEOMAGNETISM IN DETERMINING VERTICAL-AXIS TECTONIC ROTATIONS

Primary detrital or thermo-remanent magnetisation preserved in rocks can record the direction of the instantaneous geomagnetic field at the time of formation of the rock [Butler, 1992]. A major assumption in palaeomagnetic studies is that the time-averaged geomagnetic field can be modelled by a geocentric axial dipole (GAD). This is the GAD hypothesis [Butler, 1992]. The declination of a normal polarity GAD field is zero at all locations. The mean inclination, I, varies depending on the latitude of the site in question and is determined by the equation:

$$\tan I = 2 \times \tan \lambda,$$

where λ is the site latitude [Butler, 1992]. In Marlborough, at a latitude of ~41.9° S, the GAD inclination is –60.9°. The present day magnetic field direction is D: 22.2°, I: –69.7° [International Geomagnetic Reference Field (IGRF)][†]. The difference is due to non-GAD components of the field. These non-GAD components vary with time (as does the magnitude of the GAD), resulting in the secular variation observed in all elements of the field (declination, inclination and magnitude). At mid-latitudes, the amplitudes of typical variations in declination and inclination are ±40° and ±20°, respectively. Palaeomagnetic time series suggest that the non-GAD field averages to zero over periods of between 10^4 to 10^5 years. A mean palaeomagnetic direction, averaged over a stratigraphic interval spanning in excess of 10^5 years, should therefore correspond to the GAD field direction for the site location unless:

1) there has been continental drift of the locality;

2) and/or there has been tectonic crustal block movement relative to the continental interior (where the crustal block is defined as being sub-continental in size);

3) and/or there are outcrop-scale structural variations in the bedding attitude of the locality.

If drift of the continental plate on which the site is located is documented in terms of an apparent polar wander path (APWP), then the expected time-averaged palaeomagnetic direction for the site for a particular time interval can be calculated

[†] The IGRF is published every 5 years by the International Association for Geomagnetism and Aeronomy (AGSO). Software for calculating individual magnetic field components is available at the AGSO website: www.agso.gov.au.

from the palaeomagnetic pole of the appropriate age. Marlborough lies well to the east of the Alpine Fault, which has been a locus of deformation between the Pacific and Australian plates since the Miocene [Norris et al., 1990; Sutherland, 1995; Walcott, 1998]. Therefore, it seems most fitting to regard this NE part of Marlborough as belonging to the Pacific Plate and palaeomagnetic directions are compared with reference (or expected mean) directions calculated from the Pacific Plate APWP [Petronotis et al., 1994].

Over the last 60 Ma, the Pacific Plate palaeopole has moved mostly northward with little variation in longitude [Petronotis et al., 1994]. Marlborough, at a longitude of 174° E. is near the 180° meridian, along which the Pacific Plate palaeopole has moved. Therefore, there has been negligible difference in palaeomagnetic declination along this line of longitude due to Tertiary APW of the Pacific Plate.

Petronotis et al. [1994] calculated a 57 Ma palaeopole at 78.2° N, 4.8° E (dp = 4.1°, dm = 6.4° @ 93° from north) for the Pacific Plate based on a skewness analysis of crossing marine magnetic anomaly 25r. The palaeopole has moved little between 57 Ma and 39 Ma, therefore this pole can be used to calculate the reference directions for both the ~60 Ma Amuri Formation limestone and the ~50 Ma Woodside member of the Amuri Formation. These poles are listed in Table 2.1.

If we have confidence in local structural corrections, based on extensive and detailed structural mapping (see below), we would expect the mean direction of a palaeomagnetic pole measured in 60 Ma old rocks to coincide with this expected palaeopole unless there have been local vertical-axis rotations. This expected direction is termed the "reference direction". The "declination anomaly" (positive clockwise) is the angular difference between the measured mean declination of a set of palaeomagnetic data and the declination of the reference direction for the time of rock formation. The declination anomaly is presumed to be a measure of the amount of tectonic vertical axis rotation of a locality.

Between 26 Ma and the present-day, the Pacific Plate palaeopole has moved from a latitude of ~80° N to its current location, along the 0° meridian [Acton & Gordon, 1994]. This means that, although the expected inclination has shallowed from –68.5° to –60.9° over the past 26 Ma, the expected declination has changed only from 358.8 to 0°, which is well within the uncertainty calculated from the 95% confidence limit on the pole.

	Palaeopole latitude	Palaeopole longitude
Pacific Plate pole (57 Ma)	78.2° N	4.8° E

	Locality latitude	Locality longitude
Woodside Creek	41.932° S	174.025° E
Blue Mountain Stream	41.875° S	173.994° E

	Reference declination	Reference inclination
Woodside Creek	356.3° ± 6.9°	-69.7°± 2.8°
Blue Mountain Stream	356.3° ± 6.9°	-69.6°± 2.8°

Table 2.1. Summary of palaeomagnetic poles, site location parameters and expected directions for 57 Ma old rocks of the Pacific Plate (95% confidence dm = 6.4° @ 93° from north; dp = 4.1°) [after Petronotis et al., 1994]. Blue Mountain Stream is in the far NW of the study area, while the Woodside Creek locality is near the coast. There is negligible difference in reference field declination or inclination across the region studied.

Local structural corrections performed on new palaeomagnetic data

All of the new palaeomagnetic sites reported in this study are contained within rocks that have been a part of, and have remained within, the New Zealand plate boundary zone since its formation in the Late Oligocene – Early Miocene [Chapter 3]. The locality-mean vectors in Palaeogene rocks are interpreted here as primary detrital or thermo-remanent magnetisation directions (see below). These directions have been variably rotated due to deformation associated with episodes of Miocene thrusting and folding and later by Pliocene to Recent strike-slip faulting [e.g., Lamb & Bibby, 1989]. Structural corrections of bedding to account for the effect of Miocene deformation are relatively simple, because folding of strata originally took place about sub-horizontal axes which have been tilted approximately 30° to the NE since the Late Miocene [Chapter 3]. Removal of the "regional" plunge of the folds is achieved by untilting bedding and the site magnetisation vector about a horizontal axis that is perpendicular to the 052°-trending fold hinge (Fig. 2.6A). This restoration removes the regional fold plunge (~28° in the lowest thrust sheet) which has been confidently determined by detailed structural mapping of the FCFS [Chapter 3]. The second step in the correction is to restore bedding to horizontal by rotation about its strike (Fig. 2.6B). This 2-stage process yields a magnetisation vector in "corrected" coordinates (Fig. 2.6C).

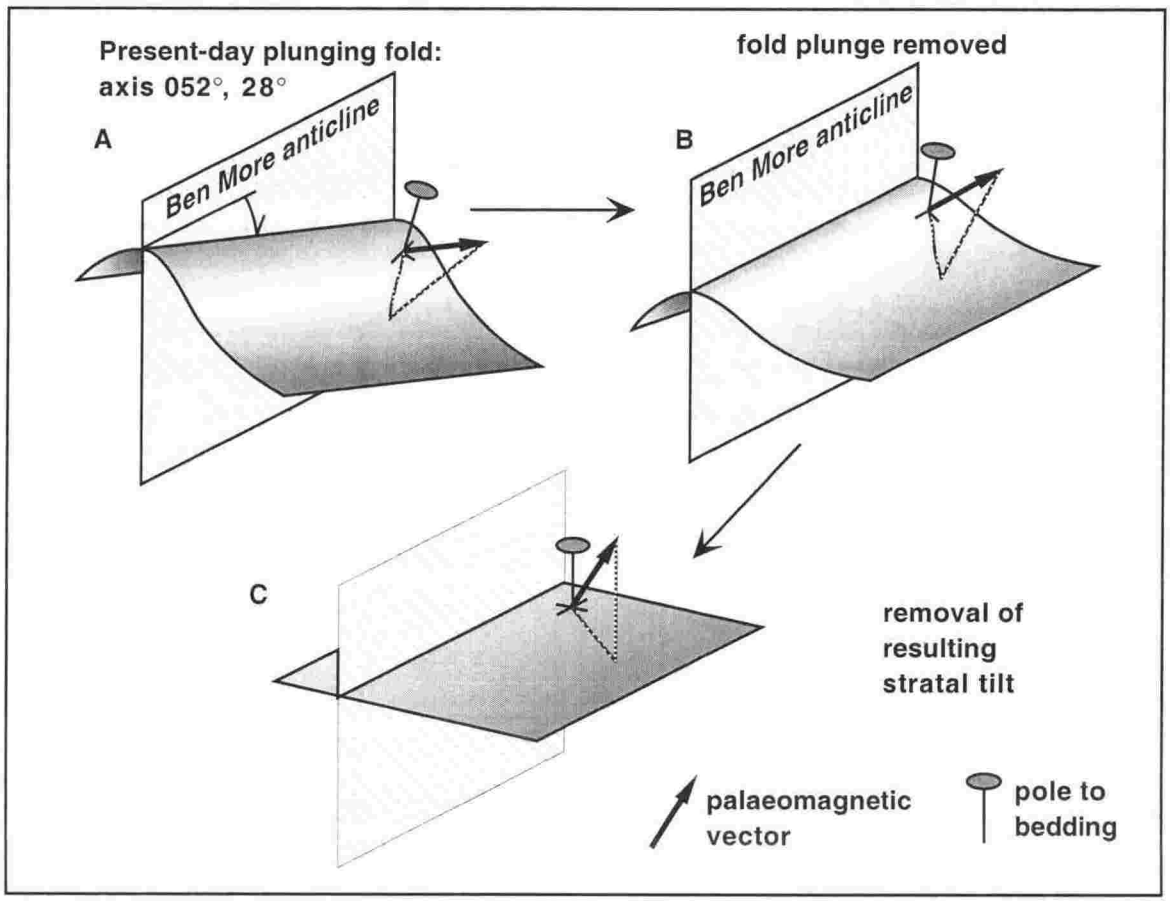

Figure 2.6. Plunging fold correction performed on the new palaeomagnetic data. The regional fold plunge (052°, 28°) is subtracted from all data during the first step. The second step involves a rotation of bedding about its (plunge-corrected) strike back to the horizontal.

NEW PALAEOMAGNETIC DATA FROM EASTERN MARLBOROUGH

Sampling strategy

One sampling strategy was to target the pink member of the Palaeocene Amuri Formation limestone, from which Vickery [1994] reported stable palaeomagnetic results. Sites were chosen from around the arcuate Ben More massif to determine the nature of folding and role of vertical axis rotations, if any, in development of the Ben More anticline (Fig. 2.3). Where possible, the overlying Early Miocene Waima Formation siltstone was also sampled to constrain temporal changes in the vertical axis rotation history. Thus, clarification of both spatial and temporal variations of vertical-axis rotations in this part of the plate boundary zone was attempted.

Samples were drilled with a standard petrol-powered drill with a diamond tipped bit. Water was used as a drilling lubricant and pumped in to the drill by a garden sprayer pump. Once cores had been oriented, labelled and wrapped, they were immediately transferred to a μ-metal magnetic shield for transport and storage.

At each new locality, samples were taken from a wide enough stratigraphic interval to average out the non-dipole effects of secular variation, as discussed above. For slowly-accumulating lithologies such as the micritic Amuri Formation limestone [Moore, 1988], sampling over a distance of greater than approximately 2m will ensure that secular variation is averaged. For lithologies such as Waima Formation siltstone, that may have accumulated more rapidly than the fine-grained limestone, the sediment accumulation rate is more difficult establish. Where possible, sampling of the siltstone lithology was executed over several tens of metres.

Laboratory procedures and conventions

Demagnetisation of cores was carried out at three different laboratories: by the author at Victoria University of Wellington and Oxford University and by Dr. Gillian Turner at the Australian Geological Survey Organisation, Canberra, Australia. A subset of cores from each site or lithology was demagnetised using the alternating field (AF) technique, but the majority of samples underwent stepwise thermal demagnetisation. Bulk magnetic susceptibility was measured after each thermal demagnetisation step to monitor the alteration and/or growth of magnetic minerals as a result of heating. Other selectively applied rock-magnetism laboratory experiments include acquisition of isothermal remanent magnetisation (IRM) and temperature-dependent susceptibility measurements. Examination of Zijderveld plots, together with principal component

analysis, were used to identify and determine the direction of the characteristic component of the natural remanent magnetisation (NRM). These directions were then structurally corrected for folding and local bedding dip using the stereographic projection program "Stereonet 4.6a" [Allmendinger, 1988].

Site descriptions

Each new site is described below in a present-day geographic order, rather than in a chronostratigraphic reference frame, followed by a summary of the demagnetisation characteristics of localities that yielded reliable palaeomagnetic data (see below). The eastern, coastal part of the field area is described first, followed by the more inland sites (Fig. 2.7, Table 2.2). The palaeomagnetic data, including the declination anomalies, with respect to the Pacific Plate, are summarised at the end of this section in Table 2.3. All demagnetisation data for new localities are archived on CD-ROM in Appendix 1, back pocket.

Localities that did not yield stable demagnetisation characteristics (WF, WR, NS2, UW, MS) and/or are statistically undersampled (e.g., WF, LN, WR –Table 2.2) are not considered for tectonic analysis. Other localities from this complexly deformed region (e.g., NS1, BM) are difficult to interpret, displaying a complicated pattern of remanent magnetisation directions. These localities are included but are not weighted greatly in the overall analysis. All of these sites are described in Appendix 2. Other sites, considered to have yielded reliable data, are described below.

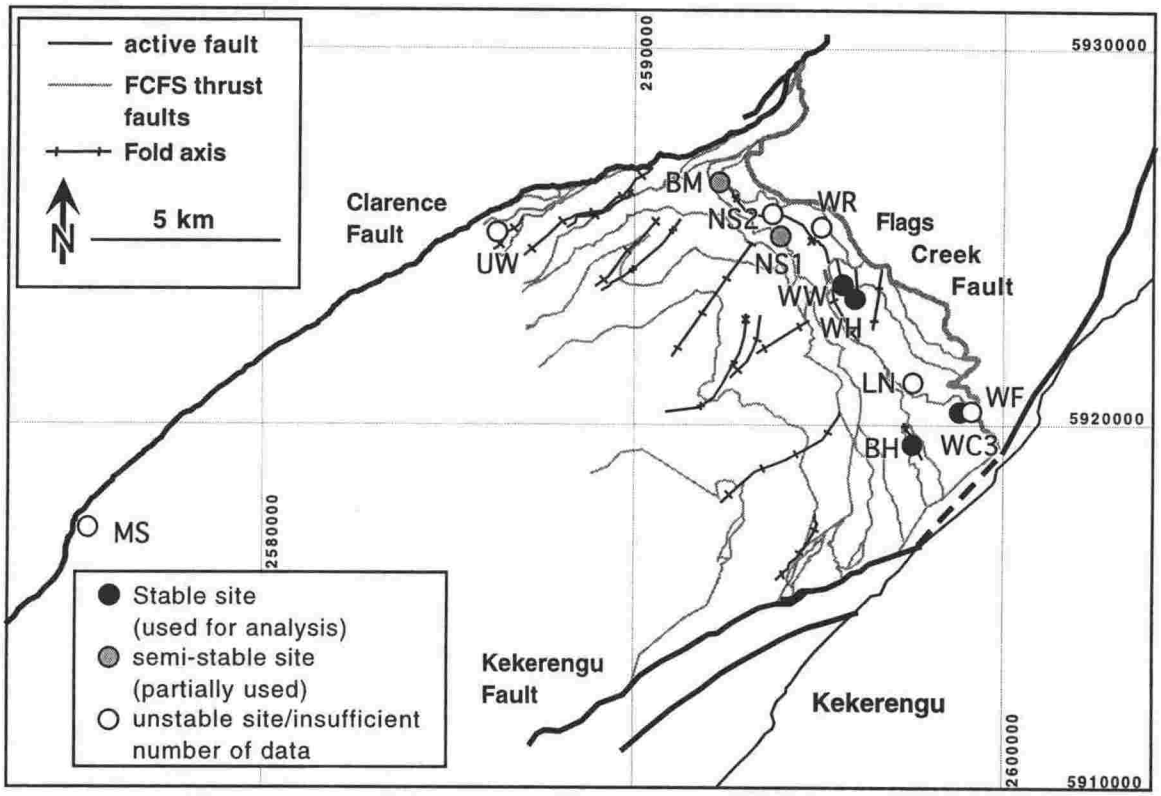

Figure 2.7. Location of the new palaeomagnetic sites (see Table 2.2). Abbreviations are BH: Black Hill Station; WC3: Woodside Creek Amuri Formation limestone; WF: Woodside Creek Amuri Formation (Woodside member); LN: Laings Nut; WH: Waima Hills Amuri Formation; WW: Waima Hills Amuri Formation (Woodside member); WR: Waima River; NS1& 2: Narrows syncline; BM: Blue Mountain Stream; UW: Upper Waima River and MS: Mead Stream.

Black Hill Station locality (BH)

Black Hill Station is the southernmost of the new palaeomagnetic localities on the eastern limb of the Ben More anticline (Fig. 2.5), where a ~10m-thick sliver of NW-dipping pink Amuri Formation limestone crops out between refolded splays of the Deep Creek Fault (DCF). This sequence of Herring Formation and Amuri Formation, which lies on the hangingwall of the DCF, tectonically overlies Miocene Waima Siltstone to the west of the fault trace (Fig. 2.8.1). Parts of the limestone may have been contact metamorphosed in proximity to a nearby gabbro sill that crops out along the DCF, as some outcrops have a sugary, recrystallised texture. These rocks are assumed to be similar in age to the 60 Ma old pink limestone [Vickery, 1994] ~3 km to the NE at Woodside Gorge, as pink limestone seems to occur at only one stratigraphic position in the Amuri Formation.

Locality (abbreviation)	Grid Ref. (P30, P29)	No. samples/ sites	Structural integrity	Lithology	Mean bedding (RHR)	Used for study?
Black Hill Station (BH)	9770-1808	4/4	Poor	LST	077/32	Y
Woodside Creek (WC3)	9894-1912	12/4	Excellent	LST	300/50	Y
Woodside Formation (WF)	9915-1919	4/4	Satisfactory	SST/MST	343/46	N
Laings Nut (LN)	9752-2031	5/5	Excellent	LST	218/35	N
Waima Hills (WH)	9658-2182	22/10	Satisfactory	LST	325/30	Y
Waima Woodside F. (WW)	9618-2218	24/7	Satisfactory	SST/gabbro	322/40	Y
Narrows 1 (NS1)	9434-2408	69/15	Excellent	ZST/W LST	310/40	Y?
Waima River (WR)	9517-2437	12/4	Poor	ZST/W LST	160/40	N
Narrows 2 (NS2)	9396-2473	18/5	Satisfactory	ZST/W LST	060/22	N
Blue Mountain Str. (BM)	9265-2667	18/7	Poor	LST/basalt	053/58	Y?
Upper Waima R. (UW)	8591-2356	20/7	Excellent	ZST	170/50	N
Mead Stream (MS)	7605-1595 7540-1629	59/21	Excellent	LST/ZST	General: 230/50	N

Table 2.2. Summary of palaeomagnetic localities sampled in this study. "Structural integrity" indicates whether the outcrop can be confidently placed within a regional structural and stratigraphic framework. LST = Amuri Formation limestone; SST/MST = Amuri F., Woodside member; ZST = Waima F. siltstone; W LST = Whalesback limestone.

Four cores were sampled over an interval of ~2m as an initial investigation into the magnetic characteristics of the pink limestone. Several of these cores were long enough to yield 2 or 3 specimens, totalling 12 for this site. Demagnetisation of samples from this locality showed that a single component was progressively removed up to ~400°C, interpreted here as a primary detrital magnetic remanence (Fig. 2.8.2). The tight clustering of the data (Fig. 2.8.3) suggests that this site has not successfully averaged secular variation. This may be due to sampling over a narrow stratigraphic range. At sediment accumulation rates of < 2 cm ka^{-1} for pelagic limestones [Morris, 1987], 2 metres of outcrop represents a minimum of 0.1 m.y. of accumulation. It is desirable to

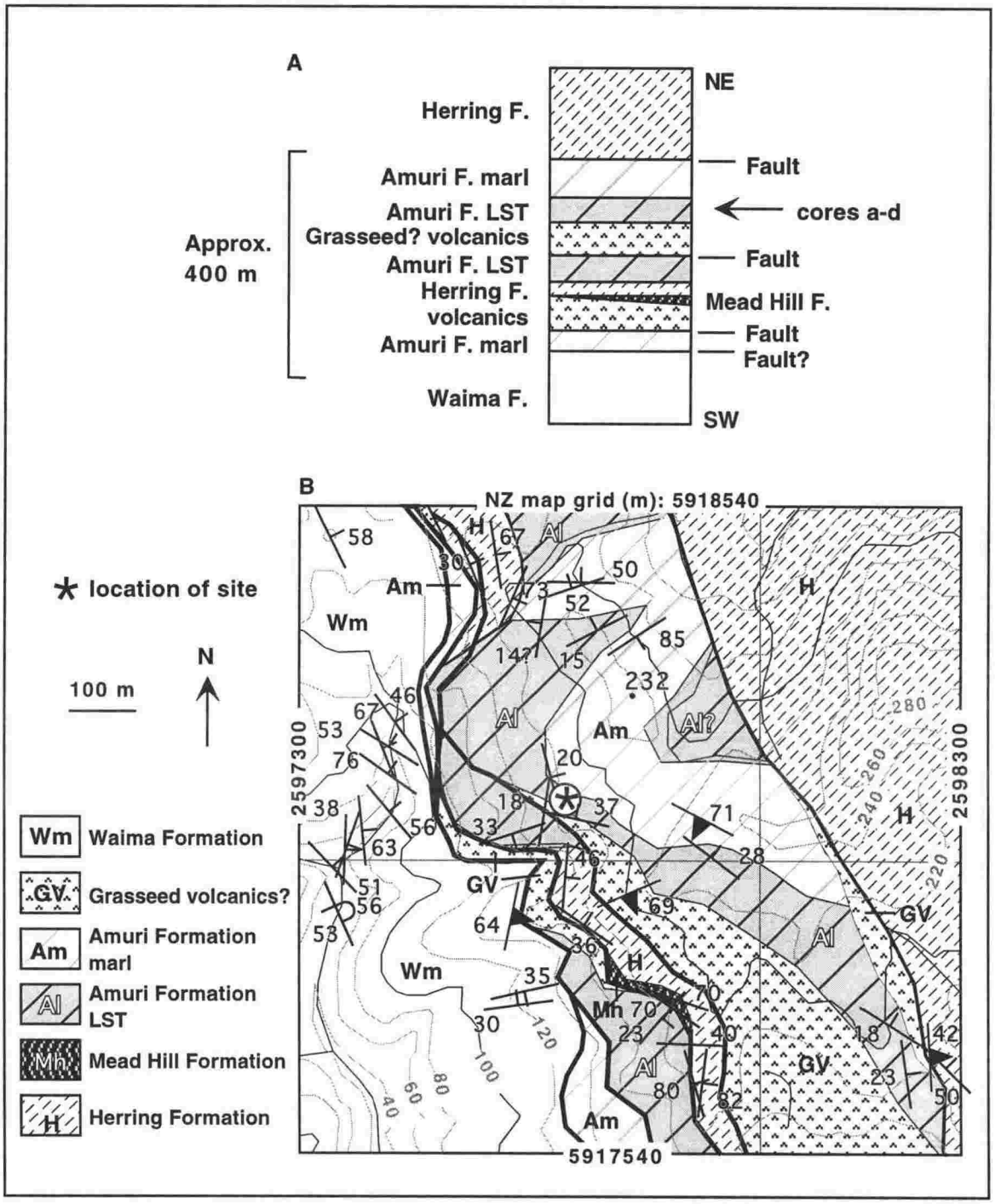

Figure 2.8.1. A: General stratigraphy of the BH locality, showing tectonic repetition of the section; B: location map with imbricates of pink Amuri Formation limestone, Grasseed(?) volcanics and Herring Formation which are "thrust" over Waima Formation across the Deep Creek Fault, forming a tectonic melange.

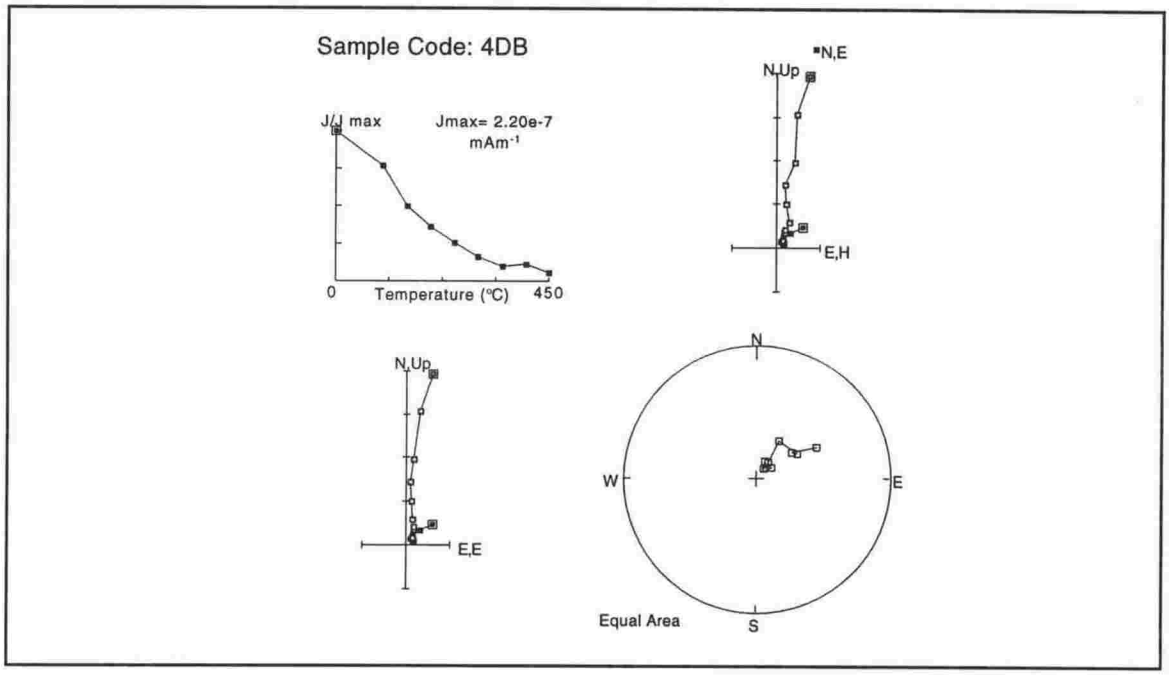

Figure 2.8.2. Thermal demagnetisation of the stable, single magnetic component in the pink Amuri Formation limestone from Black Hill Station. All plots are *in situ* coordinates. Top left: magnetisation decay during stepwise thermal demagnetisation. Top right and bottom left: vector component diagrams with the vertical component plotted against an arbitrary horizontal and east, respectively. Open (closed) symbols indicate projections onto the vertical (horizontal) plane. Bottom right: stereographic projection of demagnetisation data. Open symbols indicate projections onto the upper hemisphere.

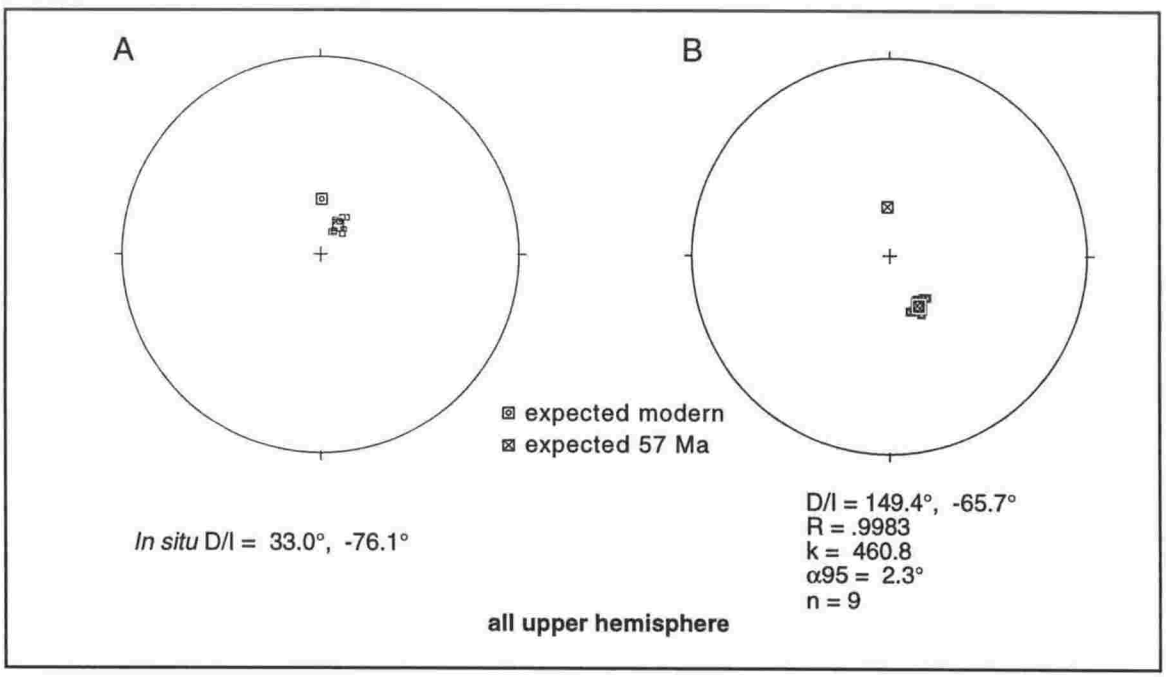

Figure 2.8.3. Primary magnetisation component from the Black Hill site; A: *in situ* coordinates and, B: corrected for folding and bedding tilt. Expected declination and inclination for these rocks is ~356°, -69°, hence 153° of clockwise rotation is inferred at this site. The tightly clustered data suggest that secular variation may not be averaged for this locality. See text for discussion.

average secular variation by sampling a time interval of $1 \times 10^4 - 10^5$ years [Butler, 1992], which may not be the case at this site. Alternatively, proximity to a gabbroic body cropping out along the nearby Deep Creek Fault may have thermally reset the magnetic remanence. However, Amuri limestone at the Blue Mountain Stream site (Appendix 2.3), which is in contact with volcanic rocks, yielded data that suggest a thermal overprint did not occur at that location. Therefore, the mean *in situ* remanence vector of 033°, -76° at the Black Hill site is interpreted as detrital and primary. The structurally corrected vector is 149°, -66° (Fig. 2.8.3B). Comparison with the 57 Ma reference direction for rocks of the Pacific Plate (Table 2.1) yields an inferred clockwise rotation of 153°. This is similar in magnitude to locality WC2, near Woodside Creek [Vickery, 1994], which yielded a clockwise vertical axis rotation of 154° for the same lithology.

Woodside Creek locality (WC3)

While many palaeomagnetic samples have been taken from Woodside Creek, notably at the Cretaceous – Tertiary boundary, few data have been published [e.g. Vickery, 1994]. The pink Amuri Formation limestone at Woodside Creek was resampled in March 1998, with a total of 12 samples drilled at 4 stratigraphic horizons over a stratigraphic range of ~20 m. To preserve this world-renowned outcrop, the oldest samples were taken from a stratigraphic distance of ~25m above the Cretaceous – Tertiary boundary (Fig. 2.9.1).

Demagnetisation of the pink limestone removed a low temperature/coercivity component that cleaned off by ~10 mT or 150°C (Fig. 2.9.2 A & B). This component is well-grouped and in the direction of a reversed geomagnetic field with a modern declination (176.5, 51°; $\alpha 95 = 4.2°$), which is anomalous. The tight clustering of this reverse polarity overprint leads to the suspicion of a rapidly imparted alteration of the rocks during some tectonic or thermal "event", possibly a lightning strike [e.g. Butler, 1992]. Progressive demagnetisation of the reversed polarity component increased the maximum intensity (J_{max}) to values of approximately 3 mAm^{-1}. A stable, underlying normal polarity component was removed by 40 mT or 600°C (Fig. 2.9.2). This component is also fairly well-grouped and is interpreted as a primary detrital remanence direction (Fig. 2.9.3A). IRM acquisition results have an unusual double step in the

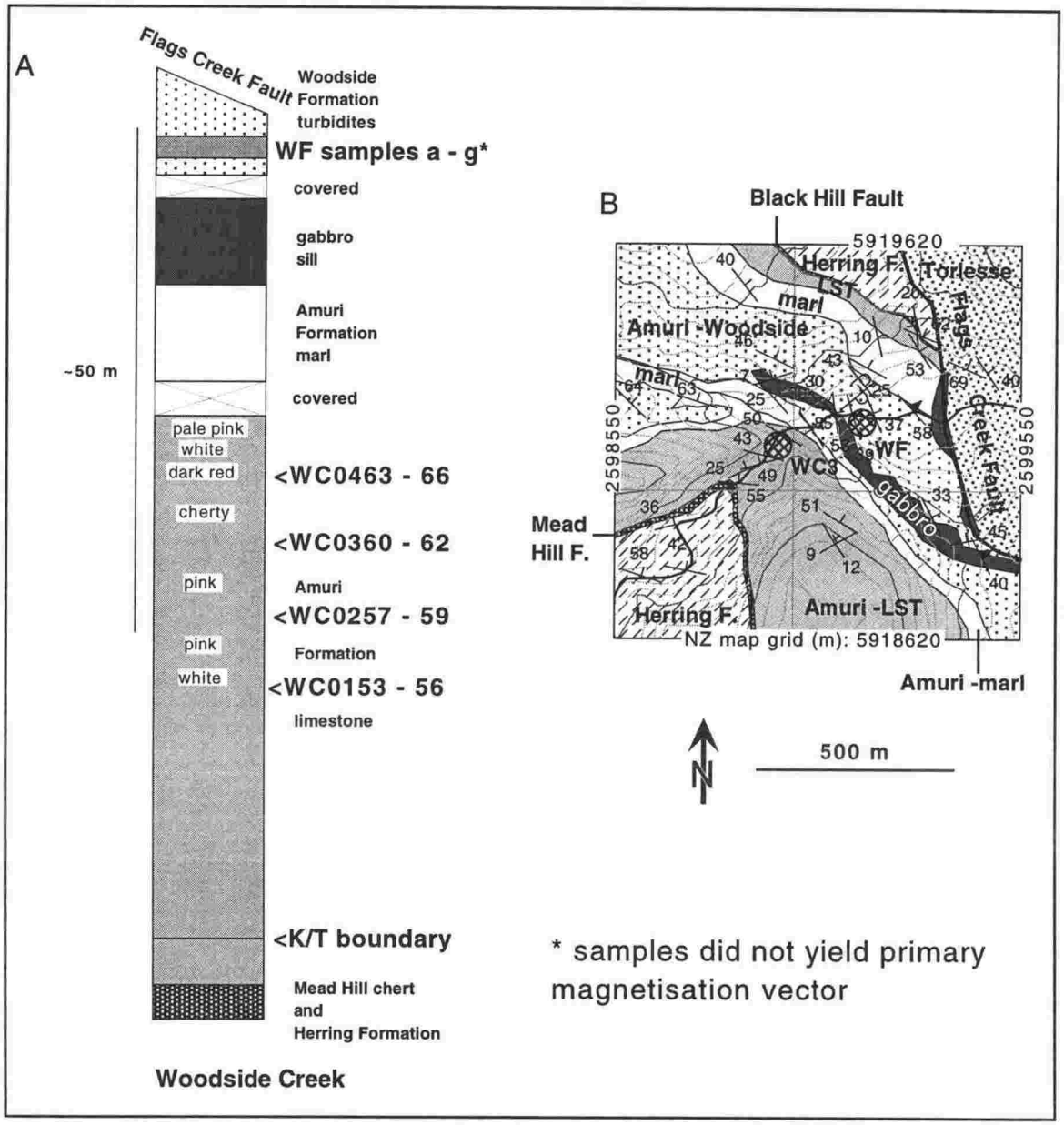

Figure 2.9.1. Geological setting of the Woodside Creek section (WC3); A: simplified stratigraphic section with location of sites WC01-04, which were taken from alternating white and pink, slightly cherty Amuri Formation limestone ~25 m above the Cretaceous - Tertiary (K/T) boundary. Erosion of the softer marl member results in a discontinuous section, that is intruded by gabbro sills. Samples of the permeable Woodside Member of the Amuri Formation (WF a-g) are not confidently placed in the stratigraphic succession. Demagnetisation of these samples failed to produce a tectonically interpretable direction. These siliciclastic rocks may also have been thermally altered in proximity to the gabbro (see Appendix 1.7); B: simpified location map of the WC3 and WF localities.

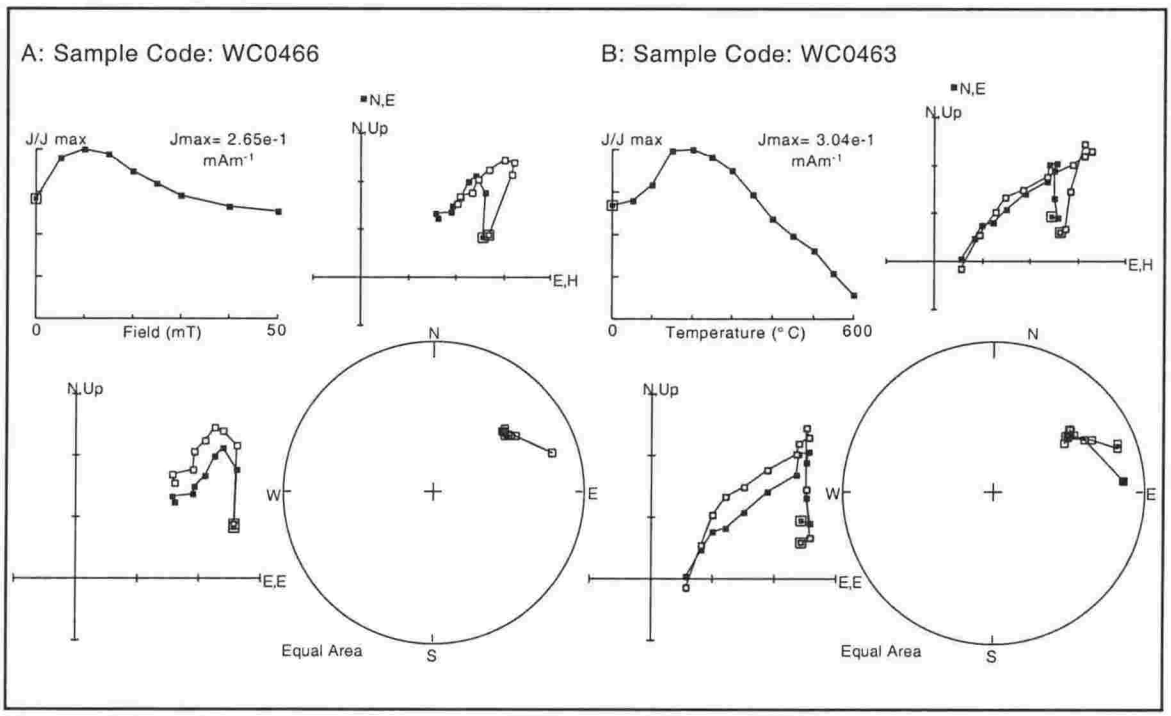

Figure 2.9.2. Typical AF (A) and thermal (B) demagnetisation plots of pink Amuri Formation limestone from Woodside Creek (WC3). All cores from this locality were normal, some with a reverse overprint, which, upon cleaning, initially causes the intensity to increase. These samples contrast with those analysed by Vickery [1994] from the same stratigraphic unit, who obtained all reverse primary magnetisations, some with a normal overprint. However, when a structural correction is applied, both data sets are in agreement with each other. The cause of the reverse overprint may possibly be a lightning strike or a recent thermal (tectonic?) event. All plots are *in situ* coordinates. Symbols are the same as in Figure 2.8.2.

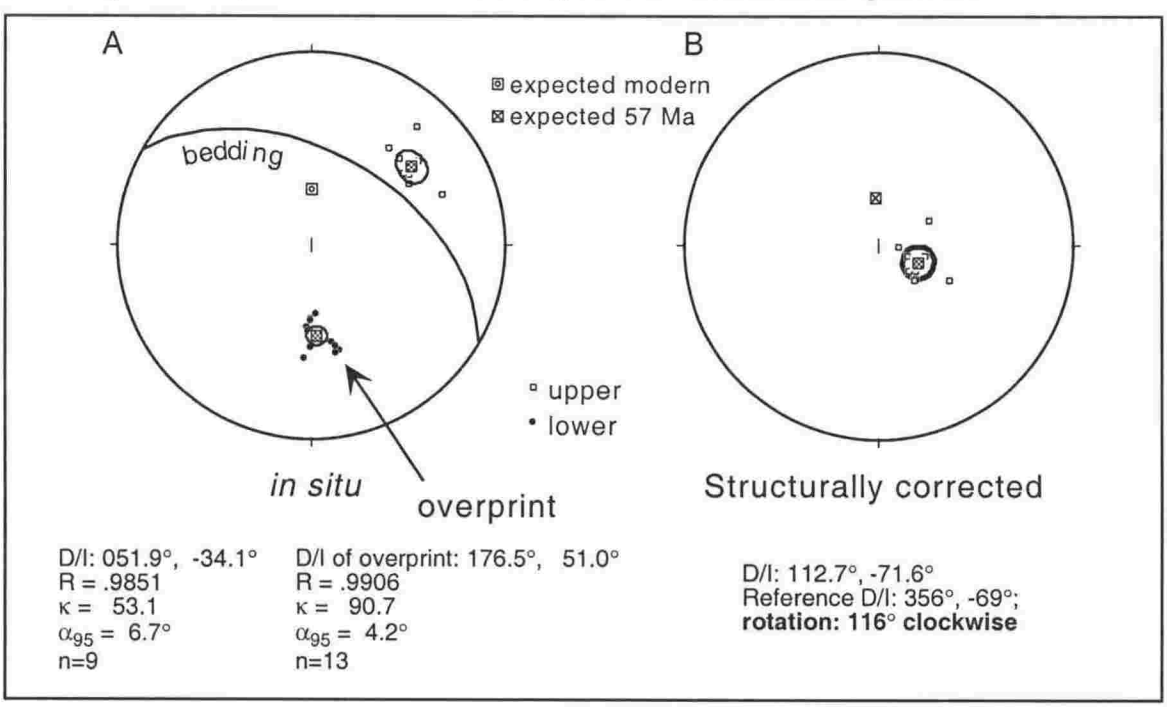

Figure 2.9.3. Magnetisation directions of samples from pink Amuri Formation limestone at Woodside Creek; A: *in situ* vectors are normal with a modern overprint; B: structurally corrected plot of the characteristic magnetisation directions. A clockwise vertical-axis rotation of ~116° is inferred from these data, which agrees reasonably well with the 138° clockwise declination anomaly of Vickery & Lamb [1995] for the same site.

curve, with a "shoulder" at ~100 mT, before increasing again to saturate at 300 mT (Fig. 2.9.4). These data indicate the presence of two possible magnetic carriers. The initial slope of the IRM acquisition curve (up to ~100 mT) is probably due to magnetite. The IRM of magnetite saturates at ~300 mT, whereas haematite can have a much higher coercivity. The fact that the IRM acquisition curve is close to saturation at 300 mT suggests that haematite is not magnetically significant in this sample. This contrasts with other samples of pink Amuri Formation limestone treated by this method (e.g. the Blue Mountain Stream locality, below; Vickery, 1994]).

The *in situ* site mean primary direction from 9 cores with interpreted stable magnetisation is 051.9°, -34.1° and the structurally corrected vector is 112.7°, -76.1 (Fig. 2.9.3B). The Early Tertiary reference declination and inclination for rocks of the Pacific Plate at this site is 356°, -69.7° [Petronotis et al., 1994], therefore ~116° of clockwise rotation is inferred. This is in fairly good agreement with the data of Vickery [1994], who obtained a clockwise declination anomaly of 134° for the same locality (Table 2.3).

Waima Hills localities (WH & WW)

A sequence of Late Cretaceous Herring Formation and Palaeocene Amuri Formation forms a topographically high-standing, NW-SE -trending ridge between the Waima River and Woodside Creek (Fig. 2.5). This sequence is part of a structural horse that is bounded by the Deep Creek Fault (DCF), to the SW and the Flags Creek Fault (FCF), to the NE. Less than 1 km to the north, the whole sequence (including the Deep Creek Fault) is complexly folded by the Narrows syncline (Fig. 2.5). Miocene strata on the footwall of the DCF are folded into a synformal structure and the DCF appears to form a footwall flat (the fault is parallel to the footwall strata). However, structurally above the DCF trace, the overthrust rocks form a folded hangingwall ramp (the fault cuts up section) and bedding is not parallel to the fault.

The NE dip of this sequence allows sampling of different stratigraphic units in proximity to each other along the ridge (Fig. 2.10.1). The Amuri Formation lower limestone member (as defined by Strong et al. [1995]) was sampled at Grid Ref. 96282179 and the younger Woodside turbidite member was sampled 600m to the west,

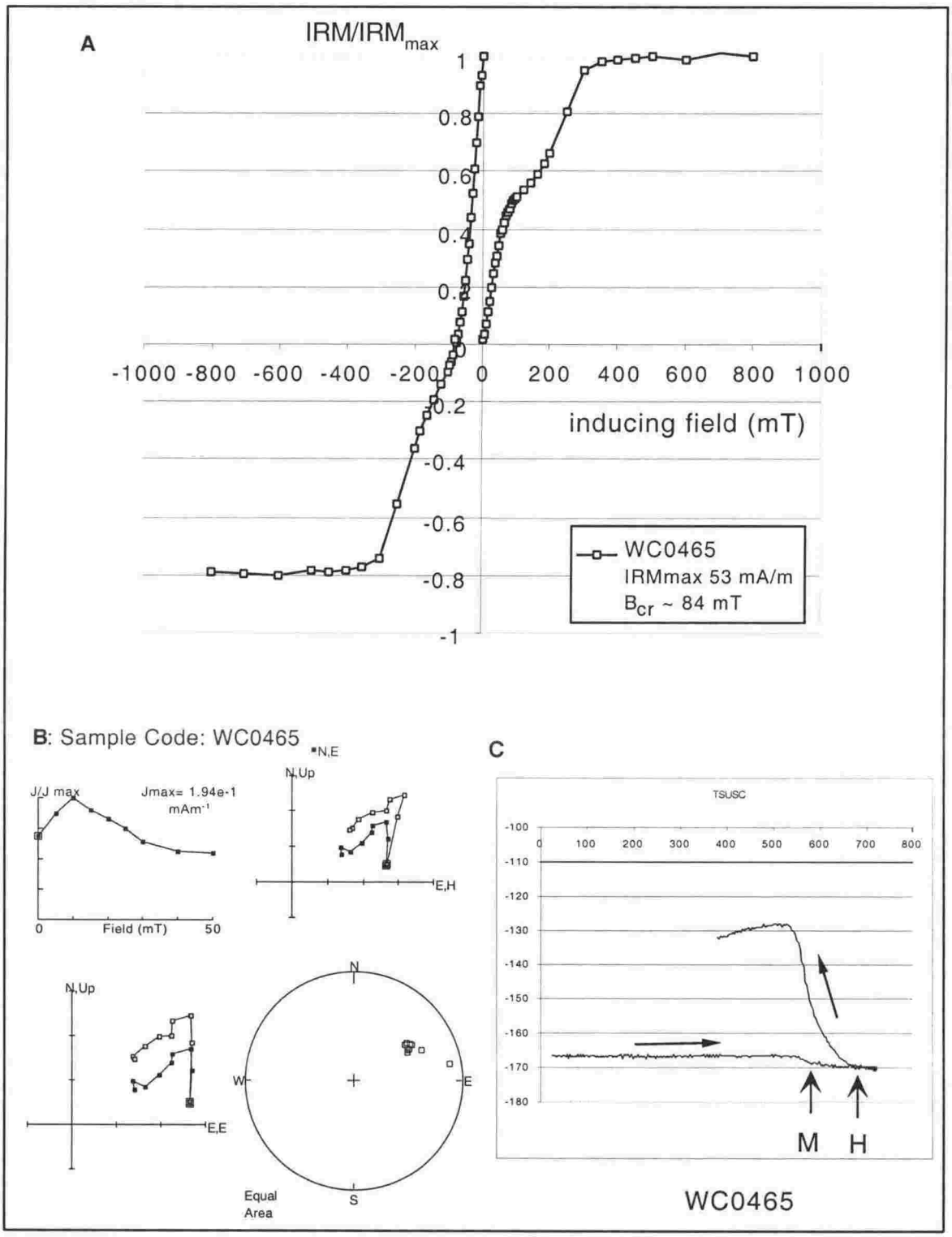

Figure 2.9.4. A: Isothermal remanent magnetisation (IRM) acquisition for samples of pink limestone from Woodside Creek (WC3) shows a two-component magnetisation, the lower coercivity component corresponding to magnetite and the higher coercivity component probably haematite. B: AF demagnetisation of the NRM of sample WC0465 and C: temperature dependent susceptibility experiments also suggests the presence of magnetite (Curie temperature ~580° C, indicated by "M"). Magnetically significant amounts of haematite (Curie temperature ~680° C, indicated by "H") are apparently not present. For B: symbols are the same as in Figure 2.8.2.

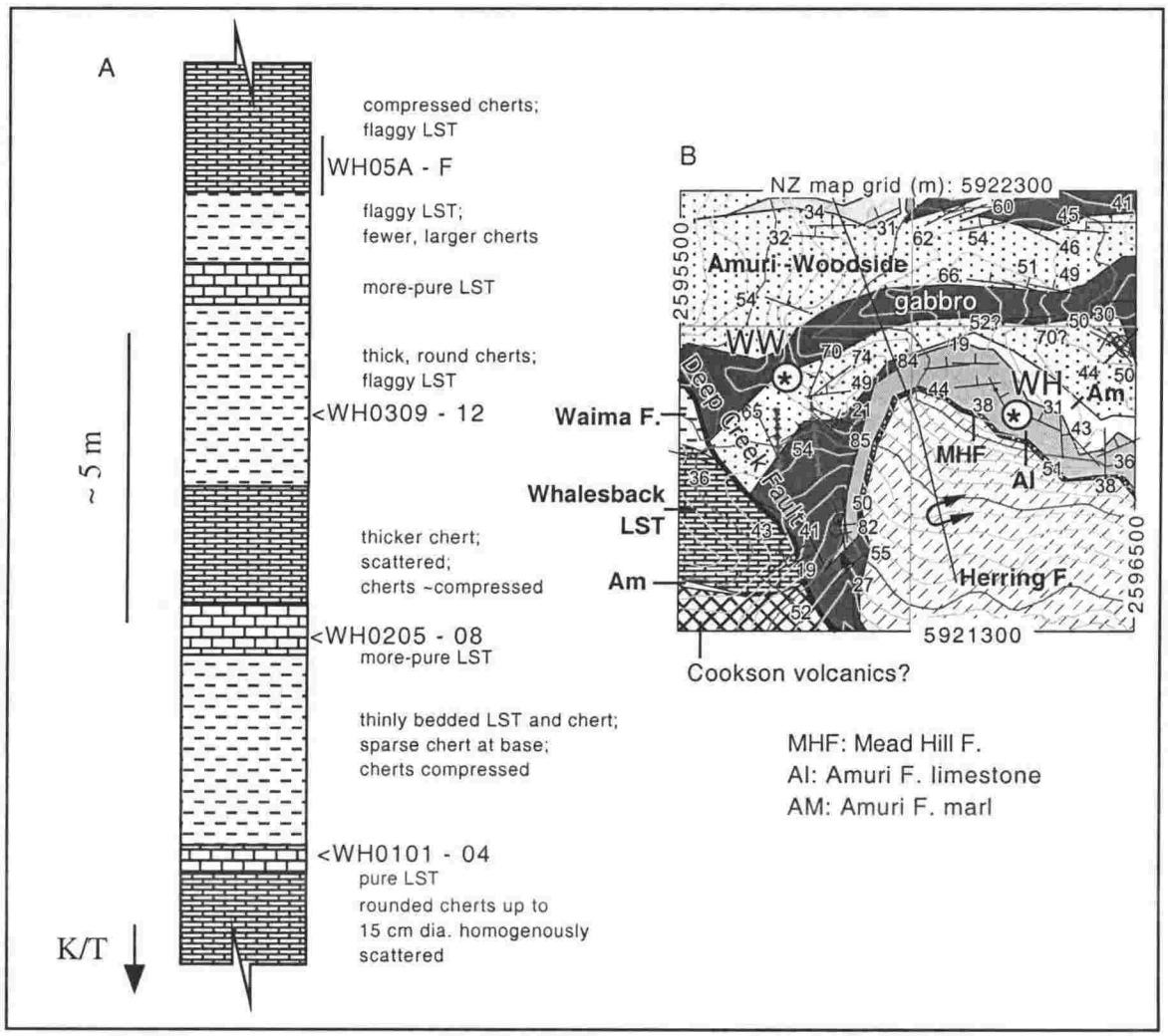

Figure 2.10.1. Stratigraphic section (A) and location (B) of the Waima Hills Amuri Formation limestone locality (WH) and location of the Waima Hills Woodside member locality (WW). This stratigraphic sequence is the lateral equivalent of strata exposed at Woodside Creek, which include the Cretaceous - Tertiary boundary and which were sampled by Vickery [1994] (WC1) and also this study (WC3).

at Grid Ref. 95682186 (NZMS P30). Although these sites are geographically close to each other, they contain different rocks and therefore are treated as two separate locations in the following description.

i) Waima Hills Amuri limestone (WH)

This locality lies within a ~30m-thick member of pink Amuri Formation limestone that crops out between Late Cretaceous Herring Formation shale, stratigraphically below and Eocene turbidites, stratigraphically above, that belong to the Woodside Member of the Amuri Formation. The sampled ~8m of exposure (Fig. 2.10.1A) is transected by meso-scale faults; however, strata can be traced with confidence across these minor structures that have << 1m offset.

Thermal demagnetisation of the pink limestone from all sites proved this lithology to be extremely magnetically stable. Most samples from the Waima Hills had NRM intensities of between 0.3 and 0.6 mAm^{-1}. Complete thermal demagnetisation at 640°C suggests that maghemite is the magnetic remanence carrier (Ozdemir, 1990), which is consistent with saturation of IRM at 300 mT (Fig. 2.10.2A). The IRM acquisition curve has a similar double step as the WC sample (above), with a shoulder at ~100 mT and saturation at ~300 mT. This double step is consistent with the presence of two populations of magnetic grains, although with the present data, it is difficult to unambiguously identify both populations.

All of the pink limestone cores from the Waima Hills location that were subjected to AF demagnetisation (up to 50 mT) initially dropped in intensity, but did not demagnetise sufficiently to isolate a primary component (e.g. Fig. 2.10.2B). Temperature-dependent susceptibility data from the pink limestone (Fig. 2.10.3) have a peak at ~550°C, which suggests that the sample has undergone thermal alteration which makes it difficult to identify a reliable Curie temperature for primary magnetic minerals. On the basis of the above evidence, it seems that the principal magnetic mineral in the pink limestone is oxidised magnetite (maghemite).

Inferred primary declination and inclination values from each sample are plotted in both *in situ* and structurally corrected coordinates on Figure 2.10.4A & B. While these data are fairly scattered (α_{95} = 11.2°), both normal and reverse polarity vectors, which are approximately antipodal, were obtained. The site mean direction of both normal and reverse polarity data is 093.6°, -59.9°. The declination and inclination of the reference direction at this site is 356.3°, -69.7° (see Table 2.1), thus a clockwise rotation of 97° is inferred for these Early Tertiary rocks.

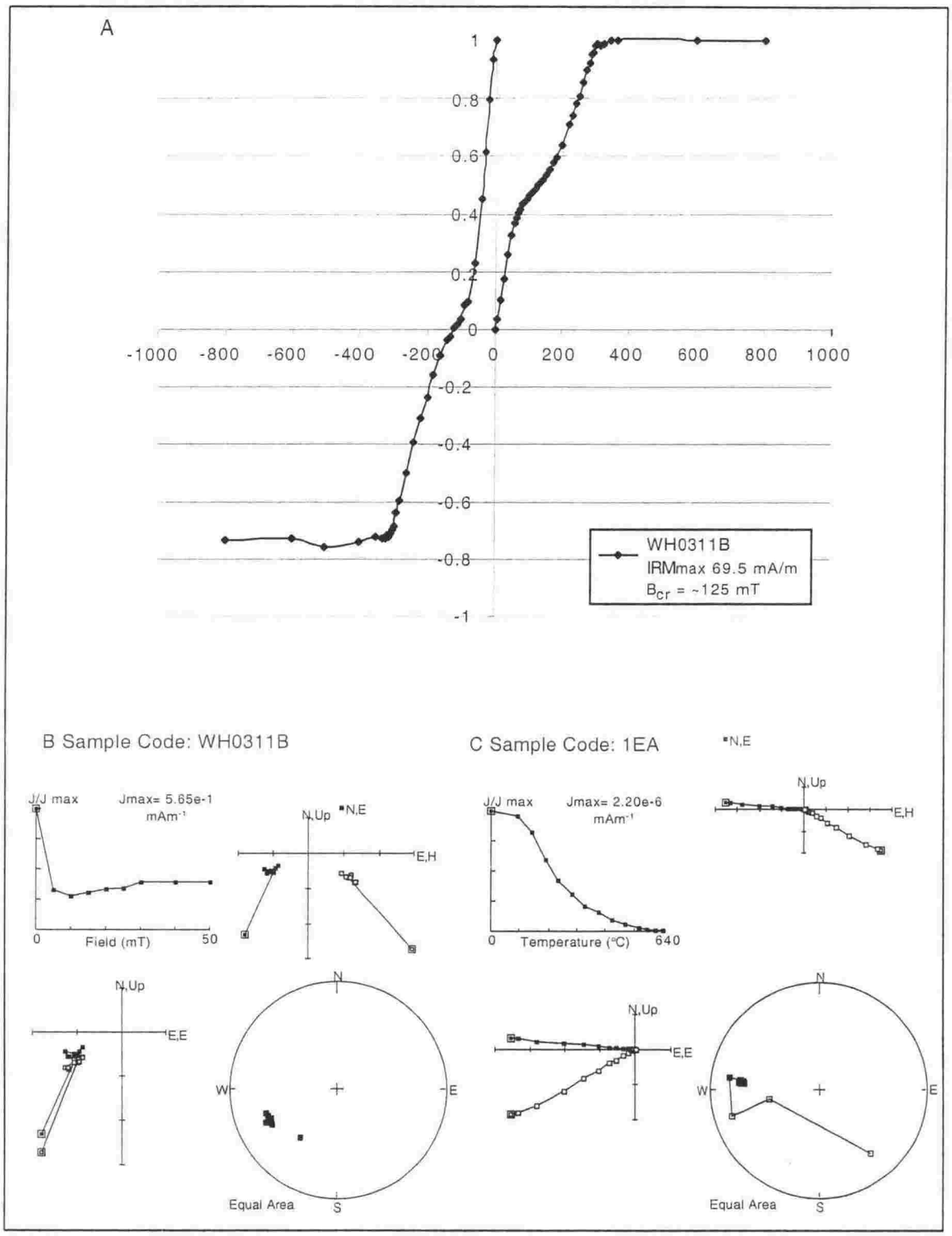

Figure 2.10.2. A: IRM acquisition data for pink Amuri Formation limestone (sample WH0311B) indicates the presence of maghemite [Ozdemir, 1990] and saturation of IRM suggests absence of haematite; B & C: typical AF and thermal demagnetisation of NRM of the pink limestone. AF demagnetisation failed to isolate a primary component, as is trypical of a high coercivity mineral such as haematite, but thermal demagnetisation was more successful. All plots are *in situ* coordinates. For B & C: symbols are the same as for Figure 2.8.2.

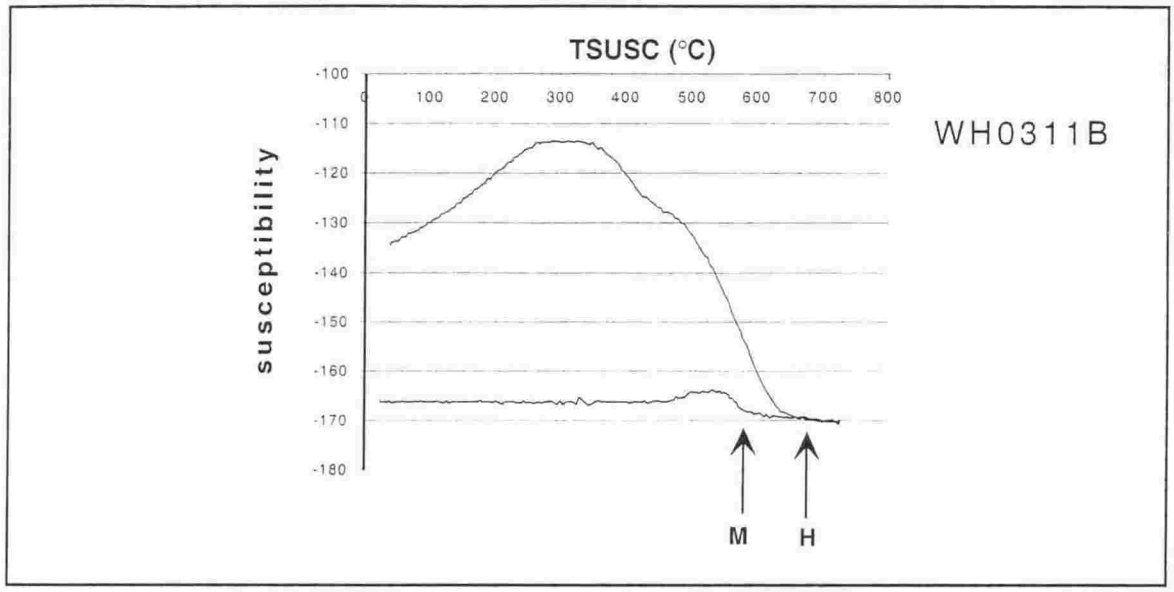

Figure 2.10.3. Temperature dependent susceptibility of pink Amuri Formation limestone sample WH0311B. Arrows on the plot mark the Curie temperature of magnetite (M; 580°C) and haematite (H; 680°C). The peak at ~500°C probably represents thermal alteration of the sample, rendering the higher temperature data for this sample ambiguous.

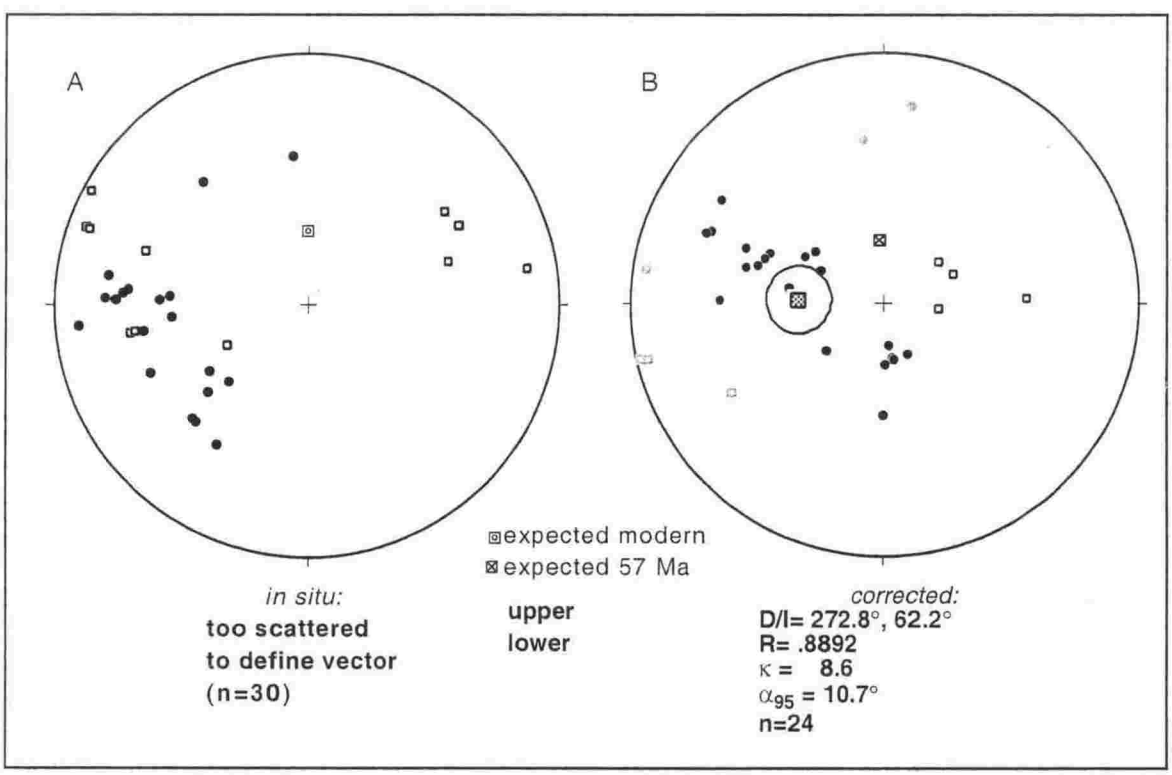

Figure 2.10.4. Primary components from the Waima Hills pink Amuri Formation limestone (WH); a: *in situ* components and b: structurally corrected. The structural correction at this locality is uniform for the fold plunge (e. g., Fig. 2.6a) but subsequent bedding tilt differs for each site. The reference declination and inclination for 57 Ma old rocks here is 356, -69°, thus 96.5° of clockwise rotation is inferred. Six specimens (shown in grey) were discarded for the final calculation, on the basis of having too shallow an inclination, or probably being a "modern" overprint.

ii) Waima Hills -Woodside Formation and gabbro sill (WW)

This section traverses a baked contact between turbidites and gabbro of the Woodside Member of the Amuri Formation, which lies ~270m stratigraphically above the WH locality (Fig. 2.11.1). The base of the sampled section is ~6m from the igneous unit and consists of fine-grained mudstone. Unfortunately, on drying, these cores became fractured and only one survived the trip to Canberra to be measured. Thermal demagnetisation removed an unstable, low temperature component to ~260°C that has a modern field direction (353°, -66°). The underlying component showed progressive demagnetisation to the origin (within error) and is interpreted as a primary component (Fig. 2.11.2). This single core has a normal-polarity *in situ* vector of 112.8°, -37.0°, which, after structural correction, becomes 121°, -64°.

Further up section, closer to the gabbro, sandstone and siltstone cores were more robust. The magnetisation of these samples decreased in a series of three steps during demagnetisation, suggesting the possibility of three components. The lowest-blocking component was removed by 180°C and is close to the modern field direction (Fig. 2.11.3). Two almost parallel components, from 300 to 350°C and 500 to 560°C, both have normal polarities and may indicate the demagnetisation of two separate magnetic mineral populations. Cores from horizons 02 – 04 have a grouped mean *in situ* direction of 050.4°, -32.3°. When a structural correction is applied, this vector becomes 039°, -75° (Fig. 2.11.1c). The data are tightly clustered and, due to their proximity to the gabbro body, which possibly cooled rapidly, probably do not fully account for secular variation.

Samples from altered sandstone at the meta-contact resist demagnetisation until the 560°C step, where a drastic decrease in magnetisation takes place (Fig. 2.11.4). The NRM of these samples is around 1 mAm^{-1}. These samples from the baked contact do not have a modern overprint, but the primary component is parallel to the two high temperature components of the sandstone samples (Fig. 2.11.3). The inferred mean *in situ* direction of site WW05 is 058.4°, -36.4°. Applying the same structural correction as above, this becomes 016.1°, -83.7°.

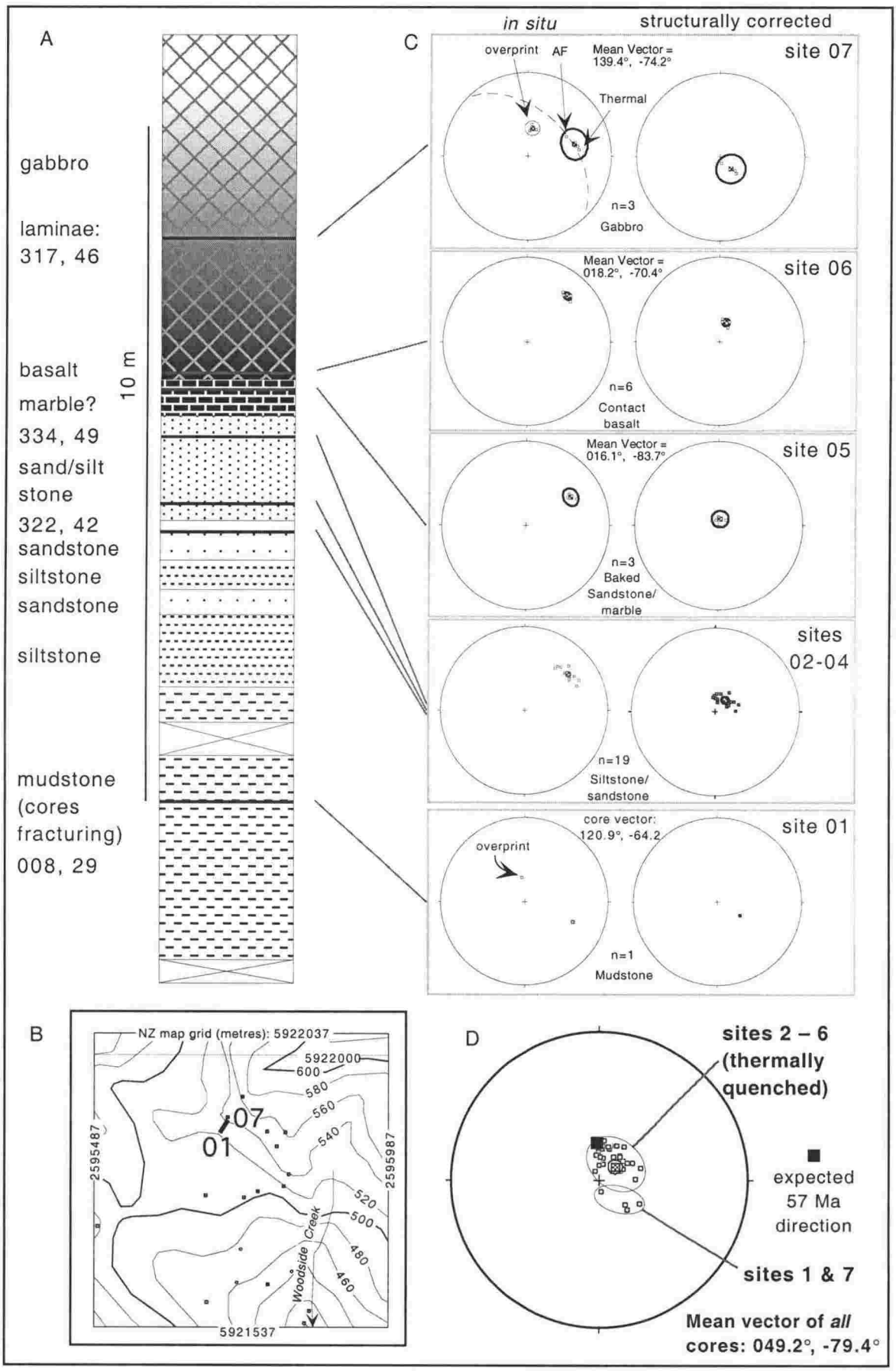

Figure 2.11.1. A: Stratigraphy of the Woodside member of the Amuri Formation at the Waima Hills palaeomagnetic locality, B: location of site, C: core magnetisation vectors in both *in situ* and structurally corrected coordinates and, D: summary of WW site data. See text for discussion.

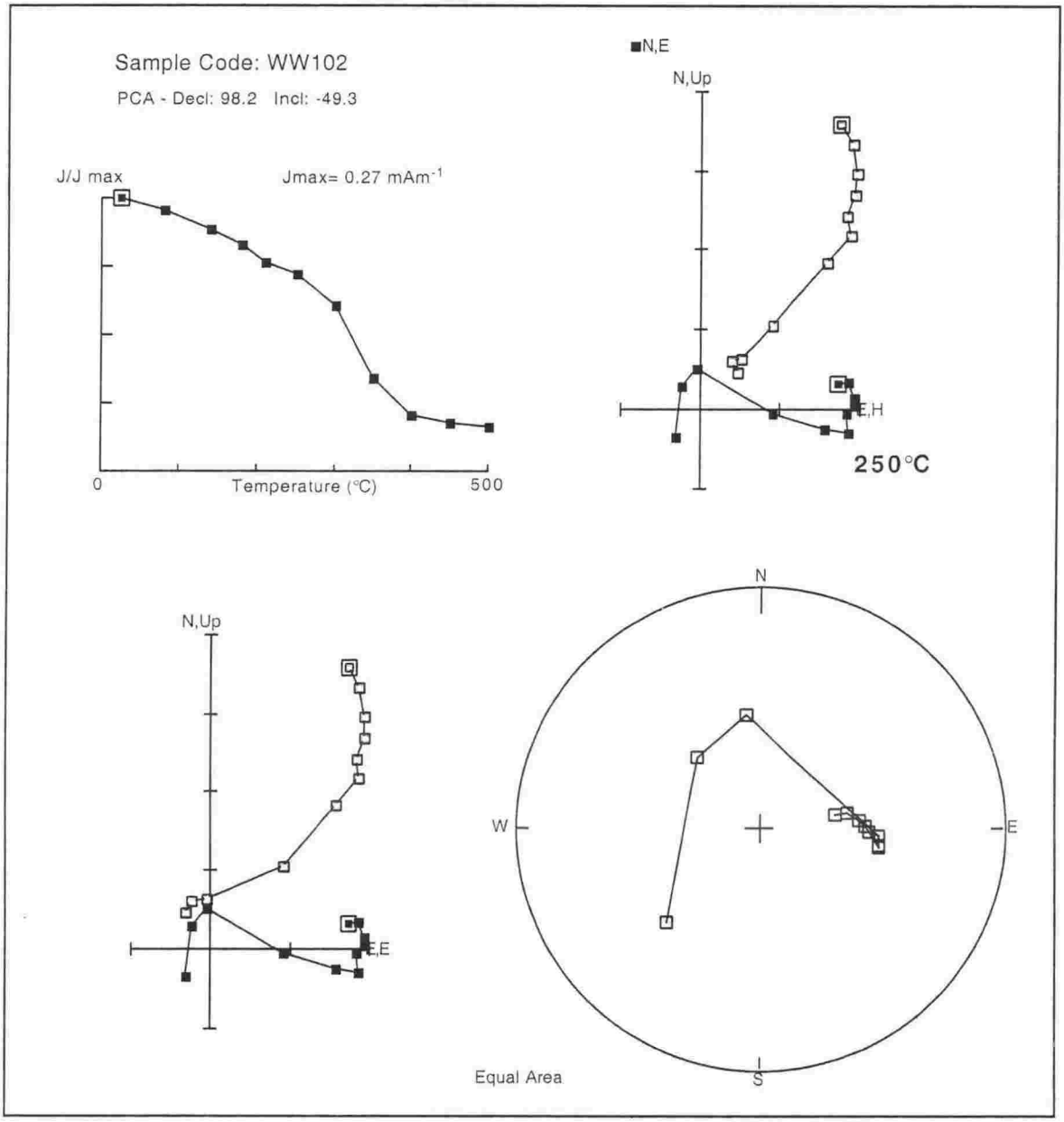

Figure 2.11.2. Demagnetisation of the sole surviving mudstone core furthest away from the gabbroic "intrusion". Thermal cleaning of a modern overprint (up to 250°C) reveals the underlying component inferred to be primary and detrital. All plots are *in situ* coordinates. Conventions are as for Figure 2.8.2.

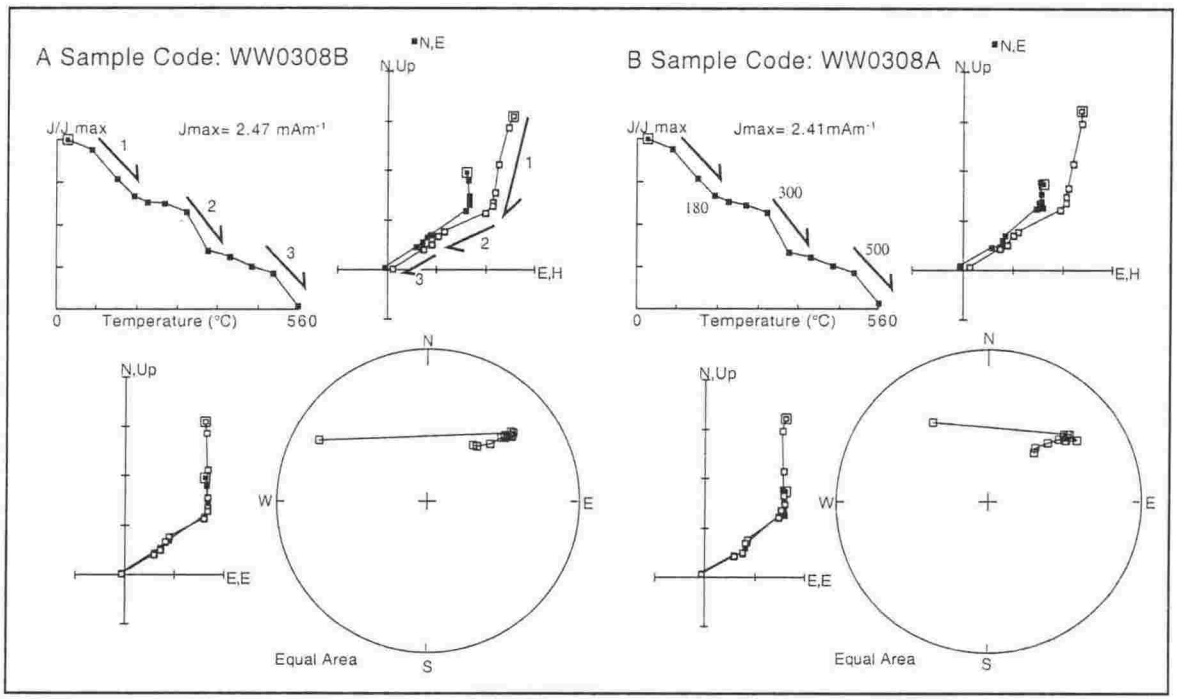

Figure 2.11.3 A & B. Typical demagnetisation data for sandstone samples of Woodside Formation from the Waima Hills (WW) location (sites 02-04 on Figure 2.11.1). Three possible components are seen: 1, the "modern" overprint that cleans off prior to 180°C; 2: an intermediate component that is dominant between 300 and 350°C and; 3: a high temperature component that appears to be parallel to the intermediate component between 500 and 560°C. All plots are *in situ* coordinates. Conventions are the same for Figure 2.8.2.

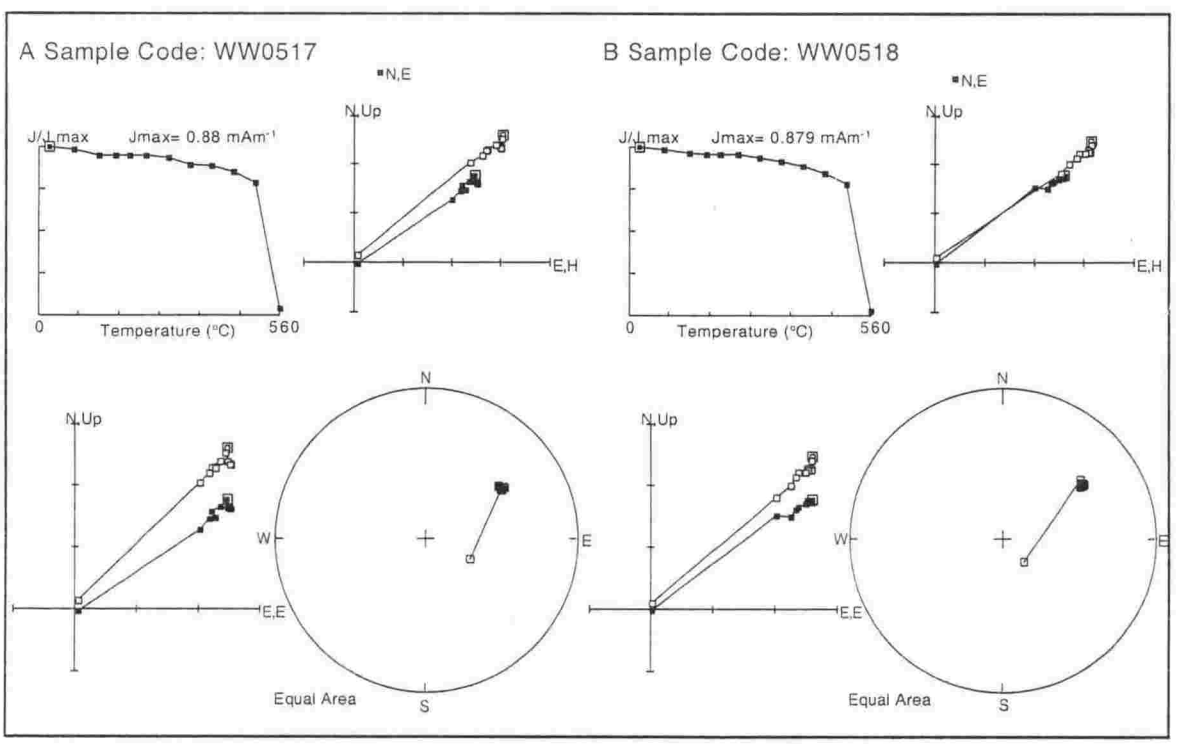

Figure 2.11.4 A & B. Typical demagnetisation plots of contact-metamorphosed sandstone from the edge of the gabbro intrusion (site 05 on Figure 2.11.1). Samples resist demagnetisation until the 560°C step, where all intensity is lost. Only a single component of magnetisation is apparent from these data. All plots are *in situ* coordinates. Conventions are the same as for Figure 2.8.2.

Basalt samples from the chilled margin of the igneous body had NRM values of 10 - 20 mAm^{-1}. Three antiparallel components were noted during both thermal and AF demagnetisation. The low blocking temperature/coercivity component was removed during the first demagnetisation step and is only constrained by two points (Fig. 2.11.5A & B). An overlying, intermediate component has a direction that is almost antiparallel with the low-blocking component and is dominant between 5 and 10 mT or 80 and 250°C. The third component was cleaned off by 350°C and is almost parallel with the low-blocking component (Fig. 2.11.5). IRM acquisition (Fig. 2.11.6A) reveals saturation of the basalt at ~70 mT, suggesting that the remanence carrier is a low coercivity phase. Temperature dependent susceptibility experiments (Fig. 2.11.6B) indicate sample WW06 underwent thermal alteration, making the primary mineral assemblage difficult to determine.

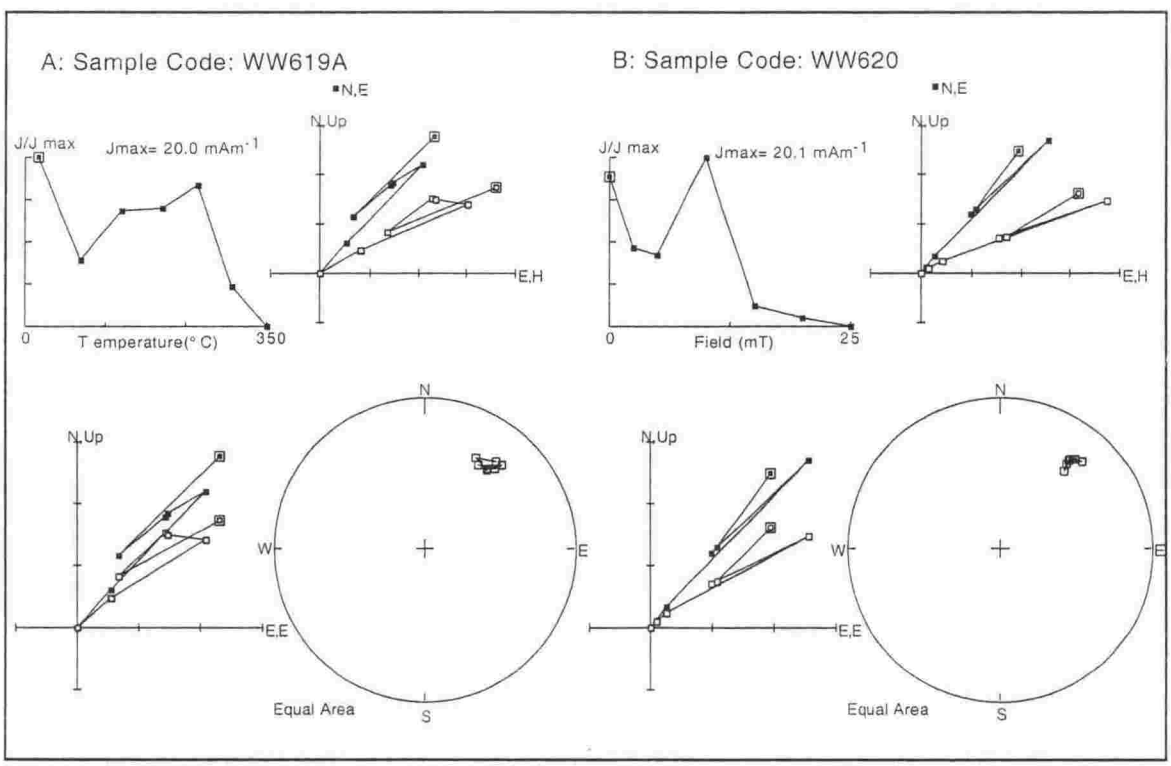

Figure 2.11.5. Chilled margin basalt demagnetised with thermal (A) and AF (B) techniques (site 06 on Figure 2.11.1). Samples reveal three anti-parallel components that constructively or destructively add to the NRM intensity. All plots are *in situ* coordinates. Conventions are as in Figure 2.8.2.

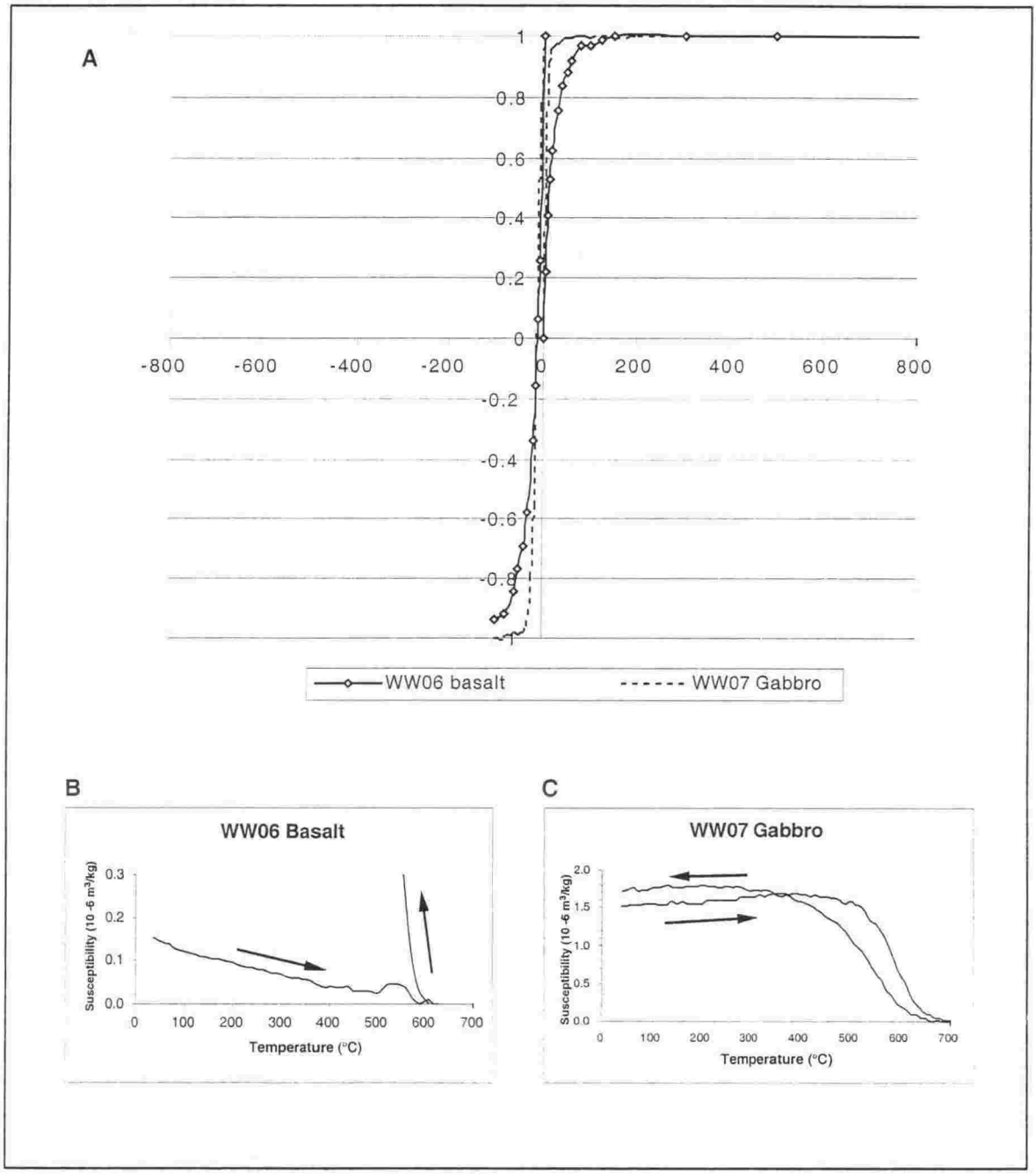

Figure 2.11.6. Magnetic properties of basalt samples from the chilled margin and gabbro from several meters into the igneous body at locality WW; A: IRM acquisition data for both rock types indicate that the more crystalline gabbro is "magnetically soft" and magnetisation is easily re-set to the applied field, while the chemically identical basalt, with its smaller grains, is harder; B & C: temperature dependent susceptibility experiments for both lithologies reveal thermal alteration of the basalt at ~550°C, while the gabbro data are consistent with the presence of maghemite [Ozdemir, 1990].

The *in situ* site mean direction of the high-temperature component is 041.6°, -27.8° for these samples and is tightly clustered (α_{95} = 3.6°). Due to the geologically instantaneous cooling of basalt, this direction cannot allow for secular variation. The structurally corrected direction (using the adjacent sandstone bedding attitude of 334°, 49° NE) is 018.2°, -70.4° (Fig. 2.11.1).

Gabbro samples from within the sill had NRM intensities of ~180 mAm^{-1}, approximately 10 times stronger than the basalt at the margins. Both thermal and AF demagnetisation removed a low temperature/coercivity component up to 300°C, or 15 mT, that is parallel to the modern field (009.6°, –62°; n = 3). A stable, underlying component demagnetises toward the origin from 350°C to be almost completely removed by 500°C (Fig. 2.11.7A & B). The greater NRM in the gabbro is partly explained by the three competing components in the basalt that are not observed in the gabbro. IRM acquisition shows the gabbro to be magnetically "soft", with a sharply

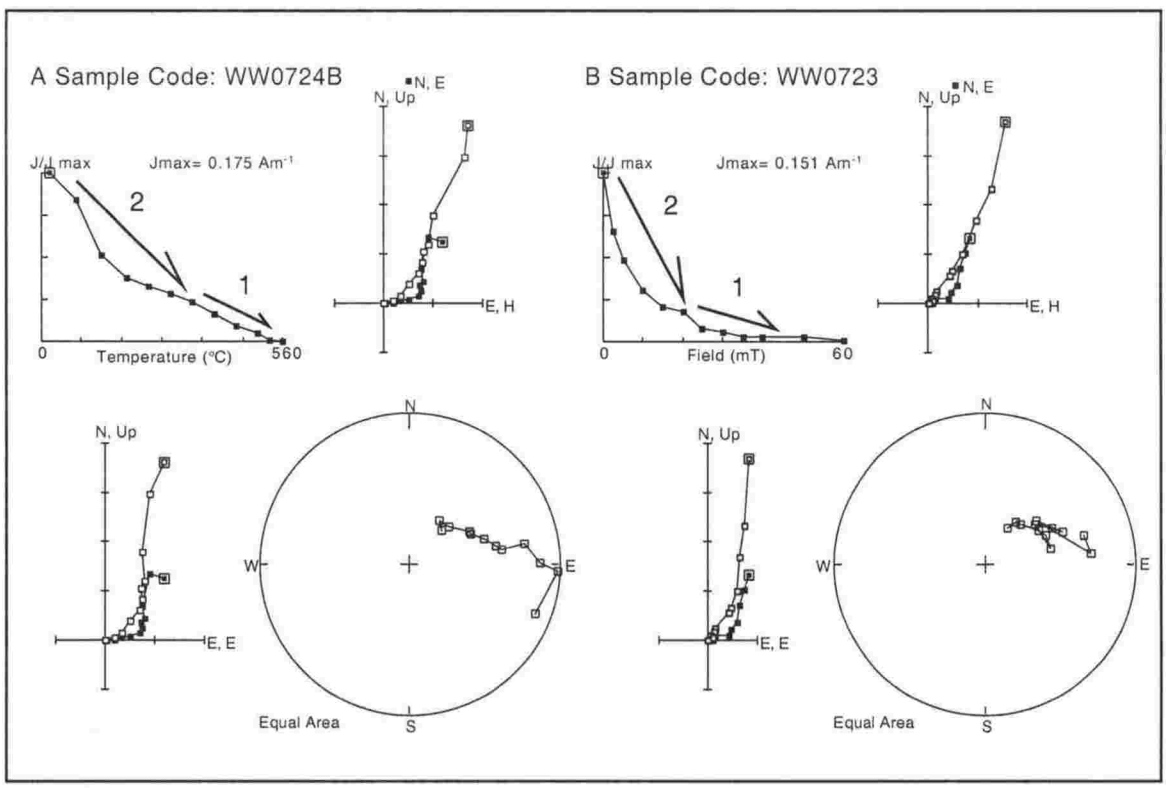

Figure 2.11.7. Representative thermal (A) and AF (B) demagnetisation plots of WW gabbro, from several metres into the igneous body. Two components are noted, the lower-blocking one (2, above) is parallel to a modern field direction and the higher coercivity component (1, above) is interpreted as a primary thermal remanent magnetisation. All plots are *in situ* coordinates. Conventions are as in Figure 2.8.2.

defined saturation point at ~20 mT (Fig. 2.11.6A). This is not surprising given the larger grain size which probably includes multi-domain grains that are easily reset to the applied field. Temperature dependent susceptibility experiments for site WW07 reveal a Curie point near 640°C, indicating the presence of maghemite (Fig. 2.11.6C). The 350 – 500°C component is interpreted as a primary thermo-remanent magnetisation and has a mean *in situ* direction of 075.6°, -41.3°. A faint lamination in the gabbro is observed to be approximately parallel to nearby bedding in the sedimentary rocks and is used for the local "bedding" correction at this horizon. The structurally corrected mean direction of the gabbro samples is 139.4°, -74.2°.

The site mean directions are summarised on Figure 2.11.1D. The high temperature/ coercivity components of sites 2 – 6 are similar in direction and have been grouped. These give a primary (thermal) direction from the baked zone of 039°, -75°. This direction probably does not average secular variation. Because the directions of inferred primary remanence from the lowermost (mudstone) and the uppermost (gabbro) horizon are similar in declination and inclination, it is interpreted here that the igneous "intrusion" occurred soon after deposition of the sedimentary rocks and that both lithologies acquired their magnetisation directions in the same geomagnetic field. The overall structurally corrected locality mean of 049, -79° is heavily biased by sampling of the baked sites, which shows a smaller declination anomaly than the other sites, possibly due to a westward excursion of secular variation at the time of quenching. Thus, the statistical mean vector is likely to underestimate the actual declination anomaly, which may be better approximated half way between the minimum and maximum declinations observed, i.e., slightly more than 090°. Consequently, a tentative clockwise rotation of 095° is assigned to this location, which compares well with 097° of clockwise vertical-axis rotation inferred from the nearby WH locality in Amuri Formation limestone (above).

Narrows syncline (NS1)

The Narrows syncline (Fig. 2.5) is a WNW–ESE -trending fold with a sub-horizontal hinge that is thought to have formed in response to reactivation of the Flags Creek Fault (FCF) as a SW-verging thrust fault in the Late Miocene [Chapter 3]. Palaeomagnetic samples were taken from three locations with different bedding attitudes within the trough-like syncline in order to perform a fold test (Fig. 2.12). Localities NS2 and WR were weakly magnetised and did not yield stable magnetisation directions (see Appendix 2.4).

Samples from locality NS1, however, were more strongly magnetised, but yielded magnetisation directions that are not straightforward to interpret. Locality NS1 traverses Waterfall Stream (unofficial name), that crosses Blue Mountain Road approximately 8 km inland (Fig. 2.12). This site lies on the SW limb of the Narrows syncline, where strata dip moderately to the NE. Erosion resistant Early Miocene Whalesback limestone is exposed at the base of the section. The gradational, ~15m-thick interbedded contact zone into overlying softer Waima siltstone, downstream, forms the waterfall. The stratigraphic range sampled at this locality is approximately 90 m, with 68 cores taken from both above and below the road (Fig. 2.12). The base of the Whalesback limestone (not exposed in this section) is Earliest Miocene in age [Reay, 1993]. Thin beds of Otaian – Altonian [Prebble, 1976] GMC crop out ~30m above the top of the sampled section, therefore the age of these rocks is inferred to be late Otaian – earliest Altonian (18 – 23 Ma).

Demagnetisation of almost all samples from NS1 sites yielded shallow mean directions compared with the GAD field inclination, that cannot be steepened by structural correction (Appendix 2.5). Two possibilities arise as to why this locality exhibits shallow directions: 1) it is possible that the shallow directions are not characteristic magnetisation directions, but an overprint resulting from the complex sequence of tectonic events that have affected this region [see Chapter 3]; 2) the shallow inclinations of magnetisation directions expressed at NS1 are genuine detrital magnetisation directions formed in a shallow GAD field (e.g., during a polarity transition or geomagnetic excursion). Two sites from NS1 (N01 & N05) are from either end of a shallow sequence and have nearly antipodal mean directions with inclinations approximately parallel to the Miocene reference inclination (Appendix 2.5). These two

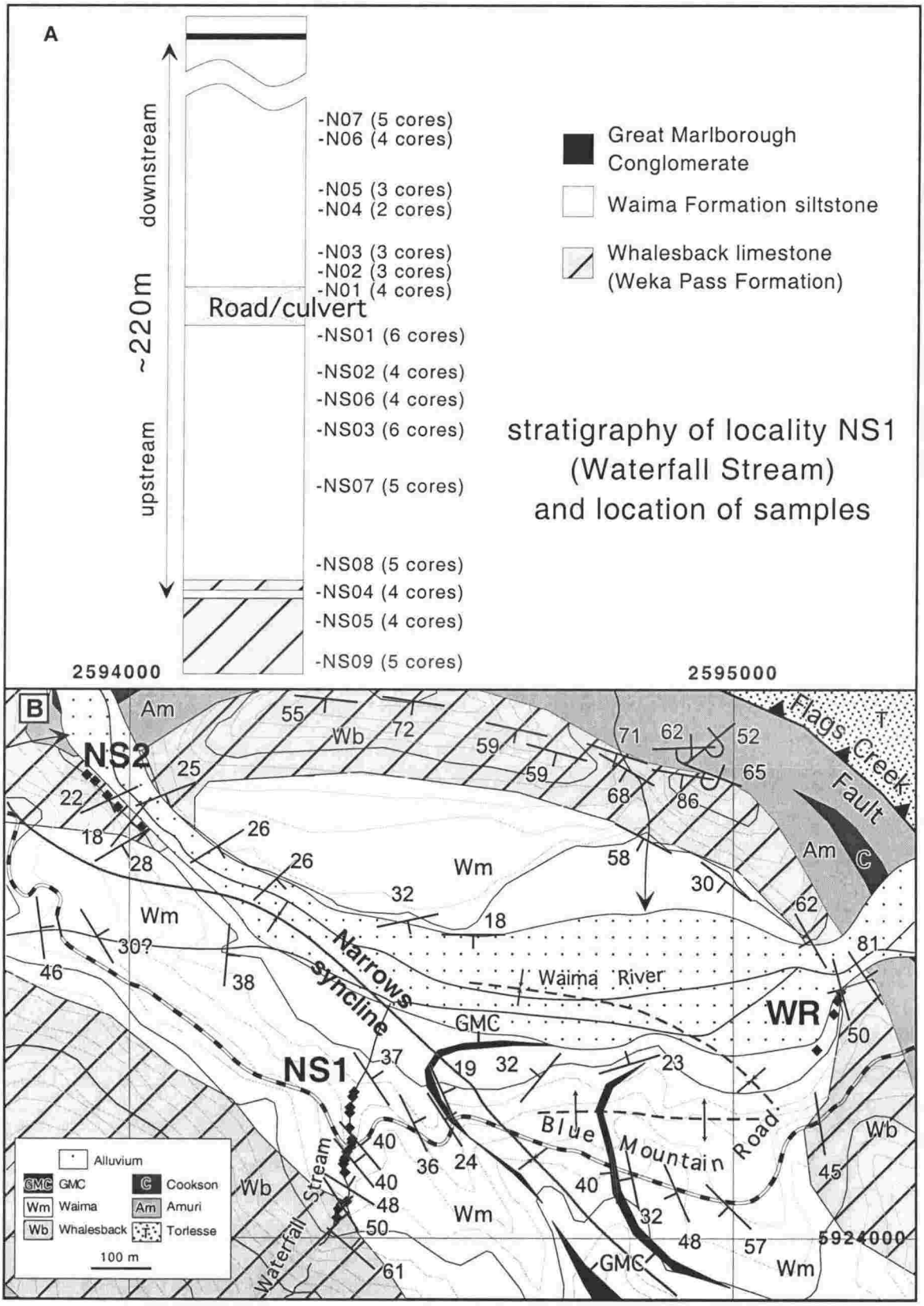

Figure 2.12. A: Stratigraphy of locality NS1 (Waterfall Stream), both above and below Blue Mountain Road. Basal samples are from Whalesback limestone but the majority are from Waima Formation siltstone. A thin bed of Great Marlborough Conglomerate (GMC) projects to near the top of the section; B: relative positions of the three sample locations from the Narrows syncline. Sites WR and NS2 produced only shallow or unstable results. See Fig. 2.5 for location of map and text for discussion.

sites have a structurally corrected mean direction of 303°, -56.6°. The samples between these sites (N02, N03, N04) display a tracking in their direction from reverse to normal polarity, indicating a transitional period during a magnetic field reversal (see Appendix 2.5). This gives a more sound reason to reject the shallow directions but to keep the steep ones and interpret a tentative vertical axis tectonic rotation from these data. If these two sites are representative of the GAD declination during deposition of the Waima Formation, then 123° of clockwise rotation since the Middle Miocene is implied. This direction probably does not average secular variation, as it is obtained from only two sites.

Blue Mountain Stream locality (BM)

Near the confluence of Blue Mountain Stream and Waima River (Fig. 2.5), submarine volcanic rocks are exposed, including a section of pillow basalt with interstitial, reticulate pink limestone (Fig. 2.13; Appendix 2.3). This limestone is inferred to be part of the Early Eocene "lower limestone" member of the Amuri Formation [Strong et al., 1995], the pink colour arising from precipitation of volcanogenic haematite and sulphides. Both submarine and terrestrial volcanic rocks are well documented in Marlborough [Reay, 1993]. In the Clarence Valley, they occur as the Eocene "Grasseed" and early Miocene "Cookson" volcanics, which are sequences of pillow basalts and basalt flows interdigitated with localised basaltic conglomerate and occasional gabbroic sills, variably in stratigraphic contact with the Amuri Formation. A fossilised shark tooth found at the local contact between limestone and basalt pillows at the Blue Mountain Stream locality confirms the eruption of this basalt into a marine environment. The formation of pillow structures suggests flow onto wet (pre-lithified) sediment, thus, the volcanic rocks at Blue Mountain Stream are interpreted as being contemporaneous with the Amuri Formation limestone and belonging to the Eocene-aged Grasseed volcanic group [Reay, 1993]. Remnant rafts of limestone "bedding" within areas of basalt flows dip steeply to the SE, similar in orientation to the strike of beds elsewhere on the western limb of the Ben More anticline; however, their dip to the SE is anomalous. The anomalous dip of bedding at this site is interpreted as a result of tilting on the NW limb of the Narrows syncline (Fig. 2.5), which was folded about a sub-horizontal hinge [Chapter 3]. Toward the eastern end of the outcrop, the basalt has a pyroclastic texture defined by a weak fabric of poorly fused lapilli, breaking into tabular

strata. This fabric, which dips to the NW, may be cooling-related and may not have formed horizontally (e.g. columnar– type jointing).

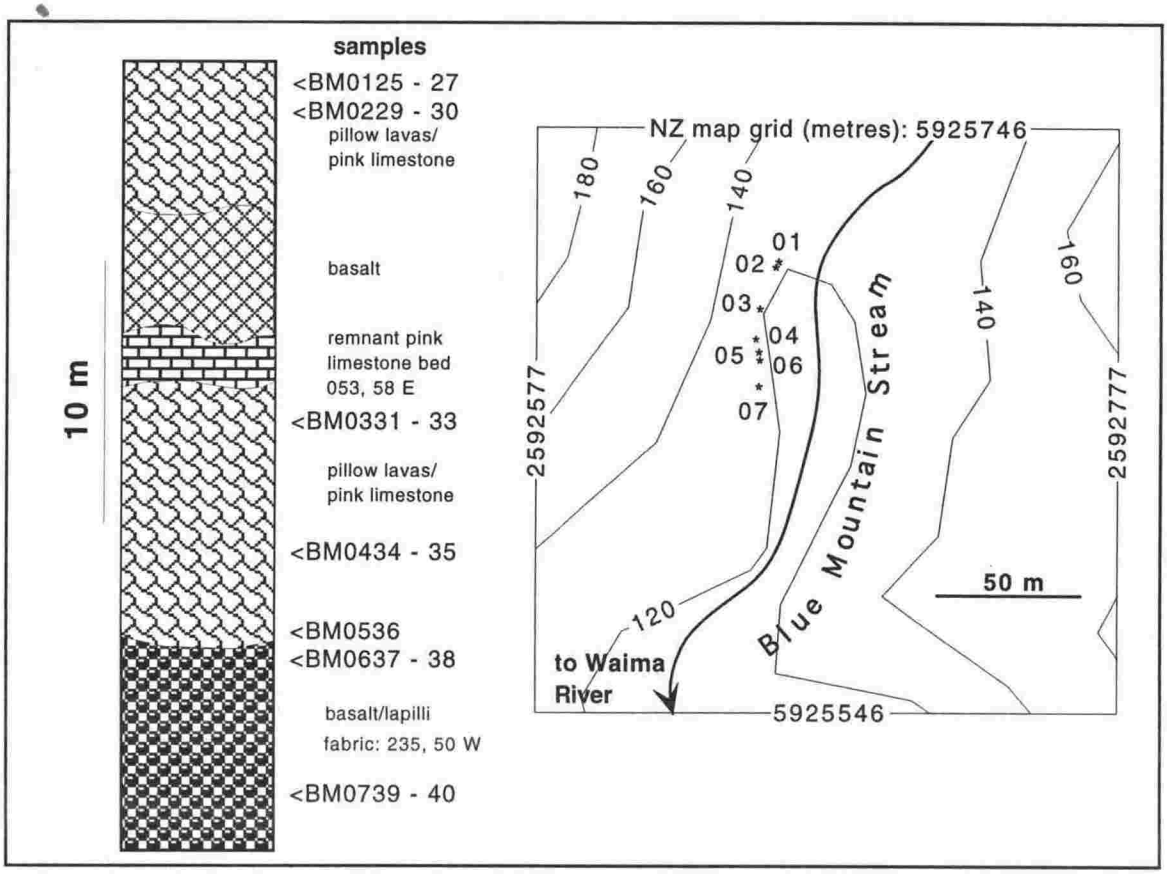

Figure 2.13. Stratigraphy and setting of locality BM (Blue Mountain Stream). A: Representative column showing sequence of limestone and pillow basalt with location of cores; B: location diagram.

Samples from the limestone exhibited two to three components of magnetisation, both of which have apparently random orientations (Appendix 2.3). Basalt samples from stratigraphically above the limestone at Blue Mountain Stream, however, have a single component of magnetisation. The mean *in situ* direction of these basalt samples (~131°, -11°) is well-grouped (k=370.6; α_{95} = 3.2°; n = 6) as would be expected for thermally "quenched" rocks that do not average out secular variation (Appendix 2.3). Structural correction using the remnant bedding attitude restores this direction to 097.5°, -66.1°. The mean expected declination for 57 Ma rocks at this site is 356° (Table 2.1), therefore, a clockwise rotation of the Eocene volcanic rocks at Blue Mountain Stream of 102° (not accounting for secular variation, which could be ± 40°) is implied. The magnetic directions from all new localities are summarised on Table 2.3.

This study	*In situ* D/I (°)	Corrected D/I (°)	REF I (°)	α_{95} (°)	N	κ	Anomaly (+/–)	Age (Ma)	Modern component removed	Ref
BM basalt	131/-11	096/-66	69	3.2	6	370.6	100±?	50±5	-	
NS1 01 & 02	272/27	302/54	65	7.4	8	49.5	122±?	22±2	?	
WW		102/-78	69	3.4	31	18.2	105±?	50±5	Yes	
WH		273/62	69	10.7	24	8.6	97±23	60±5	-	
WC3	052/-34	113/-72	69	6.7	9	53.1	117±21	60±5	Yes	
BH	033/-76	149/-66	69	2.3	9	460.8	153±10	60±5	-	
Previous studies										
WC1	235/45	310/66	65	3.2	30	67	138±6	59±5		4
WC2	330/76	318/57	65	8	4	133	146±11	59±5		4
BB2-2	309/0	315/55	65	12	22	8	135±17	30±5		4
SS1-2	118/54	122/-44	65	11	8	37	122±12	20±4		4
DS		279/59	65	6.4	46		99±10	18±1		2
HC2	147/21	121/-69	65	17	26	26	121±55	17±1		4
HC3	118/-10	106/-70	65	6.4	7	90	106±15	17±1		4
BS		200/63	63	7.4	14		17±13	8±1		3
CC		024/-61	63	5.4	12		24±9	8±1		1
WV		200/61	63	2.4	42		20±4	8±1		3
NC		215/60	61	3.5	31		35±6	5.4±0.6		3
FC		180/59	62?	10.6	25	40.4	0±	6-7		5
BR		213/60	61	3.5	132		33±3	4.8±0.2		3
UB		201/59	61	1.8	132		21±3	4.8±0.2		3
RB		212/62	61	3.9	25		32±7	4.2±0.6		3
WD1	092/-32	349/-55	61	3.4	15	143	-11±5	4±1		4
WD2	084/-31	356/-51	61	6.3	11	53	-4±8	4±1		4
SV		236/59	61	3.1	33		44±5	3.9±0.8		3
WB		204/-67	61	3.6	29		24±7	3.9±0.8		3
CS		175-59	61	2.8	52		-5±4	3.3±0.3		3

Table 2.3. Summary of Marlborough palaeomagnetic locality mean vectors from this study and from previous work. Data are compiled from 1: Walcott et al. [1981]; 2: Mumme & Walcott [1985]; 3: Roberts [1992]; 4: Vickery & Lamb [1995]; 5: Little & Roberts [1997].

QUALITY OF PALAEOMAGNETIC DATA SITES IN EASTERN MARLBOROUGH

Van der Voo [1990] devised a quality index for palaeomagnetic poles for North America and Europe whereby 6 parameters based on reliability were assigned to each palaeopole position. This allowed a direct comparison between sites and a semi-quantitative approach to testing reconstruction parameters for closing the North Atlantic Ocean. An adaptation of the Van Der Voo [1990] quality index is proposed here to quantify the reliability of the Marlborough palaeomagnetic declination anomalies. The six criteria, after Van der Voo [1990] are:

1) Well determined site–age and presumption that the characteristic component of magnetisation is about the same age. An acceptable range of age is ± 10%, or 5 Ma, whichever is smallest.

2) Sufficient data and statistical precision. The minimum number of samples ascribed to being statistically sound by Van der Voo [1990] is 24. For the Marlborough declination anomaly data, 12 samples are considered sufficient if they cover a wide enough stratigraphic range to average secular variation. Otherwise, 50% of palaeomagnetic localities from Marlborough fail this criterion. The precision parameter, κ, must be greater than 10 and α_{95} less than 8° [modified after Van der Voo, 1990].

3) Progressive demagnetisation must be performed, with isolation and determination of the characteristic component of magnetisation.

4) Field tests. Successful/positive fold, contact or conglomerate tests make locality mean directions much more reliable.

5) Presence of antipodal normal and reverse polarity directions (magnetic reversals). This guarantees that enough time has elapsed during deposition to ensure that there is no instantaneous remagnetisation, that short-lived non-dipole effects (secular variation) have been averaged out and that there is no systematic bias, such as that caused by a small overprint on a dual-polarity characteristic direction.

6) Structural integrity. Confidence must be held in any structural corrections performed on the data before a declination anomaly can be interpreted in terms of tectonic rotation. This may include confidence in obtaining the correct orientation of fold axes, identification of bedding indicators, uncertainty in localised disturbances by intrusion, etc.

Both new and existing palaeomagnetic data have been tabulated with regard to these criteria (Table 2.4). The result of this analysis is that some of the previous palaeomagnetic localities (and some of the new ones) have been statistically undersampled (WD2, HC3, SS, WC2, BM, WC3, BH) or have larger than acceptable confidence margins (HC2, BB). However, the declination anomalies of all localities that fail on the basis of statistical criteria (Fig. 2.14, white arrows), or are of intermediate quality (Fig. 2.14, grey arrows) are not significantly different from declination anomalies at high quality localities (Fig. 2.14, black arrows). Therefore, the incorporation of low and intermediate quality localities in the overall dataset does not bias the total amount of vertical axis rotation interpreted to have occurred in NE Marlborough (compare Figs. 2.3 & 2.14), but the poor quality data do not help to constrain the spatial distribution of vertical-axis rotations.

INTERPRETATION AND DISCUSSION

Pattern of vertical axis rotations in space and time

The vertical axis rotation history of a region may be understood by comparing the magnitudes of all anomalies with their respective ages. Vickery & Lamb [1995] identified three groups of rocks in NE Marlborough which have distinct spatial and temporal palaeomagnetic histories. New palaeomagnetic data from this study generally corroborate their interpretation and the three groups defined by Vickery & Lamb [1995] are retained. In the following discussion, the term "domain" is used in reference to vertical-axis rotations that are distinguished on a spatial basis, while the term "group" is used to compare rotations that occurred at different times. From a plot of declination anomaly versus site age of "accepted" palaeomagnetic data from Marlborough (Fig. 2.15), the three groups of differing rotation history are evident. The older group of rotation can be further divided into two subgroups that are distinguished both spatially and temporally:

- **Group 1a) rotations**

All rocks that are 17 ± 1 Ma or older are affected by clockwise vertical axis rotations of at least 100°, regardless of location within the study area. Implications are that a NE-trending, coherent crustal block that is at least 50 km long and >20 km wide

		corrected D/I	Age well determined (±5 Ma/10%)		Statistics (n>24; k>10; α95<16°)			reliability		Demagnet-isation?	Field tests (fold, contact, cgl)	Reversals present	Structural integrity	Quality index
			1	Age	2	K	A95	Theta 95	N	3	4	5	6	Q
Locality	**Abbrev.**			(Ma)				(=140/rt k)						
Fuchsia Creek[1]	FC	180/59	1	5.5±0.5	1	40.4	10.6	22.0	25	1	-	1*	1	5
Camp Stream[2]	CS	175/59	1	3.3±0.3	1	50.8	2.8	19.6	52	1	-	?	1	4
Washdyke Stream[3]	WD1	349/-55	1	4±1	-	143.0	3.4	11.7	15	1	?	-	1	3
Washdyke Stream[3]	WD2	356/-51	1	4±1	-	53.0	6.3	19.2	11	1	?	-	1	3
Boundary Stream[2]	BS	200/63	1	8±1	-	29.6	7.4	25.7	14	1	-	?	1	3
Waihopai Valley[2]	WV	200/61	1	8±1	1	84.6	2.4	15.2	42	1	-	1*	1	5
White Bluffs[2]	WB	204/67	1	3.9±0.8	1	58.1	3.6	18.4	29	1	-	1*	1	5
Upton Brook[2]	UB	201/59	1	4.8±0.2	1	48.2	1.8	20.2	132	1	-	1	1	5
Richmond Brook[2]	RB	212/62	1	4.2±0.6	1	56.5	3.9	18.6	25	1	-	1*	1	5
Blind River[2]	BR	213/60	1	4.8±0.2	1	37.5	2	22.9	132	1	-	1	1	5
Sea View[2]	SV	236/59	1	3.9±0.8	1	67.1	3.1	17.1	33	1	-	1*	1	5
Cape Campbell[4]	CC	024/-61	1	8±1	-	56.2	5.4	18.7	51	-	-	?	1	3
Needle's Creek[2]	NC	215/60	1	5.4±0.6	1	61.1	3.5	17.9	31	1	-	1*	1	5
Deadman Stream[5]	DS	279/59	1	18±1	1	10.5	6.4	43.2	46	-	-	1*	1	4
Heaver's Creek[3]	HC2	106/-70	1	17±1	-	26.0	17	27.5	26	1	-	?	1?	3
Heaver's Creek[3]	HC3	249/72	1	17±1	-	90.0	6.4	14.8	7	1	-	?	1?	3
Silver Springs[3]	SS	079/-44	1	20±4	-	37.0	11	23.0	8	1	-	?	1	3
Boo Boo Stream[3]	BBS	315/55	1	30±5	-	8.0	12	49.5	22	1	-	1*	1	4
Woodside Creek[3]	WC1	308/66	1	59±5	1	67.0	3.2	17.1	30	1	-	1*	1	5
Woodside Creek[3]	WC2	316/57	1	59±5	-	133.0	8	12.1	4	1	-	1*	?	3
Data are compiled from: 1. Little&Roberts [1997]; 2. Roberts [1992]; 3. Vickery and Lamb [1995]; 4. Walcott et al. [1981];														
5. Mumme and Walcott [1985]; 6. This study (see Table 2.2, 2.3 and Figures 2.4 and 2.7).														
This study:												* reverse only		accepted
Black Hill	BH	149/-66	1	60 ± 5	-	460.8	2.3	6.5	9	1	-	1*	?	3?
Woodside Creek	WC3	113/-72	1	60 ± 5	1	53.1	6.7	19.2	9	1	-	-	1	4
Waima Hills	WH	274/60	1	60 ± 5	1	7.7	11.2	50.5	25	1	-	1	1	5
Waima Woodside	WW	105/-78?	1	50 ± 3	1	59.4	3.4	18.2	31	1	1?	-	1	5?
Narrows 1	NS1	303/48	1	25 ± 5	-	49.5	7.4	19.9	9	1	-	1	1?	3
Blue Mountain Str.	BM	096/-66	1	60 ± 8?	-	370.6	3.2	7.3	6	1	-	-	?	2?
														rejected
Mead Stream	MS	-	1	70 -15	-						-	-	-	2
Upper Waima	UW	-	1	18 ± 3?	-						-	-	-	2
Narrows 3	NS3	-	1	25 ± 5	-						-	-	-	1
Laings Nut	LN		1	60 ± 5	-				4		-	1*	sec var?	2?
Waima River	WR	-	1	25 ± 5	-						-	-	-	1

Table 2.4. Criteria for acceptance/rejection of palaeomagnetic data from Marlborough. An index of 5 or more distinguishes good data; 4 reasonable data; 3 or less unreliable.

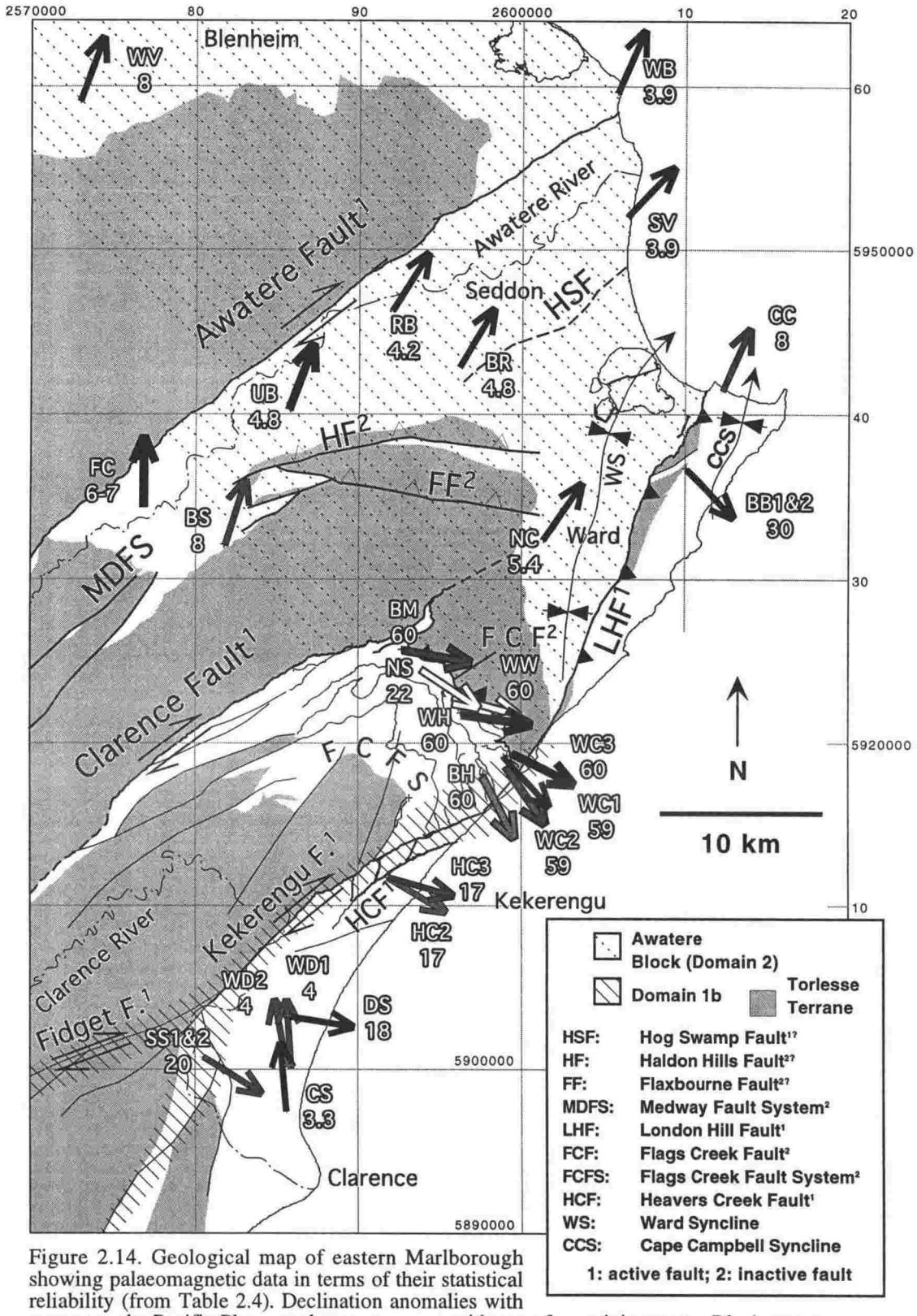

Figure 2.14. Geological map of eastern Marlborough showing palaeomagnetic data in terms of their statistical reliability (from Table 2.4). Declination anomalies with respect to the Pacific Plate are shown as arrows with age of containing strata. Black arrows represent the most reliable data, with a Quality Index of 4-5, grey arrows represent data that have some question as to their quality (Index = 3) and white arrows represent sites that are unreliable (Index ≤ 2). See Figure 2.1 for area location. Data are compiled from Walcott et al. [1981]; Mumme & Walcott [1985]; Roberts [1992]; Vickery [1994]; Little & Roberts [1997] and this study.

has rotated by ~100° since the early Middle Miocene (Fig. 2.14). The spatial extent of Group 1 rotations is poorly constrained by lack of sampling of the appropriate aged rocks to the west.

Samples from Palaeocene limestone (60 Ma) are, on average, 10 – 40° more rotated than 17 – 20 Ma rocks from the same area, suggesting that there may have been some pre-Miocene clockwise rotation. However, because of the spatial distribution of these sites of differing age, it is not possible to accurately determine whether these apparent differences are due to increasing rotation with age or proximity to active faults. Thrust faulting in the FCFS is inferred to have started earlier than 17 Ma (i.e. the GMC is Early to Middle Miocene in age, or ~24 – 20 Ma). Thus, it appears that large clockwise Class 1 rotations occurred during a late phase of FCFS fold and thrust deformation, or post-dated it entirely. Unfortunately, no data from rocks aged between 17 ± 1 & 8 ± 1 Ma have been obtained from NE Marlborough. Therefore, timing of the Class 1 rotation is poorly constrained to between 18 and 7 Ma.

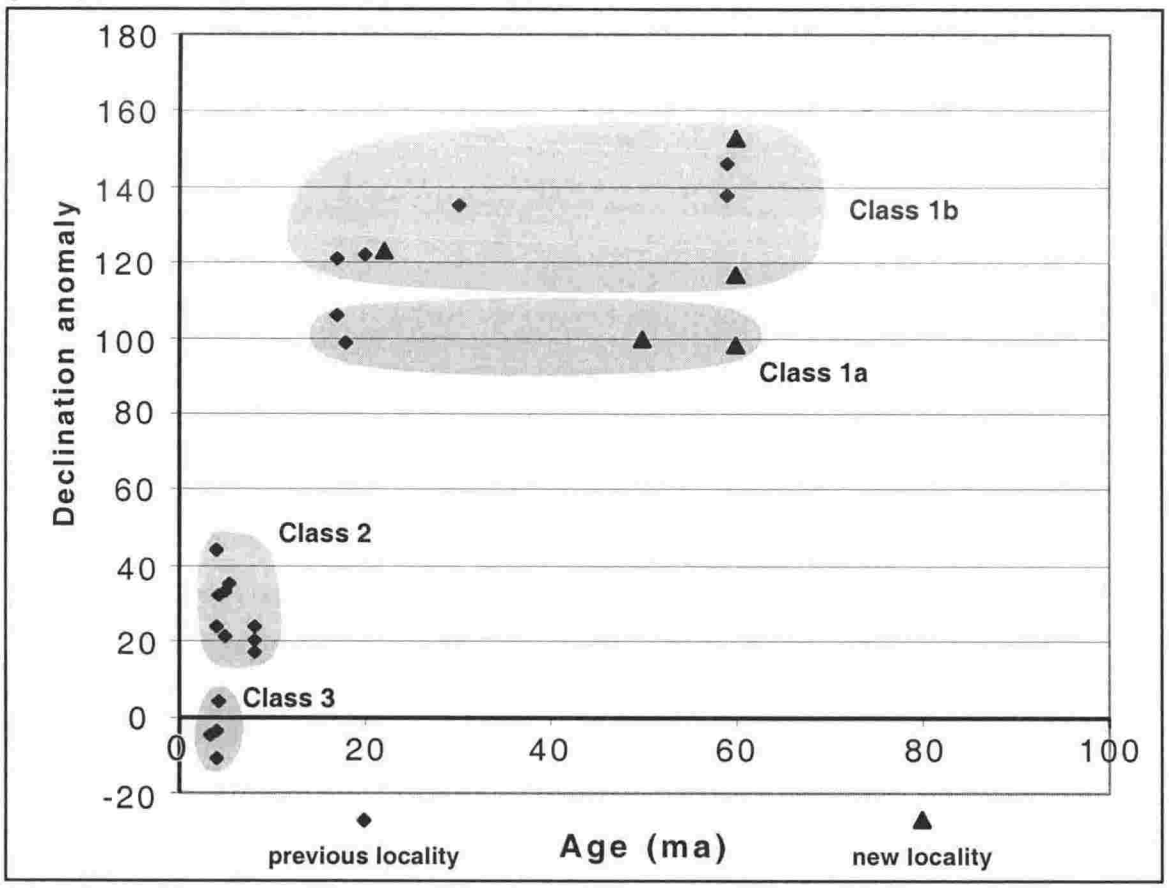

Figure 2.15. All accepted palaeomagnetic data from Marlborough plotted as declination anomaly versus site age. Three main groups [after Vickery & Lamb, 1995] can be identified. Group 1a: all rocks 17 Ma or older have been clockwise-rotated by 100° or more. Depending on their proximity to active strike-slip faults, such as the Kekerengu Fault, Group 1 locations have received an additional clockwise rotation (Group 1b) that may be related to local shear on or near those faults; Group 2 rocks of the Awatere - Wairau region between 8 and 3.5 Ma have been clockwise-rotated by up to 44°; Group 3 unrotated rocks as old as 6-7 Ma in the Awatere Valley and south of the Kekerengu Fault define the spatial limit of Group 2 vertical axis rotations.

• Group 1b) rotations

Additional clockwise rotation of up to 50° within ~5 km of the Kekerengu Fault distinguishes Domain 1b, where the total declination anomaly is 120 – 150°. The extra 20 – 50° of clockwise rotation may have occurred as distributed deformation prior to the development of through-going strike-slip fault segments that now make up the Marlborough Fault System. North of the Kekerengu Fault, the 3D map pattern of NE-dipping large-scale faults of the FCFS suggests that their eastern parts steepen through the vertical to become overturned and SW-dipping near the coast [Chapter 3]. This indicates that these thrust faults have been spectacularly "drag-folded" about an axis that is parallel to their intersection with the steeply NW-dipping Kekerengu Fault. This zone of km-scale drag-folding is conspicuous on the map (Fig. 2.5, 2.14) and apparently affects rocks within ~3-5 km of the active Kekerengu Fault, including sites WC 1, 2 & 3, BH & SS 1 & 2. This dextral-shear -related drag-folding is inferred to be responsible for an extra 20 – 50° of local clockwise rotation of Group 1b rocks relative to Group 1a rocks.

• Group 2) rotations

Late Miocene and Pliocene rocks of the lower Awatere and Wairau valleys are clockwise rotated by ~20 – 45°, defining a ~40 × 40 km crustal block, the Awatere Block [Roberts, 1992] (see Fig. 2.14). This block is transected by the active Awatere Fault and may be broken into smaller, differentially rotated structural entities. The 44° clockwise rotation of the SV site is ~15° more than the "average" ~30° rotation of the Awatere Block and the ~20° rotation of BS & UB are ~10° less. These differences may be explained by "edge effects" of the rotating Awatere Block [Roberts, 1992] and are discussed below.

• Group 3)

Sites consisting of Late Miocene and Pliocene rocks that are unrotated relative to the Pacific Plate since *c.* 6-7 Ma define the southern and western limit of Group 2 rotations. Group 2 rotations appear not to have affected the Middle Awatere Valley or the Kekerengu areas because rocks younger than 7 Ma there are unrotated, or even slightly anticlockwise-rotated (Fig. 2.14). Therefore, in this area, there is no overlap of Group 1 and 2 rotations and the magnitude of Group 1a rotations can be directly defined by the 99° clockwise rotation at the DS palaeomagnetic site. It follows that other Group

1 sites that have undergone only ~100° of clockwise rotation (BM, WH, HC2 & 3 and possibly NS) also have not experienced any additional Group 2 rotation.

Nature of the block boundaries

Palaeomagnetically determined vertical axis rotations are widely analysed in the literature, but seldom are the extent of blocks or their boundaries structurally defined [e.g. Little & Roberts, 1997]. Models of crustal deformation in strike-slip settings are mostly viewed in terms of rotations about vertical axes. This is because over-simplification of a 3-D world to a map-view can only account for two dimensions and because finite (structurally corrected) palaeomagnetic vectors record nothing about the incremental processes by which deformation accrues. Crustal deformation, however, is not two dimensional. In models of vertical axis fault block rotations, vertical boundaries of rotating blocks must deform if the system is to remain stable. If, on the other hand, a block boundary is not vertical (i.e., a thrust fault), the overlapping corners of a block that impinge on neighbouring, relatively unrotated blocks are avoided because it achieves translation of material out of the horizontal plane.

It is not currently possible to constrain the spatial extent of Group 1 rotations in Marlborough. All sampled rocks older than 17 ± 1 Ma occur east of the Clarence and London Hill faults and have declination anomalies greater than 100°. The inferred eastern boundary to the region of large rotations (Domains 1a & 1b) is the offshore Hikurangi margin subduction thrust. The other boundaries are more difficult to establish due to the lack of rocks of the appropriate age, but if the gradual folding of basement rocks in the South Island from NW- to NE-striking as one approaches the Alpine Fault (e.g., Fig. 2.1) is a consequence of Group 1 rotations, then the remaining boundaries of Domain 1 rocks may be represented by km-scale folding. This implies that the western boundary of Group 1 rotations may lie west of the Alpine Fault, as rocks in the Nelson region (Fig. 2.1) are also NE-striking and 30 Ma old rocks there are clockwise-rotated by 79° [Mumme & Walcott, 1985].

Class 2 rotations, however, have a more complicated pattern. The western boundary of Domain 2, located between sites FC and BS in the Middle Awatere Valley, is interpreted by Little & Roberts [1997] as a 0.5 to 2 km wide zone of pervasive faulting and jointing at the outcrop scale. The BS and UB sites are inferred to lie on or near the diffuse boundary marking the western edge of the Awatere Block [Little & Roberts,

1997] and for this reason may not have experienced the full rotation compared with sites closer to the centre of the block. The southern boundary of the Awatere Block must lie between NC/BS and the new palaeomagnetic sites BM, WH and WW, because the latter Palaeogene rocks are interpreted to have experienced only the ~100° Class 1a rotation. Little & Roberts [1997] place this NW-SE -trending boundary between the Middle Awatere Valley and Kekerengu, transecting the Clarence Fault (Fig. 2.14). However, if this Pliocene to present-day rotation boundary did transect the Clarence Fault, imbricated rocks of the FCFS, that lie to the SE of the Clarence Fault, would also be deflected across this boundary, which is clearly not the case (Fig. 2.14). These observations lead to the possibility that the northern part of the Clarence Fault and the FCF form the southern bounding structures of the younger Group 2 rotations observed in the Awatere Block and that Group 2 rotations do not occur anywhere to the south of these faults. Late Miocene reactivation of the FCF as a SW-verging thrust fault is inferred from overprinted deformation fabrics observed in outcrops along the fault trace and from stratigraphic relationships in the Awatere Basin, on the reactivated backlimb of the FCF [Chapter 3]. More recent movement on this fault cannot be ruled out. This hypothesis is not incompatible with that of Roberts [1995] and Townsend & Little [1998], who suggest that the Awatere Block is pivoting about the termination of the Clarence Fault due to NE termination of dextral strike-slip on this crustal-scale fault.

The eastern boundary of Group 2 rotations is also apparent. The CC site is inferred by Townsend & Little [1998] to be part of a crustal block that is structurally separated from the Awatere Block by the major London Hill thrust fault (Fig. 2.14). the 24° clockwise rotation of the CC site since *c.* 8 Ma is significantly less than the 30-40° rotation recorded from Pliocene rocks of the Awatere Block, immediately to the west of the London Hill Fault. Recent (post-Holocene) faulting adjacent to the London Hill Fault and active folding of the NE-plunging Ward Syncline [Townsend, 1996] may be accommodating differential vertical-axis rotation between these two crustal blocks on either side of the LHF. The northern boundary of the Awatere Block is inferred by Little & Roberts [1997] to be the Wairau Fault, which terminates in the Cook Strait area.

Regional versus local rotations

Plate reconstructions for New Zealand based on palaeomagnetic data indicate that the Hikurangi margin has rotated clockwise by more than 90° since the Early Miocene [Walcott, 1978; Lamb & Bibby, 1989; Vickery & Lamb, 1995]. Initiation of the subduction zone at ~25 Ma [Kamp, 1987] and its failure to propagate south of the Chatham Rise is an important factor in the development of the plate boundary through New Zealand (Fig. 2.16). Between ~24 and ~18 Ma, seaward-verging thrust faulting in the FCFS of Marlborough preceded accumulation of large vertical axis rotations there; thrusting began in the early Miocene but middle Miocene rocks are clockwise-rotated as much as Palaeogene rocks. More than 20 km of shortening in the NE-vergent FCFS is likely to have resulted in an accumulation of dextral shear strain in the (then) unfaulted, overriding plate near the subduction termination (Fig. 2.16). At this time, Mesozoic basement rocks were already tilted and folded to near-vertical, with overlying Tertiary rocks deposited above a regional angular unconformity. If the vertically dipping Torlesse basement rocks accommodated this crustal-scale dextral shear strain by a vertical axis rotation or folding [e.g., Little & Roberts, 1997], the overlying subhorizontal Tertiary strata would also have been rotated about a vertical axis as deformation ensued. Thus, in the early stages of the new plate boundary propagating through New Zealand, dextral strain accumulating at the southern termination of the Hikurangi subduction margin is likely to have resulted in the formation of a crustal-scale, dextral "kink-band" spanning the proto-Alpine Fault.

The rotated southern ends of the FCFS, which are today the northern Marlborough Fault System (NMFS) were NNE-striking by end of the Miocene [Lamb & Bibby, 1989] and at an angle to relative plate motion such that they could be reactivated as oblique dextral-reverse faults. Five lines of evidence suggest this: 1) the NMD faults strike parallel with the trend of the offshore Hikurangi margin, a feature that has rotated clockwise to become NE-striking since the early Miocene [e.g. Walcott, 1978], 2) some of the Marlborough Faults contain Palaeogene and middle Miocene rocks in their footwalls that are palaeomagnetically determined to have been clockwise-rotated by 100° or more, 3) SE-vergent thrusts of the Early Miocene FCFS in the footwall of the Clarence Fault are inferred to have been clockwise-rotated by at least 90° to be viable with a seaward-verging relative plate convergence vector at the time of their formation, 4) footwall inliers of Palaeogene rocks occur along the NMFS but not to the south of the

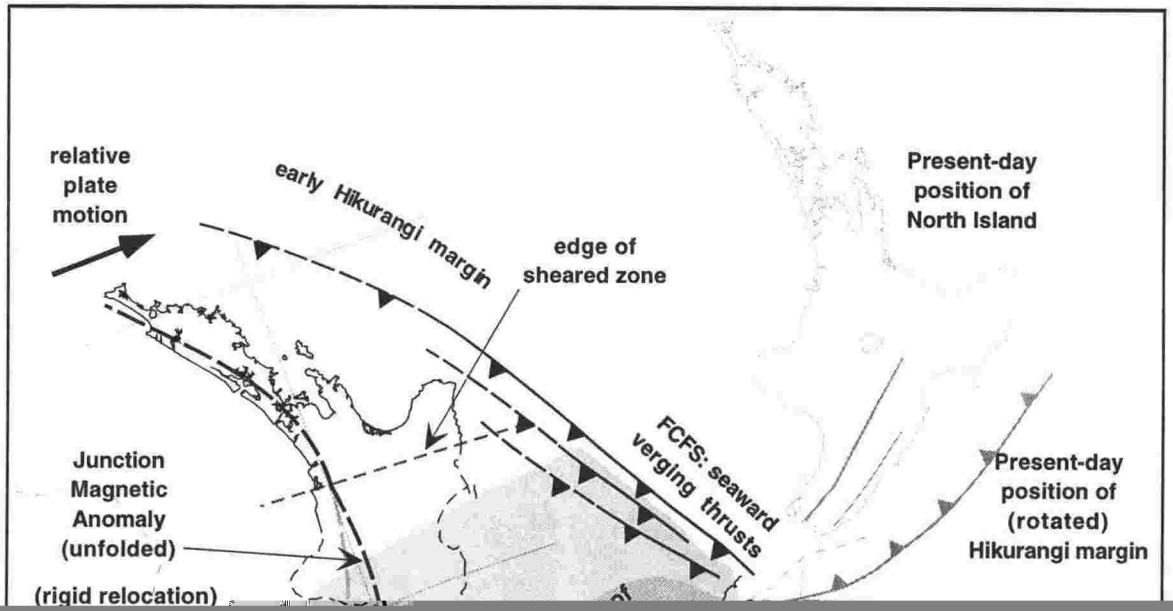
relative
plate
motion
early Hikurangi margin
edge of
sheared zone
Present-day
position of
North Island
FCFS: seaward
verging thrusts
Junction
Magnetic
Anomaly
(unfolded)
(rigid relocation)
Present-day
position of
(rotated)
Hikurangi margin

change in MFS strike at Kaikoura (Fig. 2.2). These strips of younger strata are interpreted as remnants of a more extensive sheet that was deformed by thrust faulting in the Early Miocene, in a manner similar to the FCFS, but on a broader scale and, 5) seismically active subducted Pacific Plate underlies the NMD, but not the SMD [Eberhart-Phillips & Reyners, 1997], suggesting contrasting styles of lithospheric deformation in those two areas. Thus, the NMD contains remnant faults related to the Miocene thrust deformation episode, but the SMD does not.

The Group 2 vertical axis rotations in Marlborough, which affect rocks as young as 4 Ma, are inferred to have an origin other than regional rotation about the termination of a pinned subduction zone. As the Pacific – Australia subduction interface became locked (possibly because of buoyant, thickened oceanic Pacific lithosphere choking the trench), relative motion between the Pacific and Australian plates must have been accommodated in some other manner than differential slip on the subduction thrust. The Alpine/Wairau Fault was already developed as a through-going structure by the end of the Miocene [Walcott, 1978], but its northern part may have also been clockwise-rotated beyond the critical angle for strike-slip motion (as a late part of the Group 1 rotation) [Little & Roberts, 1997], resulting in crustal deformation being shunted towards the "free edge" of the locked-plate region (or to the SE). Linking of the NMFS with slip on the Alpine Fault may have created the southern part of the Marlborough Fault System (SMFS). Because relative plate motion had become more east-west oriented by this time and because this region was not subject to the tractional effects of underlying subducted Pacific Plate, these new linking faults formed at a more-ideal angle for strike-slip deformation, clockwise to the reactivated NMFS segments and the Alpine Fault by ~30°.

While linking of the rotated NMFS segments with the Alpine Fault was occurring in southern Marlborough, slip cessation on the Clarence Fault and contemporaneous vertical axis rotation of the Awatere Block was occurring in the northern part [Roberts, 1992, 1995]. A 4 Ma reconstruction for NE Marlborough based on the available palaeomagnetic and fault-slip data is presented in Figure 2.17. The dark grey area represents the amount of shortening across faults or across block rotation boundaries, where crustal thickening is inferred to be responsible for the removal of this material. This reconstruction emphasises the effect of removing Group 1a & 2 rotations, so that at

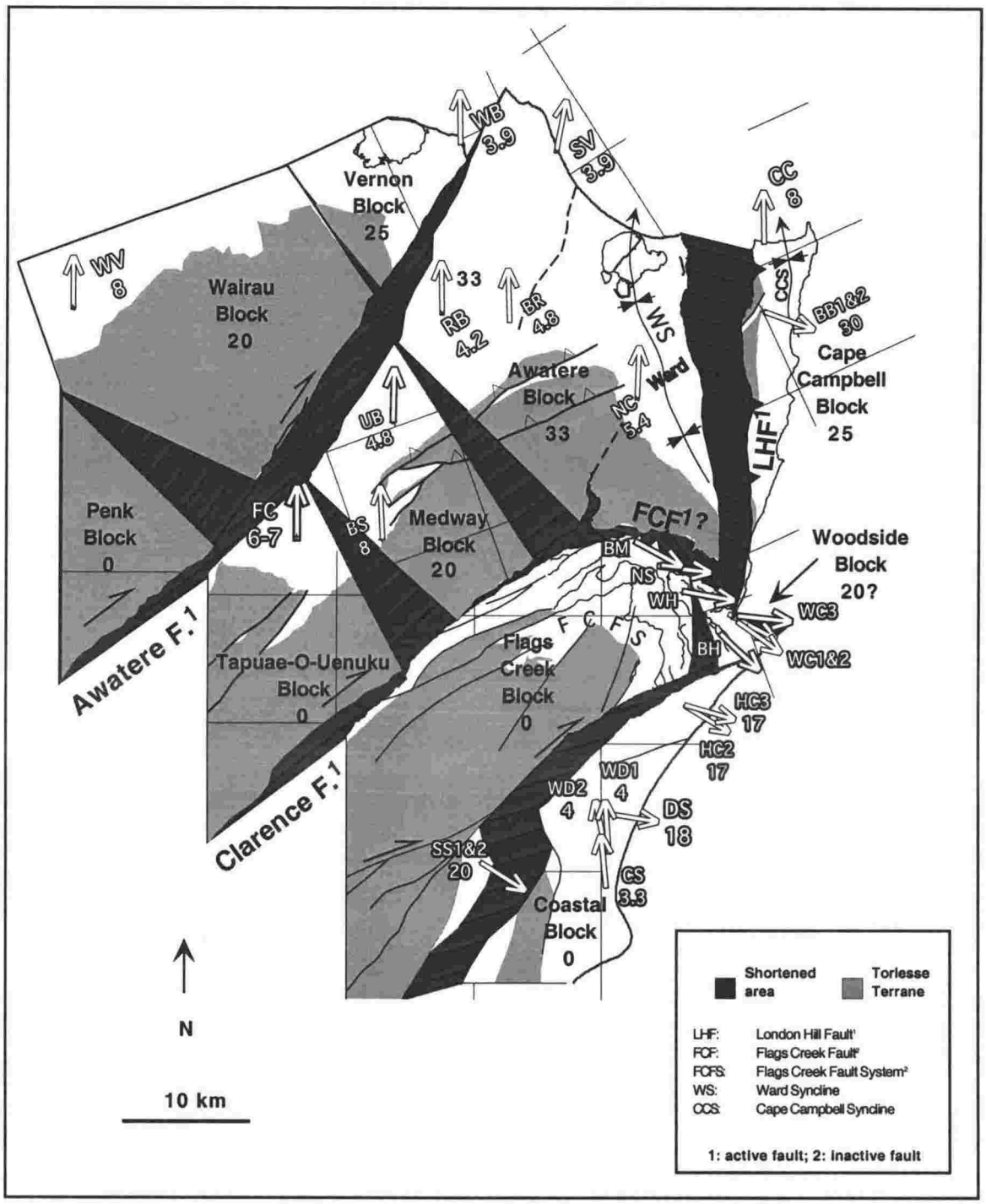

Figure 2.17. Possible Late Miocene reconstruction of Marlborough, prior to the initiation of Group 2 rotations. The region has been subdivided into rigid blocks that are assigned a rotation value according to the available palaeomagnetic data (bold numbers). The dark grey pattern represents the area that has been shortened between faults or across boundary structures (e.g., Little & Roberts [1997]) since 4 Ma; parallel lines indicate the finite direction of relative convergence between blocks. The fault slip vector for the London Hill Fault is from Townsend & Little [1998] and slip on the Awatere Fault is from Benson et al. [2001]. The four southern blocks have undergone translation but negligible rotation relative to each other, since ~4 Ma, although SS1 & 2 may have undergone additional local rotation adjacent to the active Kekerengu Fault. It is apparent that the Domain 1 rocks in the northern part of the Flags Creek Block do not require the additional Group 2 rotation to accrue their finite value, thus it seems that Group 2 rotations have not affected any part of the Penk, Tapi-O-Uenuku, Flags Creek or Coastal blocks.

4 Ma there was far less disparity among Group 1 palaeomagnetic vectors than there is today (c.f. Fig. 2.14).

CONCLUSIONS

A period of extensive thrust deformation and crustal shortening accompanied inception of the currently active subduction of Pacific Plate beneath Australian Plate in the Early Miocene (24 – 18 Ma). The subduction zone did not propagate southeast of the area that is presently the western end of the Chatham Rise.

All palaeomagnetically sampled rocks in NE Marlborough that are older than 17 ± 1 Ma exhibit clockwise declination anomalies of 100 - 150°. This rotation probably occurred as a distributed deformation event due to the accumulation of dextral crustal strain at the southern termination of the Miocene subduction zone. Consequently, as the Australian Plate has overridden the Pacific Plate, the southern end of the Hikurangi margin has acted as a pivot or hinge about which the subduction zone has rotated clockwise through ~100°. Vertical axis rotation of vertically dipping strata in the basement is the preferred method of accommodating this regional rotation, with overlying Tertiary rocks, including those in the Flags Creek Fault System (FCFS) also being rotated ~100°.

Torlesse terrane basement rocks of NE Marlborough contain a dominantly NE-SW -striking structural fabric that delineates one limb of the New Zealand orocline. Tertiary rocks unconformably overlying the Torlesse terrane have been clockwise-rotated by at least 100° since the Early Middle Miocene. Clockwise rotation of the Early Miocene Flags Creek Fault System of >90° is also required to reconcile the observed SE transport direction of thrust sheets with NE-vergent crustal shortening implied by plate reconstructions for that time.

The two new palaeomagnetic localities that are within ~3 km of the active dextral strike-slip Kekerengu Fault reveal clockwise declination anomalies of up to 150°. New structural mapping of the FCFS suggests that the eastern ends of those Early Miocene thrust faults, which are truncated by the Kekerengu Fault near the coast, are also clockwise-rotated with respect to more inland parts of the fault system. The dominant transport direction within the FCFS is to the SE, but within ~2-3 km of the Kekerengu Fault this SE-vergence direction is clockwise-rotated approximately 45° and transport directions are consistently S-directed. These lines of evidence imply the presence of a

zone of distributed dextral shear and vertical-axis rotation within 2-3 km of the Kekerengu Fault. Local clockwise vertical-axis rotation of up to 50° is interpreted to have accrued in this zone, additional to the regional, ~100° clockwise vertical-axis rotation that occurred in the Miocene.

The current NE strike of Northern Marlborough Domain (NMD) faults is inferred to have been inherited from a Miocene thrust deformation fabric that has undergone ~100° of clockwise vertical axis rotation since <18 Ma. As a result, these reactivated faults are now aligned such that there is a significant component of shortening across them. Subducted Pacific Plate that underlies the northern region may play a role in the orientation and selective reactivation of these crustal-scale structures.

Chapter 3: Evolution and tectonic significance of the Flags Creek Fault System, Marlborough, New Zealand.

ABSTRACT

The Flags Creek Fault System (FCFS) is a fold and thrust belt that formed above the Early Miocene subduction zone along the east coast of New Zealand. Syntectonic deposition of the Great Marlborough Conglomerate, an extremely poorly sorted olistostromal unit that was scoured into locally uplifted parts of the fault system, attests to the timing of fault activity. Kinematic indicators are rare on map-scale faults, but analysis of mesoscopic structures in the deformed belt, including faults, asymmetric folds, cleavage, veins and minor shear zones, preserve a consistent vergence to the southeast. Palaeomagnetically-determined regional clockwise vertical axis rotation of ~100° must be accounted for in this analysis, therefore the original vergence direction of the FCFS is to the NE, in accordance with NE-SW contraction between the Pacific and Australian plates during the Early Miocene. Fault offset accommodated at least 20 km of horizontal shortening across a leading-edge imbricate fan. Forming as a backstop to the FCFS, the proto-Clarence Fault formed an easterly-verging overthrust nappe of Torlesse Terrane rock, with a steeply-dipping western root zone (the present Clarence Fault) and a gently-dipping overthrust flap to the east (the Flags Creek Fault). By the Late Miocene, the entire region had been clockwise-rotated by ~100° and the tilted, folded Flags Creek Fault had become ideally oriented to be reactivated as a SW-directed thrust fault. This later deformation resulted in folding and overprinting of many of the (now SE-verging) mesoscopic structures in the FCFS. Now part of the transcurrent Marlborough Fault System, the eastern part of the FCFS has undergone additional deformation during the Late Pliocene to present, when an additional increment of clockwise vertical axis rotation (up to 40°) locally affected rocks adjacent to major active strike-slip faults, such as the Kekerengu Fault.

INTRODUCTION

The Flags Creek Fault System occurs in a series of imbricated Cretaceous to Miocene rocks near the east coast of the northern South Island, New Zealand (Fig. 3.1). The development of this thrust fault system is globally important for developing a general understanding of the kinematic evaluation of obliquely convergent plate boundary zones and locally important for understanding the timing and processes of plate boundary propagation through central New Zealand during the Miocene. This paper is concerned with initiation and development of the Pacific-Australia plate boundary in NE South Island and of the Flags Creek Fault System (FCFS), which was active in the Early - Middle Miocene. Evidence for timing of fault movement includes the syntectonic nature of the olistostromal Great Marlborough Conglomerate. Initiation of fault activity at ~25 Ma was probably due to the onset of westward subduction of the

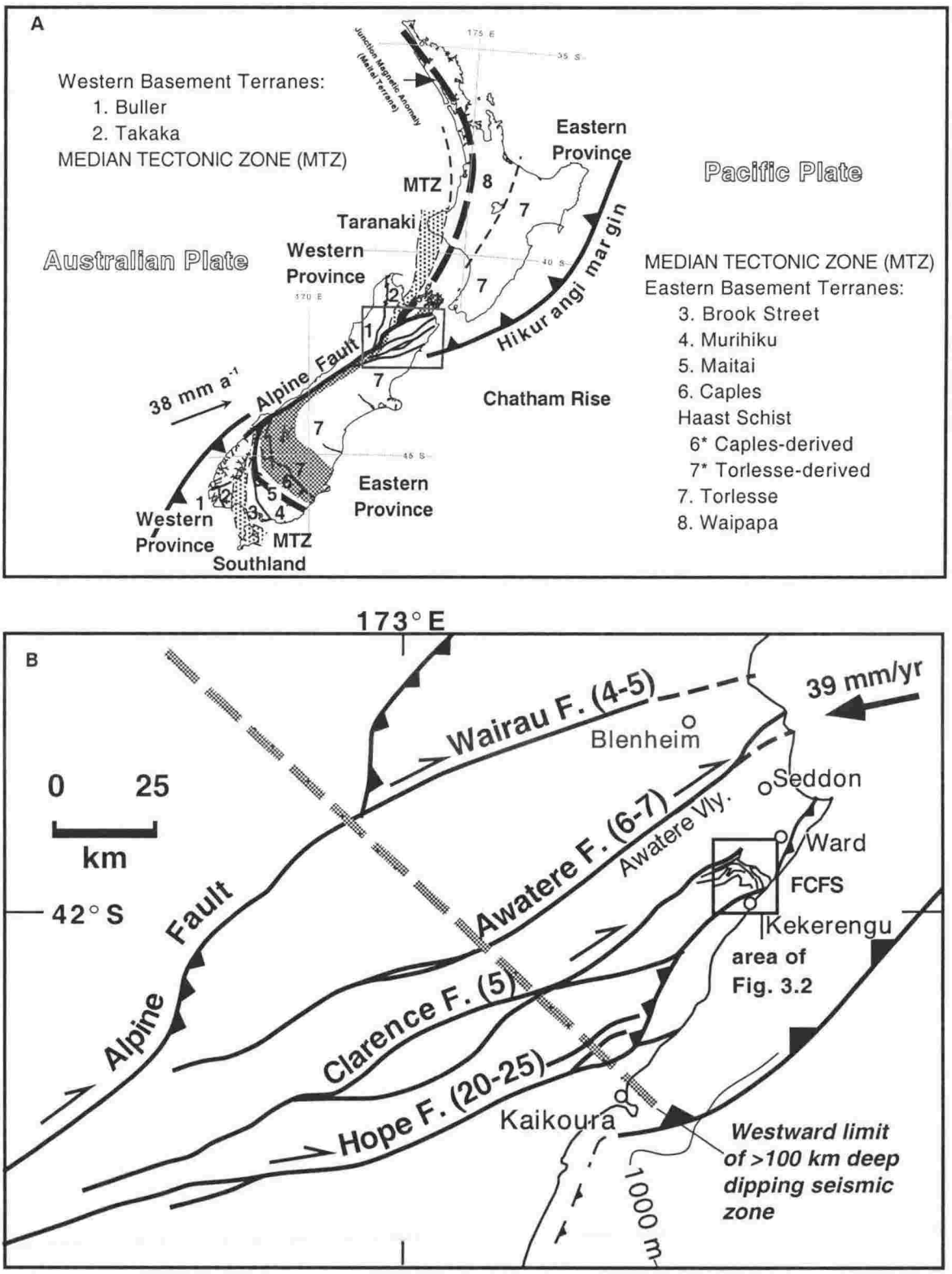

Figure 3.1A: The tectonic setting of New Zealand with emphasis on basement terranes (redrawn from Sutherland [1999]). B: The active Marlborough Fault System (MFS) currently accommodates 80 - 100% of the Pacific - Australia relative plate motion in central New Zealand [Holt & Haines, 1995]; approximate rates of strike-slip offset are shown in brackets (mm a^{-1}). After Little & Roberts [1997] and Van Dissen & Nicol [1999].

Pacific Plate beneath the Australian Plate along the Hikurangi margin [e.g. Rait et al., 1991]. Cenozoic plate reconstructions based on sea floor spreading data and New Zealand geology [Sutherland, 1995; King, 2000] require that the Australian Plate moved NE relative to the Pacific Plate in Late Oligocene – Early Miocene time. The present-day NE–SW regional strike of both thrust faults and bedrock structural grain in Marlborough (Fig. 3.2) is difficult to explain in terms of this kinematic scenario without taking into account large magnitude vertical axis rotations of the plate boundary zone in NE South Island [Lamb & Bibby, 1989, Chapter 2].

The Early Miocene Flags Creek Fault System provides valuable information about the nature and orientation of the Pacific-Australia plate boundary at the time of its formation. This paper investigates the direction, amount and timing of motion of individual faults within the FCFS and integrates new and existing palaeomagnetically determined vertical-axis rotation data [Chapter 2] to provide an interpretation of the structural history. Cretaceous and older deformation events recorded solely within the Torlesse Terrane are omitted for the purpose of this study.

The FCFS today is folded in an arcuate pattern, extending through ~180° of strike from the inland Clarence Valley to the coast near Kekerengu, forming a crustal scale structure that includes the NE-trending Ben More anticline (Fig. 3.2). This arcuate pattern might be explained by ~100° of vertical-axis rotation of the SE limb relative to the NW limb, by less rotation about a gently plunging fold hinge together with northeast-ward tilting to produce the NE-plunging arcuate map pattern, or by some combination of both. Various workers in the past have interpreted the arcuate FCFS to be the result of SE -followed by SW-vergent thrust faulting [Prebble, 1976], south-directed thrusting [Browne, 1992], SW ("landward") directed thrusting [Waters, 1988; Rait et al., 1991] or folding of a SE-vergent thrust stack about a vertical axis [Little & Roberts, 1997]. Thus, the most fundamental kinematic aspects of the FCFS have remained unclear.

Since the early Miocene, Marlborough has been at the transition between two continental areas undergoing plate boundary deformation by fundamentally different processes. Subduction of Pacific Plate beneath the Australian plate is occurring to the north, whereas continental collision and oblique dextral-reverse slip on the Alpine Fault accommodates plate motion to the south. A major influence on the different styles of deformation is the southward transition on the Pacific Plate from thickened oceanic

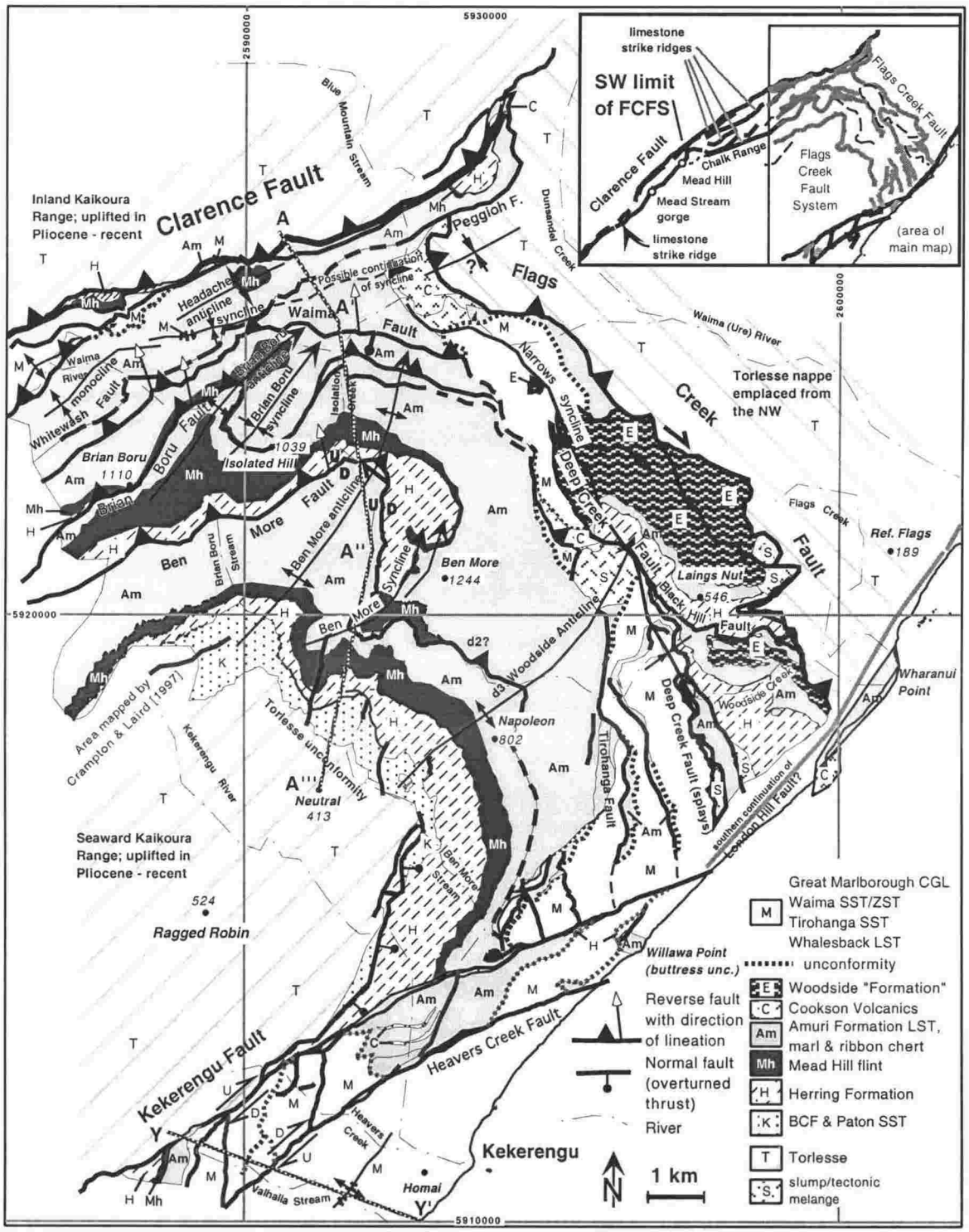

Figure 3.2. The Flags Creek Fault System and tectonic elements of the Kekerengu region. Eastern and northern thrust imbricates include younger rocks than western imbricates, consistent with thrust vergence to the SE. Torlesse rocks on the hanging walls of both the Clarence and Flags Creek faults were part of the same thrust sheet in the Early-Middle Miocene, with late Miocene reactivation of the FCF displacing its hanging wall relative to the SW. Active deformation in a zone parallel to the Kekerengu Fault mostly involves dextral shear. See text for discussion.

lithosphere of the Hikurangi Plateau to the thinned continental margin of the Chatham Rise (Fig. 3.1).

Difficulty in interpreting the kinematics from structures exposed in this highly deformed area arises, in part, from the many deformation phases that have affected the area [e.g. Lamb & Bibby, 1989]. Reactivation of large-scale structures due to changing plate boundary processes in both space and time has overprinted many of the original contact relationships between units. Further structural ambiguity is due to the complexity of the FCFS. The style of thrust imbrication in the FCFS may include different amounts of vertical-axis rotation of nappes within the structural pile [e.g., Vickery & Lamb, 1995]. Recent palaeomagnetic sampling, however [Chapter 2], suggests that 100 – 150° of clockwise vertical axis rotation has affected nappes throughout the FCFS, but with no obvious relationship between structural position and amount of rotation. If initial slip on the whole fault system was in a common direction (as concluded later), then later reactivation and folding of selected faults associated with a rapidly evolving plate boundary zone, will result in partial overprinting of early-formed structures and kinematic indicators, producing a complicated pattern of folded imbricate faults and associated fault transport and shortening directions. This is the situation of the FCFS today.

This paper describes the map-scale structure of the FCFS and interprets new meso-scale kinematic data from this complex and highly deformed region. Transport directions for Early Miocene thrust faults are inferred from these data.

Miocene tectonic setting of Marlborough

The Early Miocene was a time of major reorganisation of the plate boundary in New Zealand [e.g. Rait et al., 1991; Sutherland, 1995]. Increased early Miocene clastic sedimentation suggests that an emergent landmass was present and the onset of andesitic volcanism in the north of New Zealand indicates that subduction of the Pacific Plate beneath the Australian Plate was well established by *c.* 21 Ma [Rait et al., 1991]. Tectonic inversion of Cretaceous extensional basins at this time by reverse faulting has been documented from the West Coast of the South Island [Bishop & Buchanan, 1995], from Taranaki [King & Thrasher, 1992] and from Southland [Norris et al., 1990] (see Fig. 3.1A), indicating a change from an extensional or passive tectonic regime to one of increasing convergence or transpression. Elements of a NW-SE oriented Mesozoic

subduction zone along the eastern margin of the Torlesse Terrane, which had ceased activity in the Middle Cretaceous [Bradshaw, 1989] may have been reactivated at this time, as tectonic activity, including subduction of Pacific Plate lithosphere, migrated southward along the Hikurangi margin [Walcott, 1978]. Importantly, the early Miocene subduction front did not propagate south of the area that is today the Chatham Rise. In the early Miocene, NW-SE -striking fold and thrust belts developed above the nascent subduction zone. These are preserved onshore in Northland, Raukumara Peninsula, East Coast/Wairarapa and Marlborough (the Flags Creek Fault System; FCFS) [Prebble, 1976; Rait et al., 1991]. Stratigraphic and structural evidence in Marlborough indicate that the FCFS was active from ~24 to 18 Ma [Prebble, 1976; Vickery, 1994]. Deposition of the deep-water marine Great Marlborough Conglomerate (GMC), an extremely poorly-sorted olistostromal unit, accompanied activity of the FCFS, suggesting that Marlborough was the locus of concentrated deformation at that time.

The southward transition of Pacific Plate from oceanic to continental lithosphere across the Hikurangi plateau strongly influenced the development of the plate boundary through New Zealand (Fig. 3.1). The Chatham Rise comprises submerged continental crust, which is buoyant and difficult to subduct [Eberhart-Phillips & Reyners, 1997]. The western end of the Chatham Rise is interpreted to have formed a hinge-zone at the southern termination of the Miocene subduction zone, about which parts of the overriding Australian Plate to the north have pivoted ~100° since the middle Miocene [Lamb & Bibby, 1989]. Rocks of the FCFS, that were being accreted onto the edge of the Australian Plate in the Early Miocene, became incorporated into the plate boundary zone and experienced the full effect of this rotation [Chapter 2]. As this region has rotated clockwise, the Pacific – Australia relative plate motion vector has also changed, swinging from ~215° in the early Miocene to 258° today [DeMets et al., 1994; Sutherland, 1995]. This clockwise change in both the orientation of structures within the Hikurangi margin and the Pacific – Australia relative plate motion vector has possibly enabled some of the clockwise-rotated Early Miocene faults to remain active throughout the Pliocene to present-day. Thus, many of the NE-striking active structures that are observed in the Marlborough region today may be inherited from Miocene deformation fabrics that have been clockwise-rotated about a vertical axis by ~100°.

PRESENT TECTONIC SETTING

Marlborough is situated at the southern end of the Hikurangi margin subduction zone, where *c.* 40 mm a^{-1} of relative motion between the Pacific Plate and the Australian Plate [DeMets et al., 1994] is accommodated by a series of four crustal-scale strike-slip faults which form the Marlborough Fault System (MFS). The MFS is a transitional zone linking partitioned subduction of oceanic lithosphere to the north with continental collision, expressed as non-partitioned oblique dextral strike-slip motion on the Alpine Fault, to the south. The MFS contains four major, active dextral strike-slip faults, which are, from north to south, the Wairau, Awatere, Clarence and Hope faults (Fig. 3.1b). Several intermediate relay structures with varying rates of strike-slip motion are also included in the MFS. Bourne et al. [1998] suggest that the long-term rate of strike-slip motion within the MFS is determined by the average velocity of lower-crustal flow, producing basal tractions on rigid crustal blocks separated by the faults. The current rate of finite strike-slip motion is slowest in the north of the MFS and fastest in the south. This difference has been interpreted as a southward migration in the locus of strike-slip deformation since the Miocene formation of the MFS as the transition between subducted oceanic and continental Pacific Plate has travelled south relative to the Australian Plate [e.g., Little & Roberts, 1997; Little & Jones, 1998]. The Motunau, Ashley and Porters Pass faults, to the south of Marlborough, suggest the formation of a new "Marlborough Fault" and are attributed to this southward migration of the plate boundary and continued assimilation of Pacific Plate rocks into the plate boundary zone.

STRATIGRAPHY OF EASTERN MARLBOROUGH

Basement rocks of Marlborough comprise Torlesse Terrane sandstone, siltstone and conglomerate "greywacke" that accumulated in a Late Mesozoic subduction trench off the eastern coast of the Gondwana supercontinent. In the western Kekerengu region (Fig. 3.2), a short hiatus occurred in the Middle Cretaceous (Motuan stage) but in the east this period of non-deposition lasted a further ~10 Ma (until the Mangaotanean) [Crampton & Laird, 1997]. Deposited above an erosional unconformity cut into the Torlesse bedrock, the Burnt Creek Formation conglomerate and mudstone marks the start of a major Cretaceous - Cenozoic transgressive sequence (Fig. 3.3). The formation of the East Coast Basin, which became widespread along the entire eastern margin of

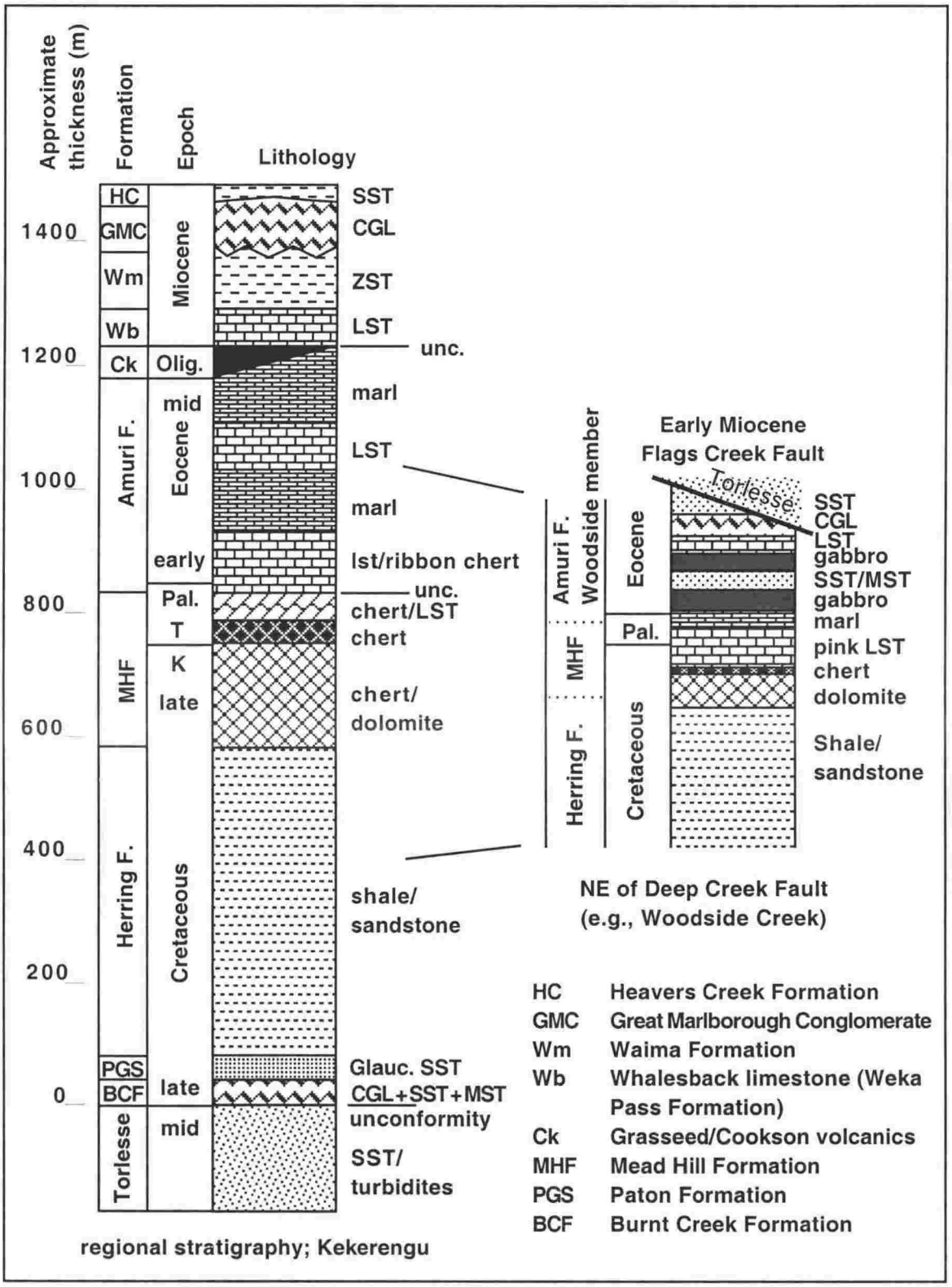

Figure 3.3. Generalised stratigraphic column for the Kekerengu area, emphasising the lithologic differences to the SW and NE of the Deep Creek Fault. Thickness of Mead Hill and Amuri formations are from Strong et al. [1995].

New Zealand, resulted from the break-up of Gondwana and opening of the Tasman Sea [e.g., King, 2000]. Localised marine basins with poor circulation accumulated the Paton Formation sandstone, Herring Formation shale and Mead Hill Formation flint. Passive margin development by the end of the Cretaceous was accompanied by a change from marine clastic-dominated to carbonate-dominated sedimentation in Marlborough, as transgression ensued. Local, anoxic basins became progressively more oceanic. Deposition of the pelagic Amuri Formation limestone and marls began in parts of Marlborough by the end of the Cretaceous. This period of tectonic quiescence lasted until ~45 Ma, when a major reorganisation of South Pacific plate motions took place [Sutherland, 1995].

During the Oligocene, maximum marine inundation of the New Zealand landmass occurred [King, 2000]. Numerous local unconformities developed along the East coast at this time [Lewis, 1992], probably as a result of both sediment starvation and the southward migration of the Hikurangi subduction margin into this region. An increase in clastic sedimentation during the latest Oligocene (Waitakian) [Vickery, 1994] marks the onset of the current subduction regime along the east coast of central New Zealand, including offshore Marlborough. This change probably corresponds to initiation of the FCFS in Marlborough [Prebble, 1976]. Early Miocene olistostromal deposits here (the Otaian to Altonian aged Great Marlborough Conglomerate [Prebble, 1976]) attest to the development of a steep submarine trench slope on an evolving plate boundary at bathyal depths. Although this deformation episode was short-lived, lasting only about 5 Ma [Rait et al., 1991], rocks of this age are well represented in the Kekerengu region. Changing sedimentation patterns accompanying development of the FCFS include a transition from the clastic-starved, earliest Miocene early–syn-tectonic Whalesback limestone (Weka Pass Formation) to the terrigenous-rich Waima siltstone (Otaian – Mid. Altonian; Vickery [1994]) as an increasing abundance of terrigenous sediment diluted the stratigraphic sequence. Locally, (e.g. at Willawa Point and Homai Hill; Fig. 3.2) combinations of thrust faulting and syntectonic erosion have resulted in pre-tectonic units (both Amuri Formation and Whalesback limestone) being exhumed at a syntectonic erosion/deposition surface and onlapped by syntectonic breccia deposits (Fig. 3.4). Lenses of Great Marlborough Conglomerate (GMC) were deposited on a scoured surface of Amuri Formation limestone, resulting in buttress unconformities with varying angular relationships to the folded and fault-deformed underlying units

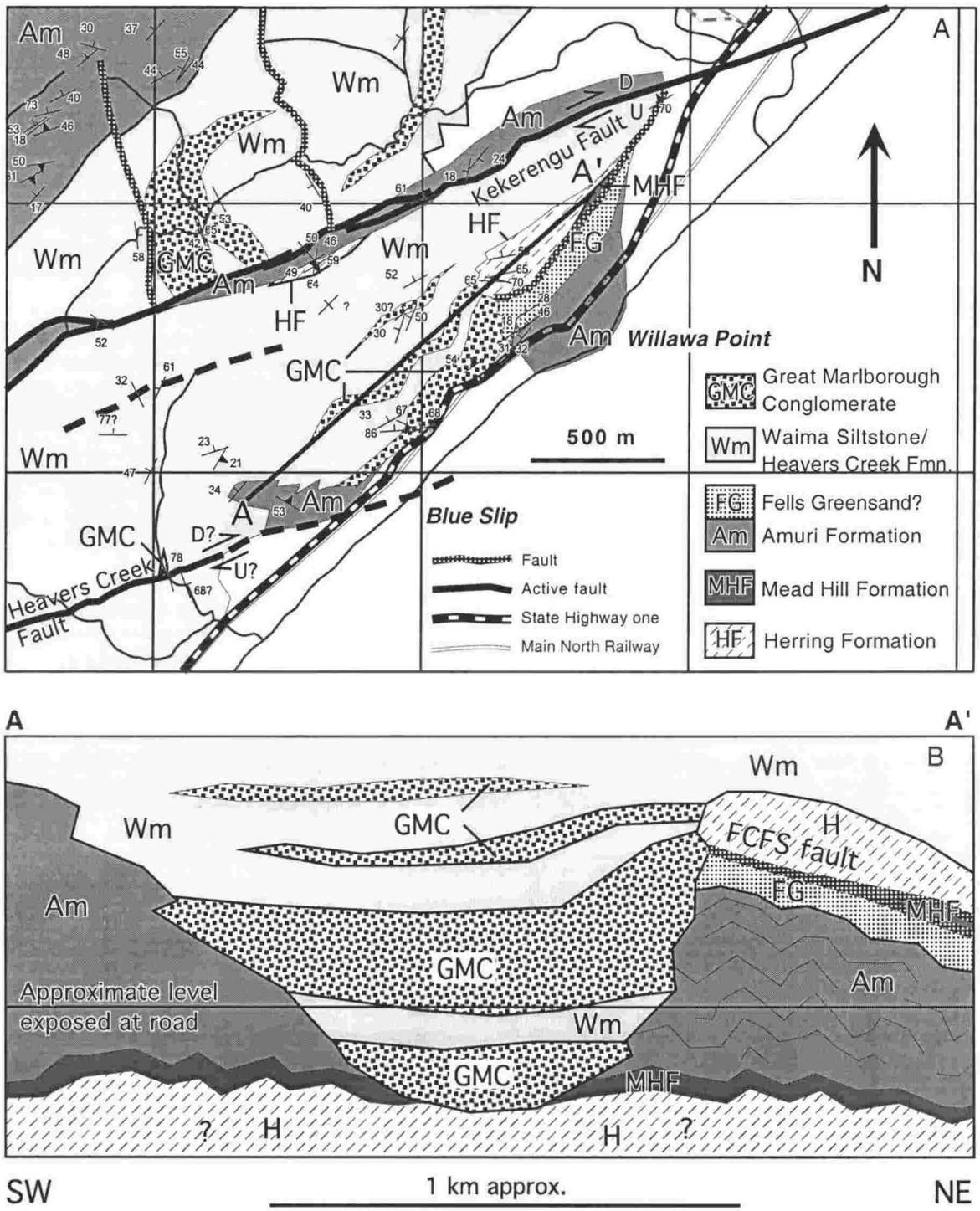

Figure 3.4. Stratigraphic relationship of units at Willawa Point, 4 km NE of Kekerengu. A: Map-view of the coastal region between the active Kekerengu and Heavers Creek faults. The region between the two coastal exposures of Amuri Formation appears to represent a scour-channel inferred to have been cut into the continental shelf at the time of localised uplift of the Flags Creek Fault System (FCFS), B: Schematic cross section along A-A' transecting the channel. The stratigraphic inversion of the units on the northern side of the channel may have occurred by overturning or repetition by thrust faulting. Either way, lenses of GMC and Waima Formation abut the older units along strike.

(Fig. 3.4A & B). These lenses of coarse clastic, tectonically derived rock often interfinger with, and/or fine upwards into the Waima Formation siltstone (e.g., Fig. 3.4). Syntectonic deposition of GMC and eastward dip-fanning is inferred from preliminary results of a shallow seismic reflection/refraction survey along the south bank of Heavers Creek [Henderson, in prep.] (Fig. 3.2). As FCFS thrust activity waned, these faulted, folded Early Miocene syntectonic sequences were overlain by Middle Miocene sandstone and siltstone of the Upper Lillburnian – Upper Waiauian [Vickery, 1994] Heavers Creek Formation. To the north of the FCFS, Late Miocene subsidence of the marine Awatere basin began by the beginning of Taranaki Series time. Increasingly convergent relative plate motion at the end of the Miocene may have resulted in thrust reactivation of the (then rotated) Flags Creek Fault and erosion of its Torlesse Terrane hanging wall rocks. This erosion is here inferred to be a major source of clastic detritus that was deposited in the Awatere basin as a fining-upwards sequence, ranging from conglomerate through to siltstone and mudstone facies. This period of activity waned in the latest Miocene (Kapitean Stage) and deposition of fine-grained clastic rocks continued into the Late Pliocene (Waipipian Stage) [Roberts & Wilson, 1992].

Some important local stratigraphic differences within the Amuri Formation also occur in the Kekerengu region. Rocks to the NE of the Deep Creek Fault (DCF; Fig. 3.2) record a different stratigraphic sequence than those to the SW of that fault. The "Woodside Formation" [Prebble, 1976] crops out only on the NE side of the DCF and consists of Heretaungan [P. Strong, pers. comm.; 1999] sandstone and mudstone turbidites that are cut at varying stratigraphic levels by gabbroic sills and locally interbedded with coarse-grained rocks of basaltic origin that could be flows or breccia deposits [Vickery, 1994]. This unit has been grouped by Prebble [1976] with the Amuri Formation, based on foraminiferal content, but is often referred to as a "formation" because of its distinctive character. In this study, the "Woodside Formation" is termed "Woodside member" of the Amuri Formation. Erosion resistant rocks forming the lower gorge at Woodside Creek lie on the hanging wall of the DCF and include a sequence of Herring Formation shale and Amuri Formation limestone (Fig. 3.2). The Mead Hill Formation there is only ~5m thick, whereas in the next lowest thrust sheet, outcropping in Isolation Creek, the Mead Hill Formation is approximately 450m thick. This difference in thickness, coupled with a new interpretation of the transport directions of major faults within the FCFS [this study], implies a thickening of the Mead Hill

Formation towards the south. These differences in stratigraphy also imply that the fault-bounded slice of rocks between the DCF and the FCF, which includes the Woodside member of the Amuri Formation, may be a far-travelled horse, transported southeastwards from a part of the basin with quite different facies associations relative to those in the footwall of the Deep Creek Fault.

PREVIOUS WORK ON THE FLAGS CREEK FAULT SYSTEM (FCFS)

Former attempts at mapping the complex Flags Creek Fault System include disparate interpretations of its kinematic and structural evolution. Prebble [1976] undertook work on the regional stratigraphy and delineated most of the major faults of the FCFS. He assumed that all fault displacements were dip-slip with respect to their current orientations and made no account for the possibility of strike-slip, oblique-slip movement, or later folding. Surprisingly, the fault planes themselves preserve little direct evidence of transport direction, an observation also noted by Prebble [1976]. Prebble [1976] interpreted the arcuate FCFS structure as the result of early, south-east verging thrust faulting on the western limb of the Ben More Anticline (BMA) followed by SW verging thrust faulting on the eastern limb, which became detached from the Torlesse Terrane "basement" by a decollement. Formation of this decollement was thought to be coeval with slip on the Kekerengu Fault, which eventually ruptured and offset the eastern limb of the Ben More anticline by wrench-style folding.

Horizontal shortening within the FCFS was estimated to be 20 km by Waters [1988], of which ~7 km is attributed to slip on the Flags Creek Fault (see Fig. 3.2). He interpreted the FCF to be the "roof thrust" of a SW-verging duplex. Waters [1988] again assumed a dip-slip motion for all faults with regard to their present-day attitude, yielding a net inferred southwest vergence for the fault system as a whole. The interpretation of Waters [1988] of southwest vergence within the FCFS is based on the present-day NE-dip of faults in the nose of the NE-plunging BMA and requires that faults on either limb of this fold were wrapped, post transport, around the fold core to become NW-dipping on the western limb and E-dipping on the eastern limb. New structural evidence, outlined below, suggests that the 20 km of shortening estimated by Waters [1988] was measured perpendicular to the mean transport direction within the thrust system and is thus invalid.

Role of vertical axis rotations in the New Zealand plate boundary zone

Vertical axis fault block rotations have been widely documented as a means of accommodating deformation in continental crust [e.g., Mumme & Walcott, 1985; Lamb, 1988; Little & Roberts, 1997]. However, many of these studies fail to successfully addresses the question of how deformation is accomplished and do not identify the structures that separate rotated regions from non-rotated regions. Palaeomagnetic data from the Amuri Formation in coastal sites near Kekerengu (Fig. 2) suggest clockwise vertical axis rotations of 100 - 150° [Mumme & Walcott, 1985; Vickery, 1994; Chapter 2]. All of these strongly clockwise-rotated sites are contained within rocks that are 17 Ma or older and suggest that large magnitude, clockwise vertical axis rotations took place throughout a broad tract of the NE South Island during the Middle Miocene [see Chapter 2]. Vickery & Lamb [1995] inferred that the Marlborough region to the east of the Clarence Fault rotated clockwise by 60 – 100° during the period 18 – 8 Ma. Roberts [1992] documented rotation of the block between the Wairau and Kekerengu faults of 20 to 45° since the Pliocene (4 Ma). Additional clockwise rotation of 30 – 40° (total 150°) has locally affected rocks adjacent to active strike slip faults near Kekerengu [Vickery & Lamb, 1995].

Torlesse strata in the core of the BMA (the "Kekerengu block") strike parallel to a NNE "regional bedding fabric" characteristic of inland Marlborough and are near-vertically dipping [Little & Roberts, 1997]. Steeply-dipping Torlesse strata to the east of the Clarence Fault (the "Clarence block") strike similarly to those in the fold core near Kekerengu; however, the strike of Torlesse Terrane bedding to the north of the FCF is WNW-ESE and moderately north-dipping (~40-70°), suggesting that this block of Torlesse rock (the "FCF block") has undergone a differential rotation relative to NNE-striking Kekerengu and Clarence Torlesse blocks to the south and west. The westerly strike of the FCF hangingwall strata in conjunction with coastal palaeomagnetic data from the footwall of the FCF, which suggest ~100° of clockwise vertical-axis rotation occurred there, imply that the difference in bedding attitude between the Clarence and Kekerengu blocks and the FCF block could be attributed to 100° of differential clockwise vertical-axis rotation [Little & Roberts, 1997]. However, it will be shown later that this difference in Torlesse bedding attitude did not result from Pliocene vertical-axis rotation [e.g., Little & Roberts, 1997], but rather occurred by folding about

a gently-plunging hinge that was coeval with development of the FCFS and an overthrust nappe of Torlesse terrane rock (the FCF block).

Vertical axis rotations continue to be a mechanism by which contemporary strain is accommodated in Marlborough. Roberts [1992, 1995] showed that a crustal block of more than 40 km^2, including the lower Awatere Valley and Ward area (Fig. 3.1), has rotated 20 – 45° since ~ 4 Ma. Little & Roberts [1997] presented palaeomagnetic data for 6-7 Ma rocks from the middle Awatere Valley, 10 km NW of the FCFS, that are unrotated relative to rocks of a similar age to the east, defining a western boundary of contemporary vertical-axis rotation of the Lower Awatere Valley - Ward region.

New palaeomagnetic data from the FCFS

Plate reconstructions and existing palaeomagnetic data suggest that the Hikurangi margin has changed from an early Miocene trend of WNW to become ENE-oriented today [Walcott, 1984; Lamb & Bibby, 1989]. If true, such a 90° change in strike would profoundly alter shortening directions in thrust fault systems that were active before or during the time that these rotations were taking place.

Published palaeomagnetic data from rocks >17 Ma in Marlborough all lie on the eastern limb of the BMA and thus fail to determine whether the limbs of this fold have experienced different vertical axis rotations. New palaeomagnetic data [Chapter 2] from the eastern limb of the BMA generally confirm the occurrence of ~100°+ clockwise vertical axis rotations of coastal Palaeogene strata. New structural data [Chapter 2] from the western part of the fold suggest that large clockwise vertical axis rotations (80 – 100°) also occurred there. These new data corroborate a hypothesis of Vickery & Lamb [1995] that most of Marlborough has been affected by large magnitude clockwise vertical-axis rotations and that the BMA is not a crustal-scale vertical axis rotation boundary. This is an important observation for analysing transport directions of faults within the FCFS because it implies that the whole fault system can be treated as part of a single, rigid crustal block.

KM-SCALE STRUCTURE OF THE FLAGS CREEK FAULT SYSTEM

The FCFS is conspicuously arcuate in map view (Fig. 3.2; stratigraphic units have been mapped in much finer detail than shown on the map). The general map pattern represents an imbricate series of reverse faults that have been folded about a gently plunging, NE-trending hinge. In the western part of the deformed belt, strata and faults dip homoclinally to the NW and erosion-resistant Amuri Formation limestone underlies the topographically high-standing Chalk Range (Fig. 3.2, inset). This topographic feature can be followed for a distance of ~30 km to the SW in the footwall of the Clarence Fault [Lensen, 1962]. At Mead Stream (Fig. 3.2, inset), a ~700m-thick stratigraphic sequence of Late Cretaceous to Miocene rocks [Strong et al., 1995] in the footwall of the Clarence Fault is not imbricated by reverse faults. At Mead Hill, 3.5 km to the NE of Mead Stream, the Clarence Fault makes a subtle anticlockwise change in strike and thus diverges to the north from the NE-striking Chalk Range. This divergence defines a NE-opening wedge, in map-view, that allows for a structurally thickening sequence of rocks that lies structurally above the Chalk Range. The abrupt increase in structural thickness between the Clarence Fault and the Chalk Range at Mead Hill is here interpreted as marking the south-western limit of the imbricate FCFS.

In the north of the study area, strata of the FCFS are folded around the BMA; however, the traces of the Clarence and Peggioh faults are not (Fig. 3.2). A narrow wedge of Late Cretaceous and Tertiary rocks constitute the footwall of the Clarence Fault in this northern region, separated from Torlesse rocks to the west by the Clarence Fault and to the east by the Peggioh Fault. The Peggioh Fault abuts the FCF in a complex structural relationship, the development of which is uncertain. This map pattern can be explained, in part, by E-W folding of the western end of the FCF to form a NE-plunging synform, with the L. Cretaceous - Tertiary rocks between the Clarence and Peggioh faults, to the west, exposed in a structural culmination.

The general map pattern of the FCFS implies a SE transport direction of the thrust sheets. Hangingwall ramps of several of the major imbricates (e.g., the Brian Boru and Ben More faults) appear to cut up-section to the SE (Fig. 3.2). Thus, on the western, NW-dipping limb of the BMA, structurally deep units persist to the NE and SW along strike. Further east, in the hinge area, where strata dip to the NNE, the FCFS is exposed in an oblique section-view at a higher structural and stratigraphic level than in the west. This region is complicated by folding of the Narrows Syncline, but faults here ramp up-

section to the east or SE, from low in the Herring Formation to varying stratigraphic levels of the Amuri Formation (e.g., in the footwall ramp of the newly recognised Black Hill Fault; Fig. 3.2). On the eastern limb of the BMA, strata dip steeply eastward and many faults and their associated mesoscopic deformation structures exhibit an apparent normal sense of dip-slip offset. Here in the coastal region, the imbricates occur at a higher stratigraphic level than in the west. Miocene rocks in the east are interpreted as syntectonic foredeep strata deposited and deformed at the emerging frontal edge of the imbricate FCFS, whereas the western region is interpreted to belong to an originally structurally deeper part of the FCFS that has only been recently exhumed. Thus, as one moves from northwest to southeast across the FCFS, increasingly shallow structural levels of a folded imbricate fan are exposed.

The BMA was previously mapped as a simple structure with a single fold hinge [e.g. Prebble, 1976; Waters, 1988]. However, detailed mapping reveals that the larger structure is an anticlinorium consisting of a train of several smaller folds (see Fig. 3.2). The westernmost fold-pair, the asymmetric Brian Boru anticline and syncline, fold both bedding and the Brian Boru Fault through a strike angle of ~160° from ~240° in the western limb to ~040° in the central (short) limb, then back to ~240° again on the eastern limb. The hinges of the Brian Boru folds, like the Ben More structure as a whole, plunge gently to the NE, at approximately 25°, a relationship which accentuates their arcuate map pattern. The actual interlimb angle of the Brian Boru folds in profile section is much larger than that implied by the map pattern, approximately 60°.

The main hinge zone of the BMA lies to the east of the Brian Boru folds, near Isolation Creek [Prebble, 1976; Waters, 1988]. This fold is expressed in map-view by a ~120° change in strike of bedding and the Ben More Fault. These curve from a strike of ~240° (west-dipping) in the west to ~000° (east-dipping) in the east. Not far to the east of the BMA, bedding strike is deflected ~60° anticlockwise, defining another asymmetric fold pair with a short limb that strikes ~300° and dips to the east. Bedding on the eastern limb of this newly recognised syncline, the Ben More syncline, strikes ~250° and dips to the NW (Fig. 3.2). To the east, in Woodside Creek, north of Mt. Napoleon and in Ben More Stream (Fig. 3.2), bedding is sharply deflected clockwise by ~60° (to become ~000° striking) around the axis of yet another antiformal structure. This eastern fold, here named the Woodside anticline, is interpreted as a younger

structure than the previously described folds on the basis of field-kinematic data (see below).

The Narrows Syncline is unusual in that its hinge trends NW-SE, approximately perpendicular to the NE-striking structural grain of NE Marlborough (Fig. 3.2). This NW strike is also a peculiarity of the FCF, suggesting a possible relationship in the kinematic evolution of these two adjacent structures. The NW trend of the Narrows Syncline and SW-directed reverse slip indicators on the FCF are key factors leading to the conclusion that the FCF was reactivated as a SW-directed contractional fault, "drag-folding" rocks in its footwall to form the Narrows Syncline. Thin beds of GMC in the core of the Narrows Syncline are overlain by rocks of the Heavers Creek Formation and suggest that folding of this map-scale structure took place after the early Middle Miocene [Vickery, 1994]. This time constraint fits well with Late Miocene clastic deposition in the Awatere basin [Roberts & Wilson, 1992], to the north of the FCF. If the FCF was reactivated as a SW-vergent thrust, the Awatere basin would lie on the reactivated back-limb, in a position to accumulate detritus eroded from the uplifting Torlesse Terrane hangingwall.

Marlborough is currently part of the Australia – Pacific transcurrent plate boundary zone and the Marlborough Fault System (MFS) is a locus of Plio-Pleistocene dextral shear that accommodates *c.* 40 mm a^{-1} of strike slip motion between the Pacific and Australian plates [DeMets et al., 1994; Holt & Haines, 1995; e.g., Fig. 3.1]. This late Pliocene – recent dextral shear is thought to be responsible for additional 20 – 40° of clockwise vertical-axis rotation of rocks that are in close proximity to active, dextral strike-slip faults, such as the Kekerengu Fault [Vickery & Lamb, 1995; Chapter 2]. The eastern part of the FCFS is truncated by the Kekerengu Fault (Fig. 3.2) and new and existing palaeomagnetic data from this eastern region imply that there has been as much as 40° of post-Miocene clockwise vertical-axis rotation over and above the regional ~100° that occurred during the period 18 – 8 Ma [Chapter 2]. The map pattern of the FCFS faults in this region imply a steepening towards the east, from gently NE-dipping, to become vertical and, eventually, overturned near the coast before being truncated by the Kekerengu Fault. This outcrop pattern may be explained by additional clockwise shear induced by "drag-folding" in a zone parallel to the Kekerengu Fault (Fig. 3.5). Because the Kekerengu Fault dips steeply to the WNW and is an oblique dextral-reverse fault [Barnes & Audru, 1999], the axis of drag folding will not be vertical, but

approximately perpendicular to the transport direction of that Fault (Fig. 3.5). This axis also happens to be approximately parallel to the intersection of the FCFS and the Kekerengu Fault. As fault offset and folding ensued, the eastern ends of the FCFS were progressively rotated about a N-plunging axis so that their coastal ends became overturned. It is possible that much of this folding took place in a zone of distributed dextral shear before being offset by the Kekerengu Fault. Thus, the map pattern of extra clockwise rotation, relative to more inland parts of the FCFS, in this zone of dextral shear adjacent to the active Kekerengu Fault has a complex 3-D relationship with the obliquity of slip and WNW dip of the fault. The steep- to overturned dip of Early Miocene Waima Formation siltstone and GMC in the Tirohanga area, also near the Kekerengu Fault, may be a consequence of this dextral/oblique shear (see structural map of FCFS, back pocket).

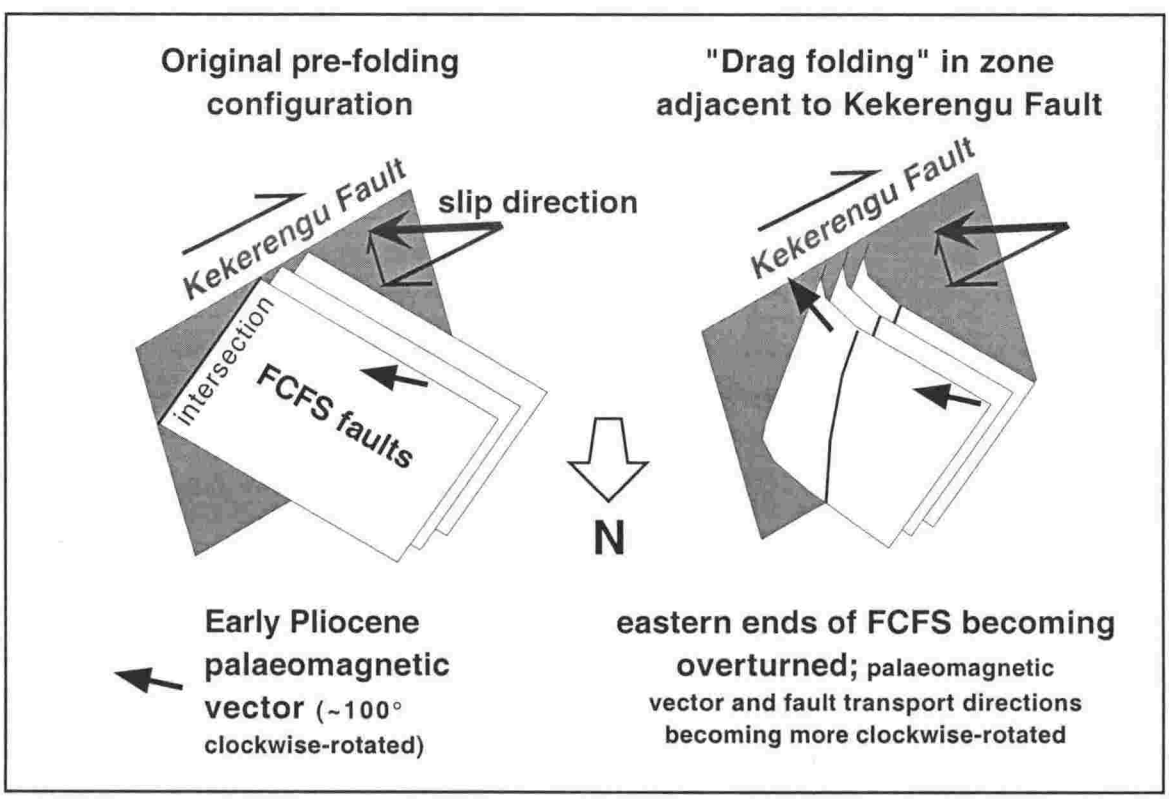

Figure 3.5. Dextral drag in a zone parallel to the Kekerengu Fault is thought to result in shearing of the eastern ends of the Flags Creek Fault System (FCFS) so that these faults have become locally overturned. This shearing is implied by palaeomagnetic data, the folded, overturned map-pattern of the eastern ends of the FCFS and southerly vergence of thrust transport directions in this area compared with SE-transport observed in the remainder of the FCFS. The situation is more complex than shown because the FCFS is not a simple parallel set of structures.

FIELD KINEMATIC DATA FROM MESOSCOPIC STRUCTURES OF THE FCFS

Transport of large-scale thrust sheets with tens of km's of offset generally result in an internal fabric that records their direction and sense of slip. Mesoscopic data in the form of faults with slickenlines, S-C ductile shear zones, folds, cleavage, veins and joints from the study region have been measured and analysed. These have been used to evaluate the principal horizontal shortening (PHS) or contraction direction at the time of thrusting. Where 3D vectors cannot be defined (as in the case for veins, joints and symmetrical folds) the direction of PHS is inferred from the strike of tensile veins/joints, or the strike of fold profile planes. Such data may yield a two-dimensional PHS vector, which implies nothing about the transport direction or vergence; however, in most cases, the transport or shear direction can also be inferred from the asymmetry of diagnostic fabric elements.

Structural correction of the data to remove the effect of later deformation and tilting include: 1) a plunge-correction for the regional folding to remove the NE plunge of the BMA, which has been determined by detailed field mapping to trend 052° and plunge 28° NE (this tilting is presumed to be younger than most of the thrust structures and), and 2) a subsequent rotation of bedding about strike to the horizontal. This last correction may not be necessary for all sites due to an expected variable original stratal tilt within the FCFS prior to folding of the BMA; however, in most cases, there are only a few degrees difference between the final transport/shortening directions of the *in situ* versus the corrected data.

Inferring thrust transport directions from meso-structures in proximity to major faults

Outcrop-scale kinematic data that are within ~500m of large faults of the FCFS are interpreted to have moved synthetically with those faults. Kinematic data on exposed fault surfaces of the major faults are rare. The lack of kinematic indicators on the macroscopic fault planes is made up for by the abundance of nearby mesoscopic faults, structures which commonly record slip vectors as calcite fibre slickenlines (Fig. 3.6A).

Shear zone fabrics (Fig. 3.6B) are commonly associated with major faults of the FCFS, the fault zones of which include a brecciated and/or cataclasitised mixture of wall-rock lithologies that is overprinted by a sigmoidal foliation that defines S-C fabrics. Poles to foliation attitudes within a single shear band define a girdle that is

parallel to the slip direction (the "m-plane," e.g., Marshak & Mitra [1988]). The intersection of the m-plane with the slip surface ("C-shear"; commonly parallel to bedding) yields an estimate of the slip vector. Additional field observations are necessary to determine the associated vergence direction or the sense of shear.

Stylolitic cleavage in Amuri Limestone forms anastomosing planes that generally lie at a moderate angle to bedding of ~40° (Fig. 3.6C). Like the S-C fabrics described above, poles to cleavage planes will define the girdle, or m-plane. Where bedding was originally subhorizontal at the time of deformation initiation, intersection of the "m-plane" with bedding yields the PHS direction. Where bedding is folded, the cleavage generally forms a constant dihedral angle to the folded beds of approximately 40°, implying that cleavage formed before those beds were tilted, as a response to early horizontal shortening strain. Other evidence that cleavage formation was early in the development of the FCFS is that limestone clasts in the GMC (deposition presumed coeval with fault movement) contain a variably oriented stylolitic cleavage that does not transect the conglomerate matrix [Vickery, 1994]. That the cleavage formed early in the FCFS deformation event is useful in that it provides a structural marker in the rocks that is presumed to have been regularly oriented with respect to the direction of fault transport.

Folds with amplitudes of ~1 – 5m and wavelengths of 0.5 – 10m are common in the study region. Most of these have hinges that trend NE, sub-parallel to the BMA (Fig. 3.6D). The vergence of asymmetric folds in bedding adjacent to map-scale faults is generally consistent with the vergence of the transport direction on those faults inferred from other slip indicators, suggesting that the folds formed in conjunction with thrust deformation.

Calcite-filled veins in limestone beds of the Amuri Formation are uncommon in the study area (Fig. 3.6E). These tensile extensional veins strike ~140°, generally parallel to the PHS direction inferred from other, nearby kinematic indicators (such as small faults and fold asymmetry), suggesting that the veins formed pene-contemporaneously with the thrust deformation.

A pervasive fracturing of the brittle lithologies (especially flint and limestone) was observed to the south of Mt. Ben More (Fig. 3.6F). These extension fractures generally strike parallel to the profile plane of the BMA and may be "ac" joints related to that fold. The restored strike of these brittle features differs slightly from the calcite

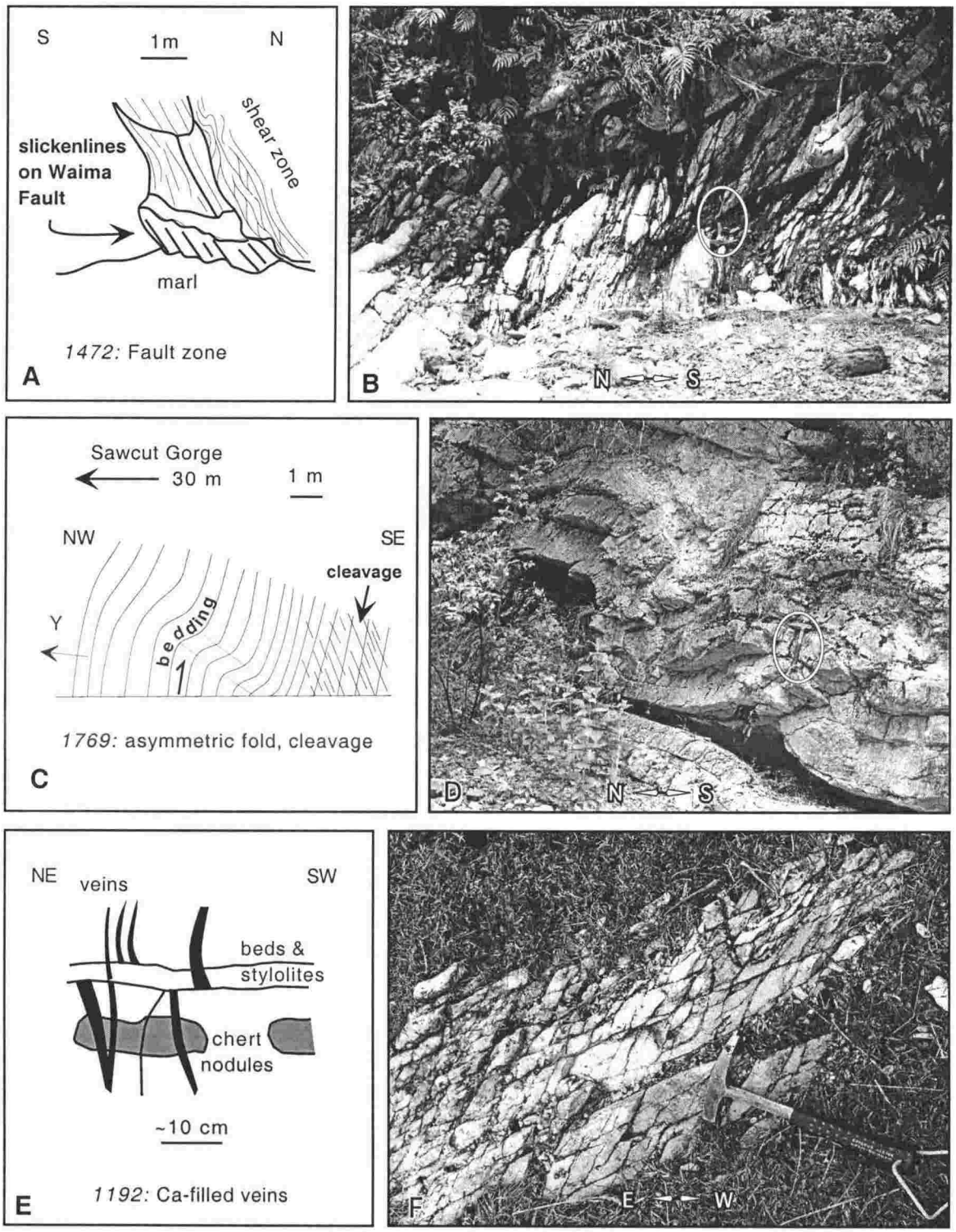

Figure 3.6. Different types of field kinematic data that have been measured and analysed for this study; A: Slickenlines at outcrop of Waima Fault; B: Sigmoidally foliated ductile shear zone in marly limestone in Isolation Creek, hammer is 33 cm long in all photos; C: Bedding-cleavage intersection relationships in Amuri Formation limestone near Sawcut Gorge, Isolation Creek; D: Asymmetric folding of limestone and marl beds in east branch of Isolation Creek; E: Field sketch of calcite filled veins cutting Amuri Formation limestone on the northern flank of Mt. Ben More and F: Pervasive brittle fracturing on limbs of Ben More Anticline. Numbers in italics refer to site locations; see Appendix 2 for more sketches and corresponding stereo-plots of data.

veins, mentioned above, as they are approximately parallel to the modern geodetic shortening direction of ~110° [Bibby, 1981].

SYNTHESIS OF KINEMATIC DATA

Mesoscopic kinematic data have been analysed in terms of both their transport directions and their principal directions of horizontal bulk strain (PHS). These data, compiled on Figure 3.7, yield remarkably consistent regional patterns throughout the western half of the field area, indicating dominance of a south or southeast direction of transport. The axes of map-scale folds (e.g., Brian Boru folds) deforming major fault traces are perpendicular to these transport directions, suggesting that motion on the FCFS and subsequent folding of those faults took place under a similar regime of NW – SE horizontal contraction.

The central and eastern parts of the study area show a more complex pattern of fault slip directions (Fig. 3.7). For example, the Ben More Fault has SE-verging thrust transport mechanisms, whereas the Tirohanga and Waima faults have a NE vergence and the Deep Creek Fault and FCF exhibit SW-directed thrust transport. The complexity of this region is interpreted as having resulted from overprinting of the original SE-directed FCF as a SW-directed thrust fault, probably in the Late Miocene (hatch pattern on Fig. 3.7).

The southern part of the FCFS on the NW side of the Kekerengu Fault exhibits mostly south-verging transport directions (Fig. 3.7). As previously mentioned, this area, close to the active Kekerengu Fault, is interpreted as having received late Pliocene to recent dextral shear (Fig. 3.7, hatch pattern), resulting in 20 – 40° more clockwise rotation than the rest of the FCFS, where transport directions are SE-verging. Thus, palaeomagnetic data, mapped outcrop traces of the FCFS and thrust sheet transport directions are in agreement that this south-eastern region of the FCFS has undergone approximately 40° more clockwise rotation than the remainder of the fault system.

The structurally complex exposures of syntectonic strata south of the Kekerengu Fault have been subjected to multiple phases of deformation [e.g., Lamb & Bibby, 1989], are stratigraphically complex and are exposed at a higher structural level than the region to the north of that fault (e.g., Fig. 3.2). Therefore, it is difficult to correlate faults in this area with structurally deeper exposures of the FCFS faults to the north of the Kekerengu Fault. Slip indicators on mesoscopic faults from the southern region

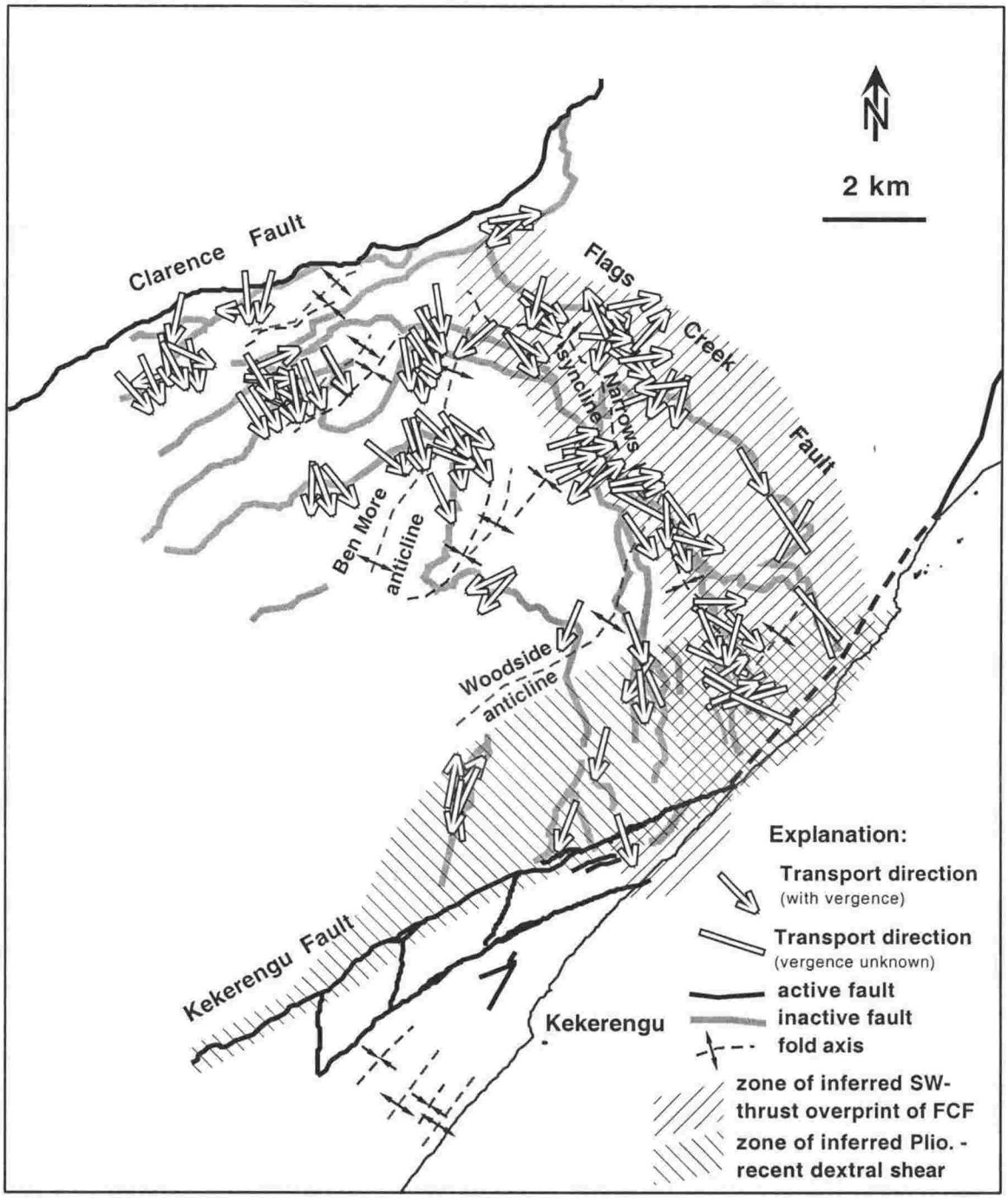

Figure 3.7. Calculated thrust sheet transport directions in the FCFS (n = 125). These directions have been structurally corrected for the effect of subsequent Pliocene - present-day folding and tilting. Arrows indicate the direction of vergence, where known. The western half of the study area shows consistently SE-vergent transport indicators, but the eastern half of the FCFS is more complicated. There, the SE-directed structures are interpreted as having been overprinted by SW-directed transport associated with reactivation of the FCF in that direction in the Late Miocene. In the Late Pliocene to present-day, dextral shear and strike-slip faulting has added to the structural complexity of the eastern FCFS, especially an apparent vertical-axis rotation of SE transport directions to a more southerly direction adjacent to the Kekerengu Fault.

cannot be directly correlated with slip on major thrust faults, but these record mostly SE transport directions, in agreement with most FCFS structures to the north of the Kekerengu Fault.

Inter-fault structures as recorders of bulk strain

Mesoscopic structures in outcrops that are >500m from the major faults of the FCFS are interpreted to have formed in response to intra-thrust sheet bulk deformation. In most cases, the analysed structures are identical to those observed near the major faults. Bulk strain PHS directions inferred from these data are similar to the transport directions near the major faults and are interpreted as mostly recording deformation relating to the thrusting event.

In addition to transport directions, the mesoscopic data have been formulated into directions of principal horizontal shortening (PHS). P- and T-axes for bulk intra-thrust sheet deformation have been calculated from inversion of slip lineations on individual mesoscopic faults, using the fault kinematic analysis program "FaultKin" [Marrett & Allmendinger, 1990]. Without an associated slip surface, a deformed quantity of fractures, joints and veins do not yield a 3-D slip vector and therefore cannot be interpreted in terms of transport directions, but the PHS direction implied by their formation can be determined. Calculated PHS directions have been further simplified by assigning each measurement within a 2 by 2 km square grid overlain across the field area (Fig. 3.8). The PHS direction of each grid square has been averaged from all of the PHS vectors of individual outcrop sets or analyses that fall in a particular square. It is apparent that, for most of the field area, contraction directions have chiefly NW – SE orientations. Exceptions to this are generally in the north and east of the study region, in the area that is inferred to have been overprinted by SW-directed contraction (hatch pattern on Fig. 3.8). Mean PHS directions in the eastern FCFS, near the Kekerengu Fault, exhibit a N-S contraction, implying a clockwise change in direction of approximately 40° from the NW-SE PHS that is interpreted as the dominant bulk shortening direction between faults of the FCFS. Most importantly for this study, near the hinge of the BMA, where bedding strike is deflected clockwise by ~110°, there is no apparent change in either direction of thrust sheet transport or intra-sheet PHS (Figs. 3.7 & 3.8). This rules out the possibility of large (~100°) differential clockwise vertical-axis

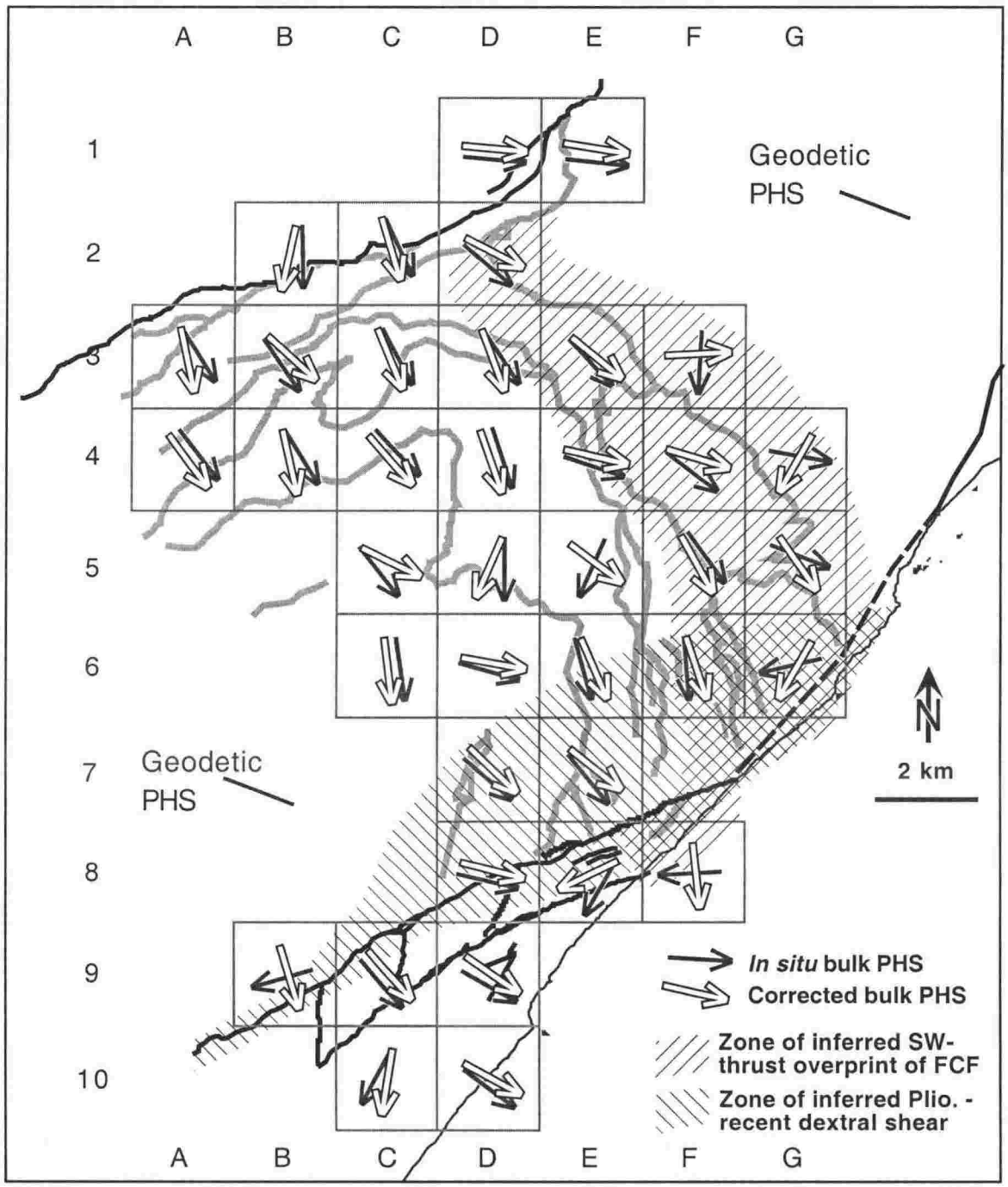

Figure 3.8. Principal directions of horizontal shortening (PHS) calculated from intra-thrust sheet field kinematic data from the FCFS, averaged over a 2x2 km square quadrant spacing. Grey arrows indicate the *in situ* mean horizontal contraction vector (PHS) for each grid square, whereas white arrows are the structurally corrected equivalent. In most cases, there is very little difference between *in situ* and corrected vectors. As most field data exhibit dip-slip displacements, contraction directions are similar to transport directions (compare with Fig. 3.7). Geodetic contraction direction of ~110° is after Bibby [1981].

rotation between the limbs of the BMA and implies that the entire FCFS may be treated as a single crustal block.

Mean bedding and fold hinge attitudes for each grid square have also been calculated using a similar vector summation method as that applied above (Fig. 3.9). It can be seen how changes in bedding strike across the BMA are not reflected by corresponding changes in the direction of bulk shortening. Fold hinge directions remain NE-plunging without being deflected across the BMA axis. In the northeast of the study area, close to the FCF, the mean fold hinge direction swings from NE-plunging to NNW-plunging in proximity to the FCF. This local reorientation of the bulk shortening direction is interpreted as more evidence for the later, SW-directed, dip-slip reactivation of the FCF (Fig. 3.9, hatch pattern). Once again, in the eastern part of the FCFS near the Kekerengu Fault, there is a consistent reorientation of the mean fold hinge directions to become more N-S oriented, a change that appears to overprint the (already) reoriented fold hinge directions in proximity to the FCF. Thus, at least three phases of deformation are interpreted from the directions of bulk PHS; the early phase is related to SE-verging thrust sheet emplacement and development of the FCFS, the second is related to reactivation of the FCF as a SW-verging thrust fault and the third is a consequence of Plio-Pleistocene dextral shear adjacent to the currently active Kekerengu Fault.

TECTONIC RECONSTRUCTION OF THE FCFS

Isolation Creek/Ben More Stream

A balanced cross-section through the FCFS, parallel to the south-easterly Early Miocene transport direction, has been constructed from detailed field mapping (see structural map; back pocket) such that faults begin to step down towards a decollement just below ground level, thus keeping the interpreted amount of shortening to a minimum (Fig. 3.10, located on Fig. 3.2). Slip is apparently tiered into three structural levels, with an upper decollement forming along the lower marl horizon of the Amuri Formation and a structurally deeper decollement forming within the Herring Formation. Surface exposures of both bedding and thrust faults in Isolation Creek are folded on a wavelength of ~1 km. This folding is interpreted as a response to horizontal contraction along an even deeper structural level, uplifting this part of the FCFS relative to the remainder of the section (Fig. 3.10). This lower slip surface is interpreted to be the unconformity between the Torlesse basement and the Burnt Creek Formation (BCF).

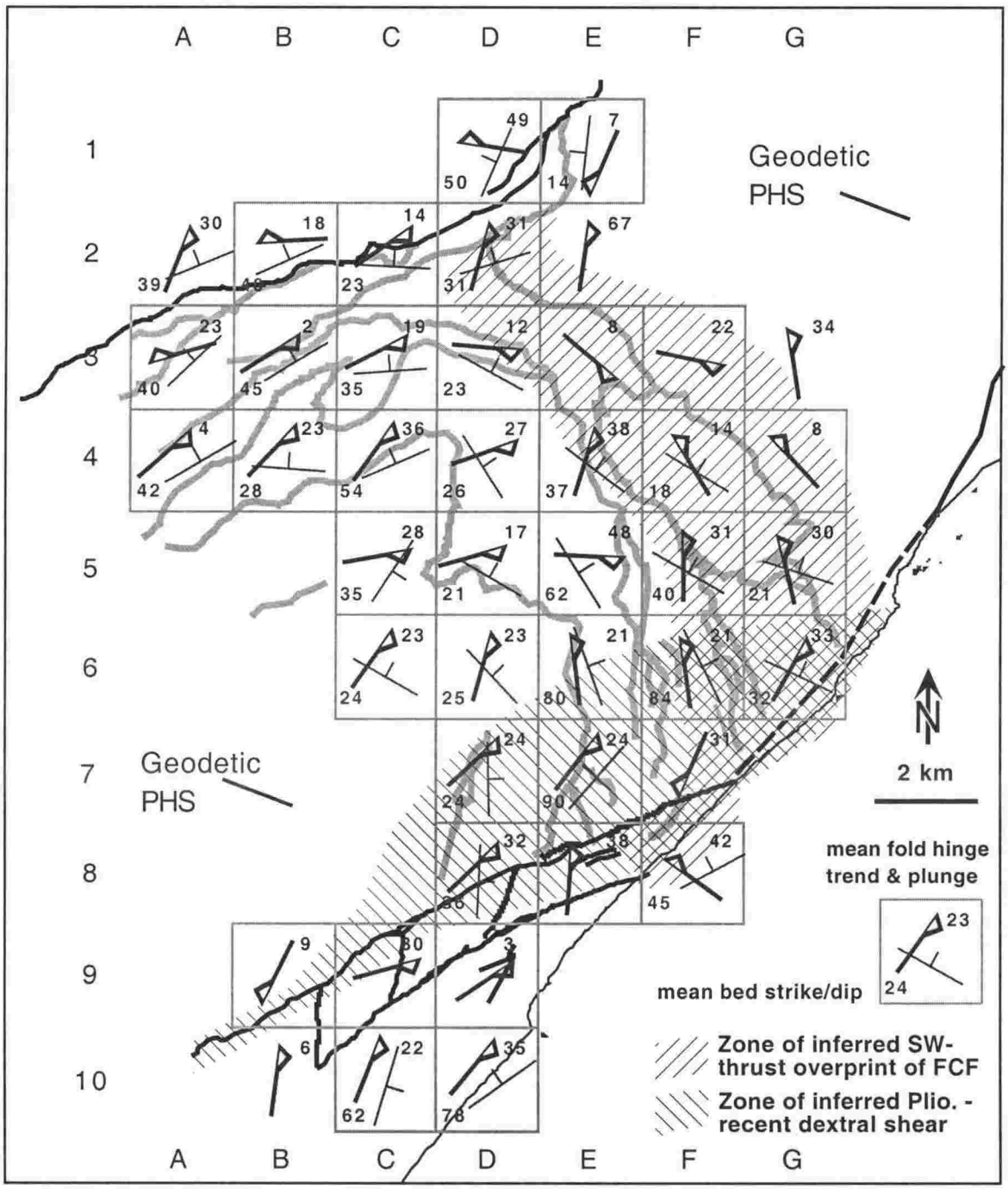

Figure 3.9. Mean bed orientation (dip given by lower left number) and mean fold hinge direction (plunge given by top right number) of each grid square. Bedding is deflected clockwise across the axis of the Ben More Anticline but hinge directions do not significantly change, suggesting that the axis of the larger fold is gently plunging and strain in this region has been co-axial (NW-SE contraction). Hinge directions do, however, significantly change orientation in the footwall of the Flags Creek Fault, interpreted as reactivation of the FCF as a SW-directed thrust fault. Pliocene to recent dextral shear is inferred to have affected the eastern part of the FCFS, adding a component of vertical-axis rotation to this area. Geodetic shortening direction of ~110° is from Bibby [1981].

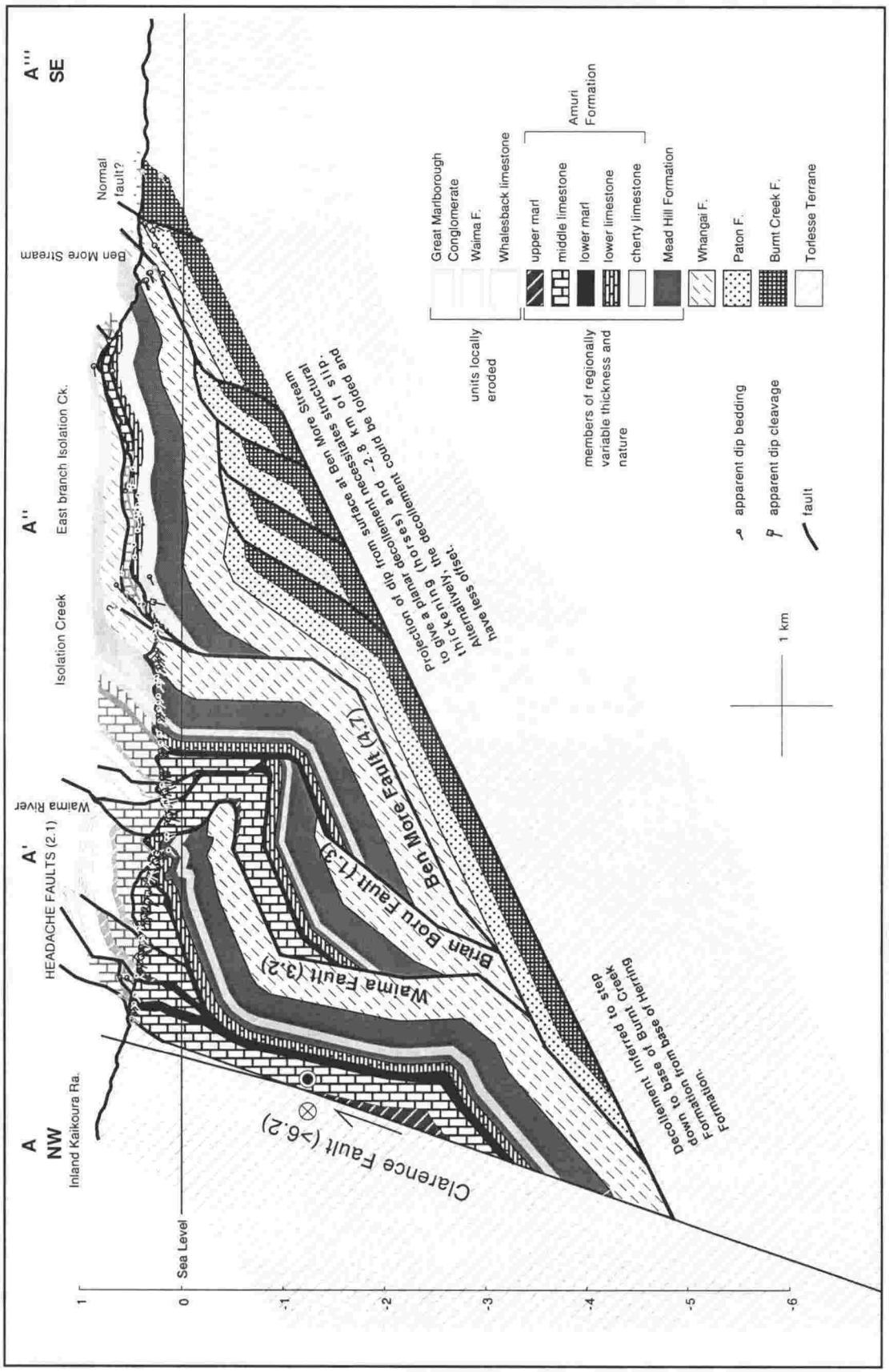

Figure 3.10. Restorable geological section A-A'-A"-A'" through the FCFS from the Clarence Fault in the NW to the decollement outcrop at Ben More Stream in the SE, made from 143 surface observations. Minimum fault offset (in km) is given for each fault. See Figure 3.2 for location of section and Figure 3.11 for restored section.

Field evidence for this lower decollement is the pulverised nature of the mud-rich and heavily slumped BCF in Ben More Stream. In addition, conglomerate pebbles in the BCF have extremely polished and, sometimes grooved, surfaces within their matrix of sheared-mudstone. This fabric is interpreted as the result of tectonic shearing along the interface between the Torlesse and non-Torlesse rocks.

Restoration of section A-A''' implies about 16 km of horizontal shortening (Fig. 3.11). The minimum amount of slip along the lower two decollements is 13.6 km (55% strain), with a further ~2 km slip along the upper decollement (43% strain), bringing the total horizontal shortening across the section to 15.7 km. The decollement dips towards the hinterland at approximately 30° (Figs. 3.10 & 3.11). This NW dip has been retained when palinspastically restoring this section, but is interpreted as having occurred due to tightening of the BMA (of which this section lies on the NW limb), after initial thrust offset. Thus, the original dip of the decollement is likely to be much less than its current 30°.

Truncation of the FCFS by the Kekerengu Fault with its downthrow to the east makes correlation of FCFS imbricates across this active fault difficult. This problem is compounded by the downthrown rocks to the east of the FCFS being structurally and stratigraphically higher than those to the NW of the present-day Kekerengu Fault, which have been subject to increased erosion. Local unconformities, e.g., at Willawa Point and Valhalla Stream (Fig. 3.2) were scoured into uplifted foreland parts of the FCFS (see Fig. 3.4). These relationships probably contribute to stratigraphic and map pattern differences across the Kekerengu Fault in the Miocene section. For this reason, it is not possible to precisely constrain the amount of bedrock offset along the Kekerengu Fault; however, a dextral strike separation of 5-6 km is inferred from offset Herring and Amuri Formations that crop out in Ben More Stream on the northern side of the Kekerengu Fault, and near the top of Valhalla Stream on the southern side of this fault (Fig. 3.2; FCFS map; back pocket). Because these units dip to the east and the Kekerengu Fault has a component of uplift to the west, the strike separation is likely to be greater than the actual dextral offset.

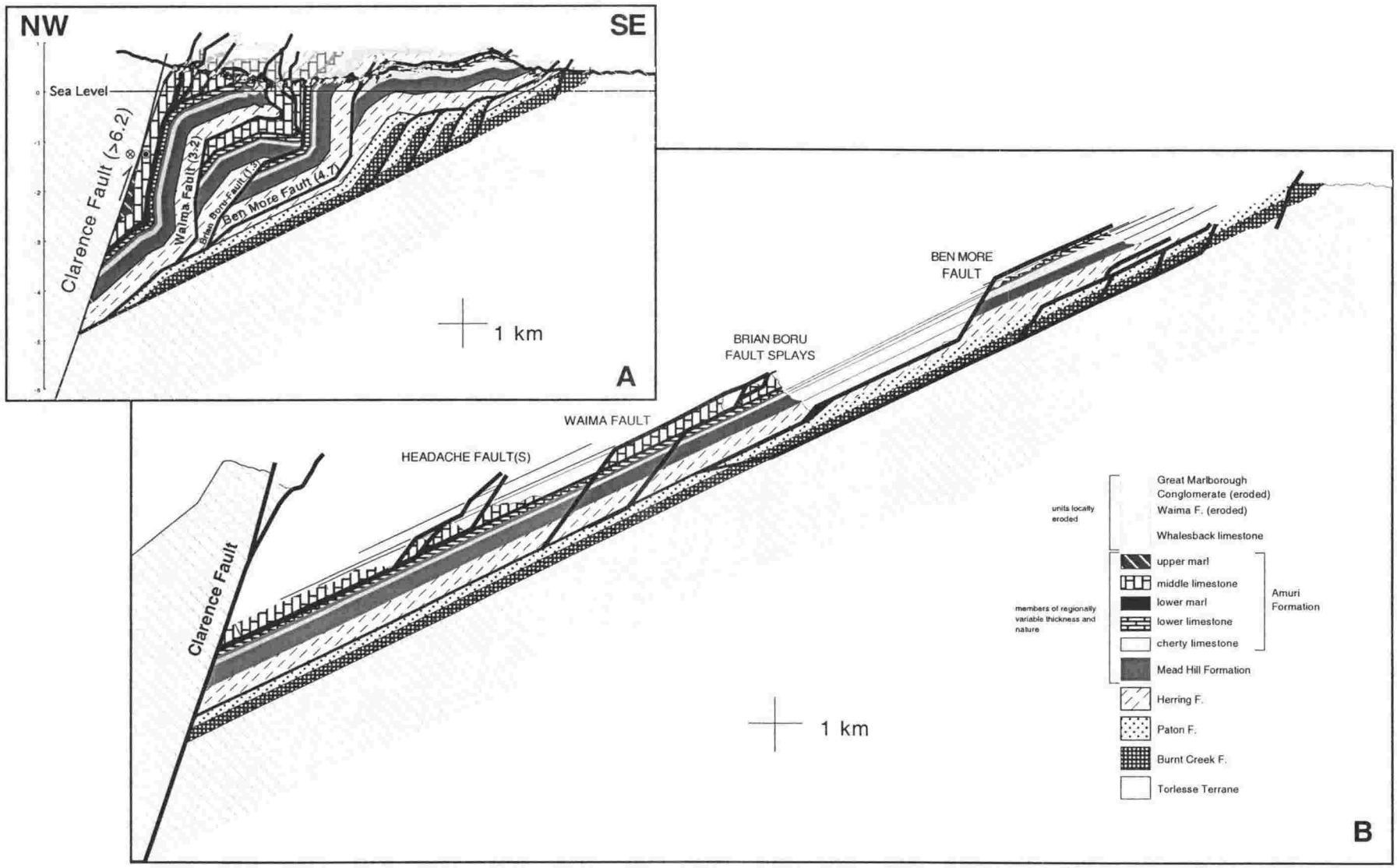

Figure 3.11. Restored cross section through the Flags Creek Fault System. A: Deformed state constructed from 143 surface observations (see Fig. 3.10), and B: the restored section, to the same scale, with ~16 km of horizontal shortening removed. The dip of the decollement is interpreted to have occurred due to later tightening of the Ben More Anticline.

Valhalla Stream

Rocks on the downthrown side of the Kekerengu Fault are well-exposed in Valhalla Stream, to the SE of the fault trace. A geological section through this area (Fig. 3.12, located on Fig. 3.2) transects mostly Early Miocene strata that are, because of their chiefly fine grain size, interpreted as having been deposited when activity of the FCFS was waning. Some parts of the sequence, however, are intensely folded, suggesting that, as thrust faulting in internal parts of the FCFS ceased, significant deformation by folding and, later, strike-slip faulting took place in its foreland to the SE. Due to the active strike-slip faulting in this area (Kekerengu & Heavers Creek faults), blocks in the section between these faults have been treated as separate structural entities. Between the Kekerengu Fault and the Heavers Creek Fault, strata dip steeply and almost homoclinally, with many beds overturned (Fig. 3.12). Between the Heavers Creek Fault and the coast, strata are intensely folded but, overall, a narrow stratigraphic range is exposed. Folding in this area may be accommodated by detachment at depth along incompetent, smectite-rich layers of Eocene-aged marl of the Amuri Formation, which is often exposed in the cores of tight anticlines and along the active faults (Fig. 3.12 & map).

The total amount of shortening in the coastal part of the section (due to folding) is calculated to be ~800m (0.3 strain; Fig. 3.13). Shortening in the western part of the section is more difficult to determine, because it relies on an interpretation of the structural history. This part of the section has been constructed so as to conform to a southeast-ward thrust fault vergence that is documented by mesoscopic deformation fabrics in the majority of the FCFS. Thus, the observed repetition of Early Miocene rocks of the inland block (Fig. 3.12) is interpreted as having occurred due to emplacement from the northwest. Due to eastward tilting of these rocks on the eastern limb of the BMA, they have become overturned in the direction of thrust fault transport, or to the SE, altering their apparent sense of motion from SE-verging thrust to SE-verging normal faults. Additional to folding on the eastern limb of the BMA, deformation interpreted to be a consequence of dextral/reverse shear adjacent to the active Kekerengu Fault has further tilted these rocks so that many structures have become downward-facing. The total amount of slip along both faults of the inland block (Fig. 3.13), parallel to the tilted bedding, is 3.6 km.

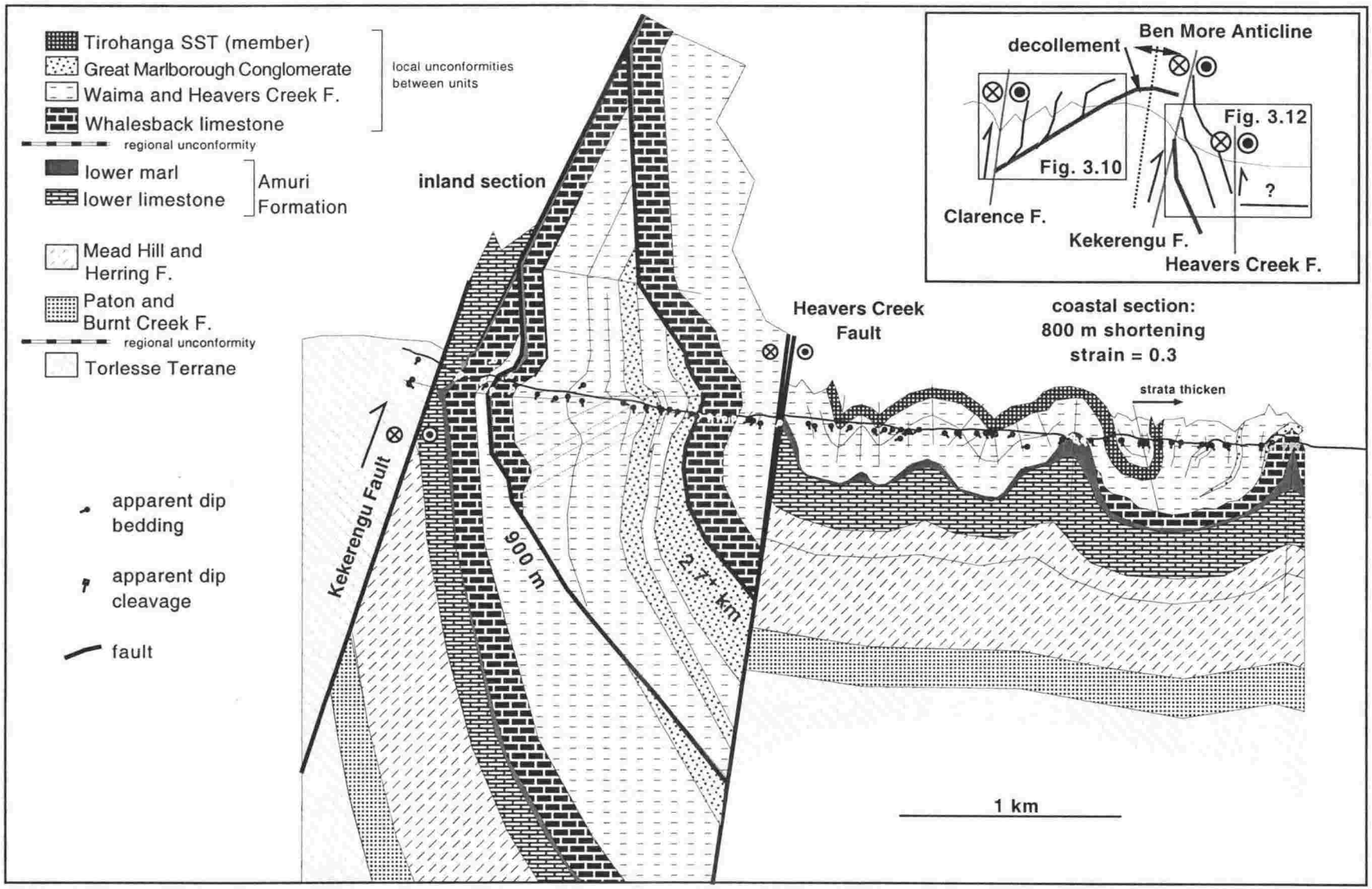

Figure 3.12. Cros-section parallel to Valhalla Stream, on the downthrown side of the Kekerengu Fault (see Figure 3.2 for location) constructed from 88 surface measurements. The section is broken into discrete parts by the active Kekerengu and Heavers Creek faults. See Figure 3.13 for restored section. The inset shows how this section relates to the previous section (Figures 3.10 & 3.11) across the regional scale Ben More Anticline.

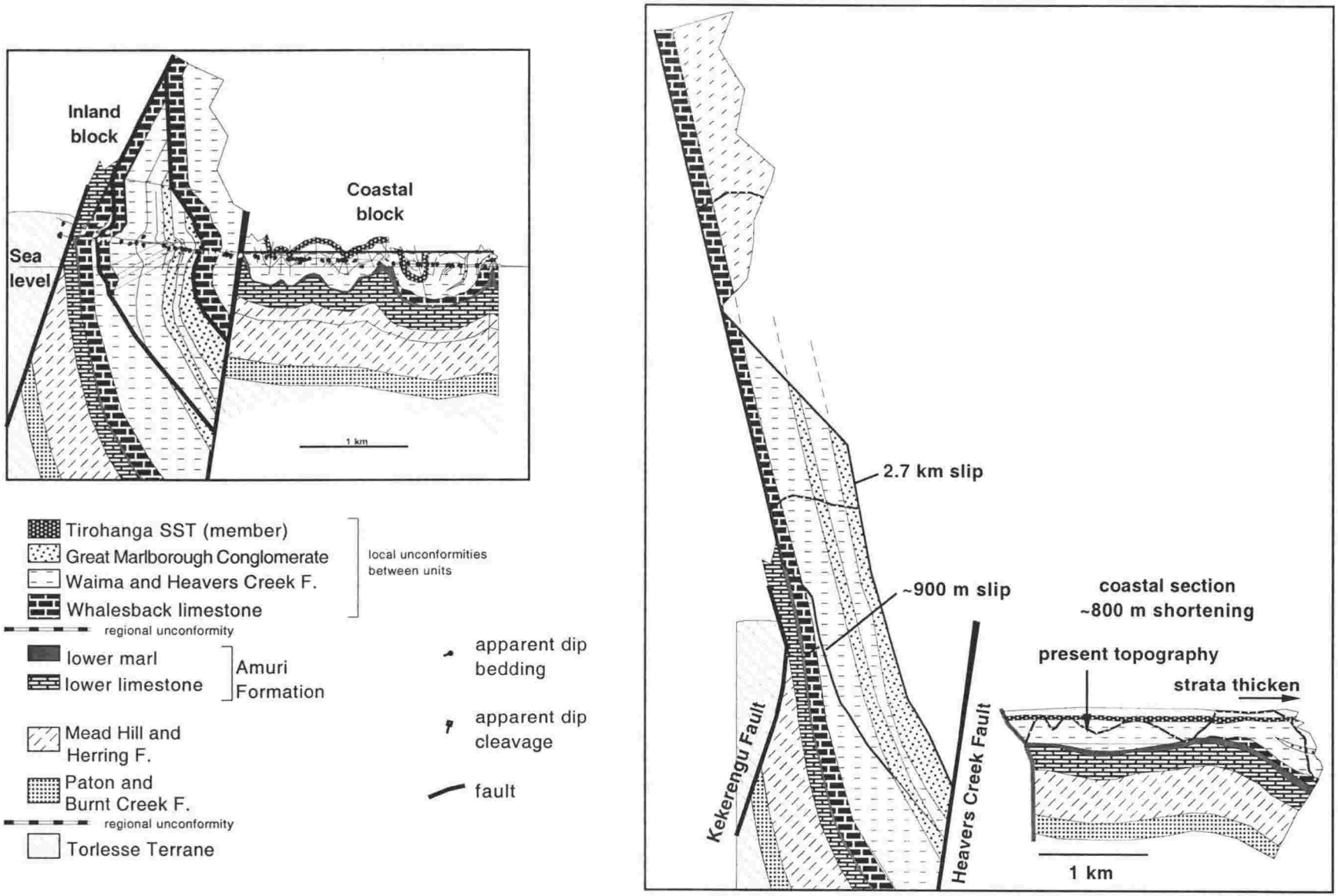

Figure 3.13. Valhalla Stream section (Y-Y'; located on Figure 3.2) restored with the coastal block unfolded so as to straighten the Tirohanga Sandstone member of the Waima Formation. The inland block has 3.3 km of fault-slip removed. Younger folding of the footwall rocks of the Kekerengu Fault, approximately 40° of eastward tilting of an upper limb, has also been removed.

TIMING OF FAULT MOVEMENT

Evidence of the timing of relative motion in different parts of the FCFS includes the folding of higher fault-bounded slices by later ramping of structurally deeper faults (e.g., Fig. 3.10). In the structurally highest thrust sheet, which constitutes the footwall of the present-day Clarence Fault, folding is generally tighter and more abundant than in lower thrust sheets. This intense deformation in parts of the fault system closer to the hinterland implies that the general style of faulting within the FCFS was of a leading edge type, with western (hinterland) thrusts having moved first, then being deformed piggy-back style by structurally deeper (foreland) faults to the east. A schematic cross-section of the early development of the upper-level Headache Creek duplex system, which closely resembles rarely-exposed meso-scale duplexes formed within interbedded limestone and marl of the Amuri Formation, is shown in Figure 3.14. Thrusting on the proto-Clarence/Flags Creek Fault is interpreted to be one of the earliest offsets within the FCFS, but offset may have been long-lived, eventually forming a nappe of Torlesse rock that overrode the FCFS to the east. Evidence for this is the SE transport directions indicated by deformation fabrics along the FCF that are interpreted to be coeval with SE-directed thrusting on the laterally contiguous Clarence Fault, along strike to the west. Other evidence for the relative timing of motion on the Clarence/FCF is derived from uplift of the Tapuae-O-Uenuku plutonic complex (TPC), which, in the Late Cretaceous, was emplaced into Torlesse rocks that now form the hangingwall of the Clarence Fault. An apatite fission-track age of 22 Ma attests to cooling of the TPC through the partial annealing zone of apatite (approximately 120 – 60°) [Baker & Seward, 1996], implying thrust fault activity of the Clarence/FCF at this time. This 22 Ma exhumation age is bracketed by the 24 – 20 Ma age of the GMC [Prebble, 1976], which was most likely sourced from erosion of uplifting parts of the FCFS, including the hangingwall of the proto-Clarence and proto-Flags Creek faults.

The youngest strata known to be deformed by the FCFS are Middle Miocene in age (U. Lillburnian – U. Waiauian Heavers Creek Formation [Vickery, 1994]). Siltstone overlying thin beds of GMC in the Waima River valley (i.e., Heavers Creek Formation) are overthrust by the Deep Creek Fault, all of which are, in turn, folded by the Narrows Syncline. Therefore, the DCF, which is structurally one of the uppermost faults in the system, must be younger than the GMC (24 – 20 Ma). If the FCFS is a leading

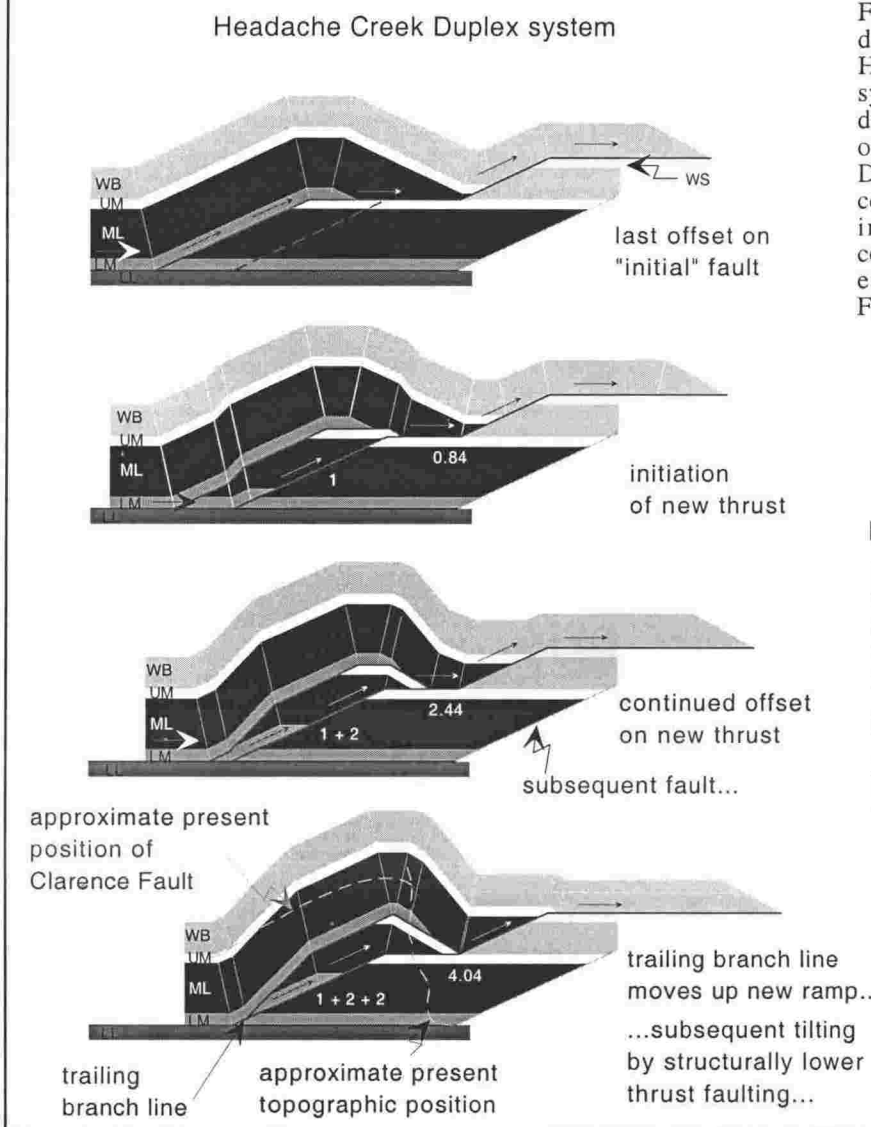

Figure 3.14a. Early development of the Headache Creek duplex system, or the upper level decollement represented on Figures 3.10 & 3.11. Detachment horizons commonly occur between incompetent marl and competent limestone layers of the Amuri Formation.

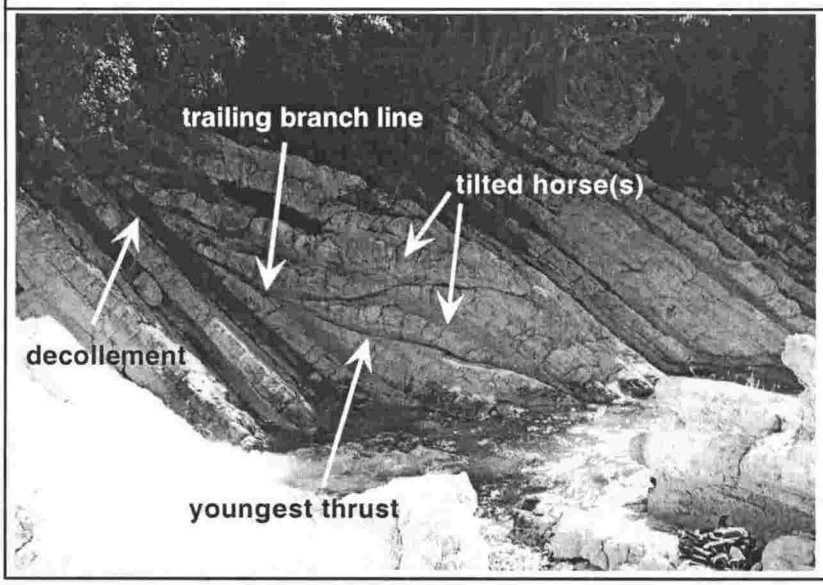

Figure 3.14b. Field example of above described duplex-style deformation in upper Waima River. Alternating layers of competent limestone and incompetent marl are repeated on a larger scale within the Amuri Formation. Vergence is to the SE (right hand side of figure) and shortening strain in the visible part of the duplex is 63% (parallel to bedding). Strata have been tilted to the east by folding subsequent to reverse offset. Back pack in right hand foreground for scale.

imbricate fan (younger faulting towards the foreland), then post-middle Miocene activity of the DCF marks one of the earliest ruptures. This relationship is also important for constraining the relative timing of folding of the Narrows Syncline (and thrust reactivation of the FCF), which must be later than the post-Middle Miocene movement on the DCF.

Due to later folding of the BMA and tilting to form its NE plunge, the youngest, structurally deep faults of the forward-propagating FCFS are now preserved within the core of this regional fold. No pre-Quaternary strata have been observed deposited above any faults of the FCFS, therefore the minimum age of displacement is not directly constrained and must be inferred from relative tectonic quiescence implied by deposition of the fine-grained Heavers Creek Formation (~15 – 12 Ma). That this post-tectonic unit is only ~5-7 Ma younger than the poorly-sorted, syntectonic GMC attests to the short time interval over which the FCFS was active.

Discussion

A reconstruction for the Kekerengu region based on new and existing palaeomagnetic and structural data is presented in Figure 3.15. NE, seaward-verging thrust faulting above an Early Miocene subduction zone was laterally continuous along the east coast for ~400 km [Rait et al., 1991, Delteil et al., 1996], with the FCFS located near the southern termination of subduction (Fig. 3.15A). Variable uplift in association with fold-thrust belt development, especially in the eastern part of the study area which was well below sea level (foraminifera from the GMC and Waima Formation suggest depths of outer shelf to upper continental slope [Vickery, 1994]), resulted in local deposition of the GMC in fans and canyons that were scoured into tectonically imbricated continental shelf (Fig. 3.15B). The proto-Clarence Fault was apparently a backstop to the FCFS and its Early Miocene movement formed a thrust nappe of Torlesse terrane rock (Fig. 3.15C), of which the WNW-striking FCF was the overthrust. Structurally restored transport markers (dextral strike-slip prior to restoration) along the FCF indicate the same SE direction of motion (present day) as for the NE-striking Clarence Fault.

In the latter stages of FCFS development, possibly as the Alpine Fault propagated along strike to become a through-going structure in the South Island, the eastern

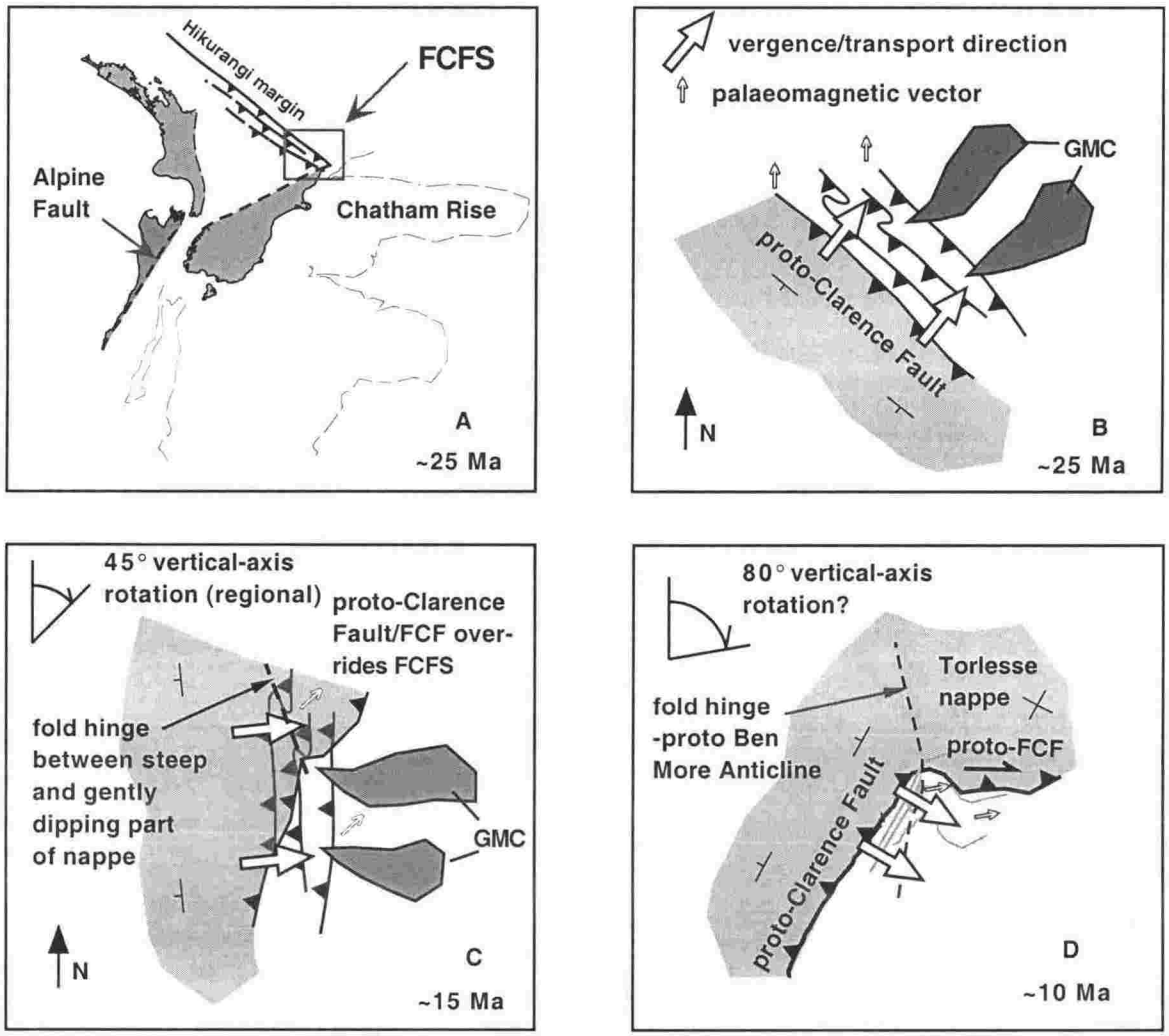

Figure 3.15. Reconstruction of the Kekerengu region for the last 25 Ma. A: Regional setting at the southern termination of the Early Miocene subduction zone, after Sutherland [1995]; B: activity of the Flags Creek Fault System (FCFS) and local deposition of the Great Marlborough Conglomerate (GMC) in submarine canyons; provenance indicates erosion of locally uplifted parts of the FCFS and hangingwall of the proto-Clarence Fault; C: formation of an overthrust nappe of Torlesse basement and folding of the overthrust limb about a gently N-plunging axis. This axis is the same structure as the "rotation boundary segment 4" of Little & Roberts [1997], but, contrary to their interpretation, folding about this structure was early Middle Miocene in age and occured about a sub-horizontal axis. Extremely rapid regional clockwise vertical-axis rotation was well underway by this time; D: regional vertical-axis rotation continues along with erosion of Torlesse nappe. Figure continues on p. 106.

Marlborough region began to rotate clockwise about a vertical axis in response to distributed strike-sip shear (Figs. 3.15C & D) [e.g., Lamb & Bibby, 1989; Vickery & Lamb, 1995]. Continued regional clockwise vertical-axis rotation, totalling ~100° by 8 Ma, resulted in the originally NE-vergent structures becoming SE-vergent by the Late Miocene (Fig. 3.15E). This regional rotation must have ceased by 6-7 Ma, as some Late Miocene clastic rocks of the middle Awatere Valley are unrotated [Little & Roberts, 1997]. New palaeomagnetic data [Chapter 2] and the similarity of thrust sheet transport directions across the regional BMA suggests that the entire FCFS acted as a rigid block during this regional rotation. Reactivation of the FCF as a SW-directed thrust fault early in the Late Miocene may have steepened Torlesse strata in its hangingwall (Fig. 3.15F) and formed the Narrows Syncline in the footwall of the FCF. This reactivation of the FCF may have been coeval with Late Miocene formation of the Medway Fault System, 10 km to the north, as recorded by syntectonic deposition of coarse-grained marine fanglomerates within the Awatere Basin (Figs. 3.15F & G). Shortening across the Ward and Cape Campbell synclines and the London Hill Fault (Fig. 3.15G; cross-hatch pattern) may also have been initiated at this time. Northeast-ward tilting of NE Marlborough throughout the Pliocene and recent times [Chapter 5] has resulted in most fold hinges obtaining a NE plunge. Dextral strike-slip deformation in the late Pliocene has reactivated the proto-Clarence Fault as a strike-slip fault, offset the eastern limb of the BMA by slip on the Kekerengu Fault and overturned the eastern, truncated ends of the FCFS by "drag folding" (Fig. 3.15H). Local clockwise vertical-axis rotation up to of 50° (Fig. 3.15H; diagonal hatch) has affected strata in proximity to these currently active faults [Vickery & Lamb, 1995], also further rotating Early Miocene transport directions to become south-verging in this zone of Plio-Pleistocene dextral shear.

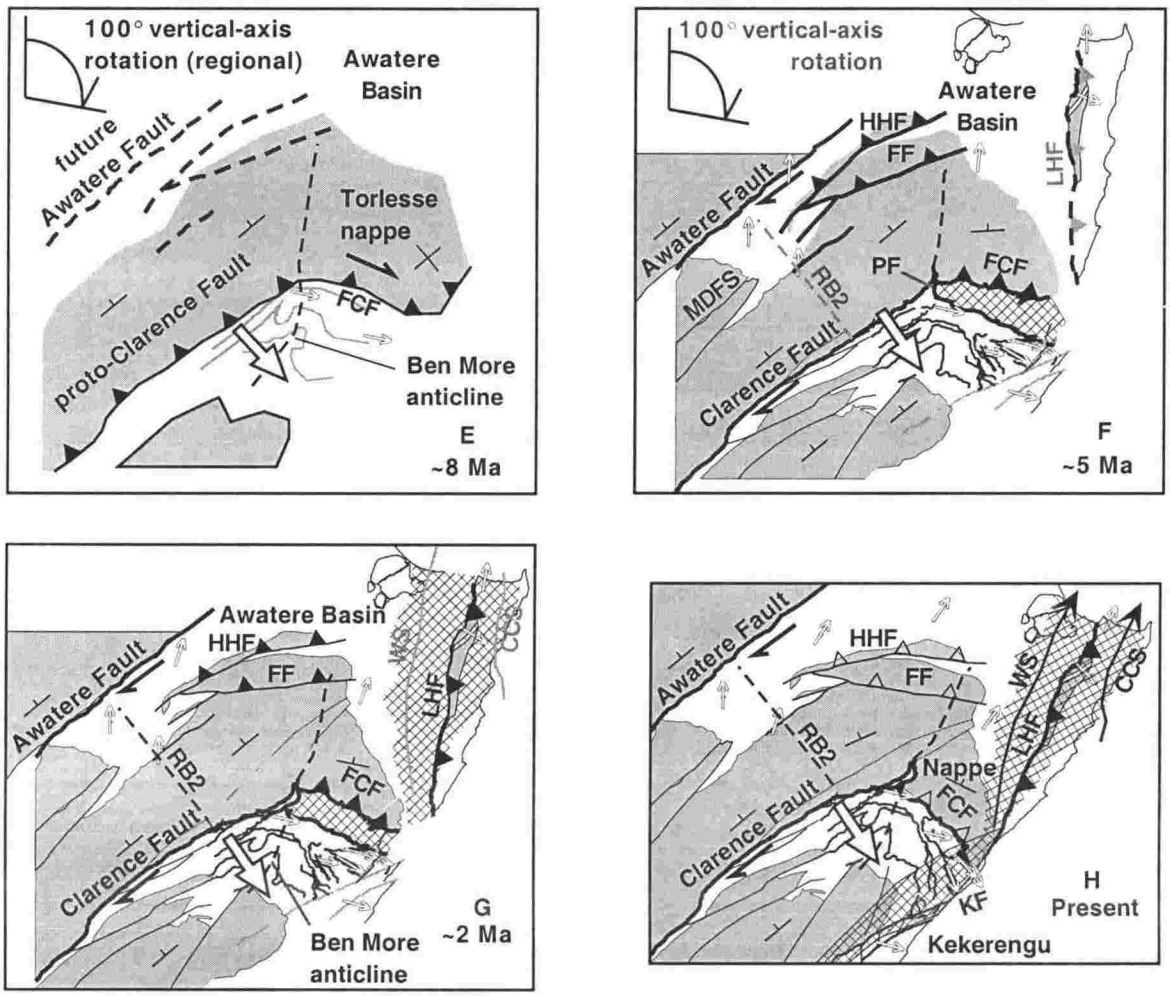

Figure 3.15 -continued. E: Regional clockwise vertical-axis rotation of ~100° was completed by 8 Ma and originally NE transport directions within the FCFS are now SE-oriented. Continued erosion of Torlesse nappe and thrust faulting in the Medway Valley/Awatere basin begins; F: reactivation of the FCF as a SW-directed thrust, tilting of Torlesse hangingwall strata, folding of the Narrows syncline (cross hatch pattern), with the Peggioh Fault (PF) possibly accommodating differential slip at the western end of the folding zone; G: late Pliocene rotation of Awatere basin, bounded to the SW along rotation boundary 2 (RB2 [Little & Roberts, 1997]) and to the east by thrusting on the London Hill Fault (LHF). Activity of the Ward and Cape Campbell synclines probably initiated at this time (cross hatch pattern); H: continued rotation of Awatere basin, up to 44° in some parts, with further contraction across LHF and Ward and Cape Campbell synclines (WS & CCS). Dextral shear of approximately 50° (clockwise) in a zone adjacent to the Kekerengu Fault and wrench folding of the eastern limb of the Ben More Anticline (cross hatch pattern) is inferred to have resulted in the overturning of the eastern, truncated ends of the FCFS and the clockwise-rotation of SE-vergent transport directions of the FCFS to become S-vergent near the coast. See text for full discussion.

Conclusions

The Flags Creek Fault System (FCFS) marks the southern limit of "thrust nappes" that are part of a > 400 km-long belt that formed above a subduction-trench system along the east coast of the North Island in the latest Oligocene – earliest Miocene. A minimum of 16 km of horizontal shortening within the FCFS since the Early Miocene is implied by restorable cross-sections through the deformed belt. Fault, fold, shear zone and cleavage –related transport directions near major faults of the FCFS record a southeast vergence and transport direction of large-scale thrust blocks, including a Torlesse Terrane nappe, that now forms the hangingwall of the Clarence and Flags Creek faults. The Flags Creek Fault (FCF) and the proto-Clarence Fault are genetically the same structure, which formed as an Early Miocene "backstop" to the FCFS. The fold hinge between the rooted limb (proto-Clarence Fault) and the nappe (FCF) was NW-trending and sub-horizontal at the time of its formation (the proto-Ben More Anticline). Regional NE tilting resulted in the nappe (FCF) having attained a moderate NE dip by the end of the Miocene. Palaeomagnetically-determined clockwise vertical-axis rotation of NE Marlborough (up to 100°) began at about this time. This rotation converted the entire, already extant FCFS from a NE-vergent thrust stack to a SE-verging one (present-day coordinates). Reactivation of the folded, tilted nappe (FCF) as a SW-directed thrust fault in the Late Miocene is inferred from NE-SW contraction of rocks on its footwall (the Narrows Syncline), by overprinting of mesoscopic fault and fold structures outcropping along the fault zone and by stratigraphic relationships on the tilted backlimb of the FCF in the Awatere basin.

The similarity in structurally corrected transport direction on all limbs of the (restored) Ben More anticline is evidence that the arcuate shape of the FCFS is not the product of differential vertical axis rotations between the limbs. Thus, the hinge of the Ben More Anticline is not a local boundary about which these very large crustal-scale rotations have occurred, affecting only part of the FCFS. Palaeomagnetic data for parts of the FCFS indicate that clockwise vertical axis rotations of ~80–100° took place during the early Middle Miocene (younger than ~17 Ma), slightly after the inception of NE-directed thrust faulting at ~24-18 Ma. These data support the theory that a large part of eastern Marlborough has undergone a regional vertical axis rotation of up to 100° [eg, Vickery & Lamb, 1995]. The Clarence Fault has since become reactivated as one of

the crustal-scale Marlborough Faults, currently accruing strike slip offset at a rate of ~5 mm a^{-1} [Van Dissen & Nicol, 1999].

Restoration of SE-vergent transport in accordance with 100° of regional clockwise vertical-axis rotation since the Early Miocene results in NE-vergent, seaward-directed thrust faulting that is consistent with the relative plate motion vector from Early Miocene plate boundary reconstructions. Although coastal parts of Marlborough have undergone large clockwise vertical-axis rotations (up to 100°), sites that record greater rotation than this are restricted to areas adjacent to active or recently active dextral faults. Pliocene to recent dextral shear is favoured as a mechanism for imparting extra clockwise vertical-axis rotation, over and above the regional amount, to rocks of coastal NE Marlborough in a zone adjacent to the active Kekerengu Fault. This shear has also affected the Early Miocene transport directions of the FCFS so that a southerly vergence is observed in this zone. The eastern ends of the folded FCFS thrusts are truncated by the Kekerengu Fault and some have become overturned in this zone of active deformation. These observations are consistent with the style of deformation in the plate boundary zone changing from subduction-related thrusting in the Early Miocene to strike-slip/transform deformation in the Pliocene, a transition that occurred both spatially and temporally along the margin.

Chapter 4: Late Quaternary fluvial terraces of eastern Marlborough and their correlation within central New Zealand

ABSTRACT

Quaternary fluvial terraces of the Awatere Valley, NE Marlborough, New Zealand, are extremely well preserved, due mainly to the aridity of the local climate and a constant regional uplift. Existing Quaternary terrace stratigraphy of the Awatere River catchment is revised by the measurement of five optically stimulated luminescence (OSL) ages on loess and applied over the wider coastal NE Marlborough region. New OSL dating indicates an abandonment age for the Starborough-1 terrace, correlated with the last major aggradational event in NE Marlborough, of 9.15 ± 7.1 ka. This date is much younger than a previous ~16 ka thermoluminescence (TL) age estimate of Starborough-1 terrace abandonment from loess at exactly the same location. Fluvial terraces assumed to be correlative of the Awatere aggradation surfaces are preserved to the south of the Awatere Valley, along the Flaxbourne River near the town of Ward. Correlation of these surfaces that are peripheral to the Awatere Valley has been achieved by assessing their morphostratigraphic position and by mapping from detailed aerial photographs. OSL dating of loess from a flight of four terraces cut by the Flaxbourne River yield abandonment ages of 70 - 80 ka and ~100 ka, indicating a mean incision rate of 1.0 mm a^{-1} over the last ~100 ka. This incision rate includes eustatic and tectonic components of fluctuating stream base level, inferred to be 0.7 and 0.3 mm a^{-1}, respectively. The elevation of other terraces at this site, that were not optically dated, have been used to infer approximate abandonment ages of ~120 ka and ~80 ka, suggesting that the chronology of terrace aggradation in NE Marlborough can be matched to warming periods on the oxygen isotope curve. It is concluded that, in this peri-glacial region, terrace aggradation is due to a downstream pulse of sediment during peak deglaciation/warming, rather than glacial outwash at the time of maximum glaciation.

INTRODUCTION

The Awatere River valley, eastern Marlborough (Fig. 4.1), has extensive flights of well-preserved fluvial terraces, some as old as ~350 ka. Preservation is due mainly to aridity of the local climate coupled with a constant uplift rate of 1-2 mm a^{-1} over the last *c*. 0.5 Ma [Wellman, 1979]. This uplift allows incision by the modern Awatere River which leaves morphologically higher lateral terrace remnants. These terraces provide an excellent record of Late Quaternary fluvial aggradation and degradation in the Awatere Valley. In this paper, previous soil and loess mapping work on terrace surfaces in the lower Awatere Valley is synthesised along with published luminescence ages, carbon dates and five new optically stimulated luminescence (OSL) ages on loess. Nine new locations of the Kawakawa Tephra (Aokautere Ash) are recognised in the study which

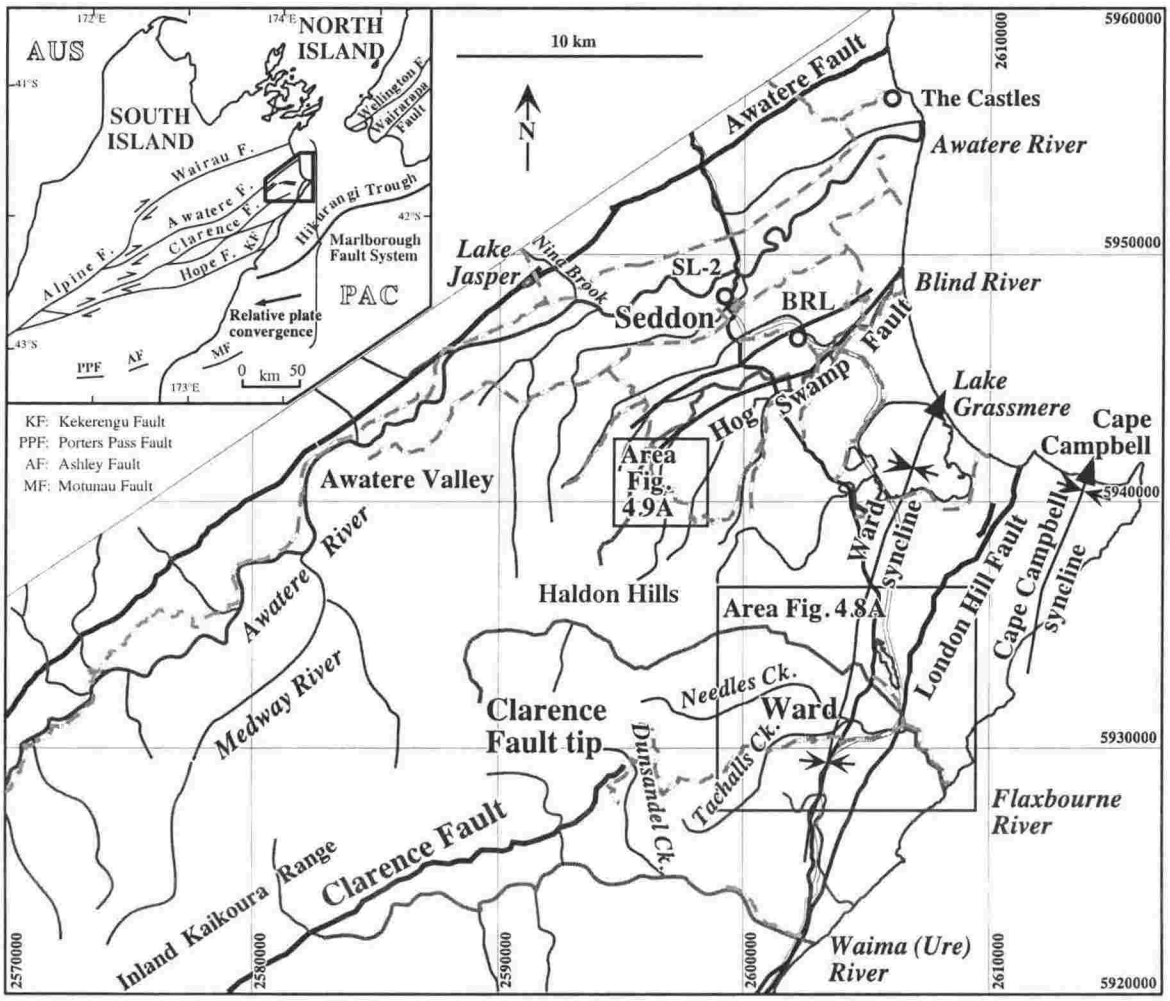

Figure 4.1. Location of the study area within the Marlborough Fault System (inset). This area, on the east coast of the South Island, New Zealand, lies within an orographic rain shadow, affording good preservation of Late Quaternary features such as fluvial terraces. PAC: Pacific Plate; AUS: Australian Plate.

provides a chronostratigraphic marker for landscapes during the last glaciation. A Late Quaternary morphostratigraphic framework is erected for eastern Marlborough from these new data and is correlated with that in other central New Zealand locations. Aggradation surfaces within the study area are correlated with each other on the basis of morphostratigraphy and detailed mapping from aerial photographs. A model for terrace aggradation during the time of peak deglaciation is presented, which incorporates changing eustatic sea level, sediment supply and tectonic uplift. This model is used to predict the relative heights of aggradation surfaces and the thickness of their gravel fill as a function of tectonic uplift and distance upstream from the river mouth.

GEOLOGICAL SETTING

Marlborough is situated at the southern end of the Hikurangi margin, where the active Marlborough Fault System accommodates *c.* 40 mm a^{-1} of relative motion between the Pacific and Australian plates [De Mets et al., 1994] (Fig. 4.1). Active deformation in this area has provided a steady uplift rate for at least the last ~0.5 Ma [Wellman, 1979; Lamb & Bibby, 1989].

A prevailing westerly wind direction means that this eastern region of South Island lies within an orographic rain-shadow. Less than 800 mm a^{-1} rainfall [Molloy, 1993] facilitates preservation of morphological features such as fluvial and marine terraces and a dry climate is optimal for entrainment and deposition of loess. Hence the Awatere and Wairau valleys are ideally situated for preserving a record of climatic fluctuations within the Late Quaternary. The area of central focus in this paper includes the coastal end of the Awatere Valley and the region to the south towards the town of Ward (Fig. 4.1).

TERRACE NOMENCLATURE AND GENERAL MODELS FOR TIMING OF AGGRADATION IN RELATION TO THE GLACIATION-DEGLACIATION CYCLE

The assumption that fluvial systems are most actively aggrading during times of peak glaciation [Penck & Bruckner, 1909] may not be valid for peri-glacial areas such as central New Zealand, where only minor (if any) glaciers were present in the upper reaches of the river systems. According to the model of Fisk [1944], who studied terraces of the Lower Mississippi River Valley, river incision is linked to glacial cycles and terrace aggradation occurs during interglacial periods. Thus, two diametrically

opposing hypotheses regarding the timing of terrace aggradation and degradation have been published.

In areas such as NE Marlborough, where bedrock is soft, lowering sea level will encourage rapid river incision. In the Awatere Valley, strath terraces which have a wide floodplain suggest that, during the incision process following a drop in sea level, the condition of "grading to base level" has generally been met. The temperate climate of central New Zealand means water is always present, even during times of peak glaciation in stream headwaters [Gage, 1965]. Physical erosion in stream headwaters produces abundant sediment in the form of screes and ultimately glacial tills and outwash in cirques (where glaciers are present), but little is transported during this period of maximum glaciation and lowered sea level. As sea level begins to rise, the climate also becomes wetter and a pulse of clastic detritus is delivered downstream. This bed-load is deposited in the stream to build an aggradation terrace. Therefore, aggradation takes place not at the time of peak glaciation, but during the period of deglaciation and sea level rise. Terrace aggradation may continue until the supply of (glacially produced) sediment "runs out" and/or until sea level stabilises at its highest level. To preserve a flight of alluvial terraces, a further necessary precondition is that the region in question is being uplifted. This would have been especially true of Holocene transgression at 17 - 6 ka, when the dramatic 120 m rise in sea level would inundate any downstream terraces that were not uplifting fast enough to avoid being drowned.

Although loess is presently accumulating in some areas of New Zealand (e.g., Marlborough), the most significant loess deposits accumulate during glacial or cold periods [Eden, 1983]. Loess deposition occurs mainly because of an abundance of over-bank silt due to physical erosion in stream headwaters and lack of significant vegetation cover on the alluvial floodplains. The climate is usually dry and windy at this time, which suits grain transportation and downwind formation of loess deposits. If terrace aggradation and loess deposition were occurring simultaneously, as in the syn-glaciation models of river aggradation, we might expect to see more interfingering of sequences of gravel and loess, rather than the generally observed sequential superposition. In NE Marlborough and other central New Zealand locations, sequences of aggradational river gravel are typically sharply overlain by younger aeolian loess and their associated soils. This point argues that major periods of gravel aggradation and loess deposition are not

pene-contemporaneous, with loess accumulating during the cold periods prior to the next cycle of fluvial aggradation.

Loess units are generally named according to when their "correlative" terrace was being incised and/or deposited. At this time, presumably during glacial/cold periods, silt becomes available for aeolian entrainment and deposition on older, higher terrace remnants above the active floodplain. Commonly, before abandonment of the active floodplain, sand-sized grains may become entrained, resulting in the localised construction of dunes [Palmer, 1982].

PREVIOUS WORK IN THE LOWER AWATERE VALLEY

Cotton [1945] concluded that there has been little time since interruption of the old fluvial aggradation cycle in Awatere River valley because the modern channel is narrow compared with the aggradational plain. Many side-streams into the Awatere River form falls or rapids down to the active river level and are largely stranded on higher terrace surfaces (in most cases the Starborough-1 surface), because unlike the Awatere River they do not have enough power to achieve modern grade.

Eden [1983, 1989] carried out important work in mapping terrace surfaces in the Awatere and Wairau valleys and describing and dating their loess coverbeds. In the Awatere Valley, Eden [1983, 1989] categorised six terrace sequences sufficiently different in morphostratigraphic position to warrant separate aggradation status (Table 4.1). Dating of terraces was achieved by recognition of the 22.6 ka Kawakawa Tephra [Wilson et. al., 1988] and in some cases the ~340 ka Rangitawa Tephra. Matching of warm/cold cycles inferred from loess stratigraphy with the oxygen isotope ratios of Hays et al. [1976] and low sea levels [Chappell, 1983] were also incorporated in the stratigraphy of Eden [1983, 1989].

Terrace	Strath	Age[1]	Age[2]	Age[3]	Sea level peak	Sea level trough
Sherbourne		*c.* 270	>340		400	?
Muritai		*c.* 240			320	270
Clifford		*c.* 150			220	200
Upton	1	*c.* 70			120	108
	2		>100		100	96
	3				80	68
Downs	1	*c.* 40	>57		60	56
	2				40	35
Starborough	1	17 ± 2		>15	12?	-
	2	12 ± 2		12	8.75?	-
	3-9	< 12			7.5?	-

Table 4.1. Morphostratigraphic sequence and age of terrace abandonment in the Awatere Valley as described by: (1) Eden [1989] who used morphostratigraphy and relative position of the Kawakawa Tephra to infer ages, and; (2) Berger & Pillans [1994] and (3) Little et al. [1998], who used thermoluminescence dating of loess. Sea level peaks for 400 - 100 ka are from oxygen isotope records of Shackleton et al. [1990] & Martinson et al. [1987], for 100 - 12 ka from Chappell & Shackleton [1986] and for 12 - 0 ka from Gibb [1979].

The nomenclature of Eden [1989] is used in this paper, not only for terraces in the Awatere Valley, but also for extrapolation of surfaces out of the main Awatere Valley catchment (see below), though his chronology has been revised. The oldest terrace recognised by Eden [1983, 1989], the Sherbourne terrace, has upon it a loess cover sequence containing 2 tephra. This surface was assigned an age of "*c.* 270 ka" by Eden, who correlated the lower tephra with the Rangitawa Tephra. This post-abandonment age was later refined by Berger and Pillans [1994], who reported a thermoluminescence (TL) age of 346 ± 70 ka for loess just below the lower tephra on this terrace and Pillans et al. [1996] who inferred an age of 340 ± 7 ka for the Rangitawa Tephra (Table 4.1). Berger and Pillans [1994] also reported TL dates of 80.6 ± 9.9 and 113 ± 18 ka for a younger loess sequence, the "Upton Loess" of Eden [1983], which is exposed not far away at The Castles in the lower Awatere Valley (Fig. 4.1). They also recorded a TL age of 57 ± 5 ka for loess cover on the younger Downs-1 terrace tread in the lower Awatere Valley.

The distribution of the Kawakawa Tephra in central New Zealand was reviewed by Campbell [1986], who integrated 22 South Island sites with North Island locations. Local tephra bed thicknesses were used to produce an isopach map of tephra airfall, on

which the Marlborough region lies between the 10 and 15 cm contours. This airfall event provides a useful last glacial maximum marker horizon in Marlborough for landscape surfaces that are older than *c.* 23 ka. Pillans et al. [1993] dated five exposures of loess close to the Kawakawa tephra in the North Island and one from Marlborough, at The Castles (see above), using TL dating. These samples were "contaminated" and consistently under-estimated the expected (generally accepted) age determined from ^{14}C dating of wood within the coeval Oruanui Ignimbrite [Wilson et al., 1988], which give an average age of 22 590 ± 230 yr BP. At Nina Brook, in the lower Awatere Valley (Fig. 4.1), the Kawakawa Tephra is exposed in colluvial/alluvial fan-glomerate, built up behind the scarp of the active Awatere Fault. Little et al. [1998] carbon-dated 4 peat samples from both above and below the tephra, all of which returned ages younger than the "accepted" 22.6 ka date. Benson et al. [2001] dated lake deposits on top of the Nina Brook fan, which contains the tephra and which have a ^{14}C age of ~21 ka.

Little et al. [1998] dated loess on the Starborough-1 terrace (St-1) at Seddon, obtaining a TL age of 15.2 ± 1.3 ka (Fig. 4.1, Table 4.1). On the basis of differential loess cover thickness and river incision levels, they inferred that the Starborough-2 terrace is about 3 ka younger than St-1. They used mean incision rates of the Awatere River, the 18% lower elevation of Starborough-2 relative to St-1 and its thinner loess cover, which is 1 m less than that of St-1. This is probably a maximum age difference due to rates of incision not being uniform during the Holocene [Little et al., 1998].

Ota et al. [1995] obtained several radiocarbon ages of shell and wood from cores in the Blind River - Lake Grassmere region, to the SE of the Awatere Valley (Fig. 4.1). Many of the sites chosen by Ota et al. [1995] are currently undergoing local subsidence in or near the axis of the active Ward Syncline [Townsend, 1996], therefore fluvial surfaces that are correlative of those within the uplifting Awatere Valley have become successively buried in this region. Beach deposits around the northern shores of Lake Grassmere that are 6-8 ka in age, based on carbon dating of wood and shell material [Ota et al., 1995], are broadly contemporaneous with degradational fluvial terraces in the Awatere Valley, including Starborough-3 to -9.

REGIONAL CORRELATION OF TERRACE SURFACES

From the morphostratigraphy of Eden [1989] (Table 4.1), who mapped terraces solely within the Awatere Valley catchment, surfaces in the Blind River - Lake Grassmere - Ward area (see Fig. 4.1) have been correlated by their morphologic position and also their characteristic degree of surface dissection (Fig. 4.2; Quaternary terrace map; back pocket). This association has been made by detailed study of aerial photographs from which terrace surfaces have been traced and digitally scanned into the GIS program "MapInfo". Photographs are registered within a global coordinate system/reference frame onto which a digital version of the NZ 1: 50 000 Map Series topographic contours can be projected. From this contour dataset, approximate elevations (± 20 metres) can be obtained for points on a specific terrace surface. Three separate Elevation Distance Meter (EDM) surveys were also carried out, in the Flaxbourne and Dunsandel valleys, and incorporated into this digital reference frame, giving millimetre precision of relative terrace heights in areas of particular interest. These surveys were constructed to resolve differences in elevation of fluvial terraces close to the tip of the Clarence Fault and are described in detail in another paper regarding the pattern of Late Quaternary uplift and subsidence in this coastal part of NE Marlborough [Chapter 5] (see Appendix 4).

Surface morphology

The degree of terrace surface dissection by streams has been used as a qualitative index of relative surface age. Where terrace surfaces are contiguous with one another, or at sites where preservation allows a good height comparison between different terraces, older surfaces can generally be distinguished from younger ones by their gross morphology, the degree of their dissection and the apparent degradation of their flanking terrace risers. In general, older surfaces have more-rounded scarp edges than the younger ones due to erosion, dissection by small streams and uneven blanketing by windblown loess. Therefore, surfaces with the sharpest edge between the tread and the riser will, in general, be the youngest ones. The oldest surfaces are commonly so dissected or blanketed with loess that no apparent terrace "surface" remains. These are sometimes devoid of loess, in which case they are interpreted as deflation surfaces. These properties are useful when correlating between disjunct surfaces as roughly contemporaneous

terraces can be categorised into age-groups by their general scarp shape. A description of the surface characteristics used in this study to achieve the correlations shown on Figure 4.2 is given in Appendix 3.1.

Kawakawa tephra as a chronostratigraphic tool

The Kawakawa Tephra (Aokautere Ash) is commonly preserved in loess and/or gravel successions in NE Marlborough. This study adds widely to the presently known outcrop distribution of the Kawakawa Tephra in NE Marlborough (Fig. 4.3). Eden [1989] used this isochronous marker as a mainstay for assigning ages within his loess stratigraphy.

Glass chemistry analysis from new sites

Electron microprobe analyses of individual tephra glass shards from new sites in Marlborough (shown on Fig. 4.3) were carried out to establish the chemical identity of tephras. This analysis was performed at Victoria University of Wellington, using the JEOL-733 super-probe with a 10 μm diameter beam and an 8 nA current. Samples from seven of the nine new locations were analysed and all sample populations have overlapping fields for CaO, FeO and 1/3 K2O (Fig. 4.4). Values were normalised to 100% and site mean data are presented in Appendix 3.2, along with scanning electron microscope photographs of representative glass shards. All seven samples also overlap the chemical field for Kawakawa Tephra averaged from well-correlated sites in the North Island [Pillans et al., 1993]. These results verify that the Marlborough tephra is the Kawakawa Tephra.

Depositional regime at the time of tephra airfall

The Kawakawa Tephra is an important tool for understanding and dating Late Quaternary stratigraphic sequences in NE Marlborough. The tephra generally forms a macroscopic horizon 2 - 10 cm thick in loess but it is often preserved within colluvial/alluvial fan deposits. For example, at Nina Brook (see Fig. 4.1), rapidly deposited alluvial fan gravel shedding from the northern hills has formed a thick sequence of coarse Torlesse-derived gravel with occasional layers of peat [Benson et al.,

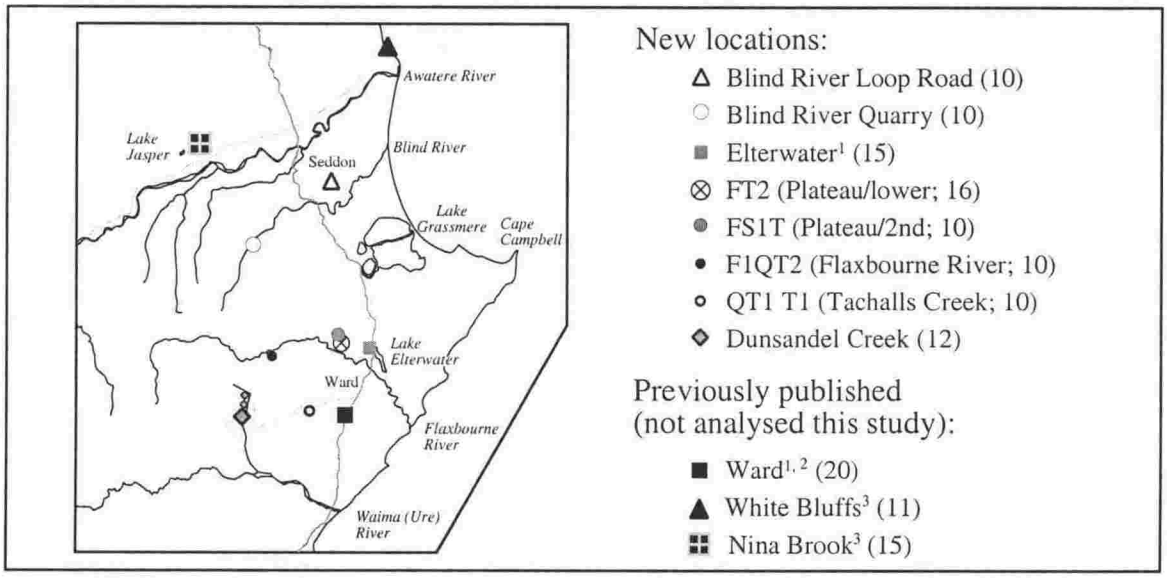

Figure 4.3. New and previously known locations of Kawakawa Tephra in eastern Marlborough. Superscripts on Figures 4.3 and 4.4 (below) refer to data from 1) Campbell [1986]; 2) Courtesy of P. Froggatt; 3) Little et al. [1998], and 4) Pillans et al. [1993].

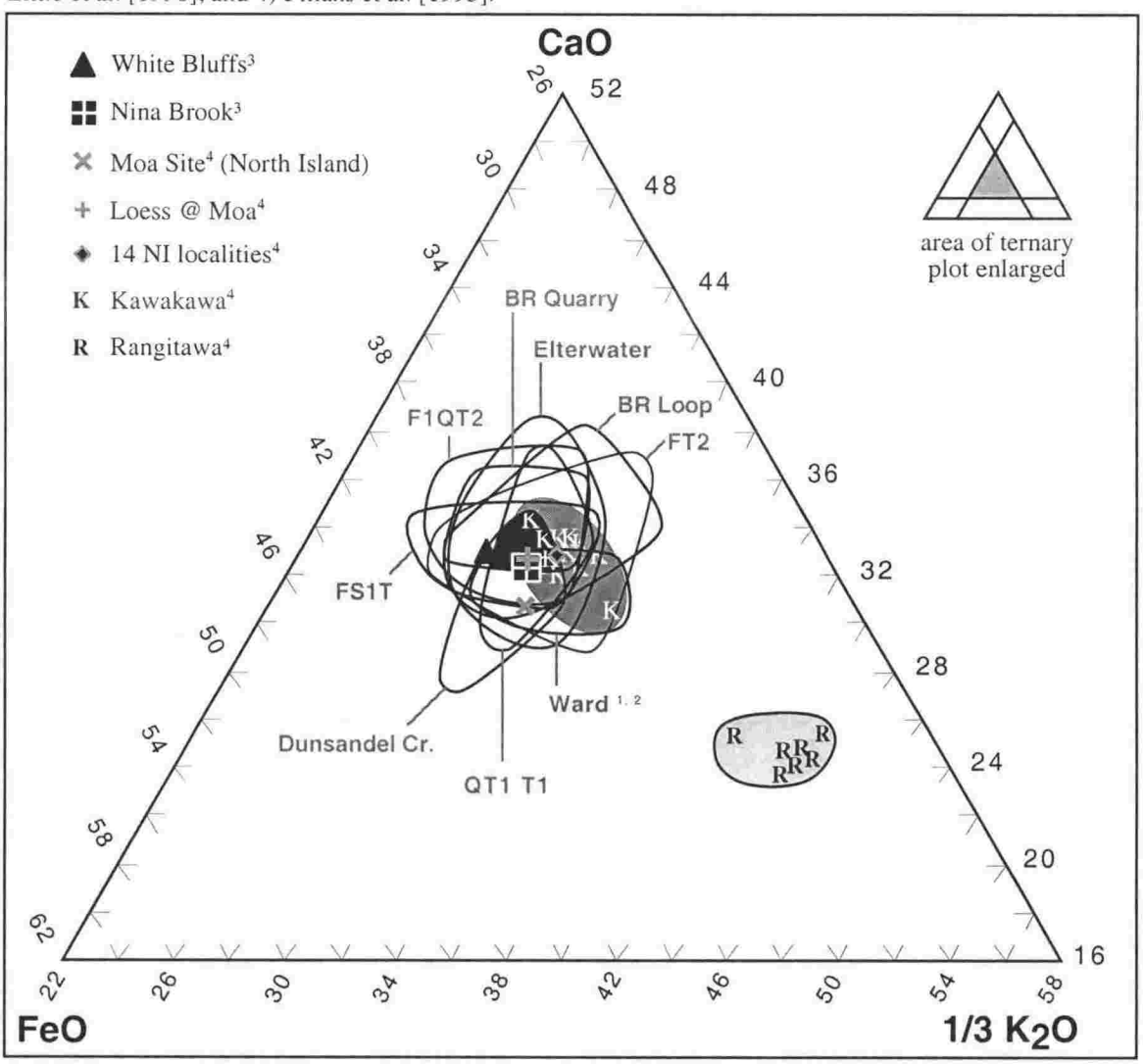

Figure 4.4. Ternary plot for distinguishing elements FeO–CaO–1/3 K_2O for new tephra samples listed in Figure 4.3 (above). Fields for Kawakawa and Rangitawa tephras (grey) are from Pillans et al. [1993]. The black area represents overlap of new samples (excl. Ward). See Appendix 3.2 for site means of analyses.

2001]. The inference of local deposition is drawn from the absence of Tapuae-O-Uenuku plutonic rocks, which are characteristic of "Awatere River" gravels and the moderately steep southward dip of the fan surface indicates a flow direction perpendicular to the present NE course of the Awatere River.

In Dunsandel Creek (see Fig. 4.1), the tephra is similarly contained within colluvial gravels and is remarkably well preserved (Fig. 4.5). As at Nina Brook, the tephra at Dunsandel Creek is preserved only within the older fan gravels, not within the gravels underlying the St-1 aggradation surface that is extensively preserved downstream (Fig. 4.5, inset).

Along SH1, approximately 1 km south of Ward (Fig. 4.1), the tephra is preserved within laminated silt that is interdigitated with bars of fine gravel, suggesting a marginal lake/deltaic environment [Townsend, 1996] and a further 3 km to the west, near Tachalls Creek, it forms thick deposits (up to 30 cm) in fine, slightly laminated silt. That the tephra is contained within or associated with, in many places, localised colluvial fan gravels and not within gravels underlying aggradation terraces suggests that, at the time of its eruption at 21.6 ka [Wilson et al., 1988], major aggradation was not taking place and instead, localised fans were being built.

EFFECTS OF LOCAL TECTONICS ON TERRACE FORMATION AND SURFACE PRESERVATION

Regional terrace correlations need to account for local variations in terrace height and character resulting from active faulting and folding and differential uplift across the region. Local tectonics can markedly affect surfaces that are inferred to be older than 60 ka. The Upton-3 terrace (*c.* 80 ka) in the Blind River area, for example, forms ridge-like remnants in the interfluves of tributary streams and has been displaced vertically by 40 - 50 m in an up-to-the-north sense of throw across the Hog Swamp Fault (Figs. 4.1 & 4.2). This displacement appears to increase along the fault trace(s) to the NE and may be responsible for a tectonic damming of this river system, causing a prominent north-east deflection of Blind River. Other north-flowing streams, shedding from the Haldon Hills, have now become pirated by Blind River where they drain into its east-flowing, deviated course. Terraces younger than the *c.* 60 ka Downs-1 appear not to be affected by this faulting, suggesting little or no movement on the Hog Swamp Fault since this time. Subsidence near the trace of the HSF may also have caused apparent burial of the

Downs-1 aggradation surface by vertical accumulation of successively younger depositional events. The stratigraphic sequence beneath the "St-1" terrace at Blind River is shown Figure 4.6. The 5 to 6m-thick basal gravel deposit is inferred to represent the Downs-1 aggradation event and thin lenses of gravel, separated from the lower gravels by Downs-1 loess, correlate with locally aggrading Downs-2 fans. The Kawakawa Tephra is preserved within a paleosol(?) as the prominent white band near the top of the sequence (Fig. 4.6) and is scoured and truncated by deposition of the youngest terrace alluvium, inferred to be equivalent to St-1 aggradation. This morphological inversion occurs at other sites that are also inferred to be undergoing local subsidence in association with active bedrock structures, notably on the footwall of the Clarence Fault (Dunsandel Creek; Fig. 4.1) and in the axis of the Ward Syncline (Tachalls & Needles creeks; Fig. 4.1). At all of these locations only a single, young terrace surface is preserved. These local differences in the Quaternary stratigraphy due to active tectonics explain why a morphologically complete set of Awatere terraces is not always preserved.

NEW OSL DATING OF LOESS FROM THE AWATERE - WARD REGION

Starborough-1 terrace at Seddon (sample SL2)

Previous dating of the Starborough-1 terrace (St-1) includes a TL age on loess [Little et al., 1998], from just north of the town of Seddon (Fig. 4.1). Loess 25 cm above the gravel (Fig. 4.7) yielded an age of 15.2 ± 1.3 ka. Assuming a linear rate of loess accumulation at this site and that loess at the ground surface has an age of 0 ka, the 25 cm of loess below the TL sample represents approximately 1000 years of accumulation. Extrapolating downward from the sampled loess to the top of the gravel yields a terrace abandonment (tread) age of 16.0 ± 1.4 ka.

OSL dating is generally regarded as being more reliable than TL techniques, especially when dealing with poorly bleached samples from fluvial or lacustrine sediments. A new OSL sample measured at exactly the same site as the TL sample of Little et al. [1998] has yielded an age of 8.4 ± 0.7 ka for loess at the same stratigraphic horizon (Table 4.2). This method uses the single aliquot regeneration (SAR) method similar to that of Murray & Wintle [2000], for coarse-grained quartz, but modified in the Victoria University of Wellington (VUW) luminescence laboratory by Dr. Uwe Rieser

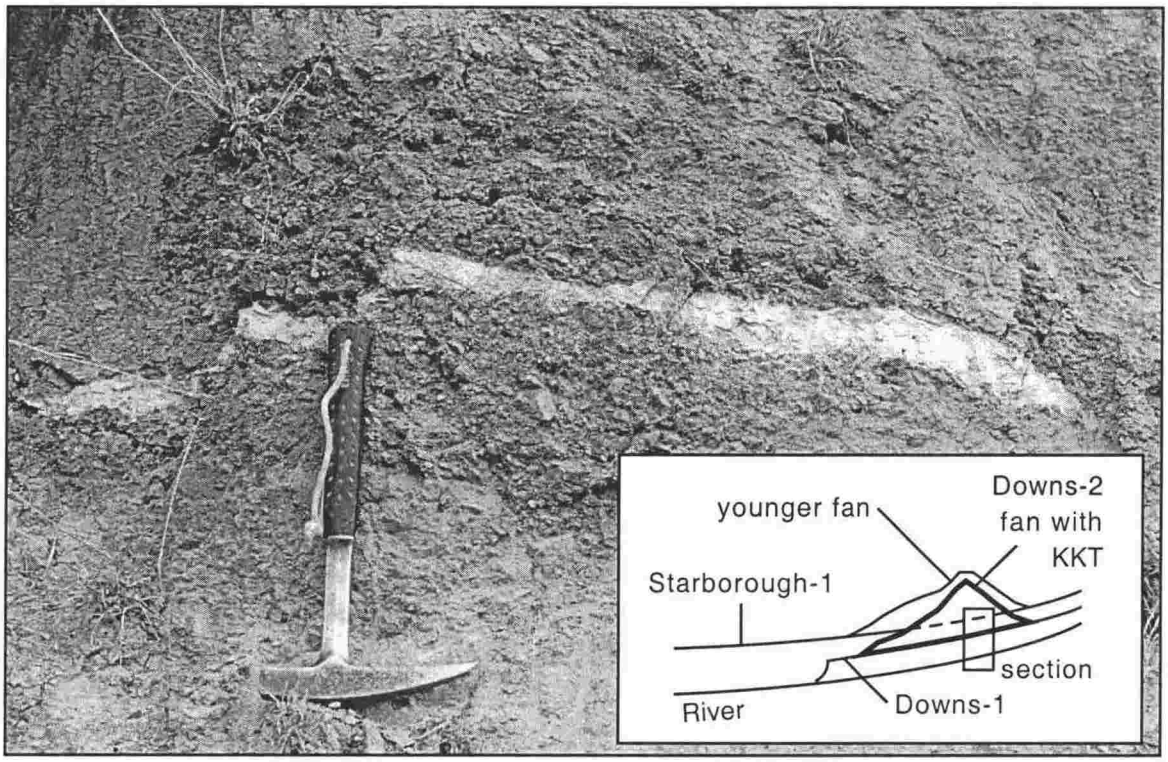

Figure 4.5. Kawakawa Tephra preserved within colluvial Torlesse-derived gravel underlying the Starborough-1 terrace near Dunsandel Creek. Hammer is 33 cm long. Inset: stratigraphic relationship of Kawakawa Tephra (KKT) to Downs-2 (?) fans and the younger Starborough-1 gravels, which have aggraded vertically, mantling the older fan surface and therefore do not contain the tephra.

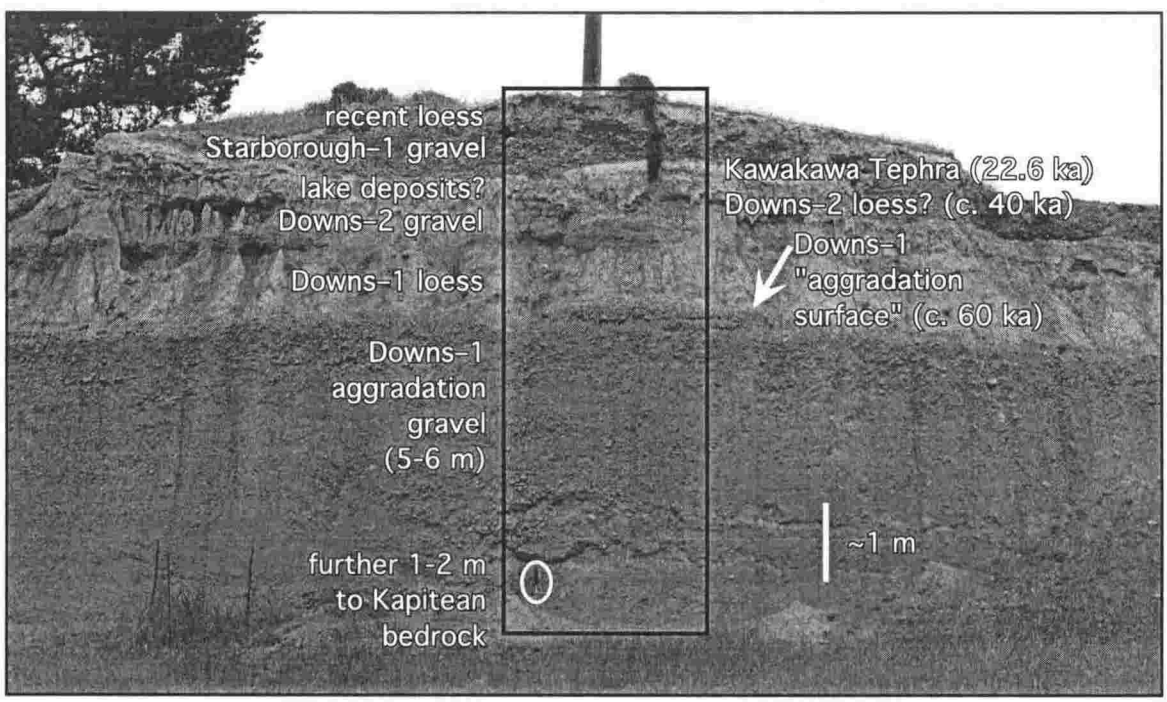

Figure 4.6. The Blind River quarry with thick Downs–1 alluvium at the base and vertically aggrading sequence containing the Kawakawa Tephra near the top. The tephra lies within possible lake deposits or a palaeosol and is scoured by younger Starborough–1 gravel. Hammer (circled) is 33 cm long.

to measure fine-grained feldspars. This is a new technique currently under review, but tests of more than 80 OSL samples by this new SAR method at the VUW luminescence laboratory suggest similar, if not more accurate, results to duplicate samples tested by the more widely accepted multiple aliquot method. For a brief description of the protocol used in SAR dating of samples presented in this paper, see Appendix 3.3. The new OSL date from Seddon indicates that abandonment of the St-1 terrace occurred much later than previously thought (extrapolated age of abandonment of 9.15 ± 0.71 ka, assuming a constant rate of loess accumulation) and that aggradation in the Awatere Valley did not cease at the end of the Last Glacial Maximum.

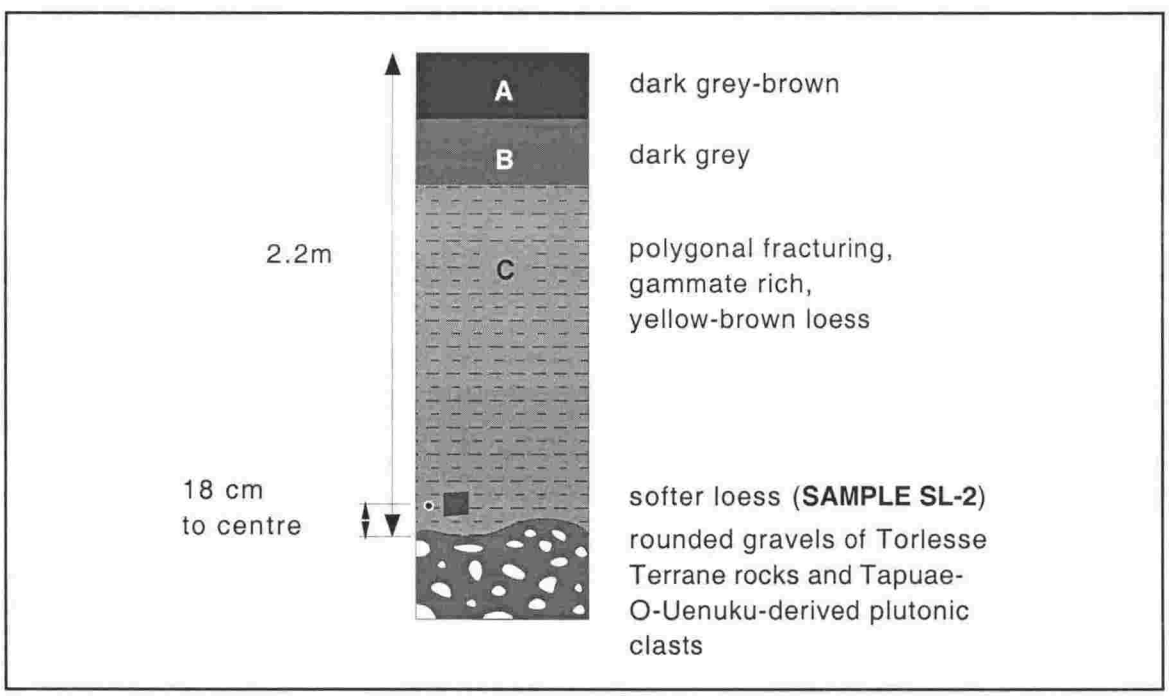

Figure 4.7. Stratigraphy of the Seddon OSL site (SL-2) in loess on the Starborough-1 terrace. The grey square marks the position of the bulk sample taken and the small circle is the pin marking the position of the TL sample of Little et al. [1998].

Sample	Material	Age (§)	error	Age (†)	error	Comments
SL-2	Loess	8.4	0.7	-		
FFS1	Silt	77.4	8.8	-		Fluvial silt?
FFS2	Silt	65.9	5.6	80.3	5.3	Fluvial silt?
FL1	Loess	64.6	6.4	70.1	4.3	
SB1	Loess	>22	2.0	>19.6	2.4	Anomalous fading

Table 4.2. New OSL dates from loess and silt in the Awatere Valley - Ward region. § - single aliquot regenerative technique [Rieser, in prep.]; † - multiple aliquot regenerative technique. See text for full explanation and description of sites.

Flaxbourne River terraces: The Plateau

Three new OSL dates have been obtained from loess and fluvial silt overlying a thick sequence of alluvium *c.* 4 km NW of Ward (Fig. 4.8A). At "Corrie Downs" station, a sequence of four terraces, known locally as The Plateau, are cut into Pliocene mudstone of the Starborough Formation. These surfaces range in elevation from approximately 80 to 130 m above the present level of the Flaxbourne River (120 to 170 m above mean sea level) and are inferred to be coeval with similar terrace flights in the nearby Awatere Valley, 15 km to the north.

The highest and oldest terrace (T1 / Upton-1?) caps an elongate, east-west-oriented ridge on the north side of the Flaxbourne River and dips at *c.* 2.5° eastward, toward the axis of the Ward Syncline (Fig. 4.8A), much more steeply than the *c.* 0.3° grade of the modern river. This ridge drops steeply away to the north where mature, low-lying, dissected terrain has escaped the rejuvenating effects of terrace aggradation. Scattered, angular clasts of Torlesse affinity lie on the T1 surface and it is assumed that these gravels were deposited by the Flaxbourne River at some time in the past before their uplift relative to the river level today. There is evidently no loess cover on this high terrace, therefore it is assumed to represent a deflation surface due to its exposure to the wind.

The next lower terrace (T2 / Upton-2?) has three narrow remnants of original surface, deeply dissected by small streams (Fig. 4.8A). The stratigraphy includes a section of fine cobble conglomerate overlain by >4.8 m of fluvial silt and sand (Fig. 4.8B). The top of the conglomerate sequence lies approximately 15.2 m below the

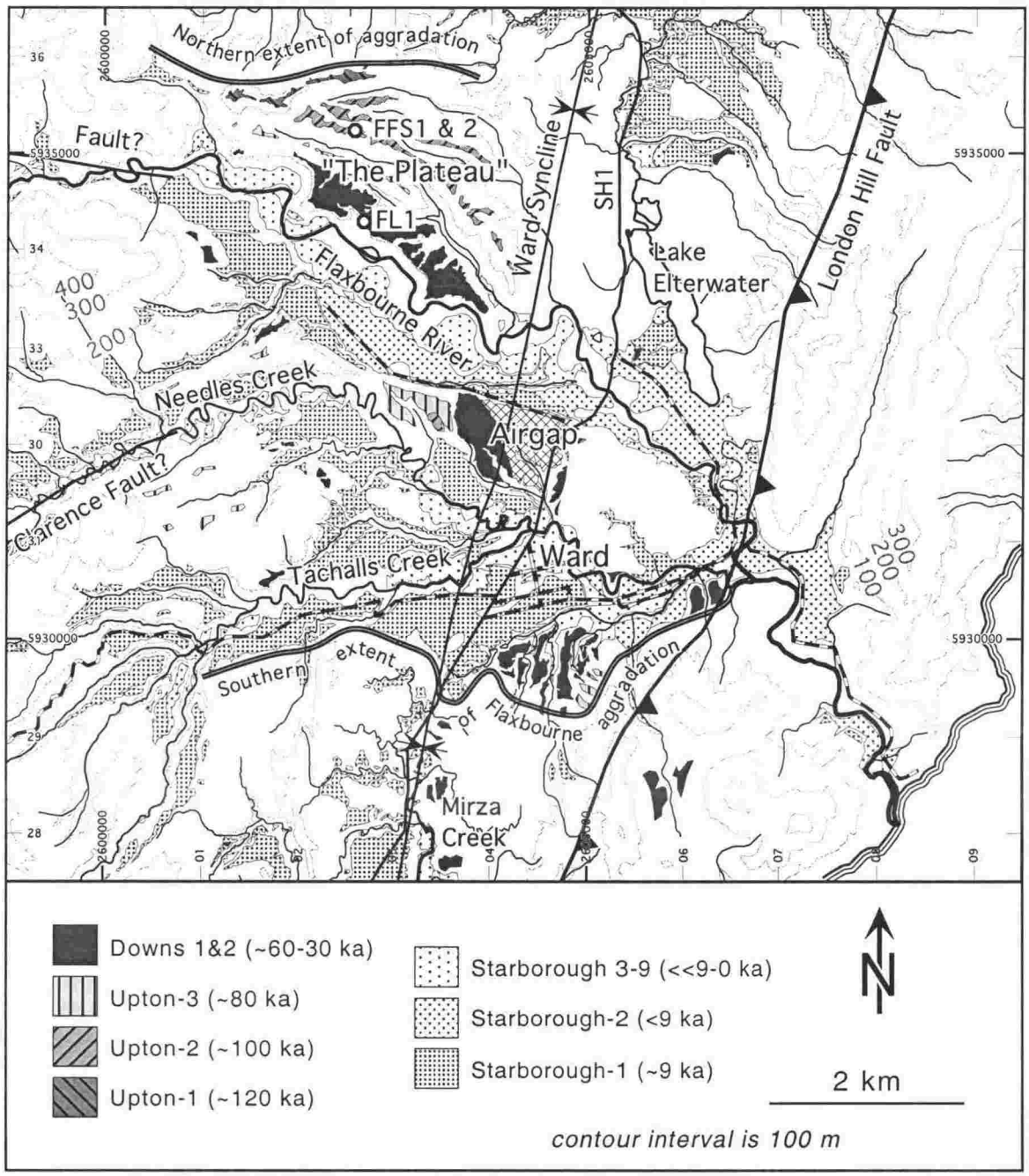

Figure 4.8A. Location of OSL samples FFS1 & 2 and FL1 (see Table 4.2) near Ward. Terraces at "The Plateau" are correlated with terraces in the Awatere Valley on the basis of morphology and new OSL dates. The oldest, highest terrace correlates with the Upton-1 surface in the Awatere Valley [Eden, 1989] and is assigned an extrapolated age of 120 ka. A slightly lower terrace yielded an abandonment age of 66 - 80 ka and is correlated with the Upton-2 terrace tread. Another slightly lower terrace fits well with the position of Upton-3 and is assigned an age of ~80 ka. The lowest of the four terraces at The Plateau yielded OSL ages of 58 - 70 ka (see Table 4.2) and is correlated with the aggradational Downs-1 surface of the Awatere Valley. This surface is underlain by a thick gravel sequence in both the Flaxbourne and Awatere catchments. See Fig. 4.1 for location of map.

terrace surface; the upper ~10.4 m of section is covered or slumped. Two samples were taken from probable fluvial silts 3.4 and 3.6 m above the top of the gravel, approximately 10 m apart. OSL dating returned ages of 77.4 ± 4.3[§] (FFS1) and 65.9 ± 5.6[§] and 80.3 ± 5.3[†] (FFS2) ka, respectively (Table 4.2). These samples are from fine over-bank silts assumed to be deposited by the Flaxbourne River but, as the top of the section is not exposed, it is unclear how thick the fluvial silts are and how much loess lies above them. No gravel, either *in situ* or as float, was noted above the silt, suggesting that this terrace ceased to be part of a major aggradational sequence after the silt was deposited. Hence these two samples record a minimum age for the last aggradational terrace-forming event at this site, but must be close to the time when abandonment occurred.

Although no OSL sample was analysed from the next lowest terrace (T3 / Upton-3?), Kawakawa Tephra (sample FT2, above) was found in its cover sequence (Fig. 4.8C). Here, the tephra lies 47 cm below the modern soil horizon, within loess and with colluvial gravel below, totalling a thickness of 5.5 m. This site is somewhat ambiguous as it may represent a side channel cut into an older terrace remnant. However, the presence of the Kawakawa Tephra in the cover sequence constrains the age minimum (of either terrace) to greater than *c.* 22.6 ka. The gravel/conglomerate is generally clast-supported and strongly iron-cemented, maintaining cementation as coherent blocks spall away from a scarp eroded by the small stream nearby. Clasts are mostly Torlesse terrane sandstone, but rare Late Cretaceous Herring Formation and Tapuae-O-Uenuku dyke lithologies were recorded, suggesting a provenance from the Awatere River.

The lowest of these locally extensive surfaces (T4 / Downs-1?) is underlain by a gravel sequence up to 40 m in thickness (Townsend [1996]; Fig. 4.8D). The clasts consist of well-rounded, weathered Torlesse rock, ranging in size from pebbles to ~10 cm in diameter, forming a consolidated, matrix-supported conglomerate. The gravels are overlain by 3.78 m of loess, which has a macroscopically visible tephra horizon 60 cm below the modern surface. Electron microprobing of this tephra chemically establishes its identity as the 22.6 ka Kawakawa Tephra (sample FS1T, above). OSL dating of loess from 36 cm above the top of the gravel terrace tread, using both single (§) and multiple (†) aliquot methods yielded ages of 64.6 ± 6.4[§] and 70.1 ± 4.3[†] ka, respectively (Table 4.2). The extrapolated age of surface abandonment, using a mean rate of loess accumulation that best-fits both dates and the tephra horizon, is between 67[§] and 74[†] ka.

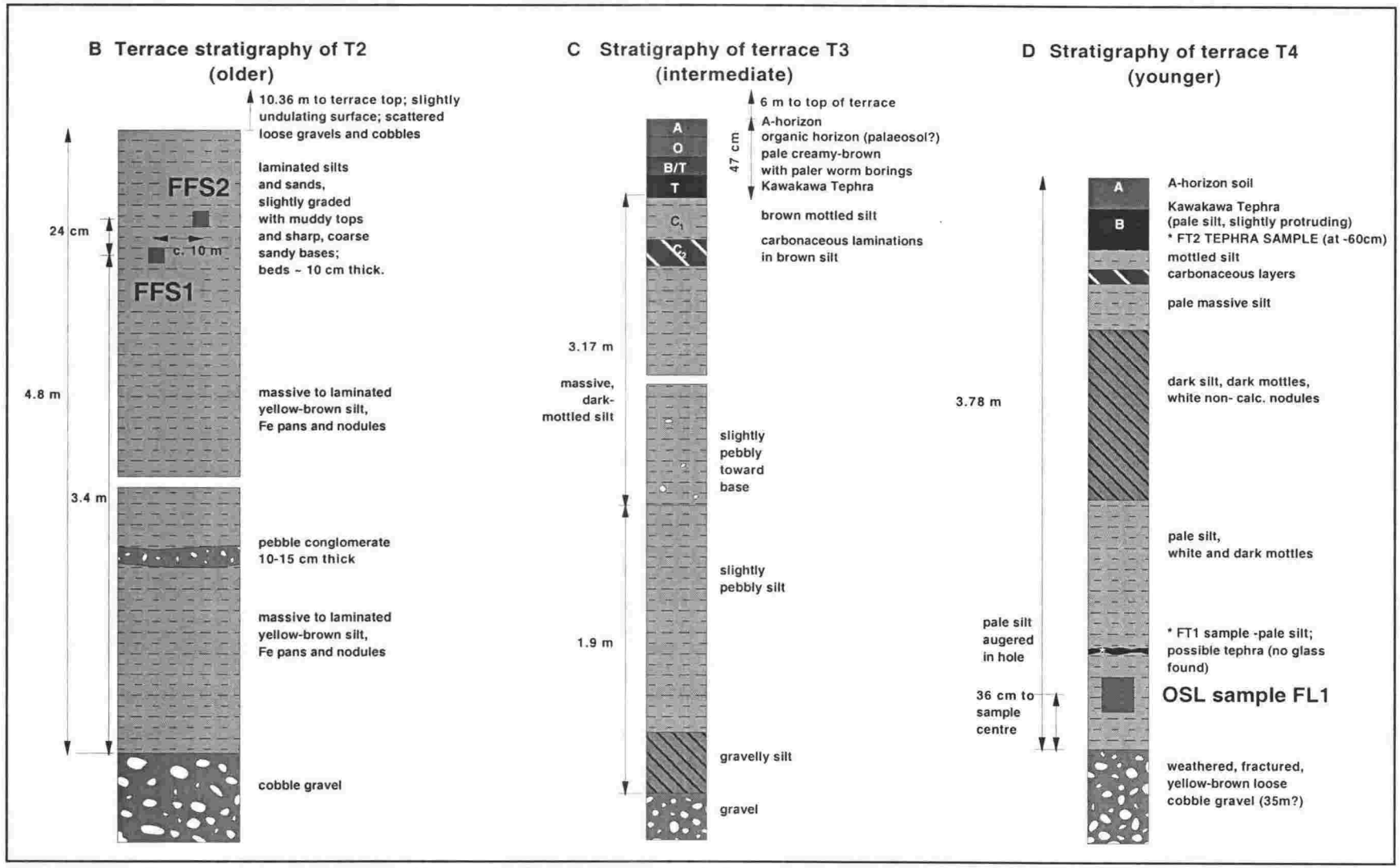

Figure 4.8B-D. Quaternary stratigraphy at The Plateau, Seddon. Columns B, C & D are representative sections from terraces T2, T3 and T4, respectively. OSL samples were collected from terraces T2 and T4. Terraces T3 and T4 contain the 22.6 ka Kawakawa Tephra (samples FS1T and FT2; Figs. 4.3 & 4.4), providing a useful control on dating.

This age is interpreted to be the time when the T4 surface was abandoned by the Flaxbourne River and loess began accumulating on the stranded terrace surface.

Younger terraces preserved in this area were not OSL sampled but are interpreted on the basis of their morphological position, relative aerial extent and the thickness or absence of loess cover to be coeval with the Downs-2, Starborough-1 and Starborough-2 terraces of the Awatere Valley (see Fig.8A).

Stirling Brook: site SB1

Alluvial terraces preserved at Stirling Brook offer a chance to date the Downs terrace tread in the Blind River area (Fig. 4.9A; located on Fig. 4.1). The Downs terrace forms remnant strips adjacent to many streams draining from the Haldon Hills, always on the south side of the NNE-trending valleys. The degree of surface dissection is characteristic of Downs-aged terraces seen in the Awatere Valley (see Appendix 3.1). Interfluves between these valleys commonly preserve remnants of the older Upton-1 surface (Fig. 4.9A). Age control of this site by tentative correlation of a possible Kawakawa Tephra outcrop (not sampled) and assuming a constant rate of loess accumulation yields an extrapolated age of abandonment of ~40 ka (Fig. 4.9B). This outcrop is similar to another site, downstream and closer to the coast (Fig. 4.9C), featuring a pale horizon containing the Kawakawa Tephra (sample BRL, above), which also yields a projected age of 40 ka using the same method.

OSL sample SB1 collected at this locality exhibited anomalous fading during OSL analysis. This means that the returned dates of 22.0 ± 2[§] and 19.6 ± 2.4[†] ka are minimum ages only. Therefore, on the basis of tephra correlation and OSL dating, cessation of Downs 1(?) aggradation is assigned an age of greater than *c.* 40 ka. An airgap (abandoned stream channel) to the north of this site appears to be coeval with aggradation of the next-youngest terrace (St-1) and attests to tectonically controlled changes in drainage patterns during the last *c.* 40 ka. This and other related topics are dealt with in Chapter 5.

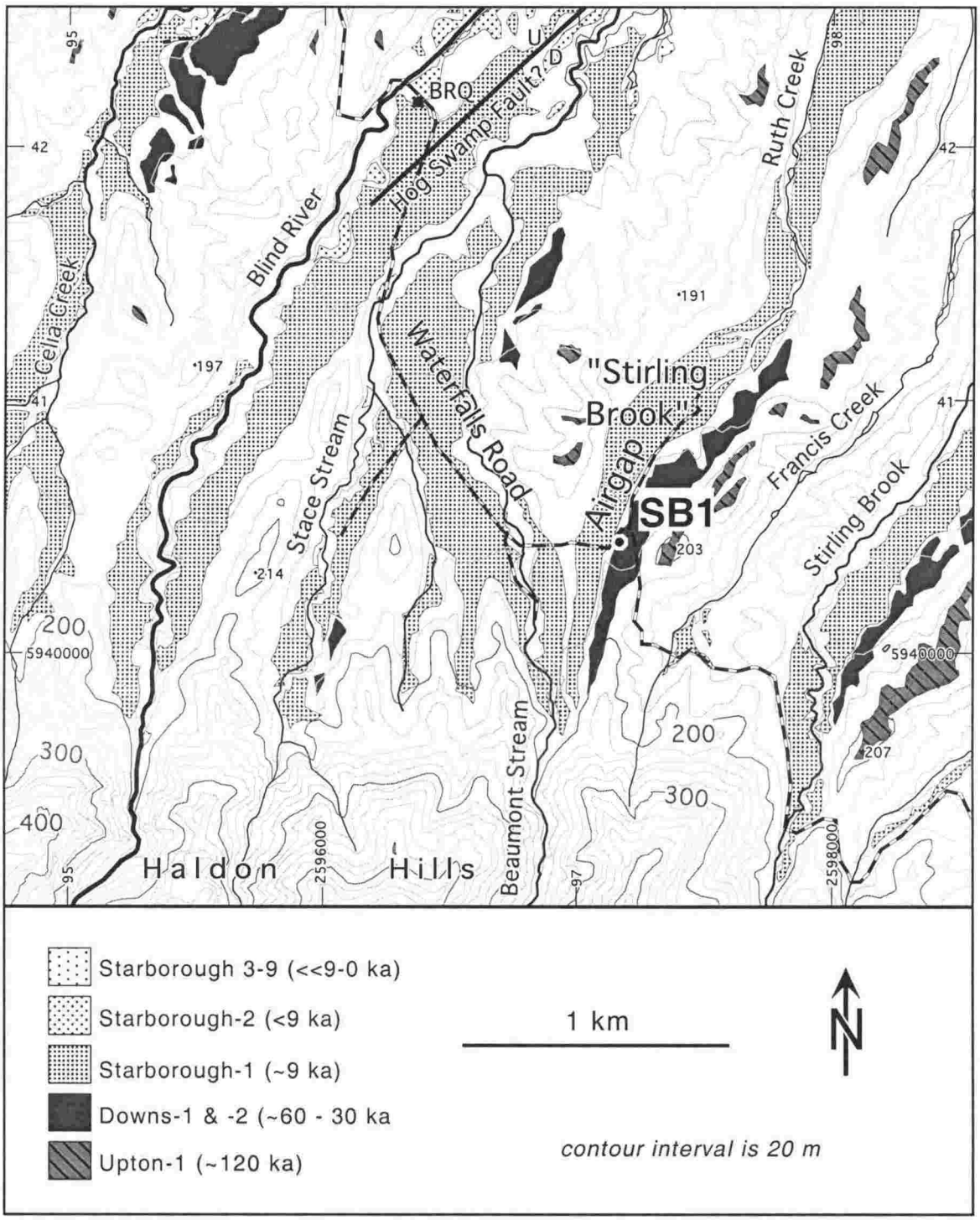

Figure 4.9A. Location of the Stirling Brook OSL sample (SB1) on the Downs-1 terrace tread (see Fig. 4.1 for area of diagram and Fig. 4.9B for stratigraphy). BRQ is the gravel quarry near Blind River where the Kawakawa Tephra crops out (see Fig. 4.6). A prominent airgap (abandoned channel) just to the north of the

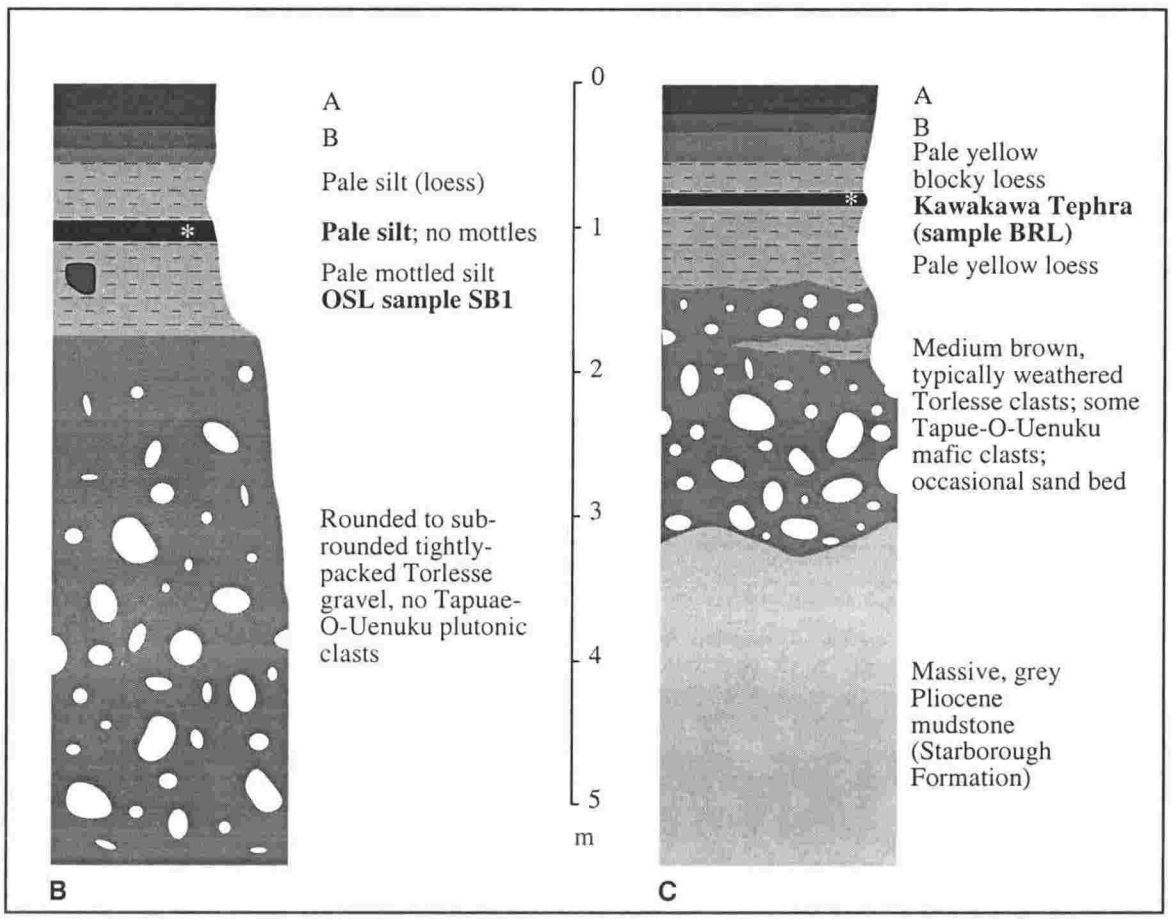

Figure 4.9. Comparison of the Downs-1 terrace at Stirling Brook and Blind River. B: OSL sample SB1 and stratigraphy at Stirling Brook; the asterisk marks the position of a possible tephra (see text). C: Comparable section interpreted to be the same terrace near Blind River Loop Road, closer to the coast (located on Fig. 4.1), containing Kawakawa Tephra (sample BRL; see Figs. 4.3 & 4.4).

RELATIONSHIP BETWEEN UPLIFT, INCISION AND SEA LEVEL

In areas where bedrock is soft, rates of incision may be able to keep pace with fluctuating stream base levels. An age-height diagram of Flaxbourne River terraces at The Plateau using dates and terrace correlations from this study is show in Figure 4.10. The rate of incision over the last *c.* 120 ka is roughly constant at 1.0 mm a^{-1}. Some time after the abandonment of T4 and before aggradation of the inferred St-1 surface, the Flaxbourne river was "deflected" eastward towards the Ward Syncline, leaving in its wake a broad airgap to the south near Ward (Fig. 4.8A). This conspicuous response of the fluvial system to tectonism attests to ongoing activity and differential subsidence related to the Ward Syncline and London Hill Fault [e.g., Townsend, 1996; Townsend & Little, 1998; Chapter 5]. This alteration of the course of the Flaxbourne River has

bypassed a major bend in the river that used to flow through the low topography occupied by the town of Ward, resulting in a shorter, more direct route to the coast and a steepening of the local stream gradient. Complex hydrodynamic responses such as this may cause young terraces (e.g., St-1 and St-2) to be cut down at a different rate than the older terraces that were formed prior to deflection of the river course.

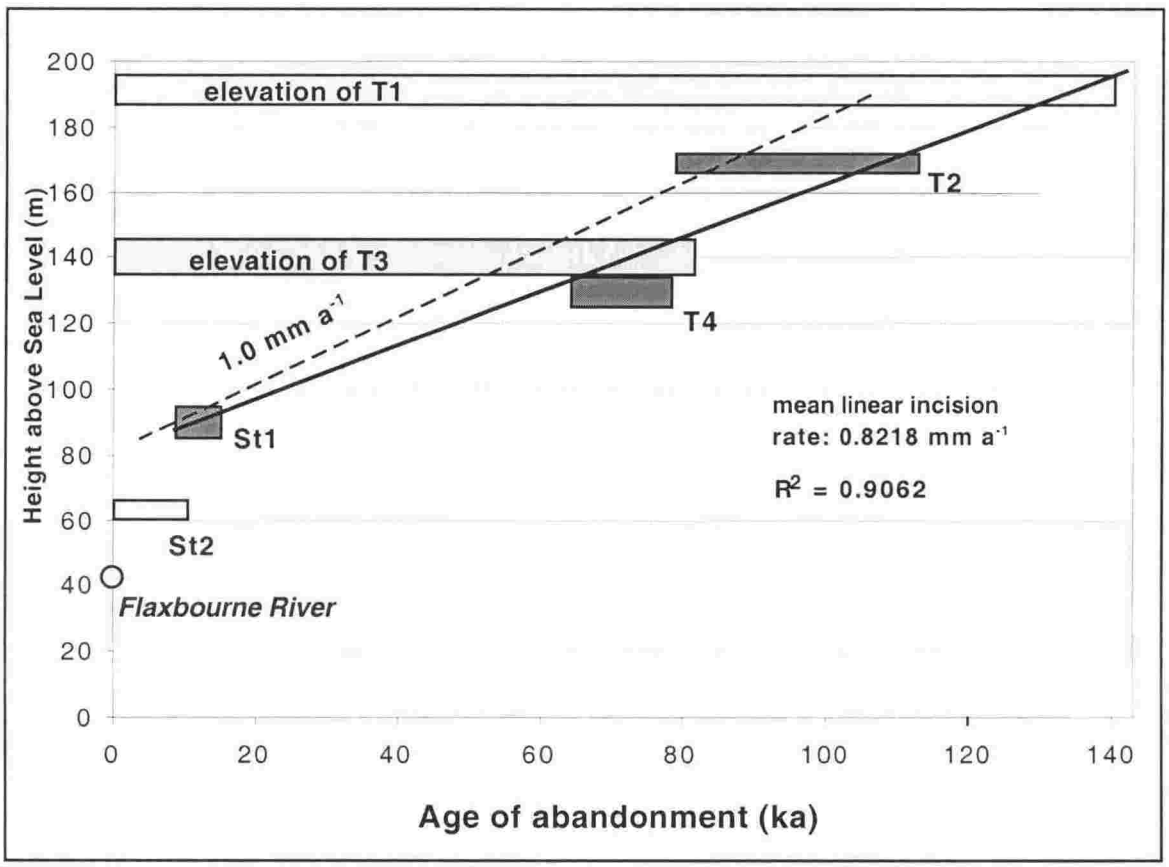

Figure 4.10. Age-height correlations for Flaxbourne River terraces at The Plateau, near Ward. Dark shaded boxes denote new OSL dates (range given; see Table 4.1) that have been extrapolated to the top of the gravel sequences to infer an age of terrace abandonment. This calculation assumes a constant rate of loess accumulation, an assumption that may not be valid for terrace T2, which is inferred to contain fluvial silts as part of its cover sequence (see Fig. 4.8B). If the dated deposits on T2 are fluvial and not aeolian, the age of abandonment is closer to 80 ka and the mean incision rate higher at 1.0 mm a^{-1}, shown by the dashed line (R^2 = 0.744). Lighter shaded boxes indicate the elevation of intermediate terraces, that were not dated, but have been projected onto the mean linear incision rate curve to yield approximate surface abandonment ages.

With a long-term incision rate of 1.0 mm a^{-1} at the Plateau (Fig. 4.10), the elevation of T1 can be used to approximate its age. It lies ~50 m above the *c.* 70 ka T4 and 130 m above the modern river. Using a linear extrapolation, the age of T1 is approximately 120 ka. This date resembles that of the Upton-1 terrace in the Awatere Valley, which is

similarly incised/degraded and is inferred to have formed during the beginning of marine oxygen isotope stage 5 [Eden, 1983]. A similar projection of the T3 surface suggests an age of abandonment of this terrace of *c.* 75 ka.

Terrace aggradation and degradation for peri-glacial areas on soft, easily erodable bedrock can be predicted from a simple model incorporating changes in sea level and tectonic uplift. A sea level curve has been constructed from the oxygen isotope data of Martinson et al. [1987], assuming that all fluctuations observed in the isotope ratio have been accompanied by proportional changes in sea level. This sea level curve has further been modified into a series of effective sea level curves for an area uplifting at rates of 0.3, 1.0 and 2.0 mm a^{-1} (Fig. 4.11). A negative slope on the effective sea level curve represents a time when sea level is rising faster than the land is uplifting. Conversely, a positive slope indicates a relative sea level fall, for example when sea level is falling eustatically. A slope of zero represents a time when sea level rise and uplift rate are the same. As the effective sea level falls, as the river attempts to retain its equilibrium grade, strath terraces would be down-cut with the amplitude of incision scaling with the magnitude of sea level fall (trough on curve in Fig. 4.11). As effective sea level rises, aggradation would begin up to a potential thickness equivalent to the amplitude of the relative sea level rise. This cycle would repeat during each glacial-deglacial cycle. As sea level rises during a deglaciation, the climate generally becomes wetter, making available sediment to build aggradation surfaces.

The 1.0 mm a^{-1} rate of incision at The Plateau (from Fig. 4.10) includes a component of tectonic uplift and also a contribution from decreasing mean sea level over the period 123 - 26.5 ka (see Fig. 4.11). The mean linear rate of sea level drop over this period is 0.7 mm a^{-1}, hence the mean tectonic uplift is the difference between the total and the sea level components, which is 0.3 mm a^{-1}. On the basis of this simple model, predictions about the expected elevation of the flight of Late Quaternary terrace surfaces and the relative thickness of each gravel fill can be made. If the top end of the river profile is fixed, so that in the headwaters, uplift is equal to erosion (not an unreasonable assumption), the relative importance of changing sea level versus uplift experienced at a particular site depends upon how far laterally from the river mouth that site is (Fig. 4.11, inset). At the mouth, ideal base level receives 100% of the effective eustatic signal. Further inland, the difference between the high and low "ideal base levels" is less because they are converging to a point at the headwaters. Superimposed on Figure 4.11

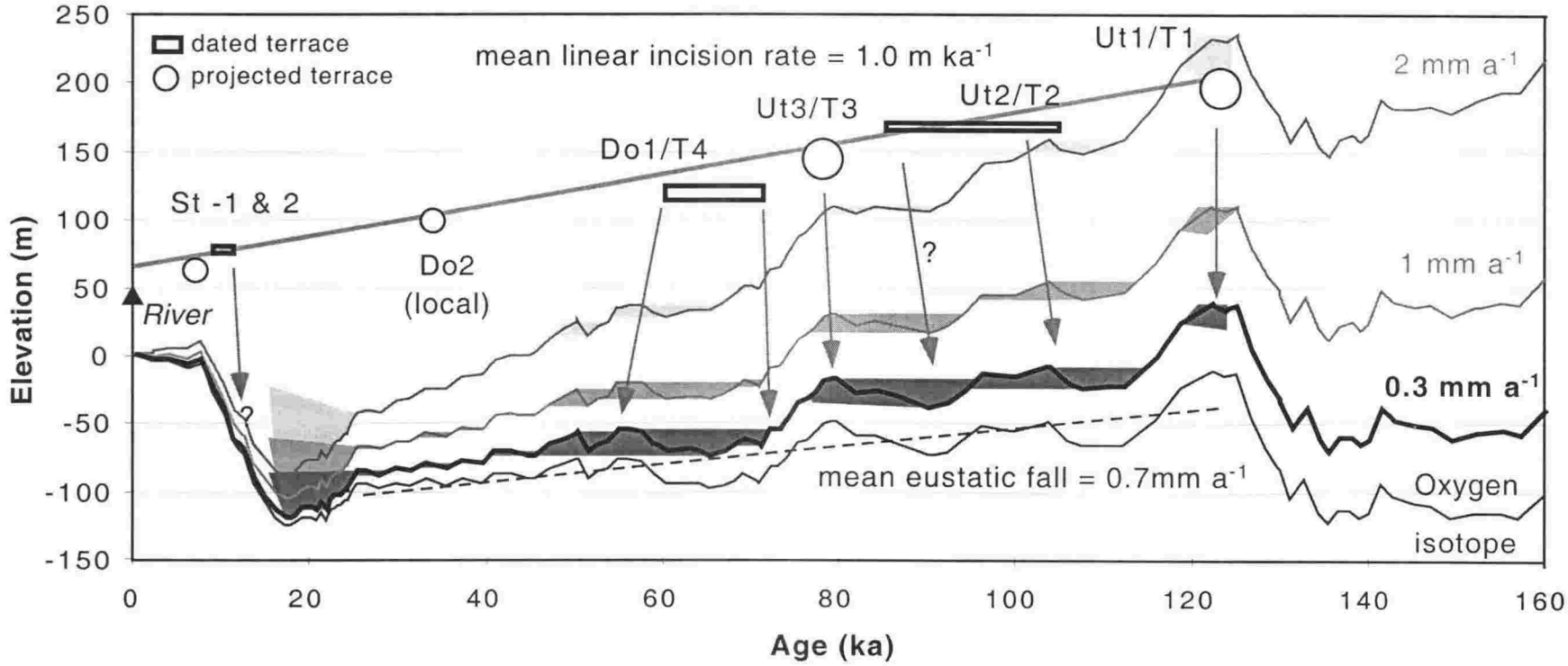

Figure 4.11. Model depicting changing effective sea level as a function of tectonic uplift. The mean linear rate of SL fall over the period 123 - 26.5 ka is 0.7 m ka^{-1} (from the oxygen isotope curve of Martinson et al. [1987]). The mean rate of incision (= eustatic + tectonic signal) is 1.0 m ka^{-1} over approximately the same period; therefore the mean tectonic signal is only 0.3 m ka^{-1} uplift. The shaded areas on the curves represent space available for filling or terrace aggradation. See Figure 4.10 for terrace elevation data. Inset (right) shows lessening effect of sea level changes with increasing distance upstream. See text for full discussion.

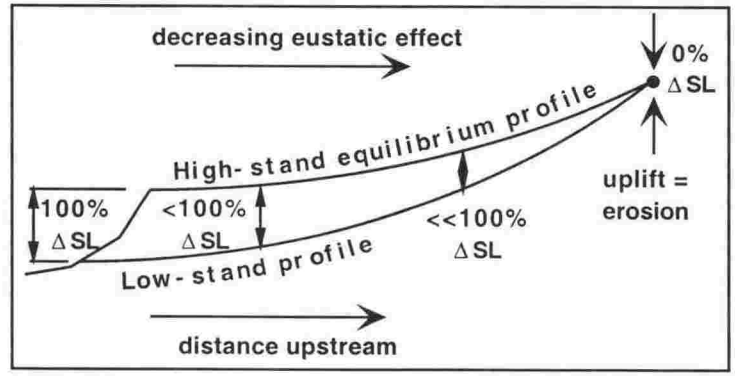

are the age-height data from Figure 4.10, for terraces at the Flaxbourne River that are cut into easily-erodable Pliocene mudstone. It can be seen from this comparison that the elevation and approximate age of terraces T1 - T4 fit the modelled terrace flight levels well. As discussed before, due to local tectonics, younger terraces at the Flaxbourne River may have been grading to a slightly different base level, therefore they might not fit as well into the expected terrace flight pattern (Fig. 4.11).

CORRELATION WITH OTHER CENTRAL NEW ZEALAND SEQUENCES

Though many robust dates have been published regarding New Zealand Quaternary stratigraphy, regional correlations remain problematical. Difficulty in regional correlation arises mainly because individual catchments are not directly linked, therefore they do not allow direct comparisons [e.g. Suggate, 1990], but also because many different types of data are presented in the literature. Care must be taken, when correlations are made between regions, that each site is responding to the same event in the same manner rather than recording local variations in response to climatic changes (e.g., comparing signals from glacial areas with peri-glacial areas). Therefore, on a regional scale, it seems more wise to recognise and correlate events rather than directly comparing sections or sequences from widely different locations and environments. To do this, we must know how different environments will react to a fluctuating climate.

Direct comparison of similar types of data can, however, be useful. The Marlborough chronology of aggradation is compared in Table 4.3 with Rangitikei River terraces from the Wanganui region in the southern North Island [Pillans, 1994]. There is remarkable consistency between the two locations, most notably the number of terraces, but also in their broad pattern of relative ages.

It is likely that the Starborough Loess [Eden, 1983], which is the youngest loess in the Awatere region, is a temporal correlative of the Ohakea Loess in the North Island. Milne [1973] described Ohakea Loess as the youngest loess in the Rangitikei/Manawatu region and it started accumulating 2-3 ka after eruption of Mangaone Tephra in the central North Island. Froggatt & Lowe [1990] ascribe the Mangaone Tephra to have a 30 ka age, based on its relationship with the overlying 28 220 ± 630 yr old Omataroa Tephra. Therefore, at Murupara in the North Island, the Ohakea Loess started accumulating at 27-28 ka (calendar years [Pillans et al., 1993]). Ohakea Loess stopped accumulating at *c.* 12 000 yrs BP., based on the 12.9 ka Kaihouri Tephra in Taranaki

Marlborough Terraces	Approx. Terrace age	Loess Unit	Rangitikei Terraces	Approx. Terrace age	Loess Unit	Tephra in loess on terrace
Starborough-3	<12 - <8?		Ohakea-3	10		
Starborough-2	12 -> 8?		Ohakea-2	12		
Starborough-1	15 -> 9?	Starborough	Ohakea-1	18	Ohakea	
Downs-2?	40		Rata	40	Rata	Kawakawa
Downs-1/T4	60	Downs	Porewa	60	Porewa	
Upton-3/T3	80	Upton-3?	Cliff	90		
Upton-2/T2	100		Greatford	100		
Upton-1/T1	120	Upton-1&2	Marton	130	Marton	
Clifford	220		Burnand	250		
Muritai	<340		Aldworth	340		
Sherbourne	400		Waituna?	360?		Rangitawa

Table 4.3. Comparison of aggradation terraces from Marlborough (this study) and Rangitikei Valley [Pillans, 1994] show a remarkable consistency in their broad pattern of ages, suggesting a common, probably climatic, influence on terrace aggradation in central New Zealand.

[Alloway, 1989], occurring just below the top of the loess section. Starborough Loess has been dated at 15.2 ± 1.3 [Little et al., 1998] and 8.0 ± 0.4 ka [this study] with the latter age probably a better estimate due to the advantages of OSL over TL dating, indicating that, while these two units are correlative, Starborough Loess continued to accumulate well after the cessation of Ohakea Loess. This difference can be attributed to local conditions; loess is accumulating in the Awatere Valley at present (e.g., Townsend [1996]), so it is not surprising that this region has had a near-continuous supply and deposition of aeolian material. The prevailing westerly wind direction may be the causal factor. The Rangitikei region lies on the west coast of North Island, therefore as sea level began to rise and inundate the shallow continental shelf that was exposed during the last glaciation [e.g. Stevens, 1974], the supply of aeolian material to the Rangitikei gradually declined, whereas the inland, upwind source of loess to the west of the lower Awatere Valley remains today.

A tentative age of 40 ka for abandonment of the Downs terrace in the Blind River area and subsequent accumulation of Downs-2 loess is comparable with the *c.* 40 ka Rata Loess in the Rangitikei Valley (Table 4. 3). The *c.* 60 ka TL age of Downs-1 Loess [Berger & Pillans, 1994] agrees well with the timing of Porewa Loess, just as the

c. 100 ka Upton Loess in the Awatere [Berger & Pillans, 1994] approximates Marton loess in the Rangitikei. Further OSL dating, in both North and South Island sequences, will be necessary to confirm these tentative correlations.

CONCLUSIONS:

- Terraces in NE Marlborough exterior to the main Awatere River catchment have been successfully correlated with known Awatere Valley aggradation surfaces using optical dating methods and mapping of surface morphological characteristics from low-altitude aerial photographs.
- New OSL dating suggests that the Starborough-1 terrace, the latest aggradation surface in the Awatere Valley, may be much younger than previously thought, as young as 9.15 ± 0.71 ka. This age indicates that aggradation in the Awatere Valley was in progress well after the last glacial maximum (*c.* 17 ka).
- The age and elevation of Late Quaternary alluvial terraces preserved in NE Marlborough suggest that these aggradation surfaces may have been forming at the time of peak de-glaciation, sea level rise and sediment flux, not during the maximum extent of glaciation, as has been previously modelled for more inland, syn-glaciation terraces.
- Terrace aggradation chronology and loess stratigraphy in eastern Marlborough has been broadly correlated with terrace stratigraphy of the Rangitikei Valley, North Island.
- The presence of Kawakawa Tephra within colluvial/alluvial fan deposits and not within aggradation surface deposits in Marlborough suggests that, in the period leading up to the last glacial maximum (*c.* 22.6 ka), localised fans were being built rather than major aggradation surfaces.
- Deformation of Late Quaternary alluvial terraces imply ongoing activity of bedrock structures such as the Ward Syncline and Hog Swamp Fault.

Chapter 5: Neotectonic patterns of uplift at the termination of the strike-slip Clarence Fault, NE Marlborough, New Zealand.

Abstract

Patterns of contemporary uplift and directions of landscape tilting in NE Marlborough have been analysed by assessing the rates of stream incision and by the evolution of drainage networks. These quantitative data have been integrated with "absolute" uplift rates gleaned from previous studies of raised coastal marine terraces in order to provide a map of Late Quaternary uplift surrounding the termination of the active strike-slip Clarence Fault. Recent estimates suggest a Late Quaternary slip rate of 5 mm a^{-1} and a total dextral strike separation of ~15 km for the Clarence Fault. These values have been used in conjunction with a model of elastic strain for a strike-slip fault termination to compare the expected and observed vertical motion attributable to crustal thickening in the tip region. Predicted values of total uplift compare well with the total observed bedrock uplift at the tip of the Clarence Fault since the late Miocene, which is on the order of 2 km. High rates of incision on indurated Mesozoic rocks compared with relatively lower rates on Neogene mudstones indicates that fast incision is not directly related to a soft bedrock, rather that the outcrop pattern of bedrock reflects the pattern of uplift.

Directions of landscape tilting, independently assessed by analysing the evolution of fluvial drainage networks, yields a pattern of tilting that is identical to the distribution of uplift inferred by assessing stream incision rates. This pattern of tilt also suggests that the tip region of the Clarence Fault is currently undergoing rapid uplift, a second-order pattern that is superimposed on a first-order regional NE tilt. Four fluvial terrace surfaces of the Awatere Valley that are younger than 120 ka all exhibit angular discordance, with progressively older terraces being progressively more tilted. Apparent regional tilting rates have not remained constant over time; in the period 120 - 60 ka, a NE tilting rate of 3° Ma^{-1} is calculated, followed by 0.2° Ma^{-1} in the period 60 - 12 ka, 6° Ma^{-1} in the period 12 - 6 ka and 15° Ma^{-1} since 6 ka. Two terraces older than 120 ka have steep, but identical downstream gradients, suggesting that the onset of the regional NE tilting in NE Marlborough was after 120 ka.

Introduction

Onshore termination of a major active strike-slip fault offers an important opportunity to study how contemporary strain is transferred from strike-slip motion on a discrete fault to distributed deformation in the tip area. The Clarence Fault, one of the four crustal-scale faults that form the Marlborough Fault System (MFS) in NE Marlborough, terminates eastward into the study area (Fig. 5.1, 5.2). This dextral strike-

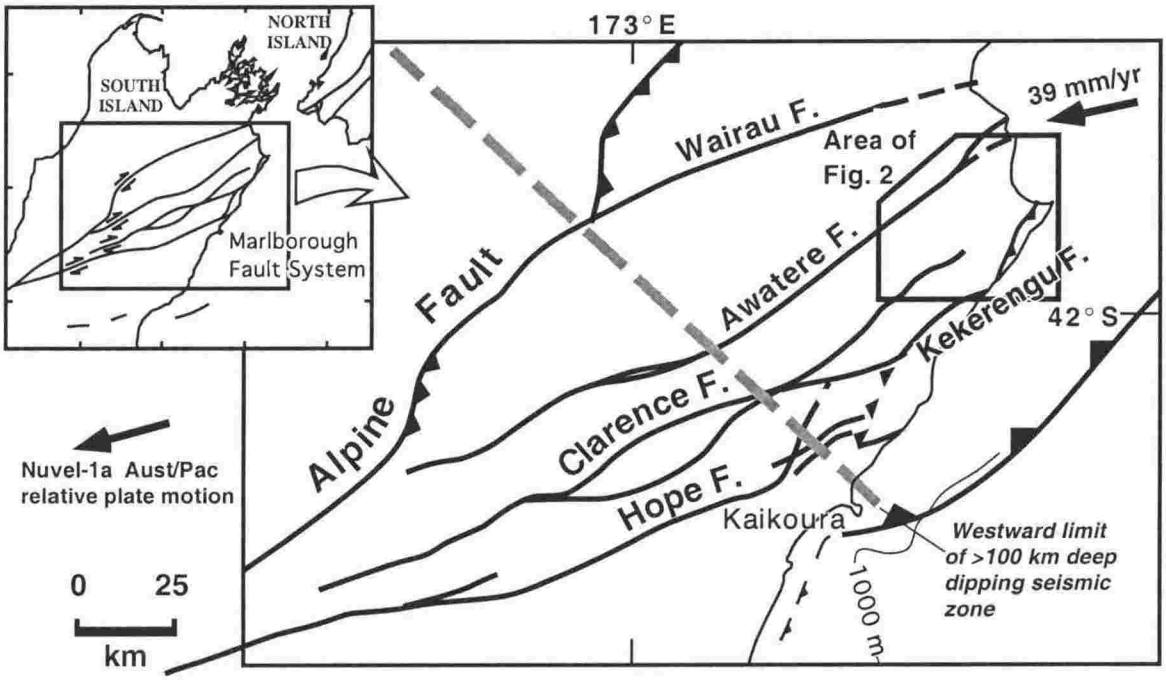

Figure 5.1. Geological setting of the study area within the Marlborough Fault System, which accommodates 80 - 100% of the Pacific-Australia relative plate motion in central New Zealand [Holt & Haines, 1995]. The active trace of the Clarence Fault, which has an inland late Quaternary strike-slip rate of 5 mm a^{-1} [Van Dissen & Nicol, 1999], terminates near the centre of the study area. Figure redrawn from Little & Roberts [1997].

slip fault has an inland slip rate of 5 mm a^{-1} [Van Dissen & Nicol, 1999], which must be accommodated by some mechanism other than fault-parallel translation to the NE of its tip. Vertical-axis block rotations are an important mechanism in accommodating Pliocene to recent deformation in the MFS, especially in the region to the NE of the termination of the Clarence Fault [Roberts, 1995; Little & Roberts, 1997; Townsend & Little, 1998]. In addition, transfer of strike-slip motion into localised crustal thickening associated with uplift may also play a role in accommodating crustal strain in the tip region. A well preserved Quaternary alluvial stratigraphic record in NE Marlborough [Chapter 4], coupled with the availability of coastal uplift rate data derived from analyses of raised marine terraces, allows the assessment of the distribution of uplift rates near the termination of the Clarence Fault over the last ~120 ka.

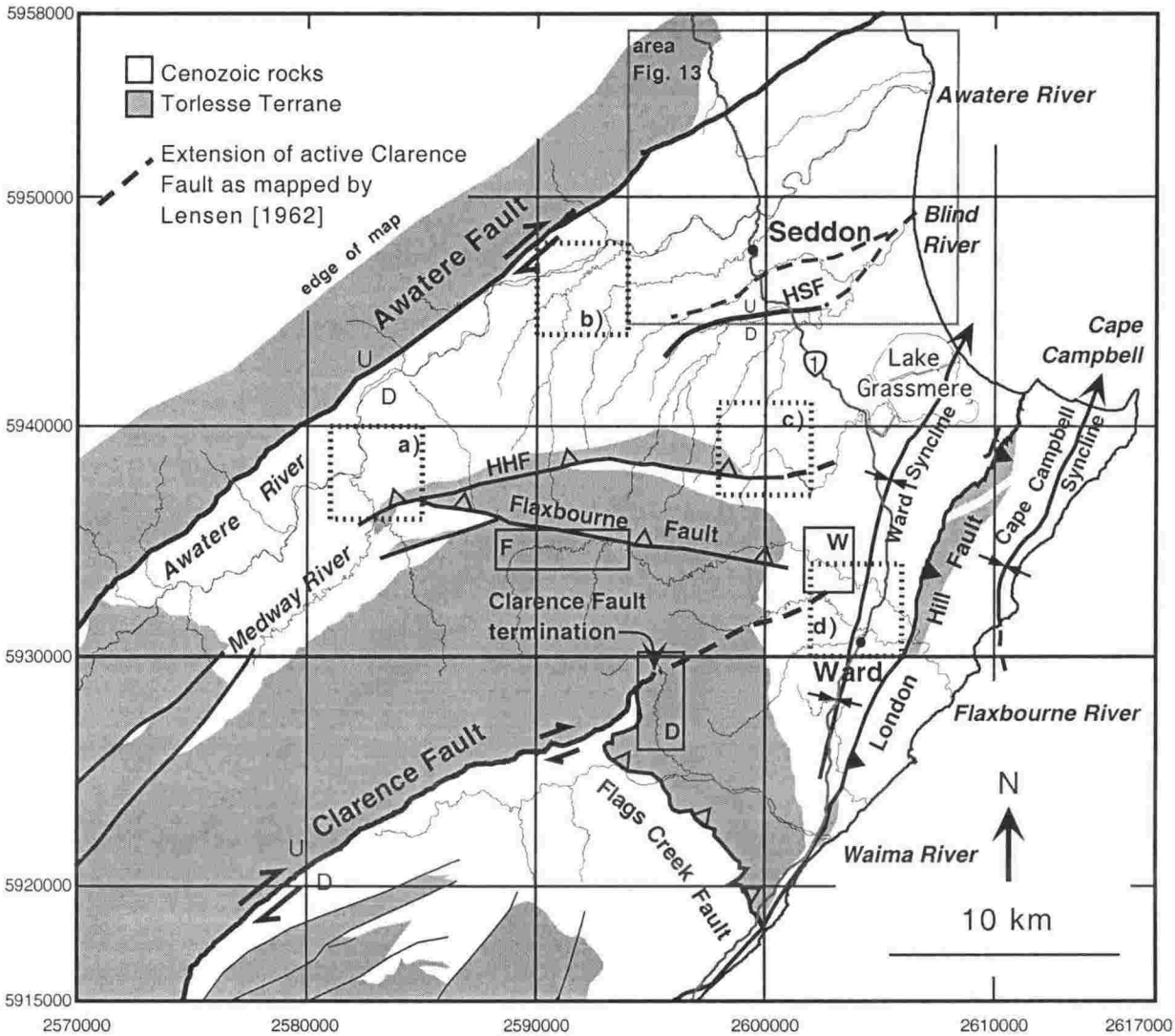

Figure 5.2. Simplified geological map of the Awatere - Ward area emphasising the distribution of Mid - Late Cretaceous Torlesse Terrane (shown in grey), after Russel [1959] and Lensen [1962]. Active structures include the Awatere, London Hill and Clarence faults, the latter of which terminates near the centre of the study area. Other faults that may be active are the Hog Swamp Fault (HSF), Haldon Hills (HHF) and Flaxbourne faults. The Ward and Cape Campbell synclines are also taking part in active deformation [Townsend, 1996]. Solid boxes with letters denote regions surveyed by EDM: F: Flaxbourne; W: Ward; D: Dunsandel (see Appendix 4) and dashed boxes a-d denote detailed examples of tilted drainage patterns shown on Figures 5.11A - D.

A study of Quaternary alluvial and marine terraces from an area that includes the NE termination of the active Clarence Fault is presented in this paper. Rates of vertical stream incision are used as a proxy for rates of uplift (with a discussion of problems therein). Bedrock underlying this area is mostly Late Miocene - Pliocene mudstone. This lithology is regionally homogenous, therefore the effect of bedrock type on drainage evolution is minimal. Directions of landscape tilting are assessed by the pattern of drainage evolution and stream piracy. These data are integrated with known "absolute" coastal uplift rates gleaned from previous studies of uplifted marine terraces and a tectonic uplift map of the NE Marlborough region is derived. The distribution of finite vertical strain determined from uplifted terraces surrounding the Clarence Fault tip is in accordance with the pattern of vertical displacement predicted by 3-D elastic models of strike-slip fault terminations [ten Brink et al. 1996]. This suggests that a component of dextral strike-slip motion of this crustal scale fault is being transferred into crustal thickening in the region to the NW of the Clarence Fault tip.

PREDICTED PATTERN OF LOCAL STRESS AND STRAIN AT THE TERMINATION OF A STRIKE-SLIP FAULT

The inhomogeneity of deformation processes in the earth often leads to distinct zones of concentrated deformation separated from relatively undeformed areas. This leads to perturbations in the regional stress field where structures terminate. Two-dimensional distinct element models of elastic media [Homberg et al., 1997] suggest that, in the tip region of a right-lateral shear discontinuity (fault), mean compressive stresses will be above average to the left of the tip and below average to the right of the tip, as viewed along the fault (Fig. 5.3A). In such elastic dislocation models, perturbation of stress magnitude is accompanied by changes in the direction of the local principal stresses (bars on Fig. 5.3A). Factors such as the magnitude of the remote differential stress, the coefficient of friction on the fault and the strike of the fault relative to the regional stress system control the direction and magnitude of stress deflection in the vicinity of the fault tip [Homberg et al., 1997].

The manifestation of increased mean compressive stress at a fault tip (e.g. Fig. 5.3A) relative to the regional stress may induce finite deformation such as pressure solution, thrust faulting and folding in the "compressional" quadrant (Fig. 5.3B & C), but because these changes in stress are relative to the regional stress, normal faulting

and extensional deformation are not necessarily characteristic of the "tensile" quadrant. Another mechanism that may accommodate deformation at a strike-slip fault termination is vertical axis rotations of crustal blocks in the tip region, such that horizontal translation is transferred into rigid body rotation [e.g. Roberts, 1995]. The fault tip may act as a "pivot" point of a series of rotating blocks (Fig. 5.3D). This mechanism may produce little vertical strain.

Alternatively, increased horizontal compressive stress in the compressional quadrant may be manifested by a component of vertical strain (crustal thickening), leading to a localised uplift of that area (Fig. 5.3E). The intensity of vertical strain predicted by 3-D elastic models [ten Brink et al., 1996] depends upon factors such as the width of the deforming zone, the strength of the fault and the total amount of fault offset, with deformation generally taking place over a broader region with increasing shear zone width and/or increasing fault strength. However, the general pattern and location of positive or negative uplift features is consistent over a wide range of boundary conditions. A component of vertical axis rotation is also predicted by these models, with the most intense rotation expected in the immediate vicinity of the fault tip. On a crustal scale, over geological time, these finite deformations will be "plastic" and non-recoverable and, rather than being a continuum, deformation will occur by slip or folding on discrete structures. In practice, deformation at a strike-slip fault termination may be accommodated by some combination of several of these mechanisms at different times and in different places.

The pattern of crustal thickening in the region surrounding the Clarence Fault tip should reflect the predicted uplift according to elastic models of strike-slip fault terminations. Study of the relative uplift of well-preserved fluvial terraces in this area allows characterisation of finite vertical crustal motions and quantification of how strike-slip /translational motion is transferred into crustal thickening where transcurrent discontinuities die out.

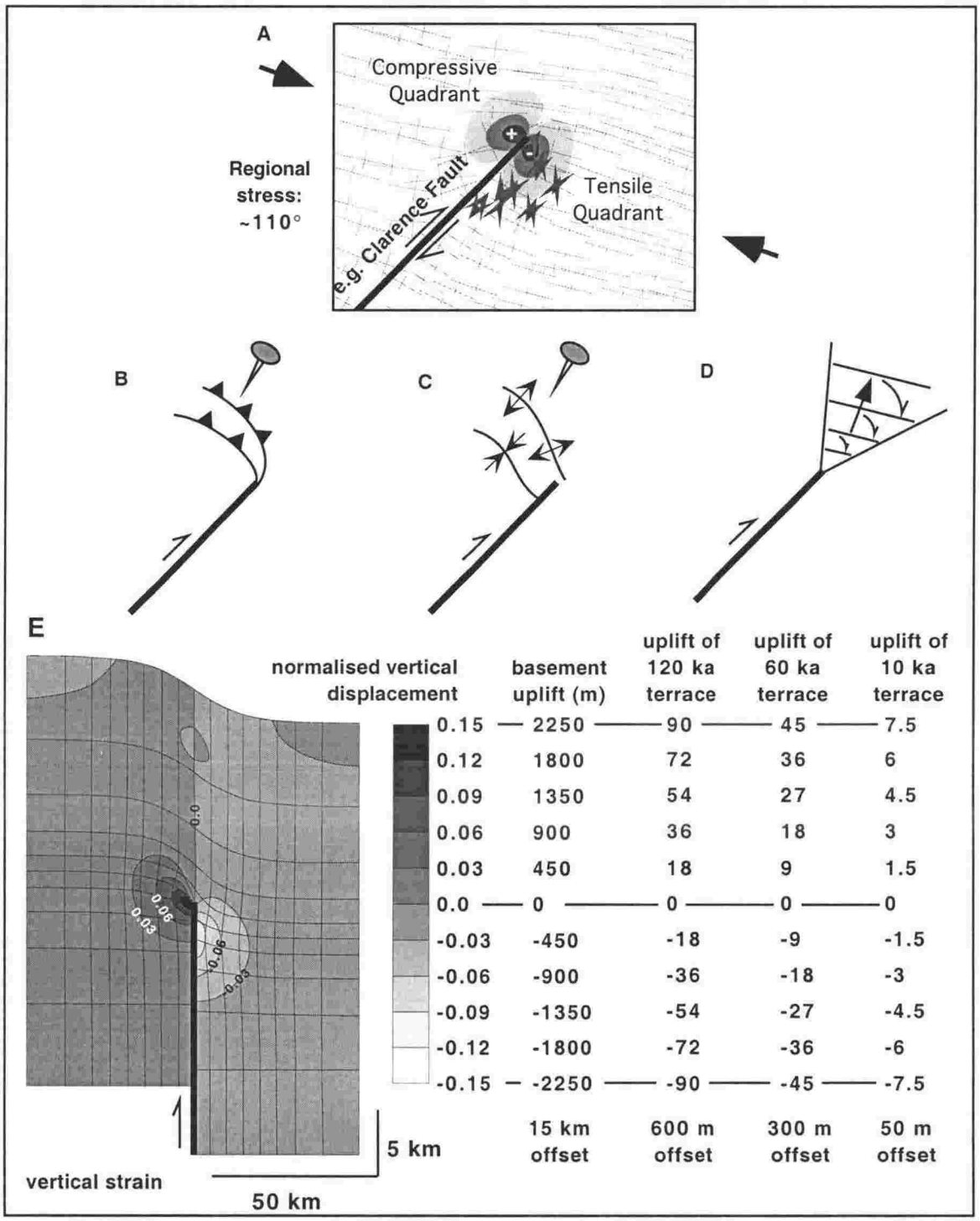

Figure 5.3. Deformation state at the termination of a strike-slip fault. A: Both the magnitude (shaded region) and direction (long bar symbol represents horizontal component of σ_1) of regional stress are locally modified in the tip area of an elastic dislocation [after Homberg et al., 1997]. Termination of dextral strike-slip may induce localised thrust faulting (B) or folding (C) in the contractional quadrant surrounding the tip, or (D) vertical axis rotation of fault-bounded blocks to accommodate differential slip [e.g., Roberts, 1995]; E: Predicted vertical displacement at the tip of a dextral discontinuity (bold line) in an elastic medium [modified from ten Brink et al., 1996]. The grid represents an originally rectangular mesh showing the horizontal deformation field near the fault tip. The basal fault offset is 5 km, the width of the shear zone is zero and the vertical scale is normalised to the amount of basal offset. The column "basement uplift" is the calculated total amount of uplift corresponding to a maximum of 15 km of dextral offset along the Clarence Fault [Little & Jones, 1998] and assuming a linear scaling of uplift with basal offset. Other columns represent the amount of uplift corresponding to terraces with ages of 120, 60 and 10 ka. These values have been calculated using an estimated Late Quaternary dextral strike-slip rate of 5 mm a^{-1} for the Clarence Fault [Van Dissen & Nicol, 1999].

PATTERN OF UPLIFT AND SUBSIDENCE IN NE MARLBOROUGH

Previous studies

Prior to this study, the extent of Late Quaternary uplift in NE Marlborough has been derived from the analysis and dating of raised coastal marine terraces [Ota et al., 1995, 1996; Townsend, 1996]. In addition, uplift gradients were identified along major river courses by analysing the tilt of alluvial terrace sequences [Eden, 1989] (Fig. 5.4). The coastal uplift data provide important constraints, or tie-points, for using stream incision rates and landscape tilting for measuring uplift rates in the inland regions. In the vicinity of the Clarence Fault termination, NE Marlborough can be divided into several neotectonic domains of Late Quaternary uplift [e.g., Ota et al., 1995] (Fig. 5.4). The Vernon domain has no available data but is inferred by Ota et al. [1995] to be undergoing "slow uplift". In the Lower Awatere domain, the difference in slope of progressively older alluvial terraces in the Awatere River Valley has been used to infer an increase in uplift rate along the river length toward the headwaters of 1 - 2 mm a^{-1} [Eden, 1989]. Using remnants of a 350 ka alluvial terrace near the coast, Little et al. [1998] inferred a tilting rate of 3° Ma^{-1} in a NE direction. The Blind River and Grassmere domains are characterised by "slight" uplift and active folding of the Ward Syncline [Ota et al., 1995; Townsend, 1996]. East of the London Hill Fault (Fig. 5.4), rapid uplift is occurring at a rate of 0.4 - 2.5 mm a^{-1} and is accompanied by active folding of the Cape Campbell Syncline. Thus, coastal NE Marlborough comprises several neotectonic domains characterised by different rates of vertical tectonic motion. By themselves, however, these scattered coastal uplift rates do not document how uplift is distributed in the large inland region or in proximity to the Clarence Fault tip.

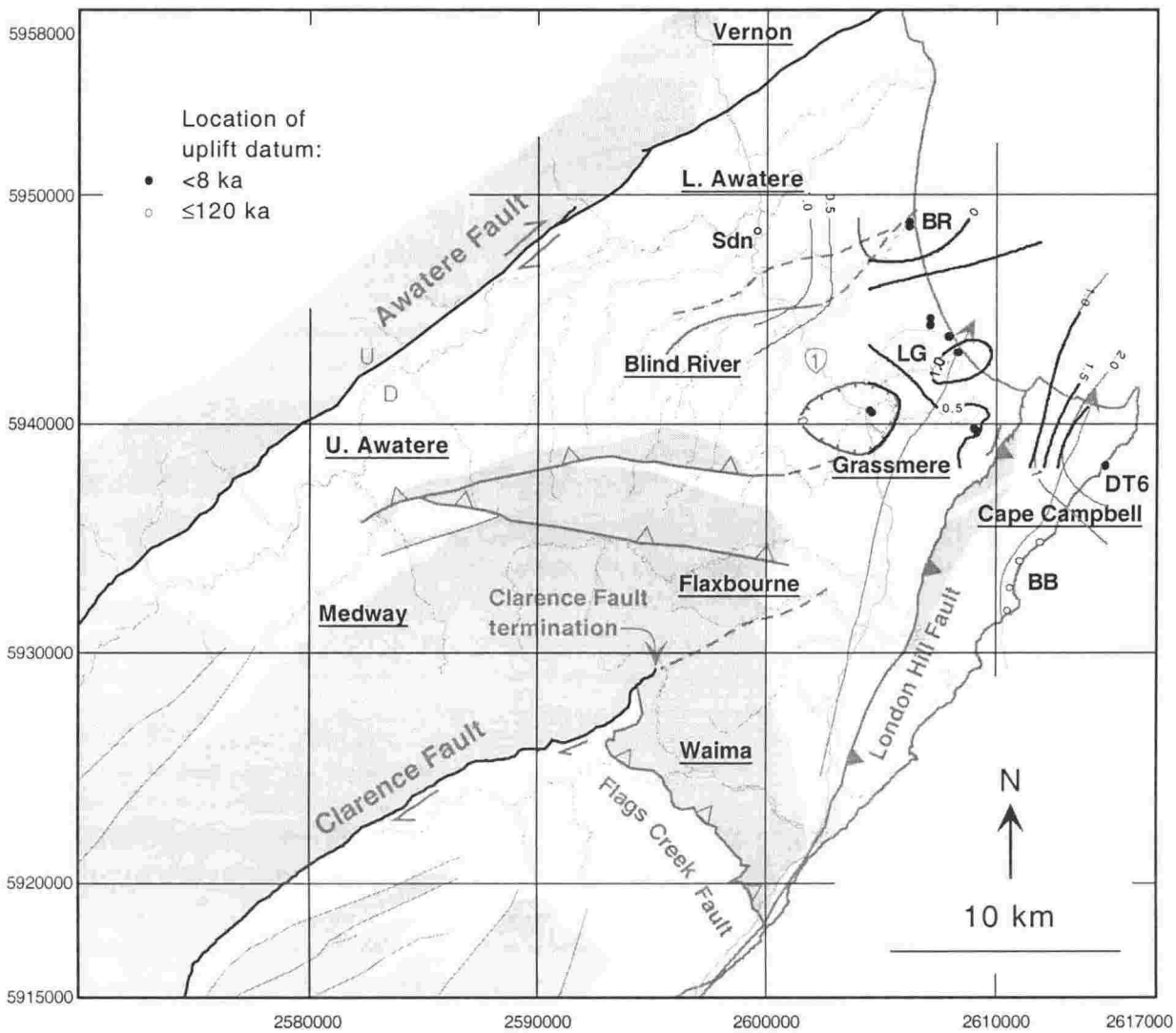

Figure 5.4. Uplift data prior to this study have mostly been derived from Late Quaternary coastal marine terraces east of the London Hill Fault and from sparse borehole data surrounding Lake Grassmere. Localities shown with a solid circle and associated black contours plot uplift data that are younger than ~8000 yrs only, whereas open circles and grey contours combine all available estimates of uplift including remnants of a 120 ka marine surface. Data are compiled from Ota et al. [1995, 1996] (Lake Grassmere: LG; Blind River: BR & Boo Boo Stream: BB), Townsend [1996] (marine terrace: DT6) and Little et al. [1998] (Seddon bridge: Sdn). These data are too sparse to define any patterns of uplift. Underlined names denote regions that are referred to in the text.

Deformation of Quaternary alluvial terraces

Morphostratigraphy and dating constraints

The lower Awatere Valley - Ward region preserves a superb flight of Late Quaternary - Holocene alluvial terraces, some as old as ~350 ka [Eden, 1989; Little, et al. 1998]. Revision of the Quaternary stratigraphy of this area (Chapter 4; Fig. 5.5; see also Quaternary terrace map in back pocket) has recently been possible in the light of analysis of five optically stimulated luminescence (OSL) ages of loess coverbeds on these regionally extensive river terraces. Fluvial terrace remnants have been regionally correlated between drainage basins on the basis of morpho-stratigraphic position, the degree of surface erosion/preservation visible from low-altitude aerial photos and the presence or absence of well-dated tephra marker beds that have been chemically identified [Chapter 4]. It has been suggested in Chapter 4 that formation of these aggradation or fill terrace surfaces coincides with the advent of warm periods following glacial maxima and can be correlated with "warming" peaks in the oxygen isotope ratios of Martinson et al. [1987] when rises in mean sea level may have occurred.

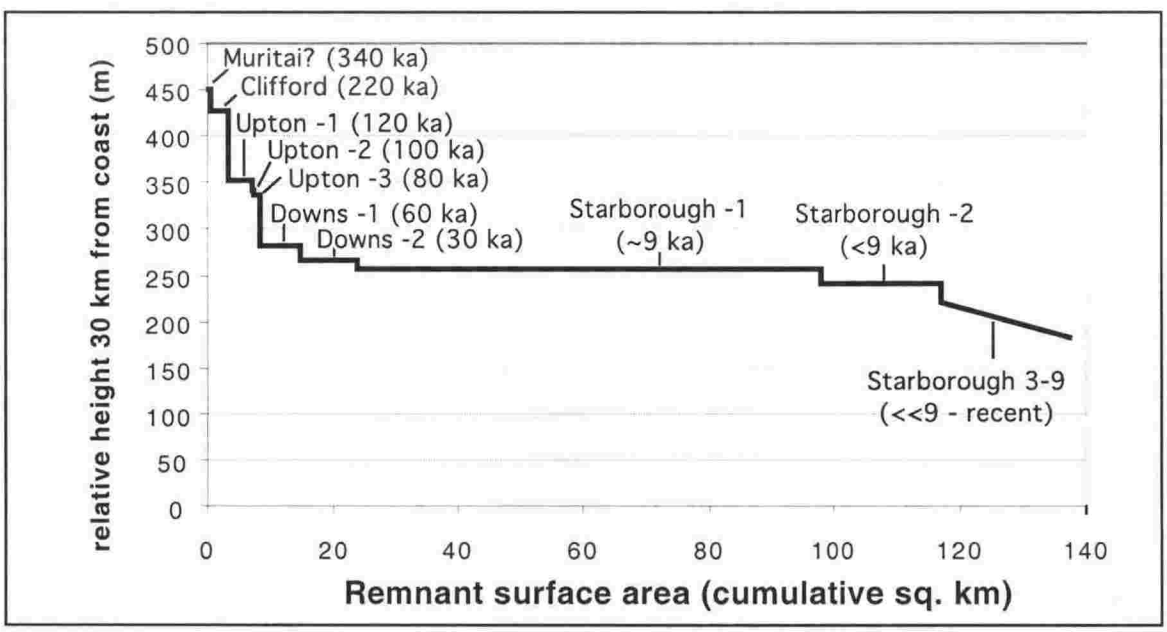

Figure 5.5. Morphostratigraphy of terraces in the Awatere Valley - Ward region [after Eden, 1989] as a function of their preserved surface area. The total area considered for analysis is ~1300 square km. Numbers in brackets refer to approximate terrace abandonment ages, in ka [Chapter, 4]. A schematic profile of relative surface elevations is taken at a distance of 30 km upstream from the Awatere River mouth. The extensive preservation of the Starborough-1 aggradation terrace makes this the most useful in terms of surface deformation analysis.

Incision rates as proxy for uplift

Differential rates of vertical stream incision have been attributed to differential tectonic uplift by various past workers [e.g., Personius, 1995; Leland et al., 1998; Maddy et al., 2000]. Using incision rate data as an estimate of uplift requires several assumptions. First, one assumes that the river had achieved its equilibrium gradient profile when all terraces formed and that the modern river is also presently graded. As the surfaces used in this study are aggradational, the assumption of grade is probably reasonable. This may not always be the case for the modern river level (see below). Other assumptions are that rates of incision are spatially uniform in the Cenozoic mudstone bedrock and only slightly lower in the stratigraphically underlying Torlesse basement rocks. The age of each surface used in this study is inferred to be the same throughout the region. Loess coverbed thickness is variable throughout the region [Eden, 1989] and has not been subtracted from terrace surface elevations used in this study. The presence of thick loess deposits on older terraces serves to increase the apparent incision rate as the present surface elevation is higher than those terraces without loess. It will be shown later that the incision rate differences introduced by this factor are negligible, because young terraces (without loess) show by far the highest incision rates.

Incision rate data have been assembled by using the Quaternary terrace correlations of Chapter 4 and elevations of terrace remnants relative to mean sea level have been taken from topographic contours plotted on the digital set of 1: 50 000 scale contours. Spot height elevations on terraces were also used in this study. The uncertainty associated with contour data is approximately 20 metres. The GIS program "MapInfo" was instrumental in this study to measure elevations between surfaces and to provide a geographic reference frame for the analysis. Elevation distance meter (EDM) surveys of terrace surfaces were also carried out in three key areas close to the termination of the Clarence Fault (boxes on Fig. 5.2) in order to measure relative terrace heights in finer detail than is possible from the 1: 50 000 contour data.

For this study, three aggradation surfaces of differing age have been used to assess both the spatial distribution of incision surrounding the termination of the Clarence Fault and its continuity over the last ~120 ka. These terraces are the ~120 ka Upton-1 terrace, the ~50 - 60 ka Downs-1 terrace and the ~9 ka Starborough 1 terrace [Eden, 1989; Chapter 4]. The older terraces are only preserved along the Awatere River or in

the Blind River - Ward region (see Fig. 5.2), therefore only a small part of the study area can be used to compare the stability of incision rates through time. However, the Starborough-1 terrace crops out extensively throughout the region and has a total surface area of more than 70 square km (Fig. 5.5), thus providing a "snapshot" in time across the entire region. The slightly younger Starborough-2 terrace is also extensively preserved along the Awatere River (e.g. Fig. 5.5), but because the only age estimates available for this surface are based on its relative position below the Starborough-1 terrace [Little et al., 1998], it is not used in this study.

The regional pattern of incision is described next for each terrace, compared with the modern stream level. Relative incision between data is also presented, which is the elevation difference between two specified terraces, divided by their age difference.

The Upton-1 surface generally shows high rates of incision in the Upper Awatere domain, as expected for a river with high stream power (Fig. 5.6A), with less incision in the Lower Awatere domain. Low values of incision rate are recorded in the Blind River domain. A positive incision anomaly is seen NW of Ward, at the eastern end of the Flaxbourne domain, and the Grassmere domain exhibits low incision rates.

Deformation of terraces that occurred between ~120 and ~60 ka can be determined by evaluating the difference in elevation between the Upton-1 and Downs-1 aggradation surfaces. Rates of incision over this period are shown on Figure 5.6B. The general pattern reveals an incision gradient along the Awatere River, from fast incision in the Upper Awatere Domain to slower incision near the coast, indicating a NE tilting along the river profile between ~120 and ~60 ka (see below). Rapid incision is again observed on the footwall of the London Hill Fault (Fig. 5.6B). Townsend [1996] noted that the structural style of deformation in this area chiefly involves flexural slip in association with active folding of the Ward Syncline, a pattern that is consistent with uplift of the eastern limb of this fold. Low rates of incision are observed in the Blind River Domain.

Downs-1 terrace incision shows a similar pattern to that of Upton-1 (compare Figs. 6A and 6C), with high rates in the Upper Awatere domain and low rates in the Blind River and Grassmere domains. The high anomaly at the eastern Flaxbourne domain persists for the younger terrace and, with limited data, it appears that incision in the rest of the Flaxbourne domain is moderate. A north-south gradient from low to high

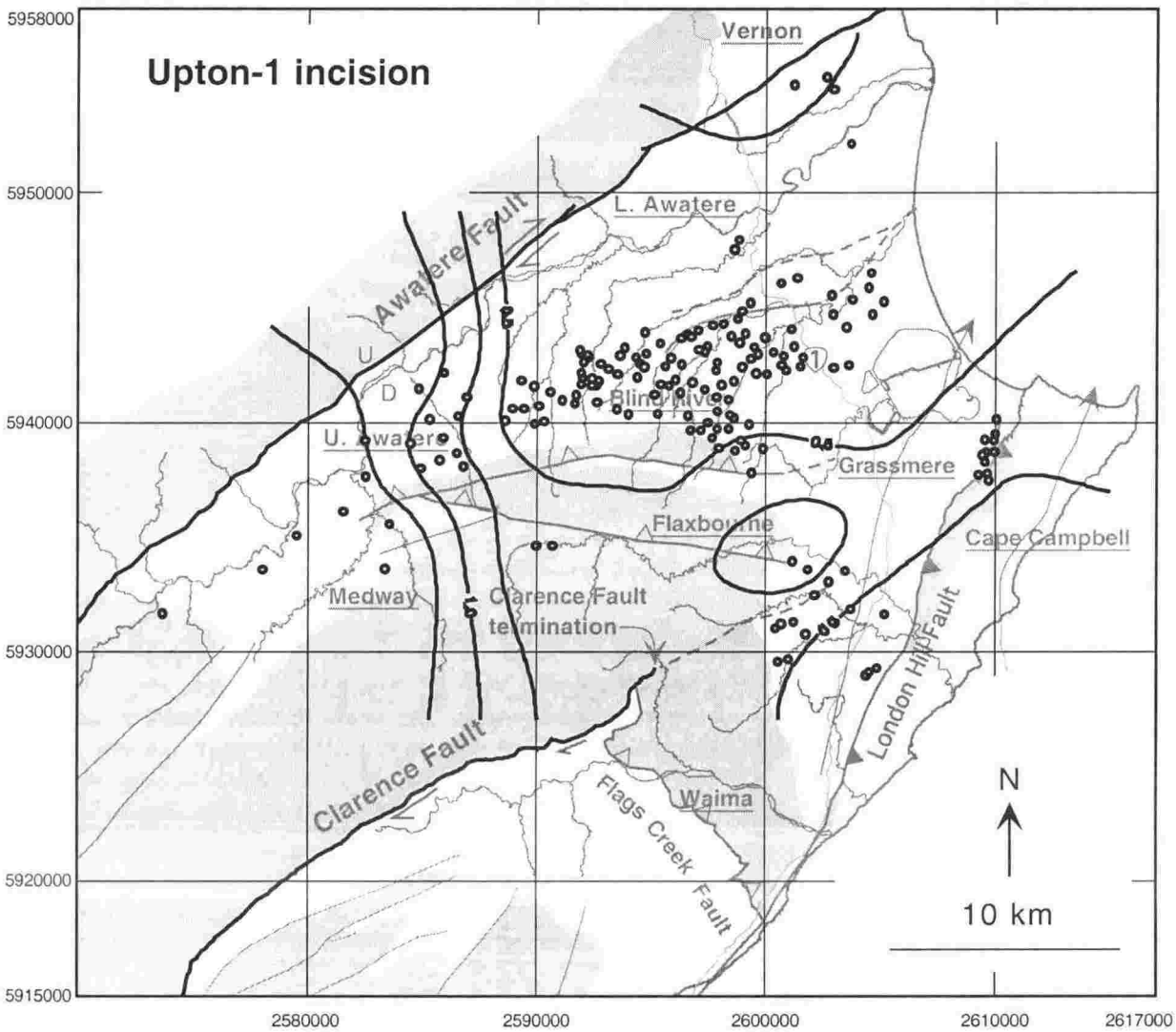

Figure 5.6A. Contoured map of terrace incision rates, in mm a^{-1}, for remnants of the ~120 ka Upton-1 terrace. Circles are point incision rate data derived from the difference in elevation between the Upton-1 terrace and the local modern river level. Incision is relatively high along the Awatere River in the west and low in the Blind River region. Fast incision is observed along strike of the Clarence Fault, NE of its termination and in the Medway area. Contour interval is 0.25 mm a^{-1}. See text for discussion.

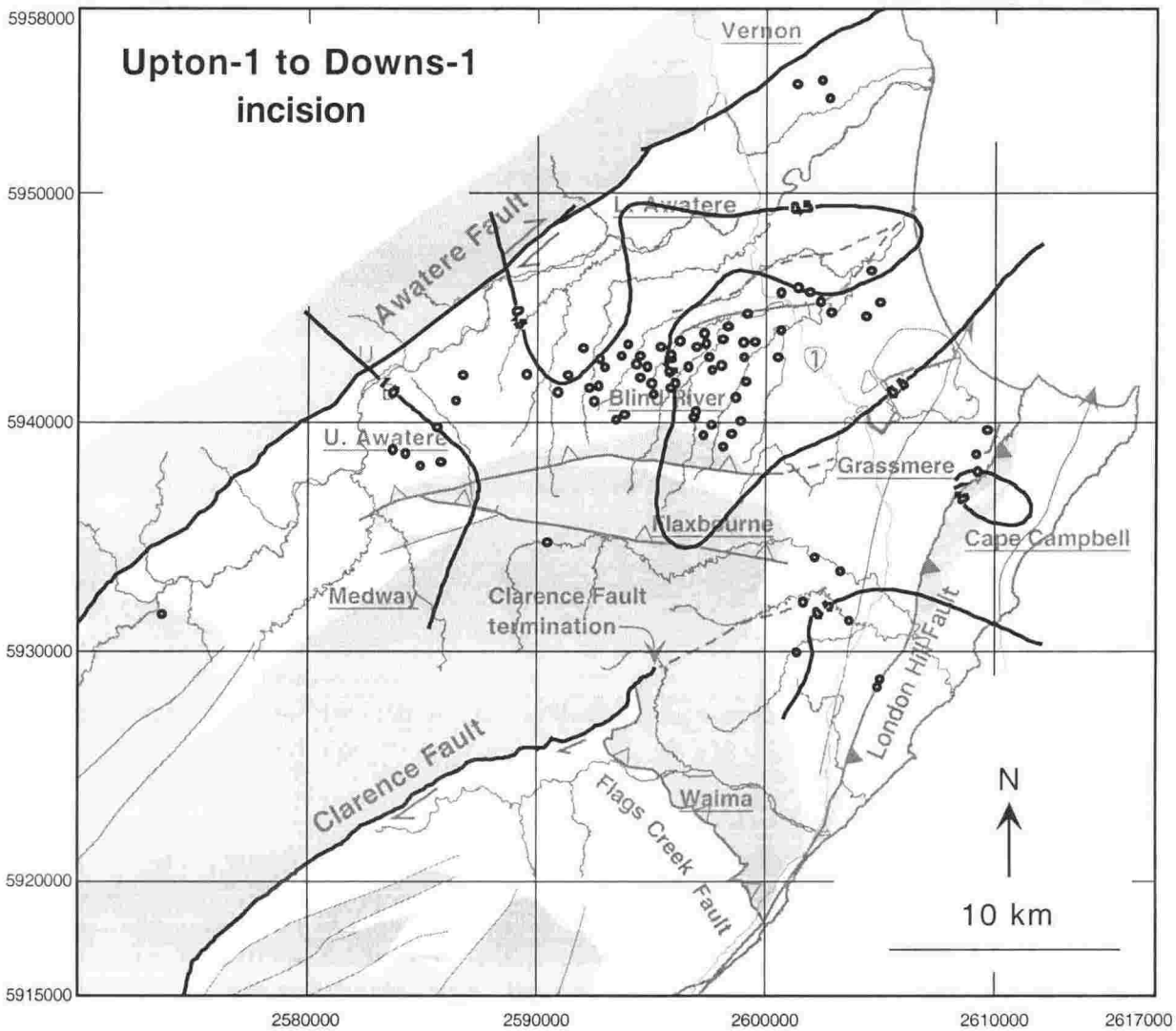

Figure 5.6B. Contoured map of terrace incision rates, in mm a^{-1}, between Upton-1 (~120 ka) and Downs-1 (~60 ka) time. Circles are point incision rate data derived from the difference in elevaton between the Upton-1 and Downs-1 terraces. Note the high incision anomalies in the west (Medway area) and close to the London Hill Fault during this time interval, with slow incision in the Blind River Lower Awatere areas. Contour interval is 0.5 mm a^{-1}. See text for discussion.

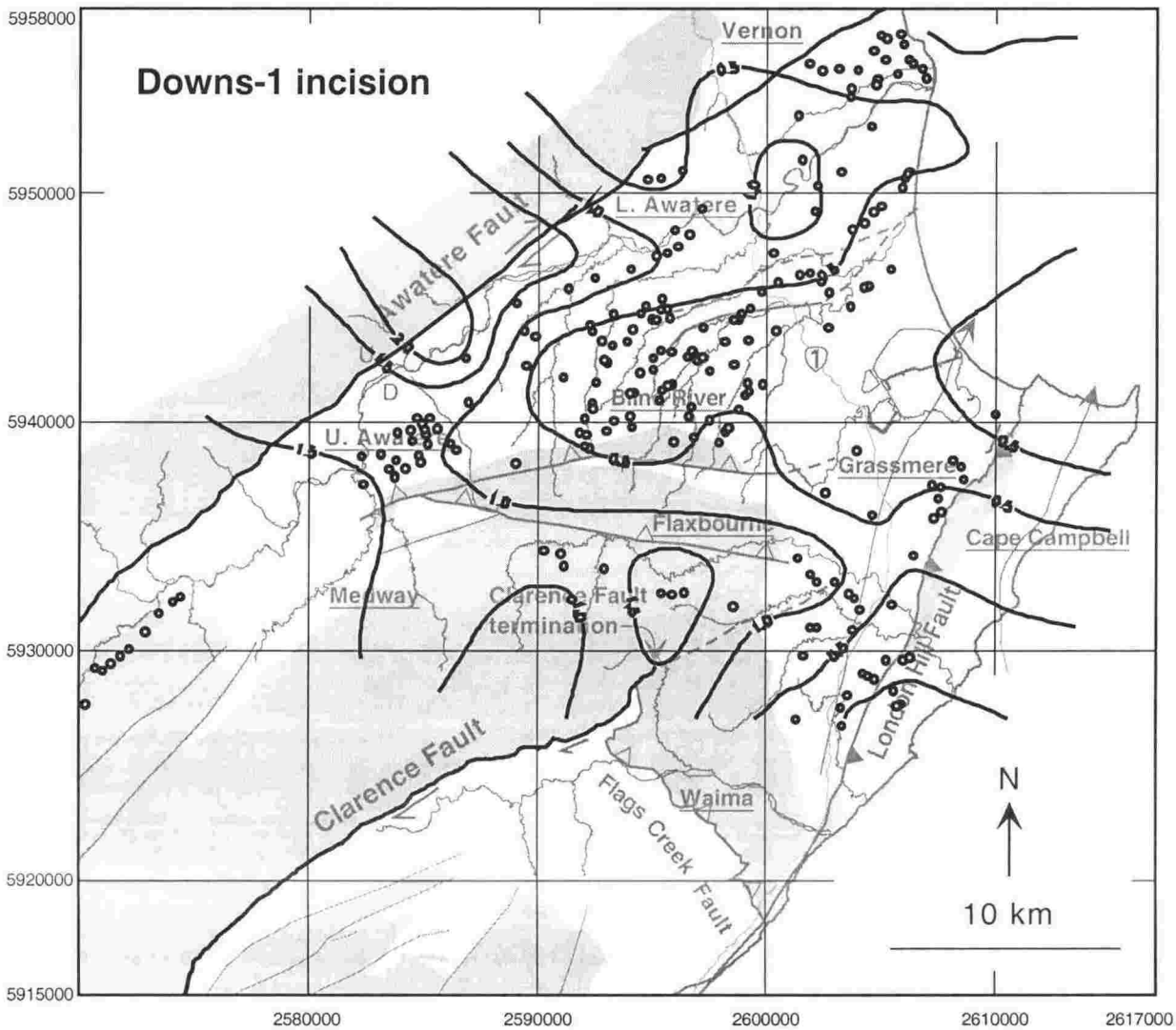

Figure 5.6C. Contoured map of terrace incision rates, in mm a^{-1}, into the ~60 ka old Downs-1 terrace. Circles are point incision rate data derived from the diffrence in elevation between the Downs-1 terrace and the local modern river level. Incision is high along the Awatere River in the west and also generally high in the Flaxbourne region. Low incision rates are seen in the Blind River and Grassmere areas. Contour interval is 0.5 mm a^{-1}. See text for discussion.

incision rates is seen across the Haldon Hills, between the Blind River and Flaxbourne domains. This gradient is the inverse of that expected were rates of incision purely related to bedrock type, as Mesozoic greywacke mostly underlies the Haldon Hills (high rates) and the Blind River area is underlain by Neogene mudstone (low rates). Thus it appears that rates of incision in NE Marlborough are not strictly controlled by bedrock type.

The difference in incision rates between the Downs-1 and Starborough-1 terraces is shown on Figure 5.6D. A striking feature is a ridge of high incision rates extending from the tip of the Clarence Fault north and east to the London Hill Fault. A region of low incision rates in the Ward area is consistent with downfolding in the axis of the Ward Syncline between ~60 and ~10 ka. Again, relatively low rates of incision are noted in the Blind River Domain.

Starborough-1 incision also reveals fast downcutting associated with the Awatere River (Fig. 5.6E), but perhaps more surprising is a high rate of incision in the Medway domain, where the Starborough-1 terrace is up to 110 m above the Medway River. Again, the Lower Awatere domain is dominated by incision of the Awatere River, but rates in the Blind River and Grassmere domains are low. The most salient features of the Flaxbourne Domain are the two high anomalies immediately NE of the Clarence Fault tip, with steep gradients to the north and east. The intervening low is associated with a hill about which the drainage has changed course, in effect creating two moderately deep channels rather than one deep one. The central part of the Flaxbourne domain also shows relatively low rates of incision compared with the upper and lower reaches. This can be explained by the central part of the Flaxbourne River not being graded to stream base level. This is discussed in more detail below. Further east, positive incision anomalies coincide with the London Hill Fault, but coastal rates in the Cape Campbell domain are moderate. A NNE-trending trough extends from the Grassmere Domain SSW along the footwall of the London Hill Fault, coincident with the position of the Ward Syncline.

The similarity in the distribution of incision into terraces ranging in age from ~120 ka to ~10 ka suggests that the pattern of incision has not changed significantly over this time interval.

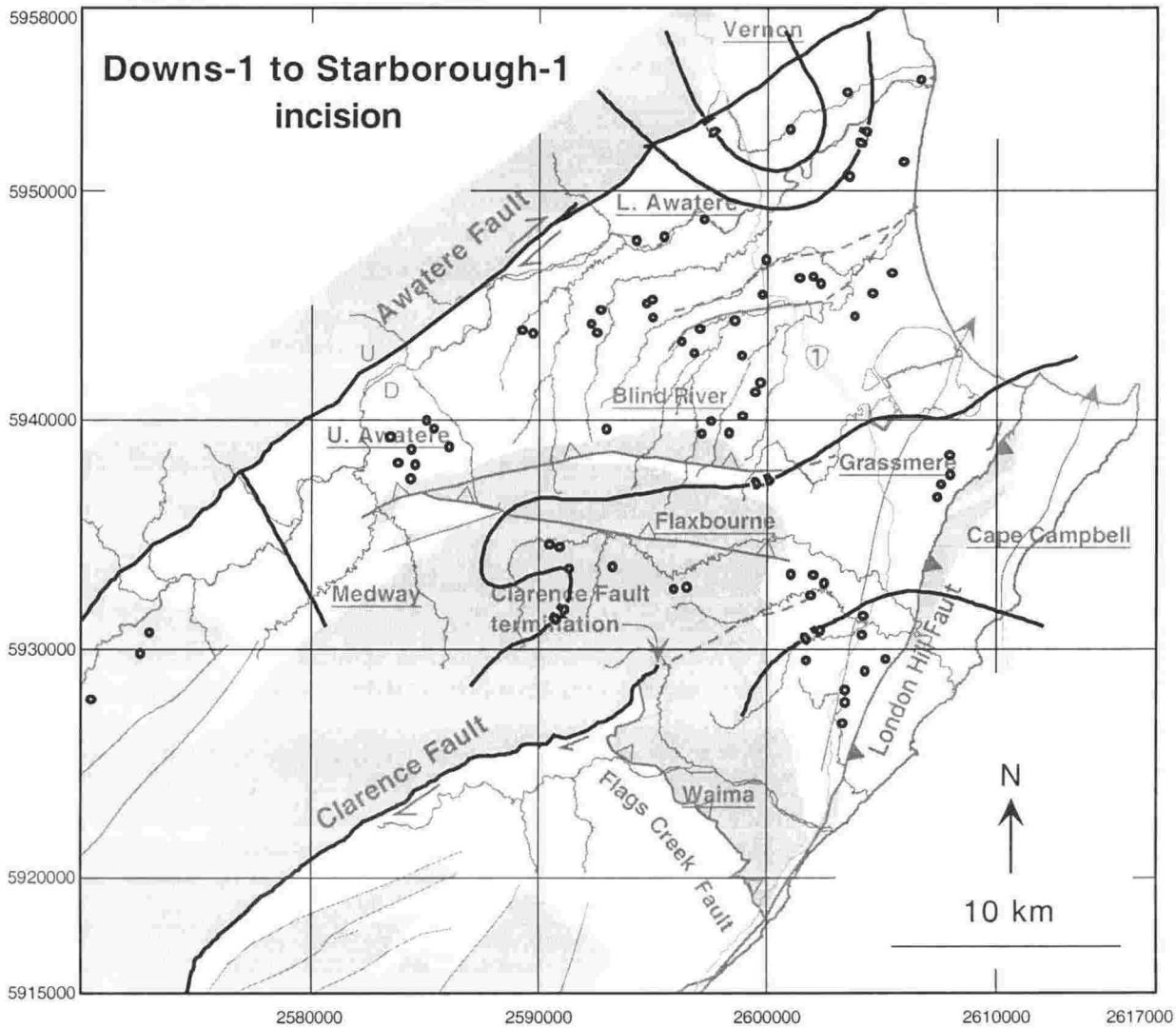

Figure 5.6D. Contour map of terrace incision rates, in mm a^{-1}, between Downs-1 (~60 ka) and Starborough-1 (~10 ka) terraces. Circles are point incision rate data derived from the difference in elevation between the Downs-1 and Starborough-1 terraces. The pattern of incision reveals moderately high rates in the Upper Awatere region and low rates in the Blind River area. A ridge of high rates is also seen in the eastern Flaxbourne area, near the Clarence Fault tip, extending (across a region of no data) to the London Hill Fault. Relatively low rates of incision occur near Ward, consistent with downfolding of the Ward syncline during this time interval. Contour interval is 0.5 mm a^{-1}.

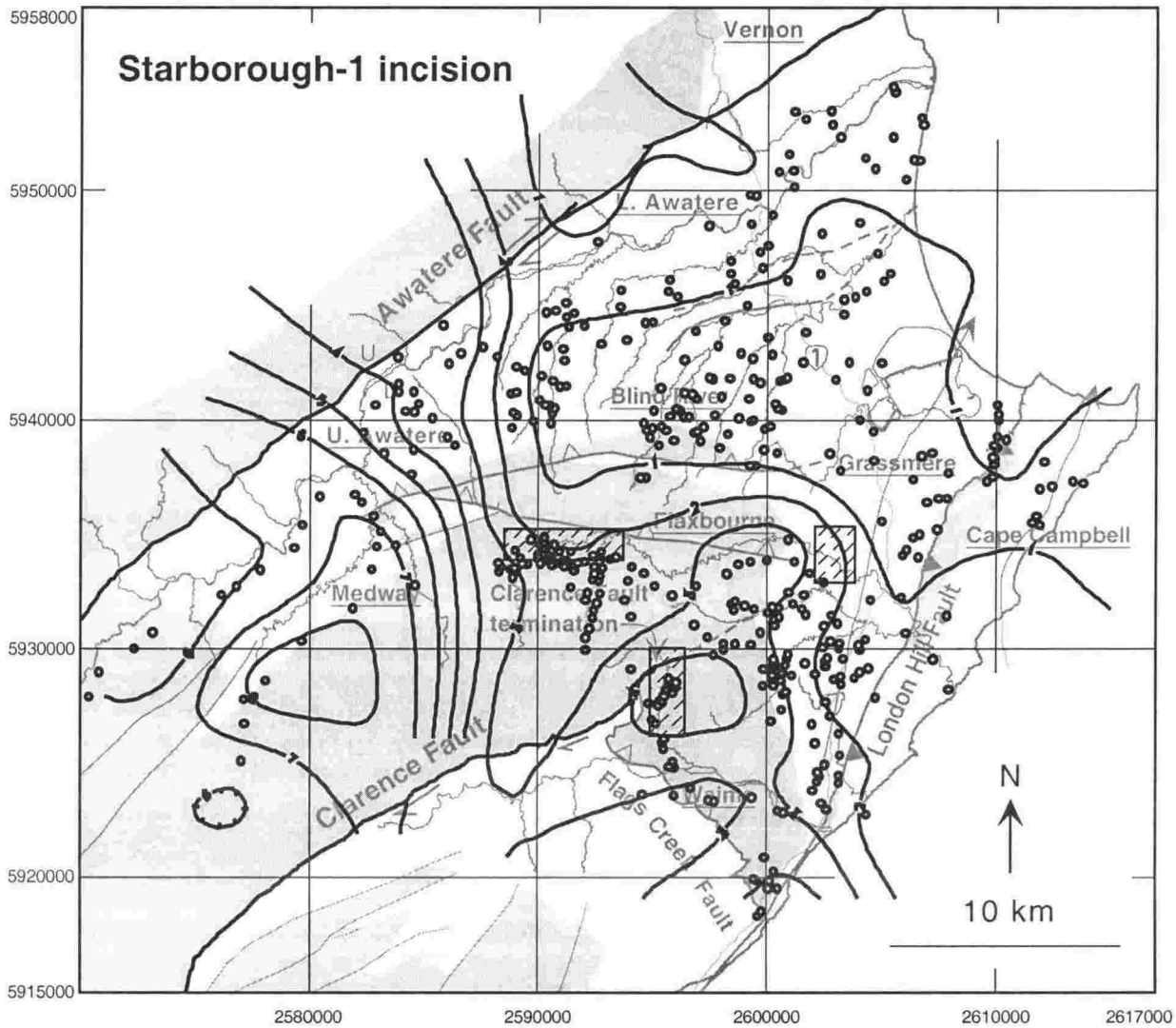

Figure 5.6E. Contour map of terrace incision rate, in mm a^{-1}, into the ~10 ka old Starborough-1 surface. Circles are point incision data derived from the difference in elevation between the Starborough-1 terrace and the local modern river level. Rates of incision are especially high along the Medway River but generally low in the Blind River area. The middle reaches of the Flaxbourne River show relatively low incision rates compared with either end, interpreted here as representing an uplifted and, still not yet-graded section of the river. Hatched boxes indicate the areas surveyed with EDM. Contour interval is 1.0 mm a^{-1}. See text for discussion.

Deformation of surfaces across the northern extension of the Clarence Fault

Flaxbourne River Profile

The west-to-east -flowing Flaxbourne River offers an opportunity to study deformation of Quaternary surfaces in a transect perpendicular to the northern extension of the Clarence Fault (Fig. 5.7, inset). Two EDM surveys were carried out in this catchment to measure in detail the relative differences in elevation of remnant fluvial terraces along its length (boxed areas on Fig. 5.7; see Appendix 4). These surveys were tied into the 1: 50 000 scale topographic database by surveying the position of geographic features visible on the map. This introduces an uncertainty in the "absolute" location of the survey, but the millimetre-accuracy within each survey is retained. This horizontal uncertainty involved in locating each survey within the topographic database is, at most, only a few metres, and is therefore negligible compared with the error associated with the topographic contours themselves.

Horizontal projection of terrace elevations onto a down-river profile reveals differences in the elevation of the variously aged terrace surfaces (Fig. 5.7). Most noticeable is the consistent eastward tilting in the eastern end of the profile, evidenced by morphologically higher terraces having progressively steeper slopes than younger, lower surfaces. These aggradation terraces are cut into soft Pliocene mudstone and are inferred to have been graded to stream base-level at the time of their abandonment. Therefore, a tectonic genesis is adopted for the tilting, which suggests continuous activity of the Ward Syncline, the axis of which lies to the east of these downstream terrace remnants (Fig. 5.7). Upstream, a range of Torlesse basement rock (the Haldon Hills) is exhumed, through which the Flaxbourne River has cut a deep gorge. The younger Starborough-1 & -2 terraces are preserved both within and on the upstream side of this gorge, where their elevations above the modern river level are high (~60 m) compared with downstream remnants of the same terraces (Fig. 5.7). Further upstream from the gorge, these younger terraces appear to converge towards the modern river (though they still dip downstream) and the modern river profile is clearly not in equilibrium (Fig. 5.7). This pattern of relative elevations can be explained by the formation of a monocline, where eastward tilting is taking place in the "central" limb (western limb of the Ward Syncline) but uplift without tilting is occurring to the west of the axis (Fig. 5.8). Since the modern stream is grading to the headwaters of the uplifting

"block", an excess of uplifted material must first be cut from above the monocline axis, where differences between the graded and uplifted base-levels are greatest. This will result in parallel, uplifted terraces upstream from the axis and discordant, tilted terraces downstream (Figs. 5.7 & 5.8).

Awatere River profile

Longitudinal valley profiles may indicate the amount and timing of relative tilting between surfaces of different age and/or morphostratigraphic position. A longitudinal profile of the Awatere River is shown in Figure 5.9, onto which the elevation of terraces preserved only on the southeast side of the river have been projected. Old terraces have a consistently steeper dip than younger terraces, indicating a continuing component of NE (downstream) tilting (Fig. 5.9). At ~30 km upstream, near the Medway River confluence, an abrupt increase in slope of all terraces is apparent. This location corresponds to the western end of the Haldon Hills, which consist of Mesozoic basement rocks exhumed and uplifted to the north of the Haldon Hills and Flaxbourne faults (Fig. 5.2). The localised convexity of these surfaces strongly suggests the presence of a previously unrecognised structure, e.g. a fault or fold, transecting the Awatere profile in this location. The regional pattern of northeast-ward tilting is well expressed in the terrace profiles up to 30 km upstream from the Awatere River mouth, below the localised deformation near the Medway confluence. There, the difference in slope between Clifford and Upton-1 terraces is negligible (Fig. 5.10), suggesting that little tilting occurred between ~215 ka and ~120 ka. Both of these older terraces have a high angular discordance relative to the ~60 ka Downs-1 terrace, however, indicating a tilting rate of ~3° m. $y.^{-1}$ in the interval ~120 - 60 ka. The slope difference between Downs-1 and Starborough-1 is relatively small across that ~50 k. y. timespan, indicating a tilting rate of ~0.2° m. $y.^{-1}$ over this period. However, the regional tilting rate appears to increase in the Late Holocene, with 6.4° m. $y.^{-1}$ indicated by the difference in slope between the Starborough-1 and-2 terraces and, if the modern Awatere River is currently graded, just over 15° m. $y.^{-1}$ since the formation of Starborough-2. In summary, the onset of tilt-related deformation in the lower Awatere Valley appears to be after ~120 ka, slowing at ~60 - 15 ka and increasing markedly over the last ~6000 years.

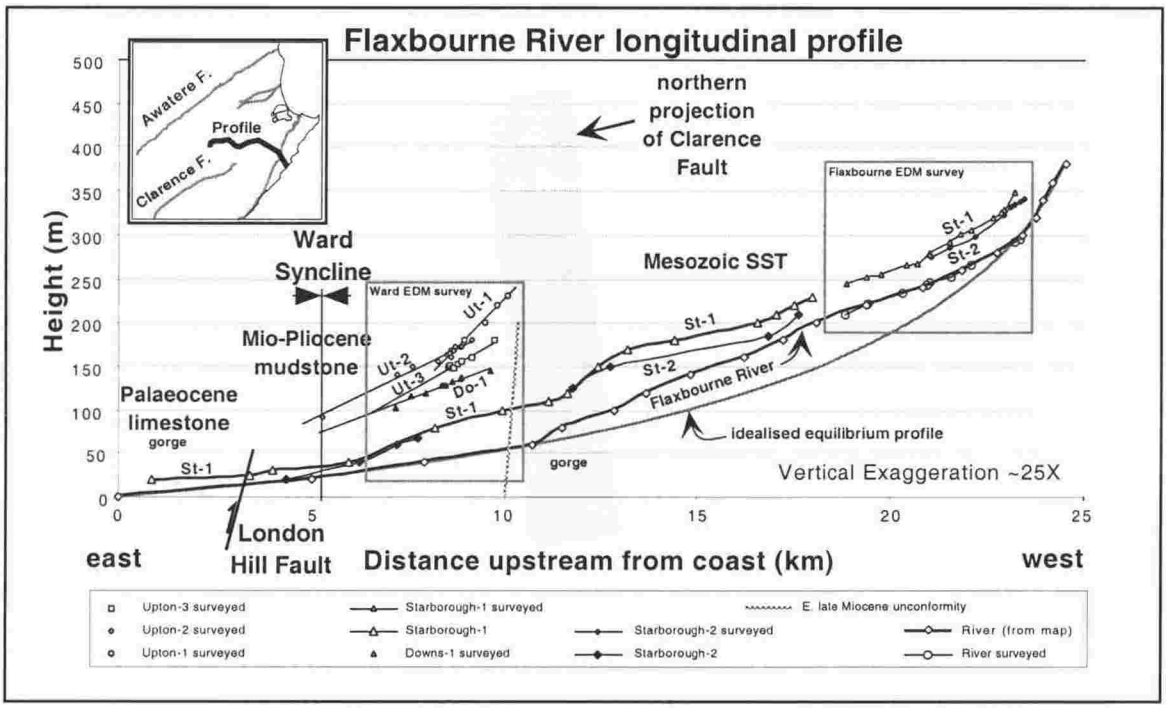

Figure 5.7. Longitudinal profile of the Flaxbourne River, showing tilting of terrace surfaces across the northern projection of the Clarence Fault (see inset). The obvious change in slope of the river (at ~12 km) defines a knickpoint, that may be related to the more resistant Torlesse bedrock, to which the upper part of the river is grading. Tilted terraces in the central region appear to define a monocline, with the greatest change in slope occurring at the projected position of the Clarence Fault (shaded band). The pattern of elevation changes is consistent with downwarping in the Ward Syncline and ~15 km wide broad doming to the west of the projected Clarence Fault position. Abbreviations of terrace names are Ut -1: Upton -1; Ut -2: Upton -2; Do -1: Downs -1; St -1: Starborough -1; St -2: Starborough -2.

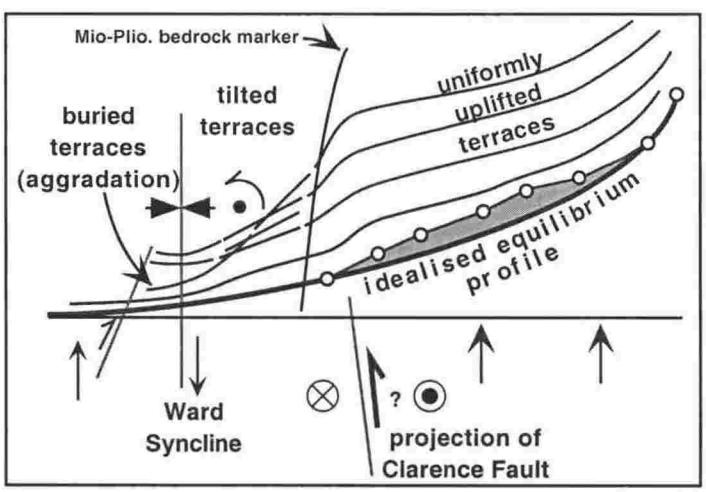

Figure 5.8. Schematic representation of Figure 5.7 (above) showing differential uplift of fluvial fill terraces above a growing monocline. The upper catchment is constantly attempting to grade to the same level, but uplift over, and upstream from, the fold axis (possibly cored by a blind reverse fault) requires that the stream incises all the way to the headwaters (shaded region). This pattern of deformation produces parallel, uplifted terraces upstream from the fold axis and tilted, sometimes buried, terraces downstream.

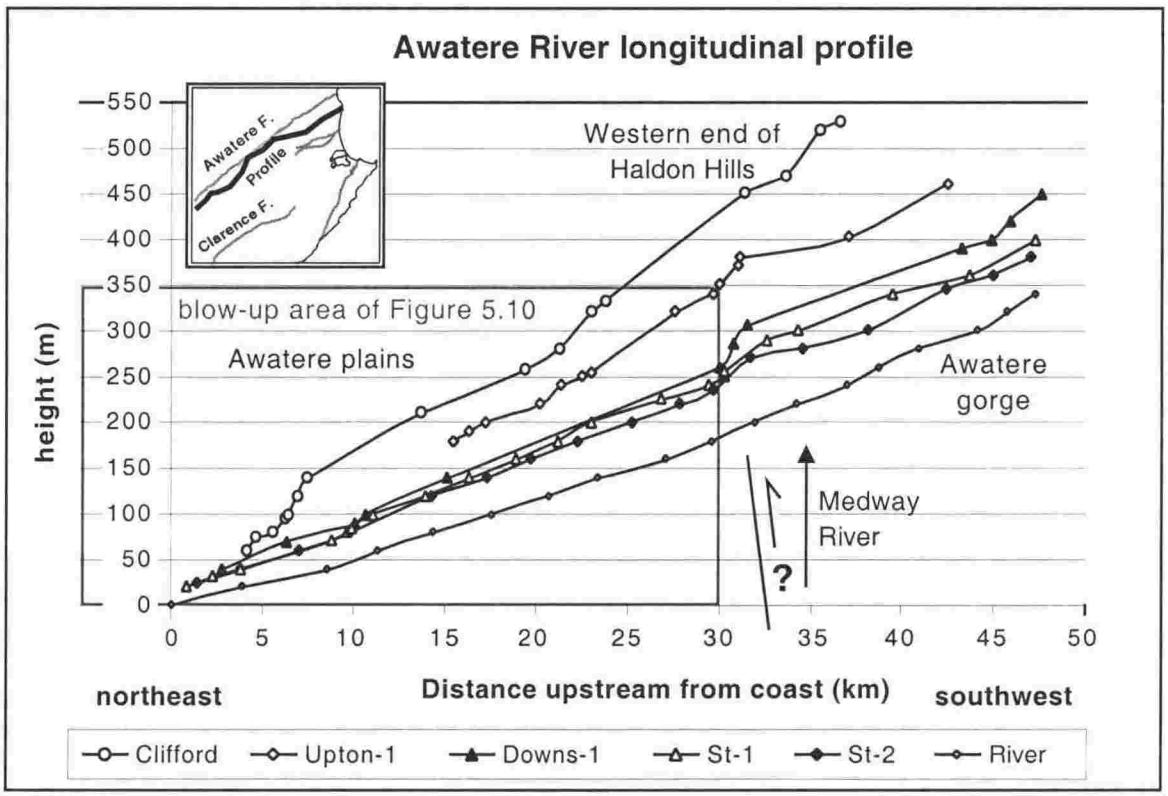

Figure 5.9. Longitudinal profile of the Awatere River and associated fluvial terraces. Contours and spot-heights on terraces have been projected onto a simplified river profile (inset), showing changes in surface elevation. A marked change in slope 30 - 35 km upstream suggests the presence of a blind, previously unknown structure. The position of this change in slope lies near the western end of the Haldon Hills.

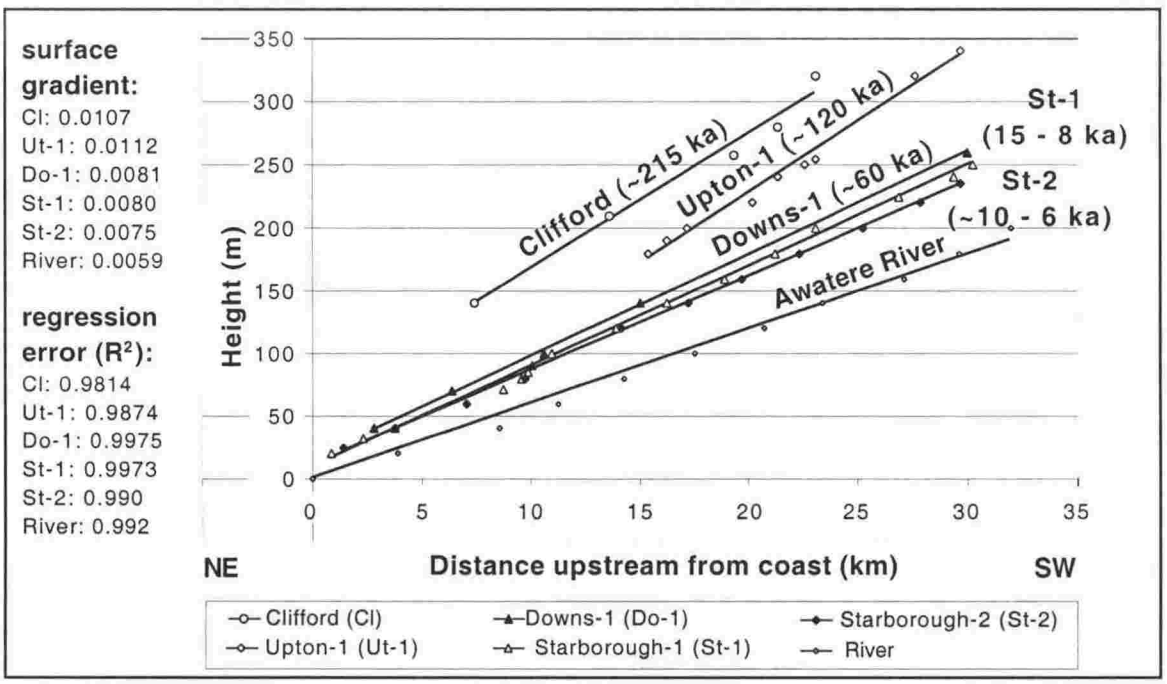

Figure 5.10. Detailed part of the graph of Figure 5.9 (above) inferred to represent the regional tilting pattern over the last ~220 ka with linear regression best-fit lines. Identical slope of the Clifford and Upton-1 terraces suggests a period where no tilt, but some uplift, was occurring. From the angular difference of younger terraces, a ~3° m.y.$^{-1}$ NE tilt is interpreted in the period ~120 - 60 ka, ~0.2° m.y.$^{-1}$ in the period ~60 to 12 ka, increasing to ~6° m.y.$^{-1}$ between ~12 and ~6 ka and 15° m.y.$^{-1}$ between 6 and 0 ka, assuming the modern river is currently graded.

DRAINAGE PATTERNS

Evolution of drainage networks in tectonically active areas

The evolution of drainage systems is often affected by active tectonics [e.g., Jackson & Leeder, 1994; Jackson et al., 1996; Townsend & Little, 1998; Markley & Norris, 1999]. In areas undergoing active deformation, particularly tilting, small streams that do not have enough power to maintain their course across an uplifted region often jump to another catchment that is topographically lower as a result of the tectonic deformation. This piracy phenomenon produces an abandoned channel segment, or "airgap" and a corresponding "watergap", which is the new stream course. Care must be taken in the interpretation of inferred tilting directions based on changing drainage patterns as stranded palaeo-channels may result from other processes. For example, the lateral migration of a river with high stream power into an adjacent, topographically higher catchment may result in "capture" of a smaller stream, or fault movement may produce an uphill-facing scarp, tectonically damming a stream that must find some other path around the obstruction. Several examples of stream piracy and capture can be seen in the area studied and these geomorphic features have been used to assess local directions of landscape tilting. Examples of tectonically-induced changes in drainage networks that have been used to infer local directions of tilting are shown in Figure 5.11 A - D.

The inferred age range of tilting "events" that have produced airgaps are indicated by the time between surface abandonment and subsequent incision and deposition of the next-youngest terrace, which cuts risers parallel to the new direction of flow. A channel deflection at a certain time does not necessarily preclude continued tilt in that direction after the event.

Pattern of tilting in NE Marlborough

Directions of active tilt based on the pattern of stream piracy and stranded palaeo-channels have been interpreted from detailed aerial photographs and field studies of selected sites. These are compiled on Figure 5.12 (see Fig. 5.11 A - D for examples). These observations of relative uplift are independent of the pattern of incision outlined above in the section on surface deformation. Data points on Figure 5.12 marked with

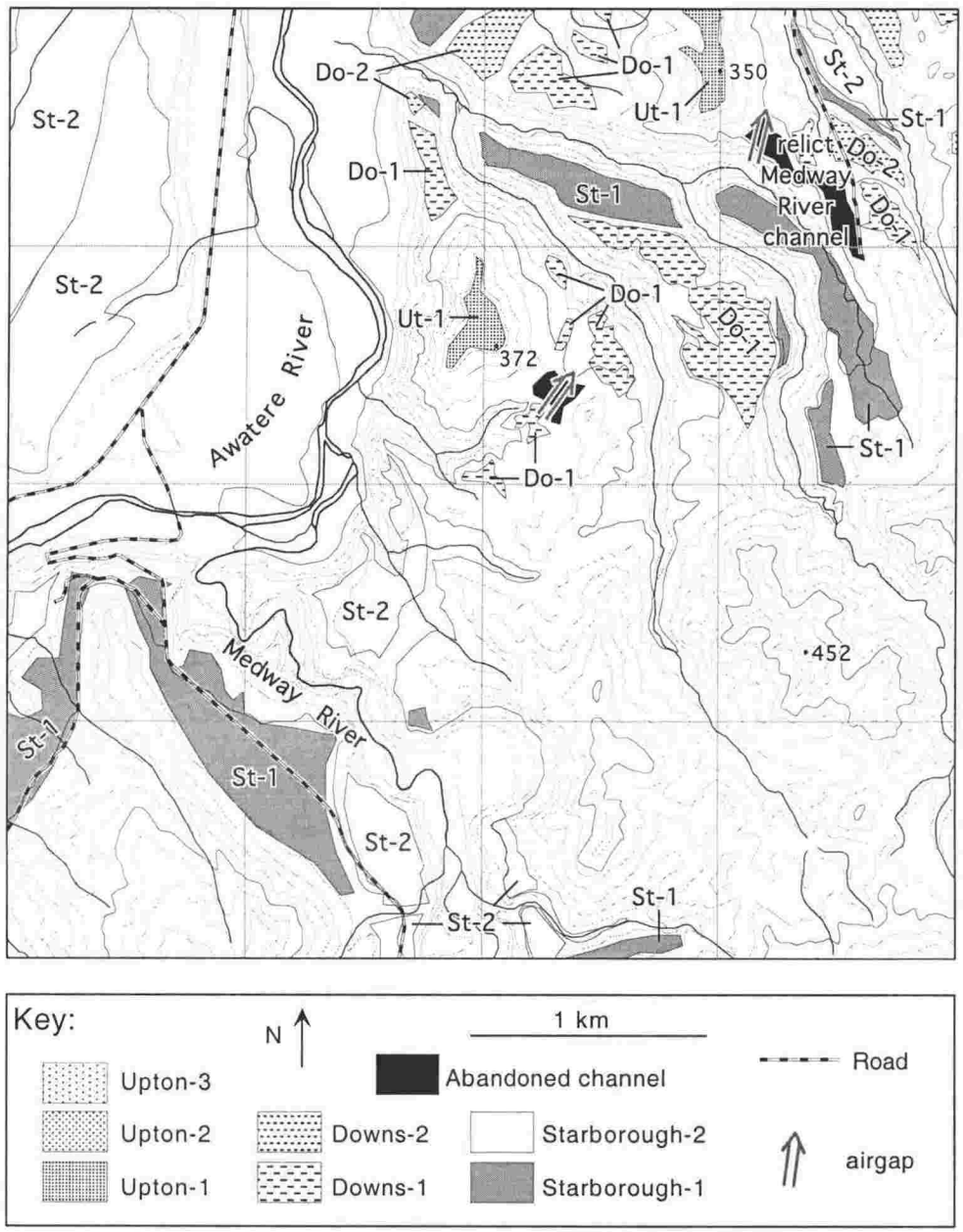

Figure 5.11A. The Medway River is an important tributary to the Awatere River and drains the mountainous region to the west of the Clarence Fault tip. The confluence of the Awatere and Medway rivers is ~30 km upstream from the coast, but is inferred on the basis of stranded Medway River terrace remnants and airgaps to have occurred ~5 km downstream from its present location, prior to the formation of the Downs-1 terrace (~60 ka). This change in the course of Medway River is interpreted as the result of NW tilting at the western end of the Haldon Hills, across which the Medway River once flowed. Since the deflection of Medway River away from this area, new streams shedding from the Haldon Hills with a NW flow direction have formed, cutting perpendicular to the previous flow.

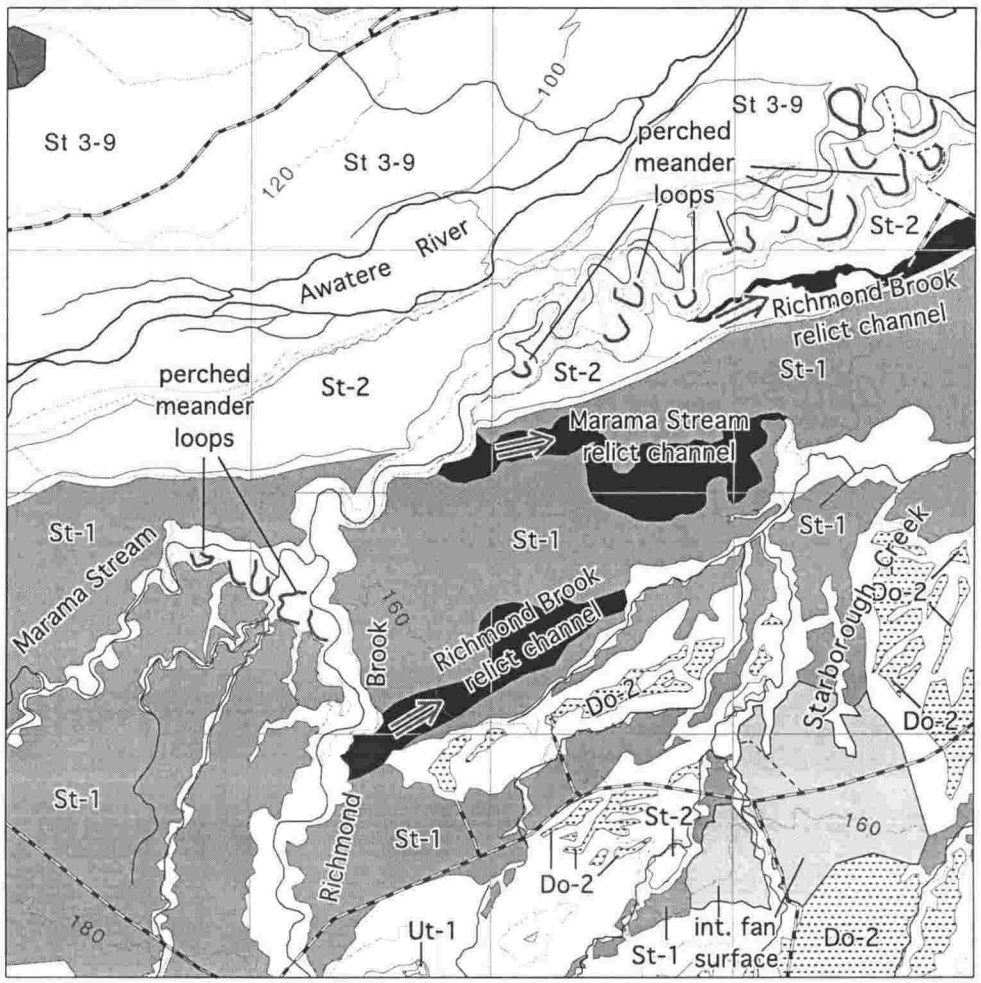

Figure 5.11B. Richmond Brook joins the Awatere River west of the town of Seddon (Fig. 5.2). The Starborough –1 and –2 terraces are deeply incised by Richmond Brook, which has a northward flow direction along its entire length. Other streams that have less downcutting power than Richmond Brook remain perched on the Starborough –1 surface where they have NE flow directions. Marama Stream (unofficial name) is interpreted to have once flowed into Starborough Creek, but has since been captured by the powerful Richmond Brook as it was diverted to a northerly flow across the Starborough –1 terrace. Also notable in this area are numerous perched, abandoned meander loops, all of which (barring one) occur on the south side of Marama Stream and Richmond Brook, hence the modern streams are eroding preferentially into their northern banks. This records a component of northward tilt, which is perhaps why the N-flowing streams in this area are so straight compared with stream sections that retain a NE flow direction.

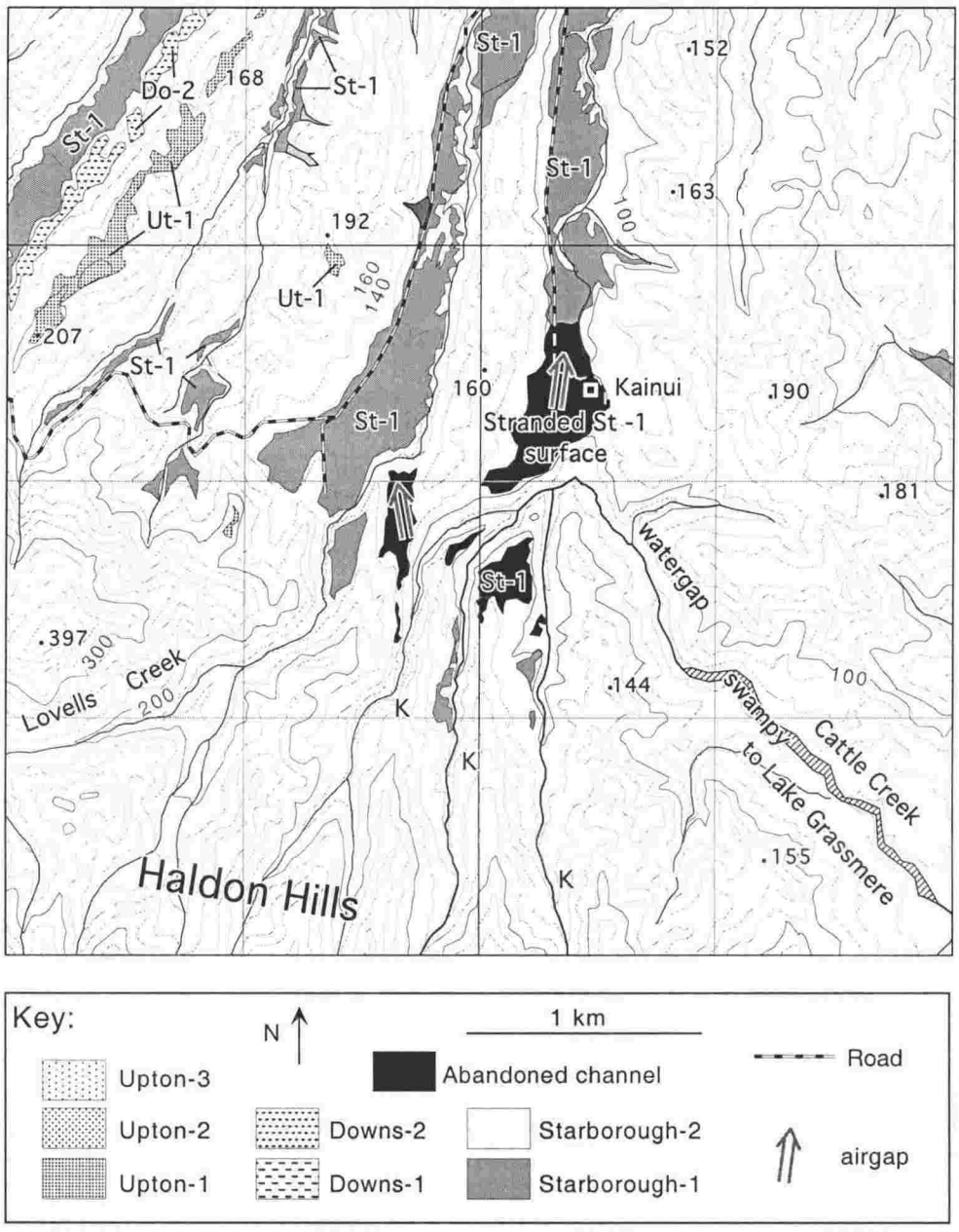

Figure 5.11C. Kainui is a striking example of ENE tilt that has resulted in the deflection of Cattle Creek by more than 270°, from a NNE to a SE flow direction. Cattle Creek is now entrenched far below the elevation of the stranded Starborough-1 terrace that is preserved in the airgap. This downcutting is probably due to a much shorter, steeper flow path to Lake Grassmere, allowing rapid incision and upstream migration of a knick-point ("K" on figure). This eastward tilting event is inferred to be younger than the ~12 ka Starborough-1 terrace. Other unnamed streams east of Lovells Creek have also been deflected into this catchment by eastward tilting, increasing the flow power of Cattle Creek.

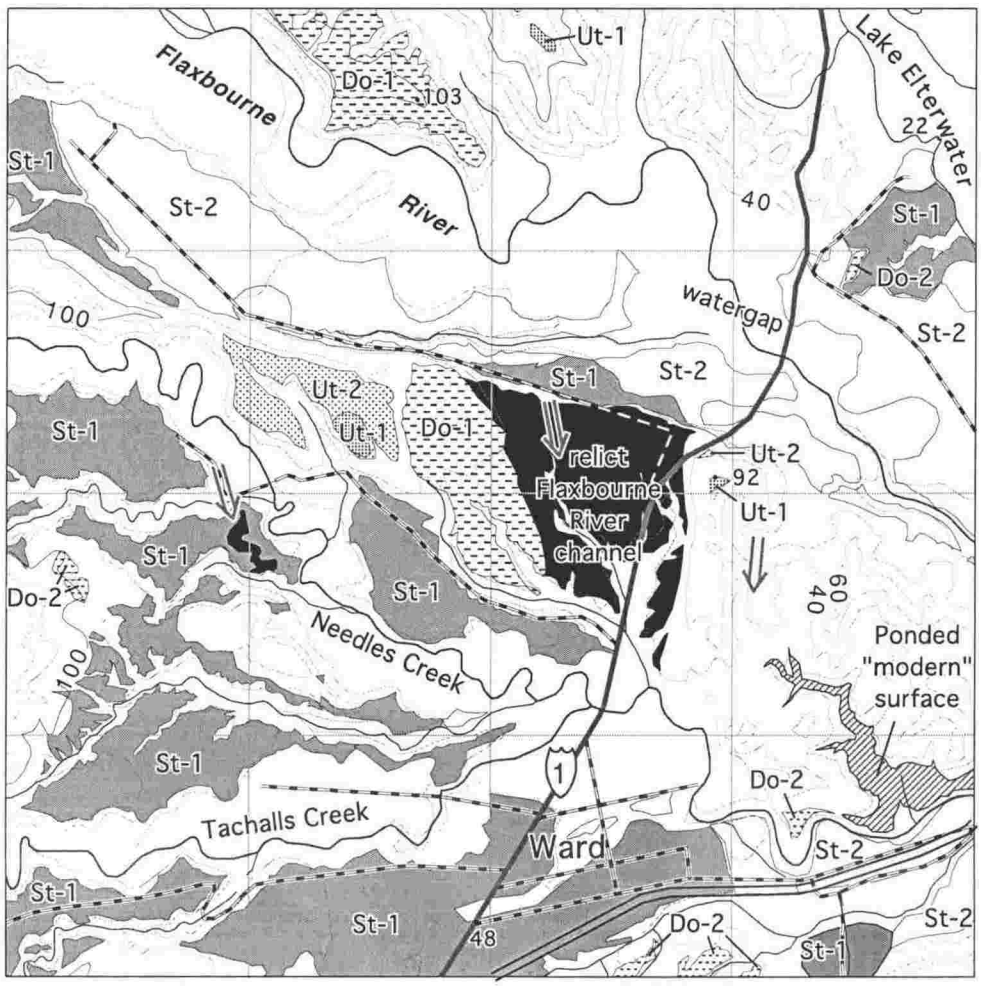

Figure 5.11D. The town of Ward lies near the axis of the active Ward Syncline [Townsend, 1996] and several instances of altered drainage indicate a strong eastward tilting on the western limb of this fold. The most startling change in drainage is the deviation in the course of the Flaxbourne River, which is interpreted to have flowed through a broad airgap towards Ward and then east into its current drainage. This change from a SSE flow to an ESE flow today is interpreted to have taken place not long after the formation of the ~60 ka Downs-1 terrace, as this surface is extensively preserved in the airgap and only slightly incised by the palaeo- river course. The younger Starborough-1 terrace is recognised in the current Flaxbourne valley (watergap), placing an age minimum of ~12 ka on the deflection. Other airgaps near this area indicate eastward tilt younger than Starborough-1, therefore the tilting direction is interpreted as constant over the last *c.* 60 ka.

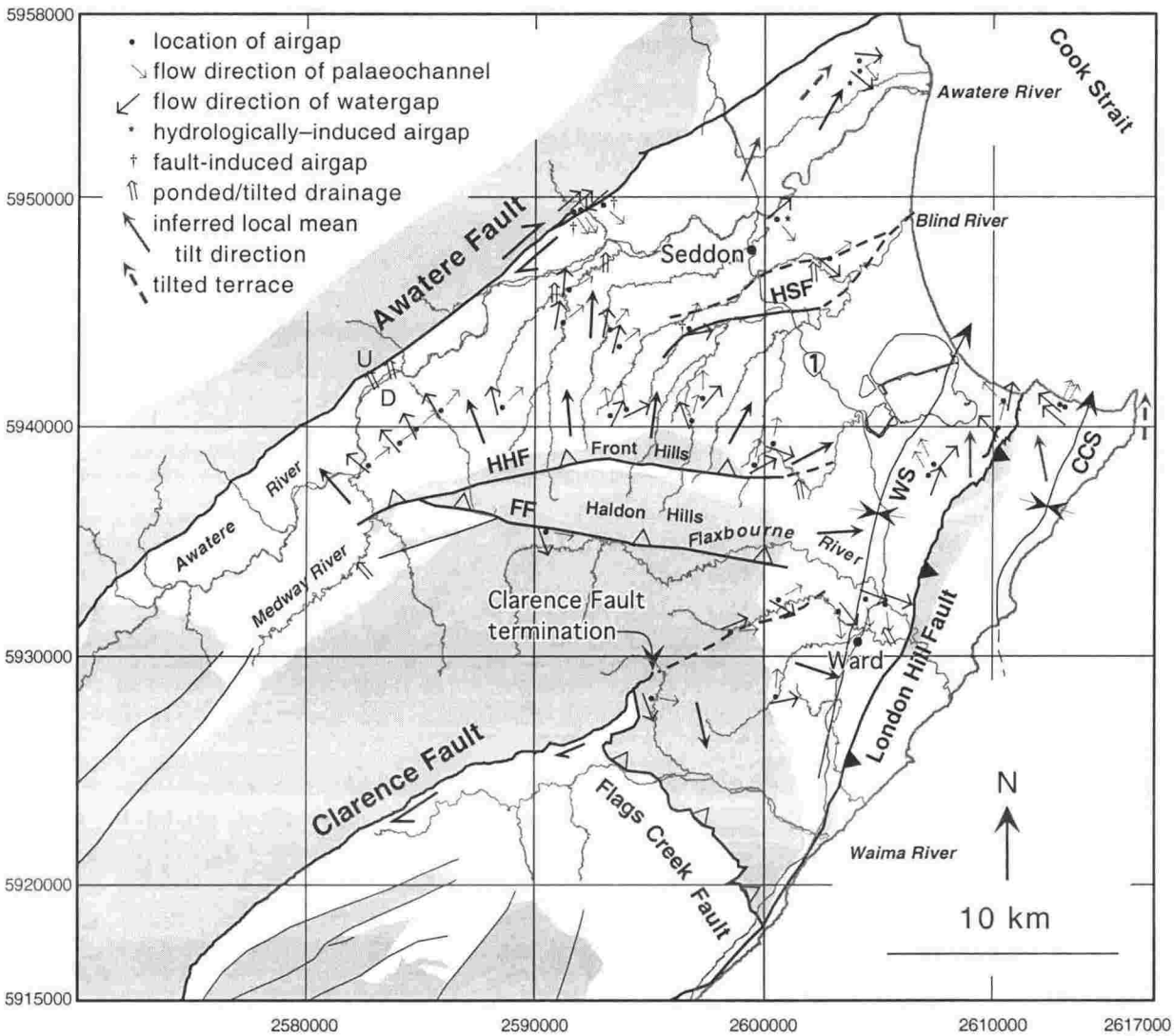

Figure 5.12. Directions of Late Quaternary landscape tilting inferred from stream piracy patterns. A broad doming centered on the Haldon Hills implies uplift north and west of the Clarence Fault tip (lower centre of figure). Eastward tilting near Ward is interpreted as activity of the Ward Syncline and N-to-NE tilting in the northern part of the area is inferred to represent a regional tilt gradient towards Cook Strait. HSF: Hog Swamp Fault; HHF: Haldon Hills Fault; FF: Flaxbourne Fault; WS: Ward Syncline; CCS: Cape Campbell Syncline. See text for full discussion.

an asterisk (*) indicate a hydrological cause for stream "piracy" (e.g., lateral migration of a channel of lower base level) and points marked with a cross (†) indicate tectonic damming of a stream attributed to direct uplift on a fault. The general pattern indicates active tilting away from the Haldon Hills in an elongate E-W dome-like shape. In the Medway and Upper Awatere domains, a NW direction of tilt is inferred, for example, from deflection of the Medway River from flowing in a NNE direction around the western end of the Haldon Hills to join the Awatere River further upstream than it originally did. In the Blind River Domain, an original network of NE-flowing streams are now connected by much shorter N-flowing segments, indicating a northward tilt. Easterly deflection of originally N-flowing streams occurs in the eastern Blind River and Grassmere domains, suggesting a tilt to the east in this near-coastal region. This pattern of tilting suggests the Haldon Hills are at the centre of an uplifting region that is approximately 15 km in width. Due to the paucity of data in the southern part of the study area, the southern extent of the doming is not well defined; however, it seems likely that, because the southern area is occupied by mountainous terrain with peaks of over 1200 m elevation, the amount of uplift here is greater than that in the Haldon Hills, where the highest peaks are on the order of 700 - 800 m in elevation. The pattern and size of the doming area loosely corresponds with the modern outcrop distribution of Torlesse basement rocks (Fig. 5.12) and suggests that exhumation of these strata is ongoing. The pattern of uplift suggested by tilting is identical to that derived independently for the distribution of high incision rates, denoting the Haldon Hills as a region of rapid uplift.

Further north and distal to uplift in the Haldon Hills, a predominantly N-NE tilting pattern is observed. The continuation to the coast of several small streams on the north bank of the Awatere River (Fig. 5.13) suggests that the Starborough-1 terrace, on which they flow, has been tilted to the N or NE, dissuading these low-power streams from joining the main Awatere River, despite its proximity and lower elevation.

Local structures also affect the pattern of inferred regional tilt. In the Blind River area, activity of the Hog Swamp Fault is interpreted as the reason for eastward deflection of Blind River (Fig. 5.12). Local up-to-the-north throw of ~35 m is interpreted from offset of the ~60 ka Downs-1 surface. This would have resulted in a south-facing scarp, to defeat the flow of Blind River and deflect it eastwards in accordance with the regional direction of tilting.

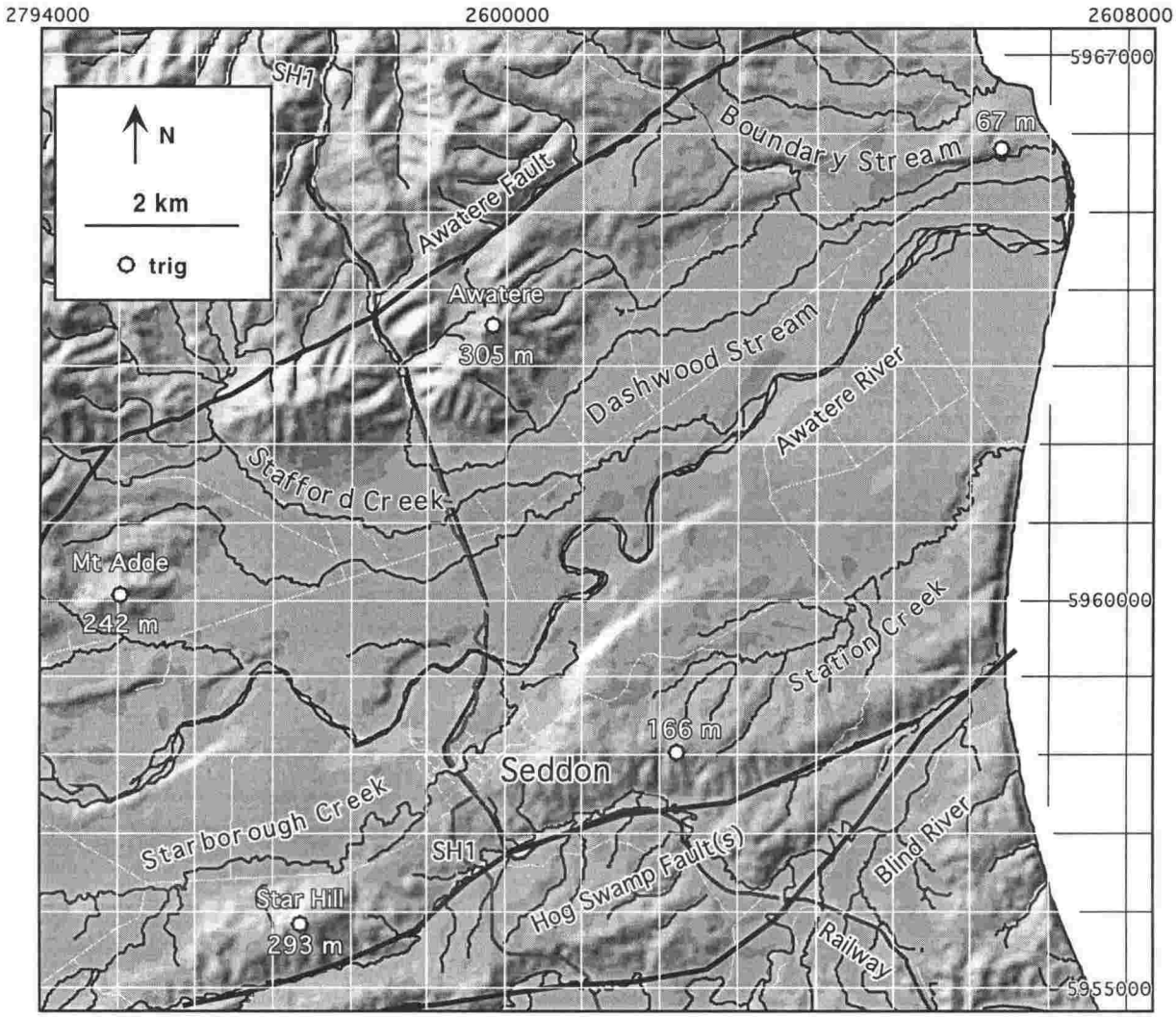

Figure 5.13. Shaded relief map of the lower Awatere River, downstream from Seddon, showing perched streams that flow down valley for several km before joining the main river (e.g., Stafford Ck), or flow all the way to the coast and do not join the Awatere River at all (e.g., Boundary and Dashwood streams). These stream courses suggest a component of northward tilting in this area. See Figure 5.2 for location.

DISCUSSION: NEOTECTONIC DEFORMATION SURROUNDING THE CLARENCE FAULT TERMINATION

If variable rates of stream incision, coupled with patterns of terrace tilting, stream abandonment and piracy in NE Marlborough can be regarded as a consequence of variable rates of vertical tectonic motion, the regional pattern of uplift delineates a ~20km-wide dome, or bulge to the west of the Clarence Fault tip (Fig. 5.14). High rates of incision on indurated Mesozoic rocks compared with relatively lower rates on Neogene mudstones indicates that fast incision is not directly related to a soft bedrock, rather that the outcrop pattern of bedrock reflects the pattern of uplift. Slightly lower incision rates are noted in the centre of the "dome" (See Fig. 5.6E). This local area of anomalously slower incision is not unexpected, as the small, low-powered streams are the slowest to respond to uplift events and will not achieve equilibrium gradient until sufficient time has elapsed for the knick point to migrate upstream (Figs. 5.7 & 5.8).

Relative uplift may be independently assessed by analysing directions of landscape tilt. Areas of uplift inferred from patterns of tilting are identical to the areas of fast incision, corroborating the inference of high uplift rates north and west of the Clarence Fault tip, in the Haldon Hills. The greywacke range of "Front Hills" (see Fig. 5.2), through which many of the Blind River tributaries have cut deep gorges, appears to lie outside the zone of most rapid uplift (Fig. 5.14). This lends support to the suggestion of Cotton [1938] that the Front Hills arose first, being uplifted on the Haldon Hills Fault, forming NE-flowing streams that incised into soft Miocene - Pliocene mudstone. During subsequent uplift on the Flaxbourne Fault (Fig. 5.14), the Haldon Hills rose and streams eroded head-ward into the uplifting block. If movement on the (northern) Haldon Hills Fault ceased prior to uplift on the (southern) Flaxbourne Fault, these small streams would have had a better chance of maintaining their northward courses rather than being defeated by the uplifting greywacke range of the Front Hills. This may explain why the Front Hills lie within a zone of relatively low uplift compared with the Haldon Hills (Fig. 5.14).

The distribution of inferred uplift in NE Marlborough involves first-order deformation by two spatially overlapping mechanisms. A lobe of "very high" incision/ uplift north of the tip of the Clarence Fault (Fig. 5.14) is reminiscent of the pattern of vertical strain predicted by elastic modelling [ten Brink et al., 1996] (Fig. 5.3E),

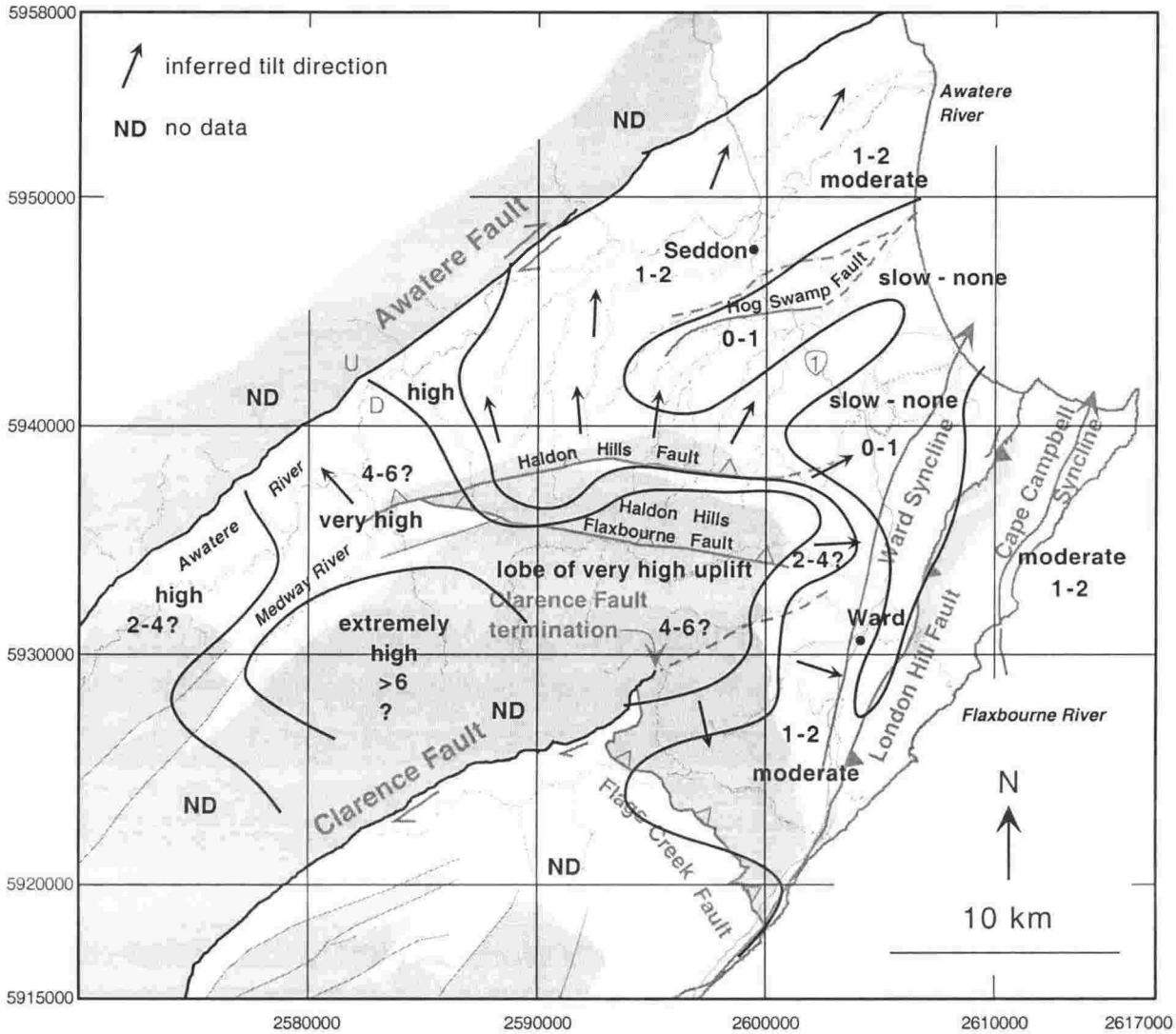

Figure 5.14. Approximation of contemporary uplift rates in NE Marlborough. Numbers are rates of uplift (in mm a^{-1}) extrapolated from uplifted coastal marine terraces and constrained by the patterns of Late Quaternary incision and tilting inland. High rates of uplift to the north and west of the Clarence Fault termination indicate uplift and crustal thickening to accommodate enhanced compressive tip stresses in this region. Lack of active surface structures suggests that the deformation may be occurring by folding or by slip on blind faults. Low rates of uplift in the Blind River - Lake Grassmere domains attest to locally active structures - the Hog Swamp Fault in the north and the Ward Syncline in the south. This pattern is superimposed on a regional north - northeast tilt of 2° $m.y.^{-1}$ since ~120 ka.

suggesting that transfer of horizontal strike-slip motion into permanent crustal thickening occurs in the immediate vicinity of the fault tip. Elevation of Torlesse basement rocks to ~700 m in the Haldon Hills implies uplift of ~1900 m in this region (with erosion of the ~1200 m thick Miocene - Pliocene rocks [Roberts & Wilson, 1992]) relative to the lower Awatere Valley. No doubt some erosion of the Torlesse rocks has also occurred, so that the overall uplift of the Haldon Hills relative to low-lying areas is more likely to be about 2000 m over an area that is ~15 km wide (e.g., Fig. 5.3E). The estimated total offset across the Clarence Fault of ~15 km [Little & Jones, 1998] and the elastic model of ten Brink et al. [1996] have been used to compare the expected total bedrock uplift at the termination of the Clarence Fault ("basement uplift" column on Figure 5.3E) with the observed uplift value of ~2000 m, assuming that elastic strain is transferred tip-ward into permanent, non-recoverable deformation. The spatial extent and total amount of crustal thickening in this region is compared using a weak fault with shear zone width of zero [ten Brink et al., 1996]. The observed 2000 m of uplift of the Haldon Hills over a width of ~15 km is only slightly higher than that predicted (900 - 1800 m regions) for a total fault offset value of 15 km (e.g., Fig. 5.3E).

Recent estimates of Late Quaternary strike-slip rate for the Clarence Fault are on the order of 5 mm a^{-1} [Van Dissen & Nicol, 1999]. Assuming terrace ages of 120, 60 and 10 ka, the corresponding dextral strike-slip offset magnitudes on the Clarence Fault are 600, 300 and 50 m, respectively. The corresponding amount of uplift for these differently aged terraces has been calculated using the elastic model of ten Brink et al. [1996] (Fig. 5.3E). It can be seen that, according to this model and using a strike-slip rate on the Clarence Fault of 5 mm a^{-1} [Van Dissen & Nicol, 1999], the maximum uplift expected in the immediate vicinity of the fault tip for a 120 ka terrace is 90 m (Fig. 5.3E). For the younger terraces of 60 and 10 ka, the expected uplift over the same area is 45 and 7.5 m, respectively. These predicted values of uplift record a linear scaling with age, or increasing fault offset; however, the observed pattern of terrace uplift/incision is such that there are smaller differences in elevation between terraces but a larger than predicted overall uplift after the formation of the (~10 ka) Starborough-1 surface (see also Figs. 5.6A - E). Several possible reasons for the disparity between predicted and observed uplift of Late Quaternary terraces in the vicinity of the Clarence Fault tip include: 1) that rates of stream incision are not linked directly to uplift and cannot be used to infer uplift rates, 2) an erratic strike-slip rate on the Clarence Fault

over the last ~120 ka may have produced real discrepancies in the rates of uplift for terraces of different age, 3) that the relatively simple elastic model of ten Brink et al. [1996] is not applicable to the termination of the Clarence Fault due to the interaction of several geological processes, such as the interaction of other faults and regional uplift, not accounted for in their model.

The mechanism by which uplift has occurred may affect the total amount and the distribution of vertical motion. For example, uplift on discrete structures, such as the Haldon Hills and Flaxbourne faults, will influence the finite pattern of deformation so that field data will not exactly resemble the modelled "elastic" distribution of uplift. Other than the Haldon Hills and Flaxbourne faults, there is no surface evidence of any discrete structure in the immediate vicinity of the Clarence Fault tip on which this deformation may occur. This is possible evidence for growth of a NE-trending anticline or monocline, that, given its asymmetry, may be cored by a SE-vergent, blind reverse fault that forms the eastern boundary of the region of high uplift along strike from the termination of the Clarence Fault (Fig. 5.14).

The second mechanism involves vertical axis rotation of the "Awatere Block" [Roberts, 1995] (Fig. 5.14). Tectonic bulging along the southwestern boundary of the Awatere Block is inferred to be responsible for the extremely high rates of uplift interpreted there. The SW boundary of the Awatere Block has been described by Little & Roberts [1997] as a "rotation boundary", constrained palaeomagnetically by unrotated 6 - 7 Ma old rocks in the middle Awatere Valley and by changes in strike of steeply dipping Torlesse bedrock. Contemporary extensional deformation is not observed along the Awatere River in the vicinity of the rotation boundary [N. Hill, Pers. Comm.]. This suggests that the pole of rotation between the Awatere Block and the unrotated rocks to the SW (Medway Block) must lie north of the Awatere River (Fig. 5.15). This model is similar to that of Roberts [1995] and Townsend & Little [1998], but the pole of rotation between the Awatere Block and the Medway Block lies further to the west (Fig. 5.15). As the Awatere Block rotates relative to the Medway Block, contraction must occur across their mutual boundary, and, the greater the distance from the pole of rotation, the greater the amount of shortening. This horizontal contraction would probably result in vertical strain (uplift) along the boundary, which overlaps with the area of high uplift due to the "elastic" deformation at the Clarence Fault tip. Thus, these two mechanisms of crustal deformation, involving strike-slip fault termination and

vertical axis block rotation, can explain the transfer of horizontal strike-slip motion into the observed pattern of uplift.

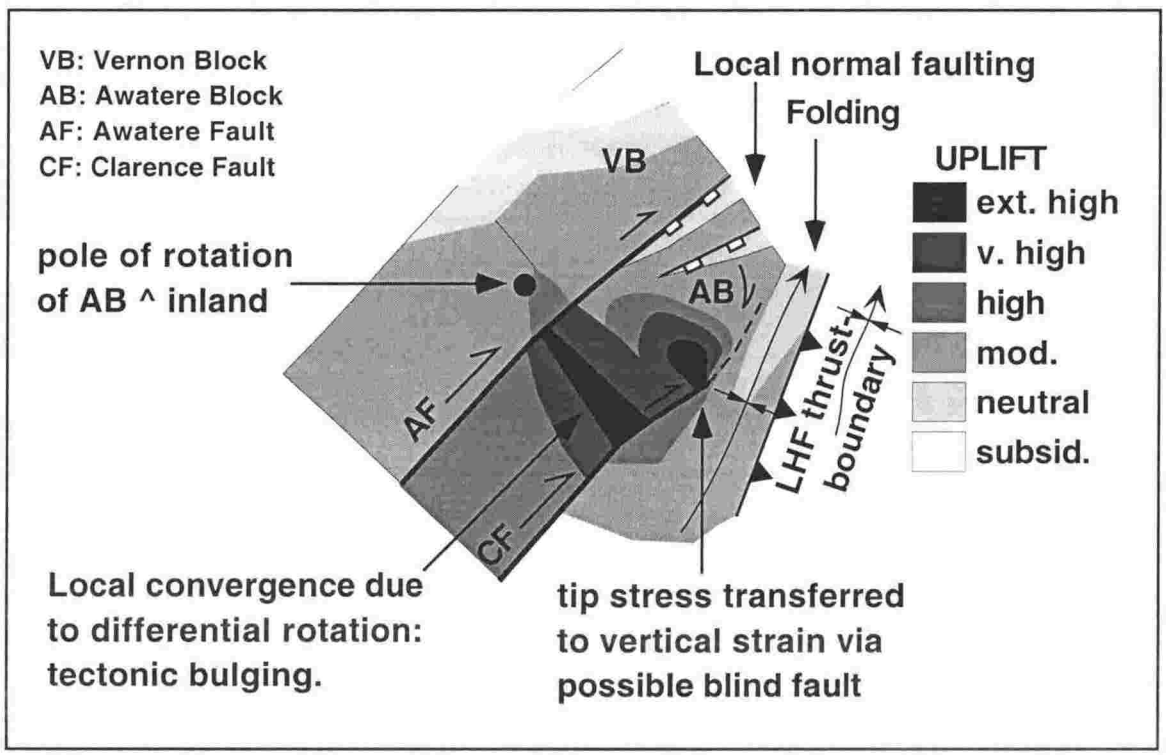

Figure 5.15. Block model of observed uplift rates in the Lower Awatere - Ward area, integrating two spatially overlapping mechanisms to accommodate strike-slip strain. Tip stresses at the termination of the Clarence Fault apparently cause deformation to be transferred onto a blind thrust along strike to the NE, giving rise to high uplift rates to the north of the tip. Vertical axis rotation of the Awatere Block (AB) relative to more inland domains causes a local convergence at the SW edge of the rotating block (dark band). This also causes the Clarence Fault to become curved, as part of the bedrock trace forms one edge of the rotating Awatere Block. Local activity of structures such as the Hog Swamp Fault and Ward Syncline are superimposed on the regional uplift, leaving a complicated pattern of deformation. See text for discussion.

CONCLUSIONS

Patterns of relative vertical tectonic motion in NE Marlborough have been assessed by analysing rates of stream incision as a proxy for uplift. The broad pattern of incision suggests rapid uplift of a ~15 km-wide area to the north and west of the Clarence Fault tip, i.e. the Haldon Hills, where Mesozoic basement rocks are exhumed and uplifted to elevations of around 700 m. Integration of previously published coastal uplift data with quantitative incision data suggest that the highest uplift rates of 4 - 6 mm a^{-1} are occurring where basement rocks are exposed. Two crustal scale deformation mechanisms are inferred to be responsible for the observed pattern of uplift rates. Vertical axis rotation of a crustal block at the termination of the dextral strike-slip Clarence Fault may produce tectonic bulging along its SW boundary, expressed as crustal thickening and uplift. The distribution of uplift is also consistent with the pattern of vertical strain predicted from elastic modelling. NE of the mapped termination of the Clarence Fault, high uplift rates suggest the presence of a growing anticline, possibly cored by a SE-verging reverse fault. Anomalously low rates of incision in the centre of the rapidly uplifting region can be accounted for by the formation of a non-graded river catchment, that is analogous to a perched valley. Terraces in the lower Awatere Valley that are older than 120 ka show parallel downstream profiles compared with younger terraces that all show some degree of angular discordance. Of the younger, tilted terraces, all successively older terraces have a progressively steeper downstream gradient. This pattern suggests that the current mode of NE tilting began after the formation of the ~120 ka Upton-1 surface and has maintained variable rates of northeast tilting since then.

Independently derived patterns of tilting based on the evolution of local drainage networks also suggest that the Haldon Hills are still undergoing uplift, with a consistent tilting away from the centre of a broad dome-like shape north and west of the Clarence Fault tip. Timing of local tilting has been estimated by the age of abandoned surfaces and palaeo-channels. Airgaps of different ages often indicate the same direction of tilting, suggesting that the pattern of local tilting over the last ~120 ka has been stable. In areas distal to the local uplift of the Haldon Hills, preferential erosion of the northern side of stream banks and preservation of terraces and relict meander loops on the south side of streams indicates regional N-NE tilting.

Chapter 7: Conclusions

Six new palaeomagnetic localities have been sampled from Late Cretaceous - Early Tertiary Amuri Formation limestone and Early Miocene Waima Formation siltstone from eastern Marlborough. Integration of new and existing palaeomagnetic data from NE Marlborough shows that all rocks that are older than 18 Ma display clockwise declination anomalies of 100 - 150°. The similarity in declination anomalies implies regional rotation of a large expanse of NE South Island after 18 Ma. Previous palaeomagnetic sampling in NE Marlborough constrains this regional clockwise rotation to have occurred before 7 Ma.

Basement rocks of NE Marlborough, the Middle Cretaceous Torlesse terrane, contain a predominantly NE-striking, steeply-dipping structural fabric that defines one limb of the New Zealand orocline. New palaeomagnetic data from Tertiary rocks of NE Marlborough, which overlie the NE-striking Torlesse terrane, imply a regional clockwise vertical-axis rotation of at least 100°. The present-day NE-SW -oriented structural fabric of Marlborough appears to be a consequence of the regional 100° vertical-axis rotation of originally NW-SE -striking basement rocks, a rotation that is also recorded throughout the palaeomagnetically sampled parts of NE Marlborough. This regional clockwise rotation is inferred to have occurred as a result of distributed dextral shear accumulating at the southern termination of the Early Miocene subduction zone, during early inception of the Alpine Fault as a through-going structure.

Near Kekerengu, NE Marlborough, the Ben More anticline is a NNE-trending, ~15 km-wide structure that folds an Early Miocene fold and thrust belt - the Flags Creek Fault System (FCFS). New palaeomagnetic and structural data from both limbs of the Ben More anticline show that the fold axis is not a vertical axis rotation boundary, as has been previously hypothesised, and that the post-Middle Miocene "regional" 100° clockwise rotation occurred in both limbs.

The two new palaeomagnetic localities that are adjacent to the dextral strike-slip Kekerengu Fault exhibit clockwise declination anomalies of up to 150°. This extra rotation is attributed to the presence of a localised zone of distributed dextral shear and vertical-axis rotation within 2 - 3 km of the Kekerengu Fault. This zone of inferred

Pliocene - Pleistocene clockwise vertical-axis rotation is also borne out by detailed structural mapping of the FCFS (see below).

Thin-skinned tectonic deformation in the FCFS accompanied the inception of the Pacific - Australia plate boundary that propagated through New Zealand in the Early Miocene. A nappe of Torlesse terrane rock formed a backstop to the FCFS and constitutes the present-day hanging-walls of the Clarence and Flags Creek faults. Transport directions of large-scale thrust sheets within the FCFS have been determined by analysis of mesoscopic deformation fabrics in proximity to the map-scale faults. These fabrics record a consistent SE direction of transport, which is anomalous with respect to the NE - SW direction of relative plate convergence implied by Early Miocene Pacific - Australia plate boundary reconstructions. If, however, the regional ~100° clockwise vertical-axis rotation is taken into account, SE transport of the thrust sheets is restored to NE (i.e. seaward-directed transport), perpendicular to the Early Miocene continental margin. The age of the thrust faults is interpreted to be younger to the east (foreland), resulting in a leading edge imbricate fan. Balanced cross sections through the FCFS imply at least 20 km of shortening in a SE direction (present-day coordinates).

Several episodes of deformation are recorded by reactivation of fault structures within the FCFS, implied by overprinting of deformation fabrics in different parts of the fault system. The Flags Creek Fault (FCF) was originally part of the Torlesse nappe that formed the backstop to the FCFS and was laterally contiguous with the proto-Clarence Fault. This fault was reactivated as a SW-directed thrust in the Late Miocene, folding rocks in its footwall to form the NW-SE -trending Narrows syncline. The eastern ends of the FCFS become steepened and eventually overturned in proximity to the active Kekerengu Fault, which truncates the eastern limb of the Ben More anticline and the FCFS near the coast. Early Miocene thrust transport directions of the FCFS are SE-directed (in present-day coordinates) over the majority of the deformed belt, but are clockwise-rotated by ~45° to become south-directed within 2-3 km of the Kekerengu Fault. This structural and palaeomagnetic (above) evidence implies the presence of a zone of Plio-Pleistocene distributed dextral shear and vertical-axis rotation within 2-3 km of the Kekerengu Fault, in which local clockwise vertical-axis rotations up to 50° have been superimposed on the older, regional 100° Miocene rotation.

Thus, three major tectonic processes are recorded from this highly complex and deformed region, attesting to the style of deformation in the evolving Pacific - Australia plate boundary zone changing from primarily thin-skinned thrusting in the Early Miocene through a period of spatially extensive (700^{+} sq. km), large-magnitude (100°) clockwise vertical-axis rotation to the current regime of dextral strike-slip and local clockwise vertical-axis rotation adjacent to active strike-slip faults.

Revision of the Quaternary stratigraphy of NE Marlborough has been enabled by five new optically stimulated luminescence (OSL) dates on loess. The Starborough-1 terrace, which formed as a result of the latest aggradation episode in the Awatere Valley, has yielded an abandonment age of *c.* 9 ka, several thousand years younger than previously thought. This age indicates that terrace aggradation, at least in the Awatere Valley, was in progress well after the last glacial maximum (~17 ka). Other terraces in the morphostratigraphic sequence of NE Marlborough have approximate ages of 40, 60, 80, 100 & 120 ka. These ages correlate with warming periods on the oxygen isotope curve, which alludes to a model of terrace aggradation and gravel outwash during maximum deglaciation rather than at the time of maximum glacial extent for peri-glacial central New Zealand.

Correlation of terrace surfaces peripheral to the Awatere Valley over a wide tract of NE Marlborough has been achieved by aerial photogrammetry and assessment of characteristic terrace surface morphology. The 22.6 ka Kawakawa Tephra has also been used as a chronostratigraphic marker in exposures of gravel and loess. Nine new exposures of the tephra have been established in NE Marlborough, seven of which have been chemically identified by electron microprobing as the Kawakawa Tephra.

The spatial and temporal distribution of stream incision patterns has been used to infer uplift rates, over the last 120 ka, for a large area of NE Marlborough that includes the Clarence Fault termination. Incision rates generally display a consistent distribution through time, with high rates of incision/uplift to the north and west of the Clarence Fault tip. Uplifted/incised terraces in this region suggest that dextral shear strain is transferred tip-ward into permanent crustal thickening. Incision rates from inland areas are compared with uplift of coastal marine terraces and assigned rates of uplift. The

fastest uplift inferred in the study area of 4 - 6 mm a^{-1} is observed immediately to the west of the Clarence Fault tip.

Patterns of landscape tilting derived from the evolution of drainage networks yield estimates of local differential uplift which are independent from the distribution of uplift inferred from patterns of stream incision. Comparison of terrace incision and drainage tilting directions indicate a similar overall distribution of uplift, with a broad doming of the area to the north and west of the Clarence Fault tip. Areas of high incision rates also mirror the outcrop distribution of indurated Mesozoic basement rocks, suggesting that the pattern of uplift observed in NE Marlborough by uplifted/incised terraces and drainage tilting directions over the last ~120 ka is a long-term pattern which can be approximated by the outcrop of Torlesse basement rocks.

The distribution of uplift is also consistent with the pattern of vertical strain predicted by models of fault terminations in elastic media. To the north of the Clarence Fault tip, high uplift rates without discrete surface structures suggest the presence of a growing anticline, that, given its asymmetry, may be cored by a SE-vergent reverse fault. Total post-Miocene uplift of ~2000 m over an area of ~15 × 15 km to the north and west of the Clarence Fault tip compares well with the elastically-modelled estimate of 12 - 1800 m over a similar area, using a total bedrock offset of 15 km for the Clarence Fault. Estimates of uplift over the last ~120 ka, using a Late Quaternary slip rate on the Clarence Fault of 5 mm a^{-1} [Van Dissen & Nicol, 1999], however, do not fit the model as well. This discrepancy between modelled and observed uplift may be due to a punctuated slip rate on the Clarence Fault or to interaction of other faults/folds in NE Marlborough that are not allowed for in the elastic model.

Vertical-axis rotation of the crustal block into which the Clarence Fault terminates, the ~40 km^2 Awatere Block, has been documented previously by palaeomagnetic studies. Clockwise rotation of the Awatere Block is also inferred from the distribution of uplift patterns. Vertical-axis rotation of this large crustal block, relative to the inland region to the SW, would cause local convergence (or divergence) along its boundaries. This local convergence is interpreted to be a key factor in the distribution of high uplift rates to the west of the Clarence Fault tip, whereas the rapid uplift observed to the north of the fault tip is inferred to be caused by the tip-ward dissipation of transcurrent strain into crustal thickening by folding.

References

Acton, G. D., Gordon, R. G. 1994: Paleomagnetic tests of Pacific plate reconstructions and implications for motion between hotspots. *Science, Vol. 263*, No. 5151. pp. 1246 - 1254

Allmendinger, R. W. 1988 - 1995: *Stereonet 4.6a*, stereographic projection program

Alloway, B. V. 1989: The Late Quaternary cover bed stratigraphy and tephrochronology of north-eastern and central Taranaki, New Zealand. Unpublished Ph. D. thesis, Massey University, Palmerston North, New Zealand

Baker, J., Seward, D. 1996: Timing of Cretaceous extension and Miocene compression in northeast South Island, New Zealand: Constraints from Rb-Sr and fission-track dating of an igneous pluton. *Tectonics, Vol. 15*, No. 5, pp. 976 - 983

Barnes, P. M., Audru, J. C. 1999: Quaternary faulting in the offshore Wairarapa and Flaxbourne Basins, southern Cook Strait, New Zealand. *New Zealand Journal of Geology and Geophysics, Vol. 42*, No. 3, pp. 349 - 367

Benson, A. M., Little, T. A., Van Dissen, R. J., Hill, N. 2001: Late Quaternary paleoseismic history and surface rupture characteristics of the eastern Awatere strike-slip fault, New Zealand. *Geological Society of America Bulletin*, in press

Berger, G. W., Pillans, B. J. 1994: Thermoluminescence dating of a loess-paleosol sequence from the Awatere River area, South Island, New Zealand. *Geological Society of America abstracts with programs 26,* No 7, A - 257

Bibby, H. M. 1981: Geodetically determined strain across the southern end of the Tonga-Kermadec-Hikurangi subduction zone. *Geophysical Journal of the Royal Astronomical Society, Vol. 66*, pp. 513 - 533

Bishop, D. J., Buchanan, P. G. 1995: *In:* Basin inversion, Editor: Buchanan, J. G. *Geological Society, London; Special Publication, Vol. 88*, pp. 549 - 585

Bradshaw, J. D. 1989: Cretaceous geotectonic patterns in the New Zealand region. *Tectonics 8*, No.4, pp. 803 - 820

Butler, R. F. 1992: *Palaeomagnetism: magnetic domains to geologic terranes.* Blackwell Scientific Publications

Campbell, I. B. 1986: New occurrences and distribution of Kawakawa Tephra in South Island, New Zealand. *New Zealand Journal of Geology and Geophysics, Vol. 29*, pp. 425 - 435

Chappell, J. 1983: A revised sea level record for the last 300 000 years from Papua New Guinea. *Search, Vol. 14*, pp. 99 - 101

Chappell, J., Shackleton, N. J. 1986: Oxygen isotopes and sea level. *Nature, Vol. 324*, pp. 137 - 140

Cotton, C. A. 1938: The Haldon Hills Problem. *Journal of Geomorphology, Vol. 1*, pp. 187 - 198

Cotton, C. A. 1945: *Geomorphology*. Whitcombe & Tombs Ltd., Wellington

Crampton, J. S., Laird, M. G. 1997: Burnt Creek Formation and Late Cretaceous basin development in Marlborough, New Zealand. *New Zealand Journal of Geology and Geophysics, Vol. 40*, pp. 199 - 222

Delteil, J., Morgans, H. E. G., Raine, J. I., Field, B. D., Cutten, H. N. C. 1996: Early Miocene thin-skinned tectonics and wrench faulting in the Pongaroa district, Hikurangi margin, North Island, New Zealand. *New Zealand Journal of Geology and Geophysics, Vol. 39*, pp. 271 - 282

DeMets, C., Gordon, R. G., Argus, D. F., Stein, S. 1994: Effect of recent revisions to the geomagnetic reversal timescale on estimates of current plate motions. *Geophysical Research Letters, Vol. 21*, No. 20, pp. 2191 - 2194

Eberhart-Phillips, D., Reyners, M. 1997: Continental subduction and three-dimensional crustal structure: The northern South Island, New Zealand. *Journal of Geophysical Research, Vol. 102*, pp. 11843 - 11861

Eden, D. N. 1983: A late Quaternary history of the Awatere and Wairau Valleys, Marlborough, New Zealand. Unpublished Ph. D. thesis lodged in the library, Victoria University of Wellington, New Zealand; 2 Vols

Eden, D. N. 1989: River terraces and their loessial cover beds, Awatere River Valley, South Island, New Zealand. *New Zealand Journal of Geology and Geophysics, Vol. 32*, pp. 487 - 497

Fisk, H. N. 1944: *Geological Investigation of the Alluvial Valley of the Lower Mississippi River*. Mississippi River Commission, Vicksburg

Froggatt, P. C., Lowe, D. J. 1990: A review of Late Quaternary silicic and some other tephra formations from New Zealand: their stratigraphy, nomenclature, distribution, volume, and age. *New Zealand Journal of Geology and Geophysics, Vol. 33,* pp. 89 - 109

Gage, M. 1965: Some characteristics of Pleistocene cold climates in New Zealand. *Transactions of the Royal Society of New Zealand: Geology, Vol. 3*, pp. 11 - 21

Gibb, J. G. 1979: Late Quaternary shoreline movements in New Zealand. Unpublished Ph. D. thesis, lodged in the library, Victoria University of Wellington, New Zealand

Hays, J. D., Imbrie, J., Shackleton, N. J. 1976: Variations in the earth's orbit; pacemaker of the ice ages. *Science, Vol. 194*, pp. 1121 - 1132

Henderson, R. in preparation: Late Cenozoic evolution of the crustal blocks to the east of the Kekerengu Fault, Marlborough, New Zealand. Unpublished M. Sc. thesis, lodged in the library, Victoria University of Wellington, New Zealand

Holt, W. E., Haines, A. J. 1995: The kinematics of northern South Island, New Zealand, determined from geologic strain rates. *Journal of Geophysical Research, Vol. 100*, pp. 17991 - 18010

Homberg, C., Hu, J. C., Angelier, J., Bergerat, F., Lacombe, O. 1997: Characterisation of stress perturbations near major fault zones: insights from 2-D distinct-element modelling and field studies (Jura Mountains). *Journal of Structural Geology, Vol. 19*, No. 5, pp. 703 - 718

Jackson, J., Leeder, M. 1994: Drainage systems and the development of normal faults: an example from Pleasant Valley, Nevada. *Journal of Structural Geology, Vol. 16*, No.8, pp. 1041 - 1059

Jackson, J. Norris, R., Youngson, J. 1996: The structural evolution of active fault and fold systems in central Otago, New Zealand: evidence revealed by drainage patterns. *Journal of Structural Geology, Vol. 18*, Nos. 2/3, pp. 217 - 234

Kamp, 1987: Age and origin of the New Zealand Orocline in relation to Alpine Fault movement. *Geological Society (London), Vol. 144*, No. 4, pp. 641 - 652

King, P. R. 2000: Tectonic reconstructions of New Zealand: 40 Ma to the Present. *New Zealand Journal of Geology and Geophysics, Vol. 43*, pp. 611 - 638

King, P. R., Thrasher, G. P. 1992: Post-Eocene development of the Taranaki basin, New Zealand: convergent overprint of a passive margin. *AAPG Memoir, 53*, In: Geology and Geophysics of Continental Margins, 1992, pp. 93 - 118

Lamb, S. H. 1987: A model for tectonic rotations about a vertical axis. *Earth and Planetary Science Letters, Vol. 84*, pp. 75 - 86

Lamb, S. H. 1988: Tectonic rotations about vertical axes during the last 4 Ma in part of the New Zealand plate-boundary zone. *Journal of Structural Geology, Vol. 10*, pp. 875 - 983

Lamb, S. H., Bibby, H. M. 1989: The last 25 Ma of rotational deformation in part of the New Zealand plate-boundary zone. *Journal of Structural Geology, Vol. 11*, No. 4, pp. 473 - 492

Leland, J., Caffee, M., Reid, M. R., Burbank, D.W., Finkel, R. 1998: Incision and differential bedrock uplift along the Indus River near Nanga Parbat, Pakistan Himalaya, from ^{10}Be and ^{26}Al exposure age dating of bedrock straths. *Earth and Planetary Science Letters, Vol. 154*, No.1-4, pp. 93 - 107

Lensen, G. J. 1962: N. Z. Geological Survey Map 1: 250 000, Sheet 16 Kaikoura, D. S. I. R., Wellington, New Zealand

Lewis, D. W. 1992: Anatomy of an unconformity on mid-Oligocene Amuri Limestone, Canterbury, New Zealand. *New Zealand Journal of Geology and Geophysics, Vol. 35,* pp. 463 - 475

Little, T. A., Roberts, A. P. 1997: Distribution and mechanism of Neogene to present-day vertical-axis rotations, Pacific-Australia plate boundary zone, South Island, New Zealand. *Journal of Geophysical Research, Vol. 102*, No. B9, pp. 20447 - 20468

Little, T. A., Jones, A. 1998: Seven million years of strike-slip and related off-fault deformation, northeastern Marlborough fault system, South Island, New Zealand. *Tectonics, Vol. 17*, No. 2, pp. 285 - 302

Little, T. A., Grapes, R., Berger, G. W. 1998: Late Quaternary strike-slip on the eastern part of the Awatere Fault, South Island, New Zealand. *Geological Society of America Bulletin, Vol. 110*, No. 2, pp. 127 - 148

Maddy, D., Bridgland, D. R., Green, C. P. 2000: Crustal uplift in southern England: evidence from the river terrace records. *Geomorphology, Vol. 33*, pp. 167 - 181

Markley, M., Norris, R. J. 1999: Structure and neotectonics of the Blackstone Hill Antiform, Central Otago, New Zealand. *New Zealand Journal of Geology and Geophysics, Vol. 42*, No. 2, pp. 205 - 218

Marrett, R., Allmendinger, R. W. 1990: Kinematic analysis of fault-slip data. *Journal of Structural Geology, Vol. 12*, pp. 973 - 986

Marshak, S., Mitra, G. 1988: *Basic Methods of Structural Geology*. Prentice Hall Inc., Englewood Cliffs, New Jersey

Martinson, D., Pisias, N., Hays, J., Imbrie, J., Moore, T., Shackleton, N. 1987: Age dating and the orbital theory of the ice ages: development of a high-resolution 0 to 300,000-year chronostratigraphy. *Quaternary Research, Vol. 27*, pp. 1 - 29

McKenzie, D., Jackson, J. 1983: The relationship between strain rates, crustal thickening, palaeomagnetism, finite strain and fault movements within a deforming zone. *Earth and Planetary Science Letters, Vol. 65*, pp. 182 - 202

Milne, J. D. G. 1973: Upper Quaternary geology of the Rangitikei drainage basin, North Island, New Zealand. Unpublished Ph. D. thesis lodged in the library, Victoria University of Wellington, New Zealand

Molloy, L. 1993: *Soils in the New Zealand Landscape: the living mantle*. Mallinson Rendel Publishers, Ltd., Wellington

Moore, P. R. 1988: Stratigraphy, composition and environment of deposition of the Whangai Formation and associated Late Cretaceous-Paleocene rocks, eastern North Island, New Zealand. *New Zealand Geological Survey Bulletin, Vol. 100*

Morris, J. C. 1987: The Stratigraphy of the Amuri Limestone Group, East Marlborough, New Zealand. Unpublished Ph. D. thesis, University of Canterbury, Christchurch, New Zealand

Mumme, T. C., Walcott, R. I., 1985: Palaeomagnetic studies at Geophysics Division 1980 - 1983. *DSIR Report No. 204*

Murray, A. S., Wintle, A. G. 2000: Luminescence dating of quartz using an improved single aliquot regenerative-dose protocol. *Radiation Measurements, Vol. 32*, pp. 57 - 73

Norris, R. J., Cooper, A. F. 1997: Erosional control on the structural evolution of a transpressional thrust complex on the Alpine Fault, New Zealand. *Journal of Structural Geology, Vol. 19*, pp. 1323 - 1342

Norris, R. J., Koons, P. O., Cooper, A. F. 1990: The obliquely-convergent plate boundary in the South Island of New Zealand: implications for ancient collision zones. *Journal of Structural Geology, Vol. 12*, No. 5/6, pp. 715 - 725

Ota, Y., Brown, L. J., Berryman, K. R., Fujimori, T., Miyauchi, T. 1995: Vertical tectonic movement in northeastern Marlborough: stratigraphic, radiocarbon, and paleoecological data from Holocene estuaries. *New Zealand Journal of Geology and Geophysics, Vol. 38*, pp. 269 - 282

Ota, Y., Pillans, B., Berryman, K., Beu, A., Fujimori, T., Miyauchi, T., Berger, G. 1996: Pleistocene marine terraces of Kaikoura Peninsula and the Marlborough coast, South Island, New Zealand. *New Zealand Journal of Geology and Geophysics, Vol. 39*, No. 1, pp. 51 - 73

Ozdemir, O. 1990: High-temperature hysteresis and thermoremanence of single-domain maghemite. *Physics of the Earth & Planetary Interiors, Vol. 65*, No. 1 - 2, pp. 125 - 136

Palmer, A. S. 1982: The stratigraphy and selected properties of loess in Wairarapa, New Zealand. Unpublished Ph. D. thesis, lodged in the library, Victoria University of Wellington, New Zealand

Penck, A., Bruckner, E. 1909: *Die Alpen im Eiszeitalter*. Tauchnitz, Leipzig

Pillans, B. 1994: Direct marine-terrestrial correlations, Wanganui basin, New Zealand: the last 1 million years. *Quaternary Science Reviews, Vol. 13*, pp. 189 - 200

Pillans, B., McGlone, M., Palmer, A., Mildenhall, D., Alloway, B., Berger, G. 1993: The Last Glacial Maximum in central and southern North Island, New Zealand: a paleoenvironmental reconstruction using the Kawakawa Tephra Formation as a chronostratigraphic marker. *Palaeogeography, Palaeoclimatology, Palaeoecology, Vol. 101*, pp. 283 - 304

Personius, S. F. 1995: Late Quaternary stream incision and uplift in the forearc of the Cascadia subduction zone, western Oregon. *Journal of Geophysical Research, Vol. 100*, No. B10, pp. 20193 - 20210

Petronotis, K. E., Gordon, R. G., Acton, G. D. 1994: A 57 Ma Pacific plate palaeomagnetic pole determined from a skewness analysis of crossing of marine magnetic anomaly 25r. *Geophysical Journal International, Vol. 118*, pp. 529 - 554

Prebble, W. M. 1976: Geology of the Kekerengu-Waima River district, North-East Marlborough. M. Sc. thesis, lodged in the library, Victoria University of Wellington, New Zealand. 103 pp

Rait, J., Chanier, F., Waters, D. W. 1991: Landward- and seaward-directed thrusting accompanying the onset of subduction beneath New Zealand. *Geology, Vol. 19*, pp. 230 - 233

Reay, M. B. 1993: *Geology of the Middle Clarence Valley*. Institute of Geological and Nuclear Sciences Geological map 10

Roberts, A. P. 1992: Paleomagnetic constraints on the tectonic rotation of the southern Hikurangi Margin, New Zealand. *New Zealand Journal of Geology and Geophysics, Vol. 35,* pp. 311 - 323

Roberts, A. P. 1995: Tectonic rotation about the termination of a major strike-slip fault, Marlborough fault system, New Zealand. *Geophysical Research Letters, Vol. 22,* No. 3, pp. 187 - 190

Roberts, A. P., Wilson, G. S. 1992: Stratigraphy of the Awatere Group, New Zealand. *Journal of the Royal Society of New Zealand, Vol. 22,* No. 3, pp. 187 - 204

Russel, W. A. C. 1959: *A geological reconnaissance of Northeast Marlborough.* Petroleum Report Series, 279

Shackleton N. J., Berger, A., Peltier W. R. 1990: An alternative astronomical calibration of the Lower Pleistocene timescale based on ODP Site 677. *Transactions - Royal Society of Edinburgh: Earth Sciences, Vol. 81,* No. 4, pp. 251 - 261

Stevens, G. R. 1974: *Rugged Landscape: the geology of Central New Zealand.* A. H. & A. W. Reed, Ltd., Wellington

Strong, C. P., Hollis, C. J., Wilson, G. J. 1995: Foraminiferal, radiolarian, and dinoflagellate biostratigraphy of Late Cretaceous to Middle Eocene pelagic sediments (Muzzle Group), Mead Stream, Marlborough, New Zealand. *New Zealand Journal of Geology and Geophysics, Vol. 38,* pp. 171 - 212

Suggate, R. P. 1990: Late Pliocene and Quaternary glaciations of New Zealand. *Quaternary Science Reviews, Vol. 9,* pp. 175 - 197

Sutherland, R. 1995: The Australia-Pacific boundary and Cenozoic plate motions in the SW Pacific: Some constraints from Geosat data. *Tectonics, Vol. 14,* No. 4, pp. 819 - 831

Sutherland, R. 1996: Transpressional development of the Australia-Pacific boundary through southern South Island, New Zealand: constraints from Miocene - Pliocene sediments, Waiho-1 borehole, South Westland. *New Zealand Journal of Geology and Geophysics, Vol. 39*, pp. 251 - 264

Sutherland, R. 1999: Cenozoic bending of New Zealand basement terranes and Alpine Fault displacement: a brief review. *New Zealand Journal of Geology and Geophysics, Vol. 42*, pp. 295 - 301

ten Brink, U. S., Katzman, R., Lin, J. 1996: Three-dimensional models of deformation near strike-slip faults. *Journal of Geophysical Research, Vol. 101*, B7, pp. 16205 - 16220

Townsend, D. B. 1996: Cenozoic to Quaternary tectonics of the Awatere/Cape Campbell area, Marlborough, New Zealand. B. Sc. (Hons) thesis, lodged in the library, Victoria University of Wellington, New Zealand. 122 pp

Townsend, D. B., Little, T. A. 1998: Pliocene-Quaternary deformation and mechanisms of near-surface strain close to the eastern tip of the Clarence Fault, northeast Marlborough, New Zealand. *New Zealand Journal of Geology and Geophysics, Vol. 41*, pp. 401 - 417

Turner, G. M. 2001: Toward an understanding of the multicomponent magnetization of uplifted Neogene marine sediments in New Zealand. *Journal of Geophysical Research B: Solid Earth, Vol. 106*, No. 4, pp. 6385 - 6397

Van der Voo, R. 1990: Phanerozoic palaeomagnetic poles from Europe and North America and comparisons with continental reconstructions. *Reviews of Geophysics, Vol. 28*, No. 2, pp. 167 - 206

Van Dissen, R., Yeats, R. S. 1991: Hope Fault, Jordan Thrust, and uplift of the Seaward Kaikoura Range, New Zealand. *Geology, Vol. 19*, No. 4, pp. 393 - 396

Van Dissen, R. J., Nicol, A. 1999: Palaeoseismicity of the middle Clarence Valley section of the Clarence Fault, Marlborough, New Zealand. *Geological Society of New Zealand Miscellaneous Publication, 107A*, p. 162

Vickery, S. 1994: Cenozoic Deformation in a Plate Boundary Zone, Marlborough, New Zealand. Unpublished Ph. D. thesis, lodged in the library, Victoria University of Wellington, New Zealand

Vickery, S., Lamb, S. H. 1995: Large tectonic rotations since the Early Miocene in a convergent plate boundary zone, South Island, New Zealand. *Earth and Planetary Science Letters, Vol. 136*, pp. 44 - 59

Walcott, R. I. 1978: Present tectonics and late Cenozoic evolution of New Zealand. *Geophysical Journal of the Royal Astronomical Society, Vol. 52*, pp. 137 - 164

Walcott, R. I. 1984: The kinematics of the plate boundary zone through New Zealand: a comparison of short-and long-term deformations. *Geophysical Journal of the Royal Astronomical Society, Vol. 79*, pp. 613 - 633

Walcott, R. I. 1998: Modes of oblique compression: late Cenozoic tectonics of the South Island, New Zealand. *Reviews of Geophysics, Vol. 36,* No. 1, pp. 1 - 26

Walcott, R. I., Christoffel, D. A., Mumme, T. C. 1981: Bending within the axial tectonic belt of New Zealand in the last 9 Myr from paleomagnetic data. *Earth and Planetary Science Letters, Vol. 52*, pp. 427 - 434

Waters, D. W. 1988: The Flags Creek Thrust. Unpublished B. Sc. (Hons) thesis, lodged in the library, Victoria University of Wellington, New Zealand

Wilson, C. J. N., Switsur, V. R., Ward, A. P. 1988: A new ^{14}C age for the Oruanui Ignimbrite (Wairakei) eruption, New Zealand. *Geological Magazine, Vol. 125*, pp. 297 - 300

Wilson, G. S., McGuire, D. M. 1995: Distributed deformation due to coupling across a subduction thrust: mechanism of young tectonic rotation within the south Wanganui basin, New Zealand. *Geology, Vol. 23,* No. 7, pp. 645 - 648

Wellman, H. W. 1979: An uplift map for the South Island of New Zealand and a model for the uplift of the Southern Alps; *in*: Walcott, R. I., Creswell, M. M. 1979: Origin of the Southern Alps. *The Royal Society of New Zealand Bulletin, Vol. 18*

Appendix 1.

See CD-ROM archive of palaeomagnetic data in back pocket.

Appendix 2.

Sites that did not yield satisfactory primary magnetisation vectors are given a precis description. All sites described below are located on Figure A2.

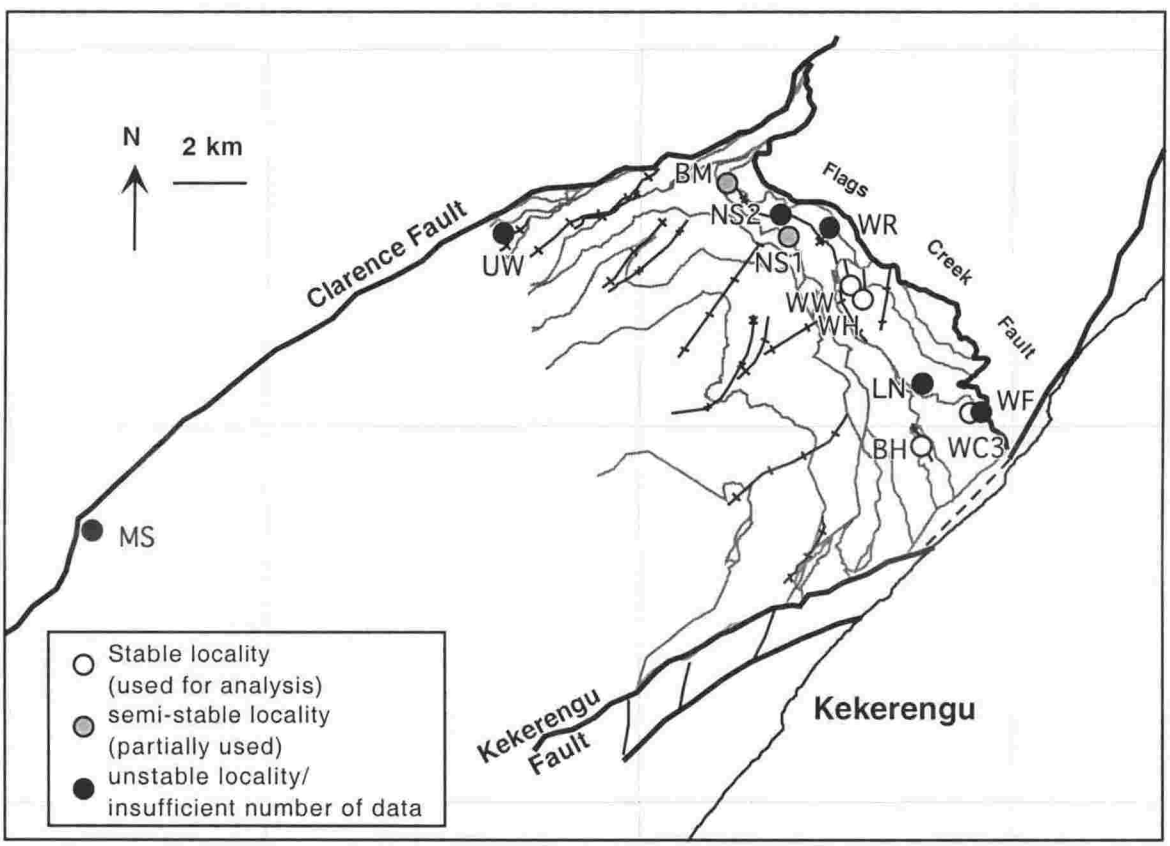

Figure A2. Location map for sites outlined in Appendix 2. Sites refer to this study only. Faults of the Early Miocene Flags Creek Fault System are also shown, for reference.

locality abbreviations:

MS	**Mead Stream**
UW	**Upper Waima River**
BM	**Blue Mountain Stream**
NS2	**Narrows syncline-2**
NS1	**Narrows syncline-1 (Waterfall Stream)**
WR	**Waima River**
WW	**Woodside member of Amuri Formation (Waima Hills)**
WH	**Amuri Formation limestone (Waima Hills)**
LN	**Laings Nut**
WC3	**Woodside Creek**
WF	**Woodside member of Amuri Formation (Woodside Creek)**
BH	**Black Hill Station**

Appendix 2.1.

Mead Stream locality (MS)

Rocks on the downthrown, SE side of the Clarence Fault, at Mead Stream, include a relatively complete stratigraphic section of Late Cretaceous – Palaeocene chert of the Mead Hill Formation, Palaeocene – Eocene Amuri Formation limestone and marl and Early Miocene clastic rocks, including the Whalesback limestone (Weka Pass stone), Waima Formation siltstone and Great Marlborough Conglomerate (GMC) [see Fig. 2.4, main text]. The lower and middle part of the section (Mead Hill & Amuri formations, Weka Pass stone, lower Waima Formation) were sampled in March 1998 as a pilot study on the magnetostratigraphy of this section, which is internationally recognised as an important Cretaceous – Tertiary boundary location. I sampled the upper part of the section in late 1998, drilling the Early Miocene Waima Formation siltstone and thin siltstone interbeds of the GMC.

Three to four cores were drilled from each sampled stratigraphic horizon. Twelve sites, from the Mead Hill Formation to the lower Waima Formation, totalling 42 samples, generally have weak natural remanent magnetisation (NRM) values (~2-4 mAm^{-1}) [Gary Wilson, Pers. Comm.] and exhibited unstable demagnetisation characteristics. Primary magnetisation components from these samples could not be unequivocally isolated for the Mead Stream locality (Fig. A2.1.A.I).

Seventeen samples from the Miocene section (Waima Formation siltstone and mudstone beds within the GMC) were demagnetised at Oxford University by the author. These also had fairly weak NRM values, typically less than 1 mAm^{-1}. The bulk magnetic susceptibility of these samples consistently increased at ~350°C during thermal demagnetisation, usually before the characteristic magnetisation had been resolved (e.g., Fig. A2.1.A.I). Demagnetisation of the low temperature component was not directed toward the origin of the vector component diagram, suggesting that the component being demagnetised was not primary.

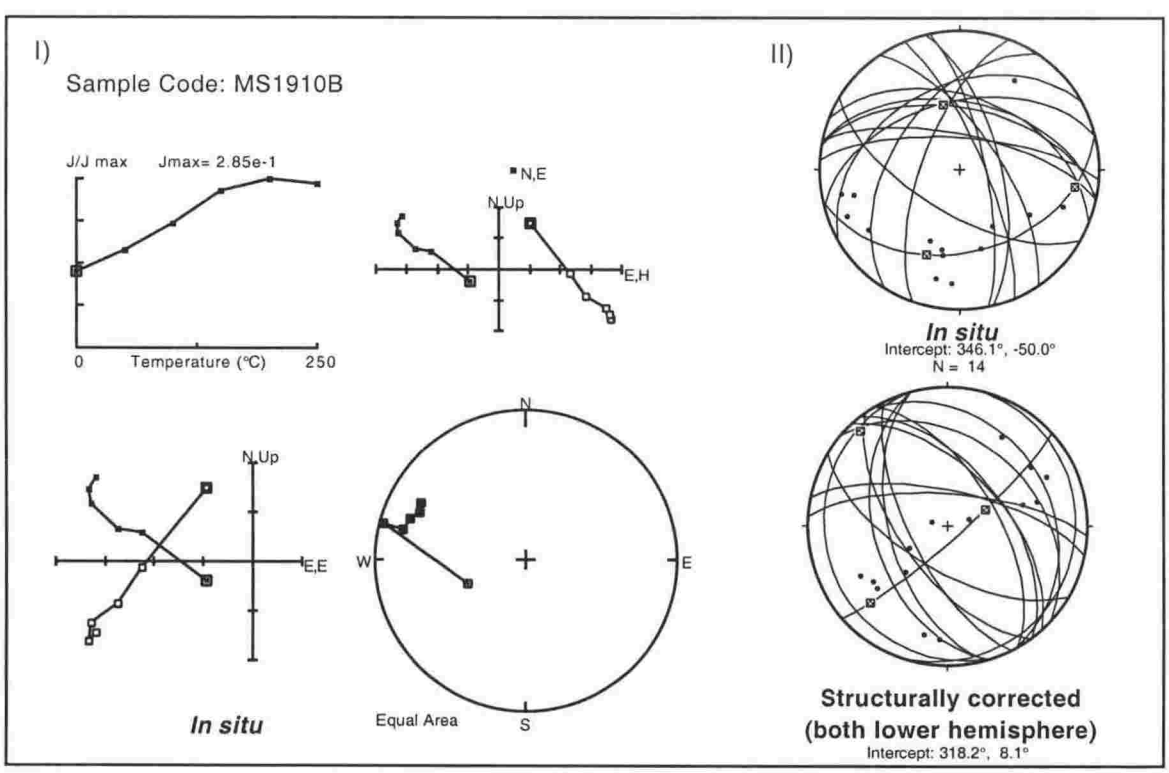

Figure A2.1.A.I: Demagnetisation plots for siltstone interbed of the Great Marlborough Conglomerate from Mead Stream that did not reach a stable endpoint (above left). II: Great circles analysis of these specimens (above right) failed to produce a component that could be differentiated from an *in situ* modern direction.

Appendix 2.2.

Upper Waima River (UW)

Palaeocene Amuri Formation limestone and marl crop out at the base of this section and are separated from Early Miocene [Reay, 1993] Whalesback limestone and Waima Formation siltstone above, by a minor fault or shear zone. After only a few metres, the Whalesback limestone grades up section into Waima Formation, which after ~20 m of stratigraphic thickness becomes a poorly sorted, matrix supported conglomerate that contains large clasts of most of the aforementioned lithologies. This conglomerate is inferred to be a lateral equivalent of the Otaian to Altonian aged Great Marlborough Conglomerate (GMC). Clasts decrease in abundance several metres further up section, giving rise to the sampled outcrop of ~50 m of blue-grey silty mudstone. At the top of the section, reintroduction of large (up to 1 m across), sub-angular clasts visibly disturbs bedding traces and the lithology here is a poorly sorted, matrix supported conglomerate that continues up section for several hundred metres. The site age is Otaian (20 – 25 Ma).

NRM values of the siltstone cores were weak (at around 1-1.5 mAm^{-1}). Bulk magnetic susceptibility increased markedly at ~350°C, before a stable characteristic magnetisation could be isolated from all but two of these samples (Gillian Turner, Pers. Comm. – see Fig. A2.2.A.I) but, owing to the low sample number, cannot be statistically ratified. Great circles analysis suggests that the component being cleaned off the other samples is a modern overprint (Fig. A2.2.A.II).

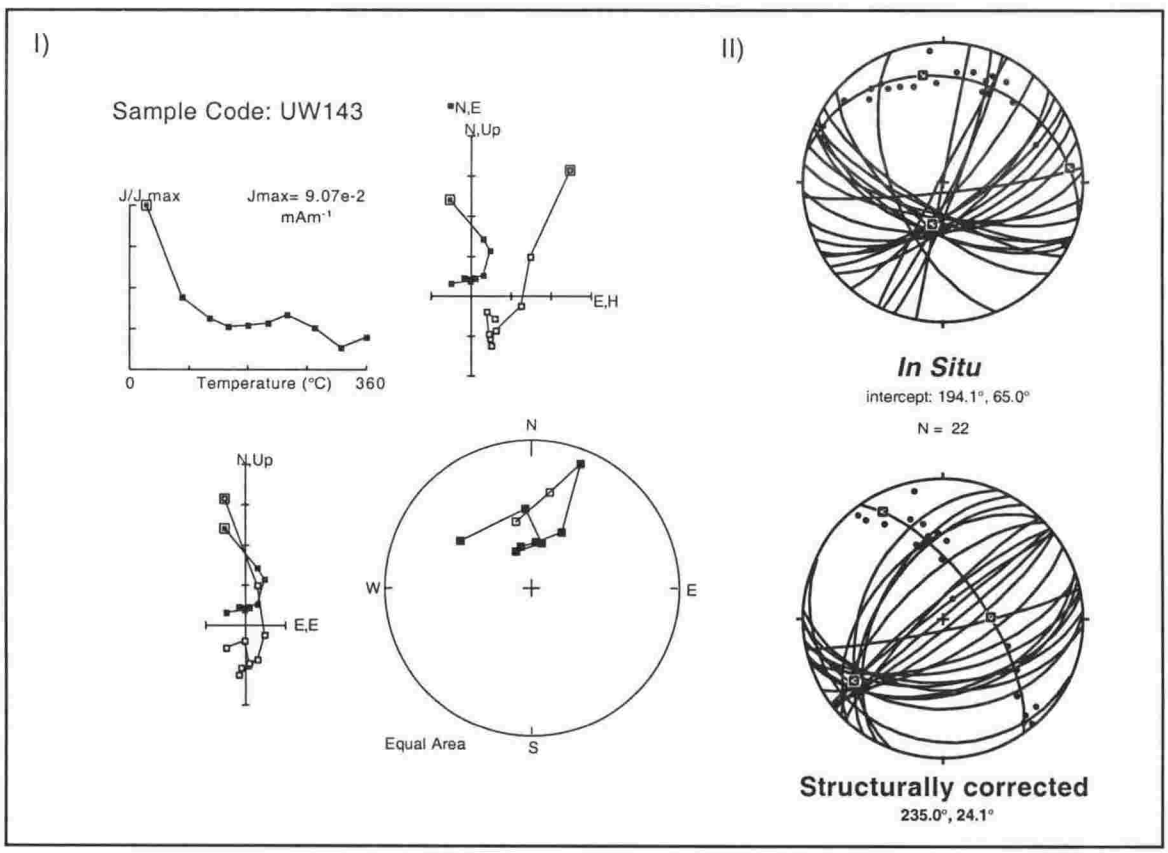

Figure A2.2.A.I: Typical demagnetisation plot for UW sample that did not reach a stable endpoint. II: Great circles analysis suggests that the component being cleaned is approximately parallel to a modern geomagnetic field when viewed *in situ* and is therefore likely to be an overprint.

Appendix 2.3.

Blue Mountain Stream (BM)

The stratigraphy at the Blue Mountain Stream locality consists of Eocene submarine volcanic pillow basalt and pink Amuri Formation limestone (Fig. A2.3.A).

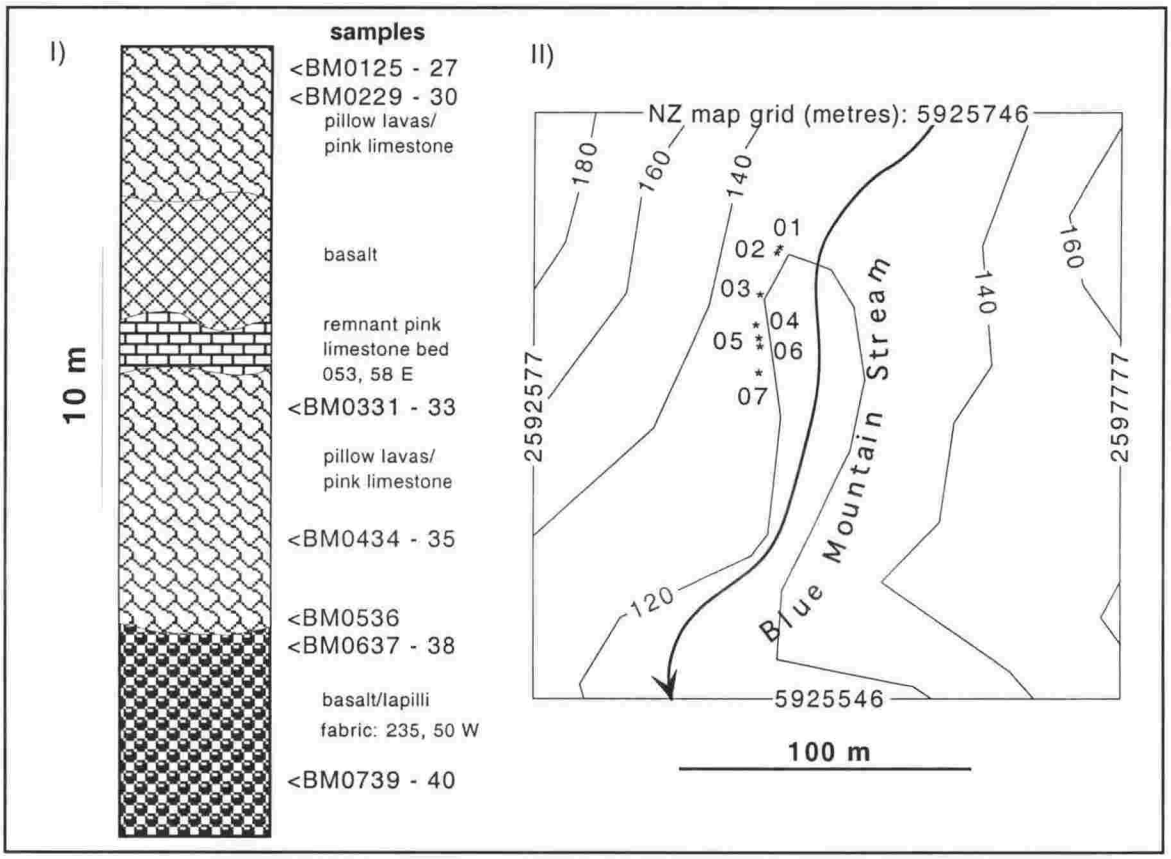

Figure A2.3.A.I): stratigraphy and setting of the Blue Mountain Stream section, showing sequence and location of samples; II): sample location map.

Appendix 2.3. -continued.

Samples were taken from both the limestone (5 cores) and basalt (10 cores) lithologies. Limestone samples exhibited two to three components of magnetisation. A low-blocking temperature component that is common to all samples (α_{95} = 7.6°) was removed on heating to ~210°C (Fig. A2.3.B I & II).

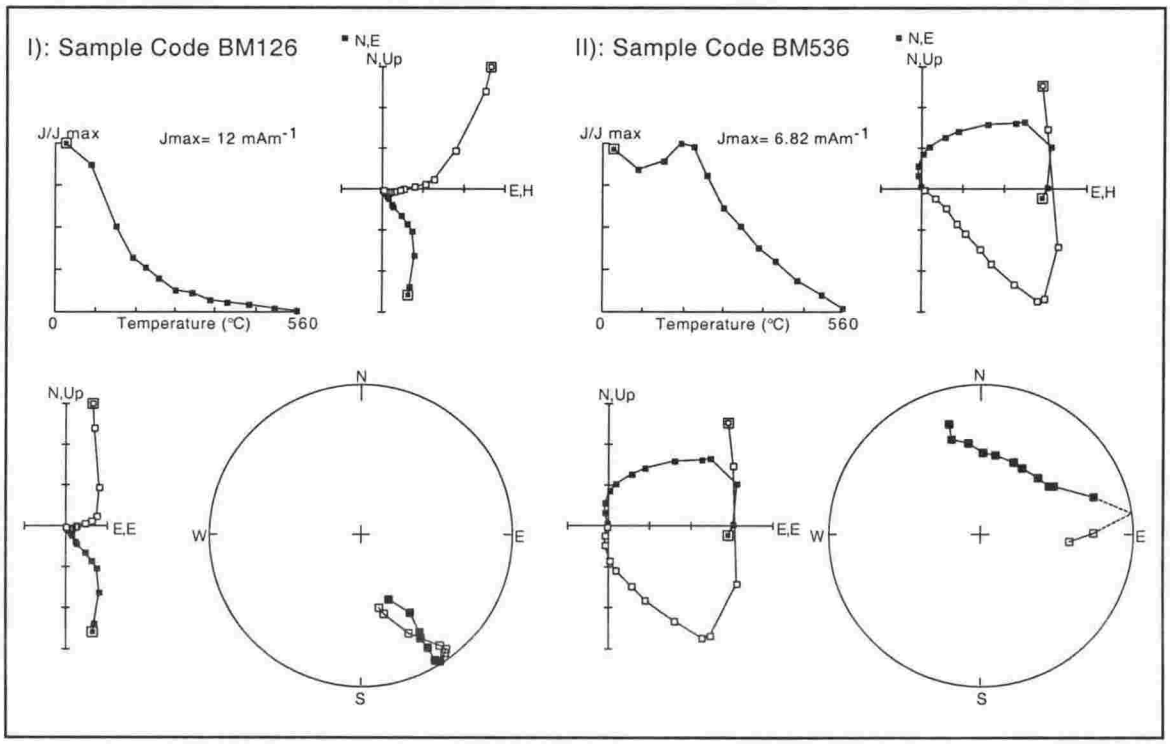

Figure A2.3.B. I & II: Demagnetisation of limestone cores, revealing overlap (curved demagnetisation path on Zijderveld plots) of two components at higher temperatures. The low temperature component is represented by the relatively straight section of the plot, where most intensity is lost. Symbols are the same as in Figure 2.8.2. Solid symbols indicate lower hemisphere equal area projection.

This component has an unusual *in situ* orientation, with a mean declination of 194° and mean inclination of –70°, that cannot be interpreted as a modern-day overprint (Fig. A2.3.C.I.). The other two components have overlapping blocking temperature / coercivity spectra, making identification of the two vectors difficult. Both of these components have apparently random orientations (Figs. A2.3.D. & E). Isothermal remanent magnetisation (IRM) acquisition and analysis of the limestone at this site suggests a component of single-domain magnetite (inflection at ~100 mT; B_{cr} = 52 mT) and non-saturation of the IRM by 850 mT indicates the presence of a high coercivity mineral, probably haematite (Fig. A2.3.F.). Three orders of magnitude difference between the NRM (~4 mAm^{-1}) and IRM_{850} (~4 Am^{-1}) is typical of a detrital or chemical remanent magnetisation [e.g., Butler, 1992]. The haematite in these samples may be authigenic and have grown grown as a separate population of secondary magnetic grains. This means that the scattered, highest blocking– component(s) may not be indicative of a primary magnetisation direction [e.g., Turner 2001] and must be regarded with suspicion.

Appendix 2.3. -continued.

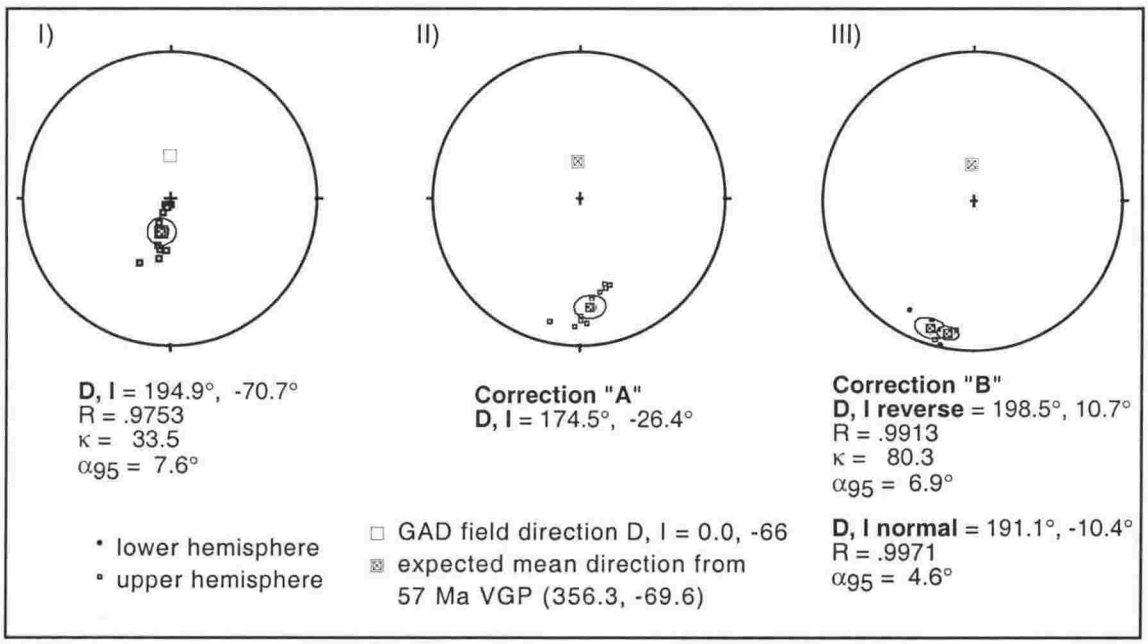

Figure A2.3C. Low-blocking temperature component of the pink limestone cores from Blue Mountain Stream. Plots are (I) *in situ,* (II) structurally corrected using the "lapilli" fabric and (III) using the remnant limestone bed. A modern magnetic field inclination best fits the *in situ* data, but the declination of these upper hemisphere components is ~195°. Both corrections A and B yield shallow inclinations for this low blocking temperature component.

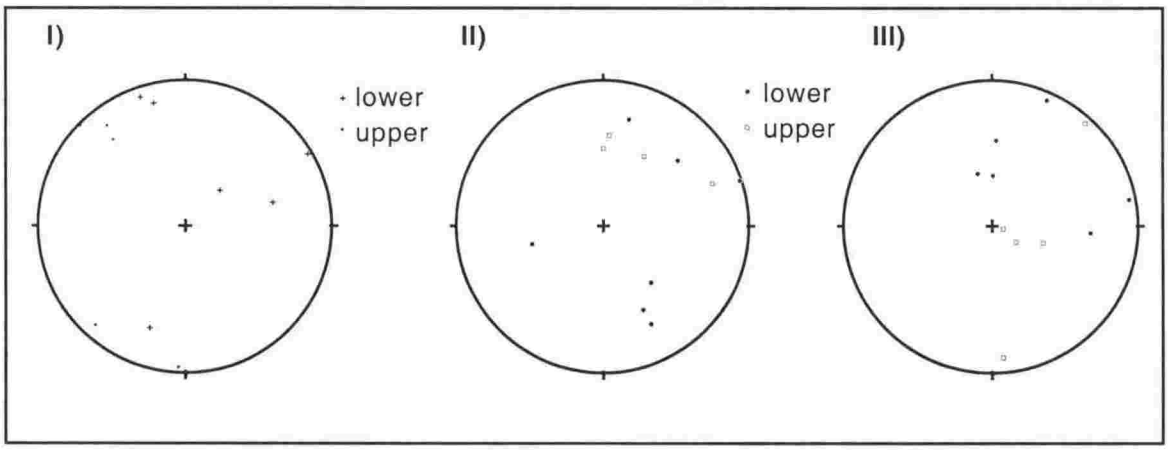

Figure A2.3.D. Intermediate blocking temperature component (from roughly 100 – 350°C) of the pink limestone samples from Blue Mountain Stream. Plots are as *in situ* (I), corrected using a lapilli fabric (II) and using the remnant limestone bed (III). This component shows no obvious grouping.

Appendix 2.3. -continued.

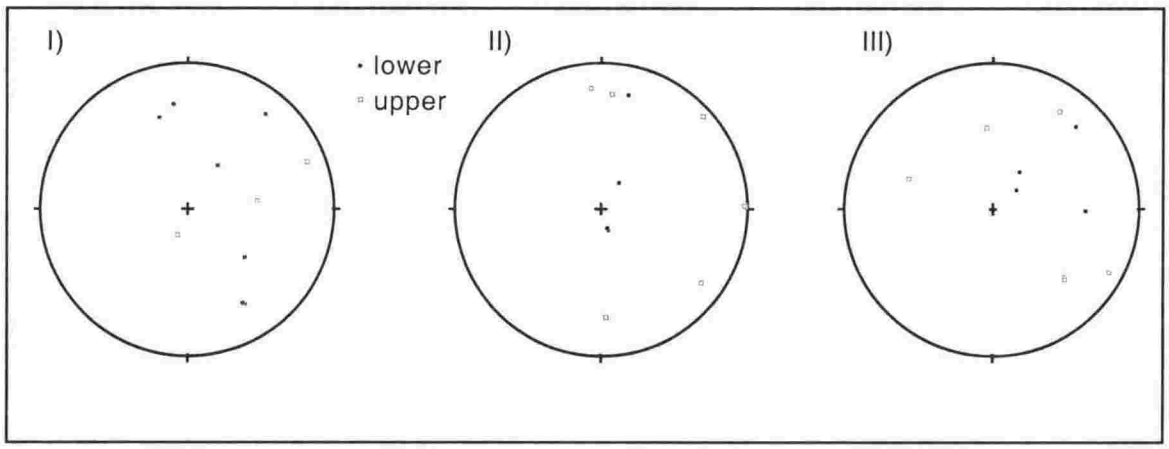

Figure A2.3.E. High temperature/coercivity component (from roughly 350 – 560°C) of the pink limestone samples from site BM. Plots are as *in situ* (I), corrected using the lapilli fabric (II) and using the remnant limestone bed (III). This component is also apparently random.

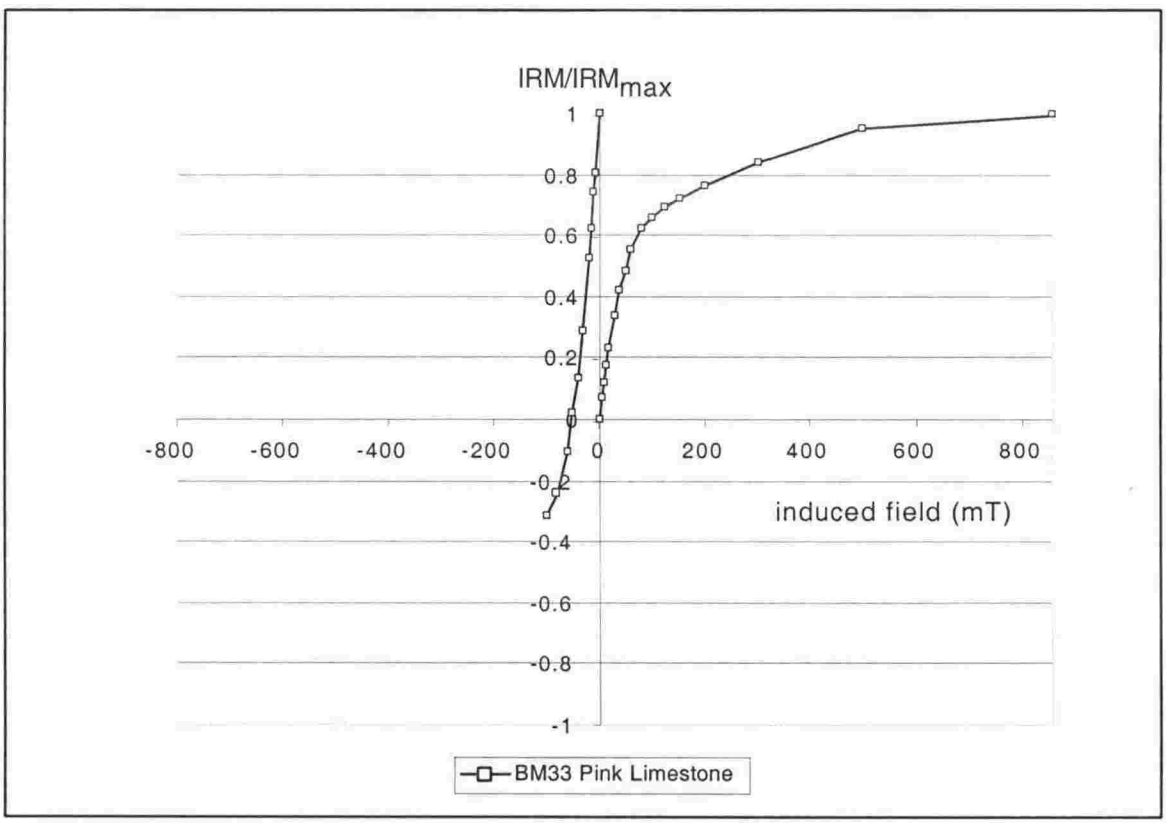

Figure A2.3.F. Isothermal Remanent Magnetisation (IRM) acquisition for a sample of pink Amuri Formation limestone from between the Blue Mountain Stream pillow basalts. The initial rapid increase to ~80 mT followed by a steady increase to ~500 mT suggests two magnetic mineral components in this rock. The first component saturates at the field strength of magnetite but non-saturation of the second component suggests the presence of haematite.

Appendix 2.3. -continued.

Basalt samples from stratigraphically above the limestone at Blue Mountain Stream were taken from three different flows over an interval of ~14 m (Fig. A2.3.G.I). These had a very strong NRM (up to 6 Am^{-1}), making it possible to measure them on a Molspin spinner magnetometer (demagnetisation performed at VUW by the author). AF demagnetisation revealed that these samples have a single component of magnetisation that starts cleaning off at ~5 mT and which is almost completely lost by peak fields of ~60 mT (Fig. A2.3.G.II). Thermal demagnetisation of basalt samples showed that this component is magnetically strong, retaining ~85% of the maximum intensity (J_{max}) to temperatures of ~450°C, finally cleaning off by 590°C, where only ~2% of J_{max} remained. The unblocking temperature of ~580°C suggests that the magnetic remanence carrier in the basalt is magnetite [Butler, 1992]. The mean *in situ* remanence direction of these basalt samples (~131°, -11°) is well-grouped (k = 370.6; α_{95} = 3.2°; n = 6) as would be expected for volcanic rocks that do not average out secular variation (Fig. A2.3.H.I).

The structural correction of the *in situ* magnetic vector may be applied in two ways at this location. Both methods account for the regional fold plunge, but use different corrections for the second step. If the pyroclastic fabric (235°, 50°) in the basalt is representative of palaeo-horizontal at the time of basalt flow (correction A), then the site magnetic vector from the basalt cores restores to a reverse polarity (141.1°, 37.3°). Alternatively, if the remnant limestone bedding (053°, 58°) is used as a horizon for the second step (correction B), the magnetic vector restores to 097.5, -66.1 (Fig. A2.3.H.II). Correction B is the preferred restoration because the restored inclination more closely matches that of the expected mean inclination at this site (-69°; see below). The mean expected declination for 57 Ma rocks at this site is 356° (Table 1), therefore, a clockwise rotation of the Eocene volcanic rocks at Blue Mountain Stream of 102°, not accounting for secular variation, which could be ± 40°, is implied.

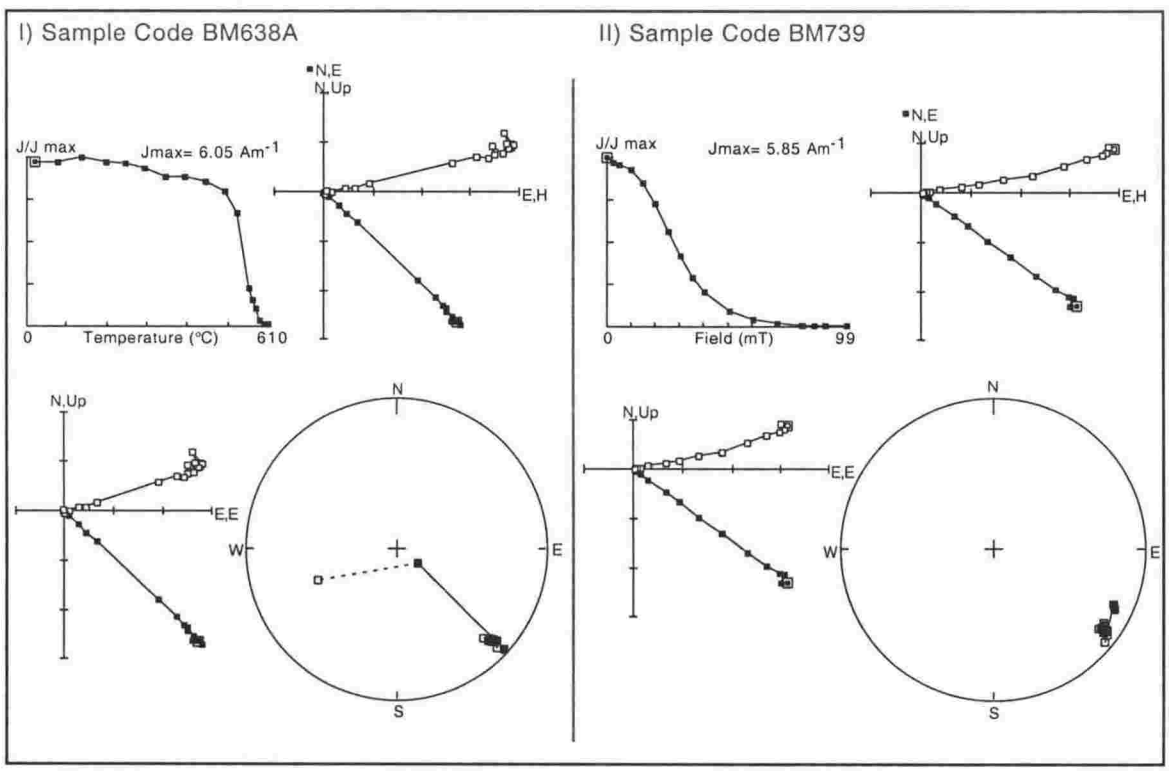

Figure A2.3.G. Examples of typical thermal (I) and alternating field (II) characteristic magnetisation of the Blue Mountain Stream basalt flows. All plots are *in situ* coordinates.

Appendix 2.3. -continued.

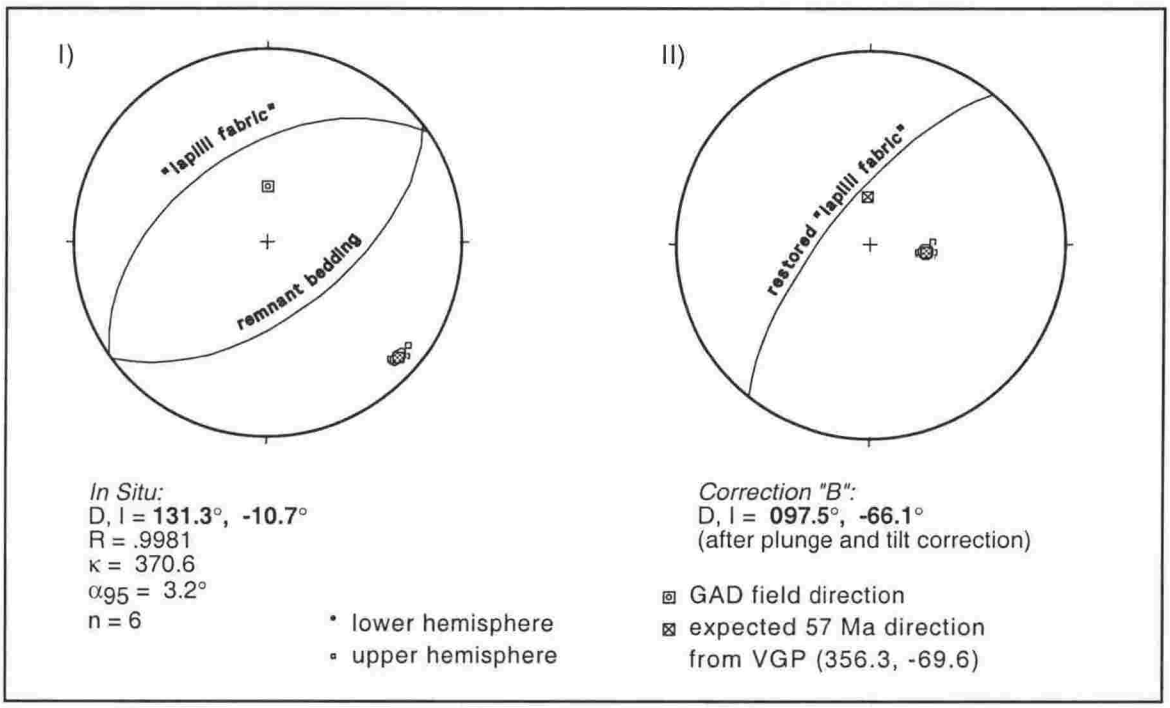

Figure A2.3.H. Stereoplots of extremely well grouped single magnetic components from basalt samples inferred to be thermal remanence directions. I: the *in situ* measured directions, showing the bedding and lapilli fabric orientations and; II: after correction "B" (see text). The expected declination and inclination for 57 Ma old rocks at this location is ~356°, -69°, therefore 102° of clockwise rotation (not accounting secular variation) is implied.

The well clustered low-blocking temperature component of the limestone cores does not restore to an orientation that can be easily interpreted. The *in situ* direction of 194.9°, -70.7° restores to 174.5°, -26.3° using correction A (above -Fig. A2.3.C) and 285.9°, -42.6° using correction B. Both of these vectors have inclinations that are shallow compared with the expected Palaeogene inclination for this site (-69°) and on this basis are not used.

If deposition of the limestone and flow of the basalt at this site are contemporaneous, we might expect to observe a thermal overprint in the magnetisation of the sedimentary rocks. The magnetic remanence component in the basalt begins demagnetisation at ~450°C and is removed by ~590°C. However, no consistent overprint of an orientation similar to the component from the basalt is apparent in the limestone cores, which are all demagnetised by ~560°C. Therefore, it seems that there is no consistent secondary thermal effect from eruption of the basalt onto/into the limestone. The same cannot be said for the physical disruption of limestone bedding and its inferred "primary/detrital" remanence (the high-blocking component), which can only be described as "random".

Appendix 2.4.

Narrows syncline (NS2 and WR)

Miocene Waima Formation siltstone is widely exposed within the Narrows Syncline, which forms a 3-sided trough-like structure in the Waima River valley. The different attitudes of bedding around this structure would be ideal to perform a fold test on palaeomagnetic data from the Waima Formation. Three sites were chosen on opposing limbs of the fold, but principal component analysis (PCA) of the siltstone from all but one horizon from all three sites either were not stable enough to yield a remanent magnetisation vector or yielded vectors that were too shallow to be regarded as primary components.

In particular, cores that were sampled across the interbedded boundary between Whalesback limestone and Waima Formation siltstone were generally weak and did not have stable demagnetisation characteristics (Fig. A2.4.A). For sites WR and NS2, this was the only part of the sequence sampled. For NS1, fresh outcrop of the muddier Waima Formation is well exposed along Waterfall Stream (unofficial name) and demagnetisation was more stable (see Appendix 2.5).

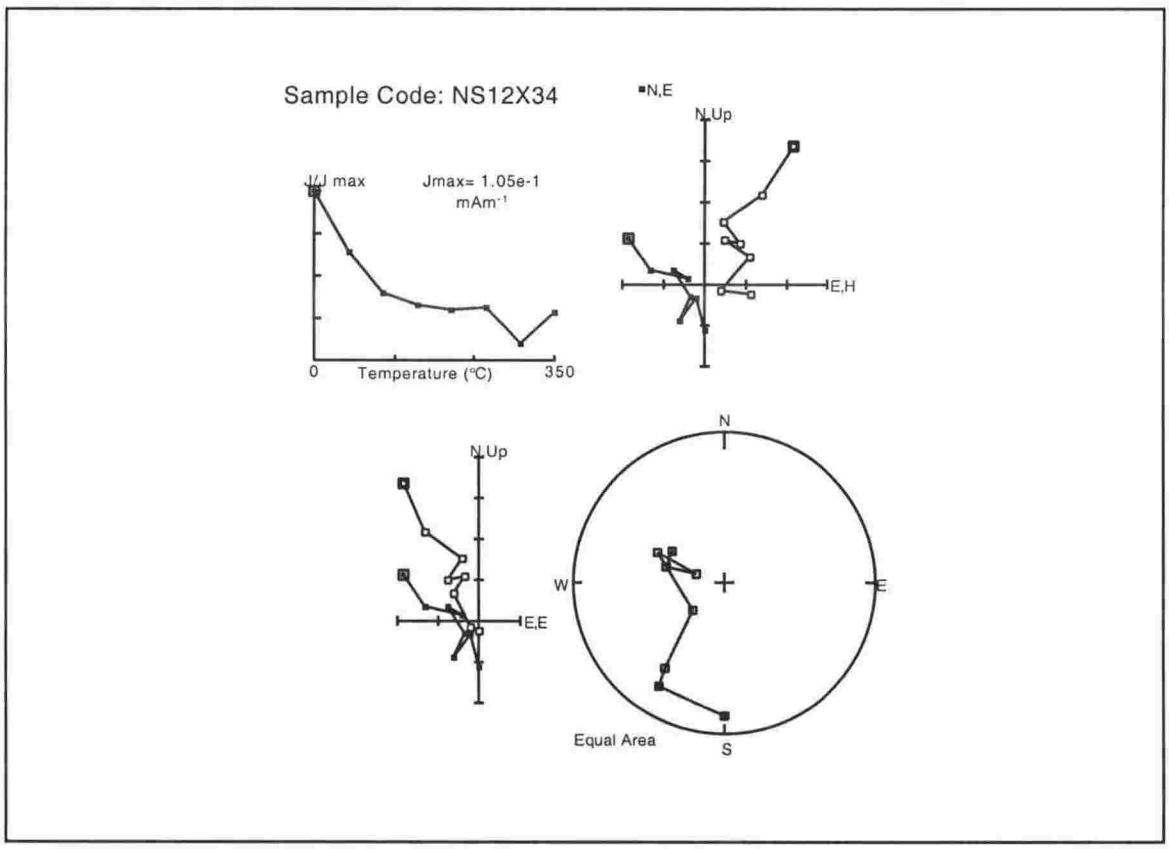

Figure A2.4.A. Demagnetisation plots for weakly magnetised calcareous siltstone from NS2. Locality WR displayed similar demagnetisation characteristics of weak samples. All plots are *in situ* coordinates. Conventions are the same as in Figure 2.8.2.

Appendix 2.5.

Narrows syncline (NS1)

Thermal and AF demagnetisation results of Whalesback limestone samples from NS1 (see Fig. 2.12) were not stable enough to isolate a primary magnetisation component. These samples were deemed unusable. Demagnetisation of cores from the muddier Waima Formation siltstone at NS1, however, reveals a fairly stable signal with a maximum NRM of around 5.3 mAm^{-1} (Fig. A2.5.A. I & II). Most samples were thermally demagnetised to ~350°C, at which point they displayed an increase in bulk magnetic susceptibility, indicating thermal alteration of the magnetic minerals. Many samples did not demagnetise toward the origin of the vector component diagram, suggesting an underlying component that was not isolated. AF demagnetisation of selected samples was not as successful in isolating the principal components as was thermal processing. Acquisition of IRM for the mudstone cores (Fig. A2.5.B.I) reached saturation at inducing field strengths of between 200 and 300 mT, indicating that the magnetic remanence carrier is a low coercivity ferrimagnetic mineral, such as magnetite.

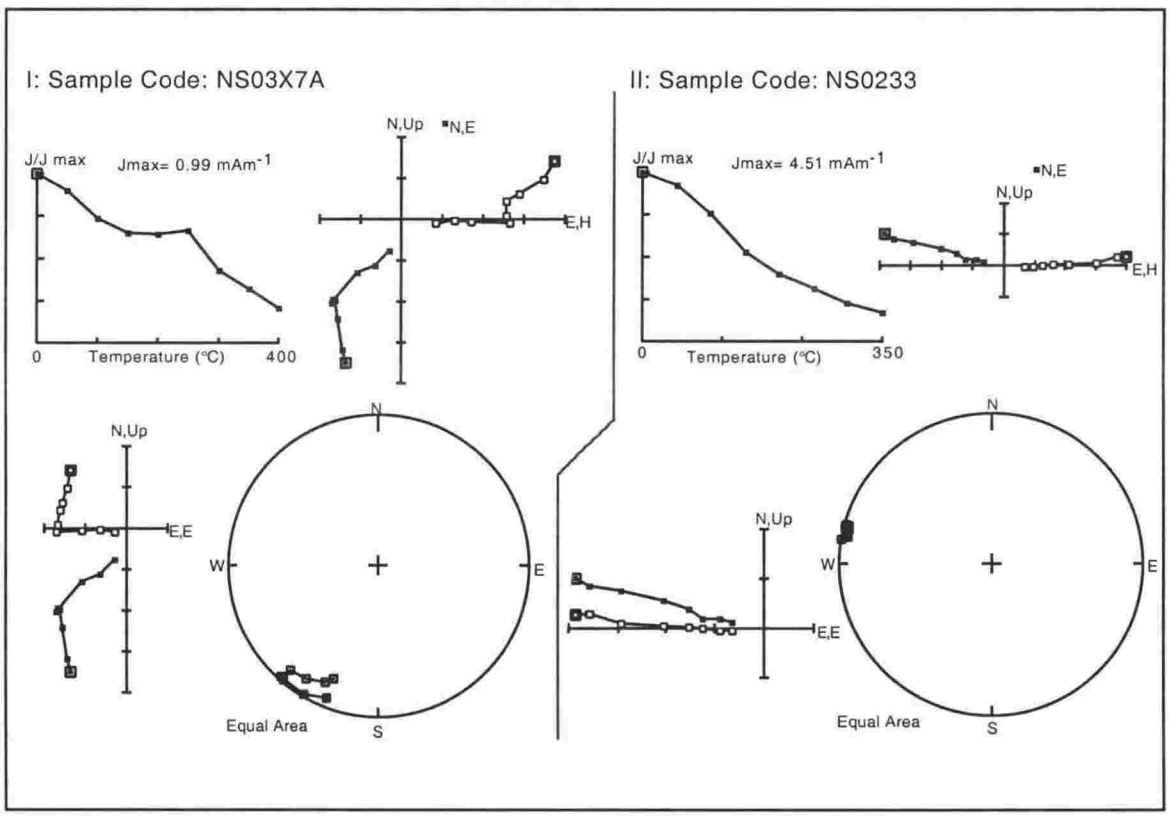

Figure A2.5.A. Examples of thermal demagnetisation of Waima Formation siltstone from locality NS-1 (Waterfall Stream); I: low-blocking temperature overprint (inferred to be "modern") cleans off by ~250°C, revealing an underlying component that resembles a primary magnetisation vector; II: no modern overprint is apparent for this sample and the entire remanence resembles a primary component. All plots are *in situ* and "primary" vectors are shallow, but the bedding correction does not satisfactorily produce final vectors that can easily be compared with the reference inclination (~ -65°). Conventions are the same as in Figure 2.8.2. See text for discussion.

Temperature dependent susceptibility experiments performed on mudstone samples (Fig. A2.5.C.) reveal an inflection at the approximate Curie temperature of magnetite (580°C) [Butler, 1992]. The maximum IRM (IRM_{max}) attained for this mudstone lithology is ~3 Am^{-1}. Compared with NRM values of ~1-10 mAm^{-1}, the IRM_{max} is strong, suggesting that the process of natural magnetisation in these rocks is inefficient and therefore probably detrital.

Appendix 2.5. -continued

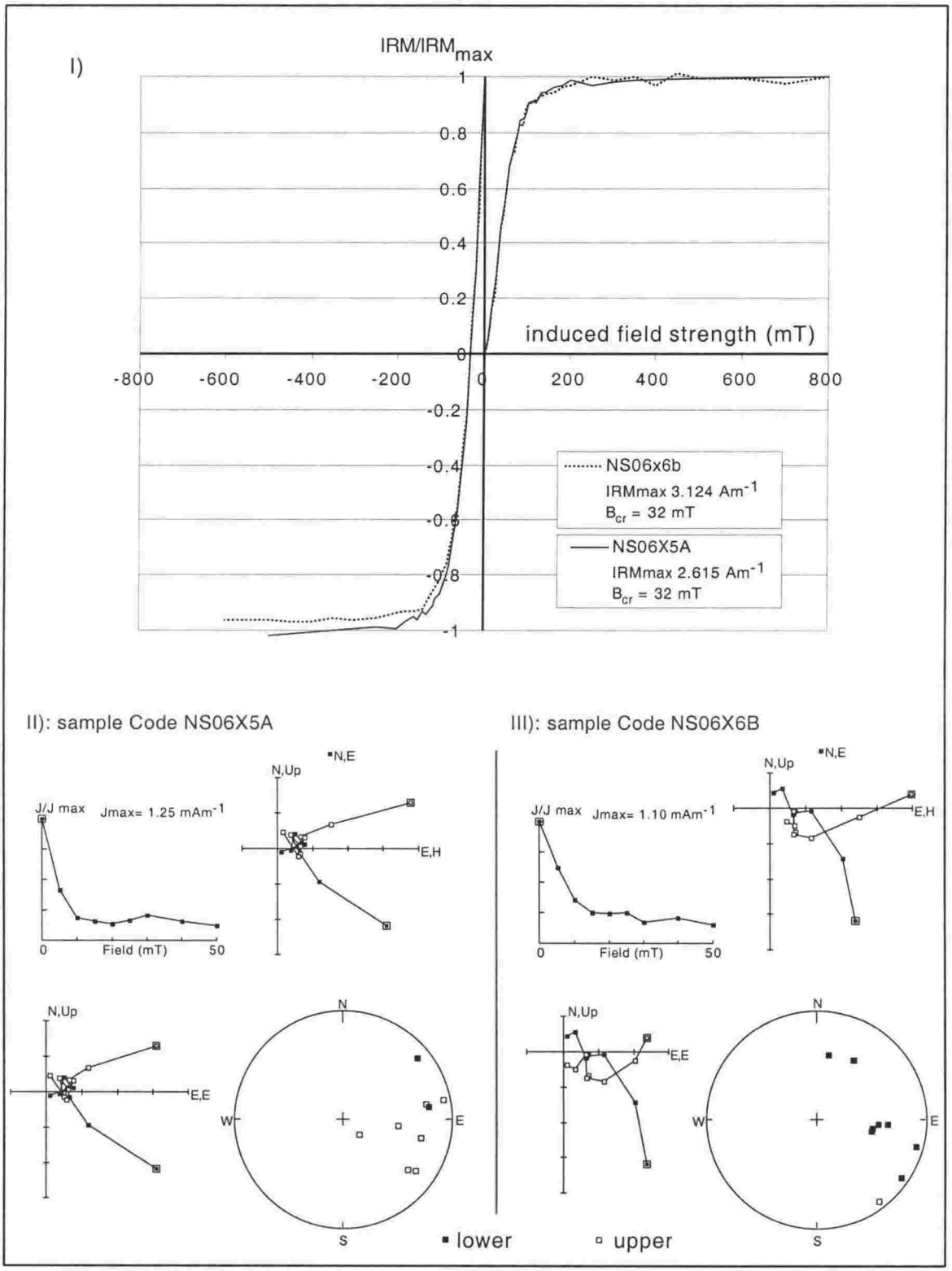

Figure A2.5.B.I: Isothermal remanent magnetisation (IRM) for 2 samples of Waima Formation siltstone from locality NS-1 (Waterfall Stream). Field saturation strength and coercivity values of remanence are typical of magnetite-bearing rocks; II & III: alternating field demagnetisation of NRM of the same samples as in A2.5.B. I. All Zijderveld plots are *in situ* coordinates. Conventions are the same as in Figure 2.8.2.

Appendix 2.5. -continued

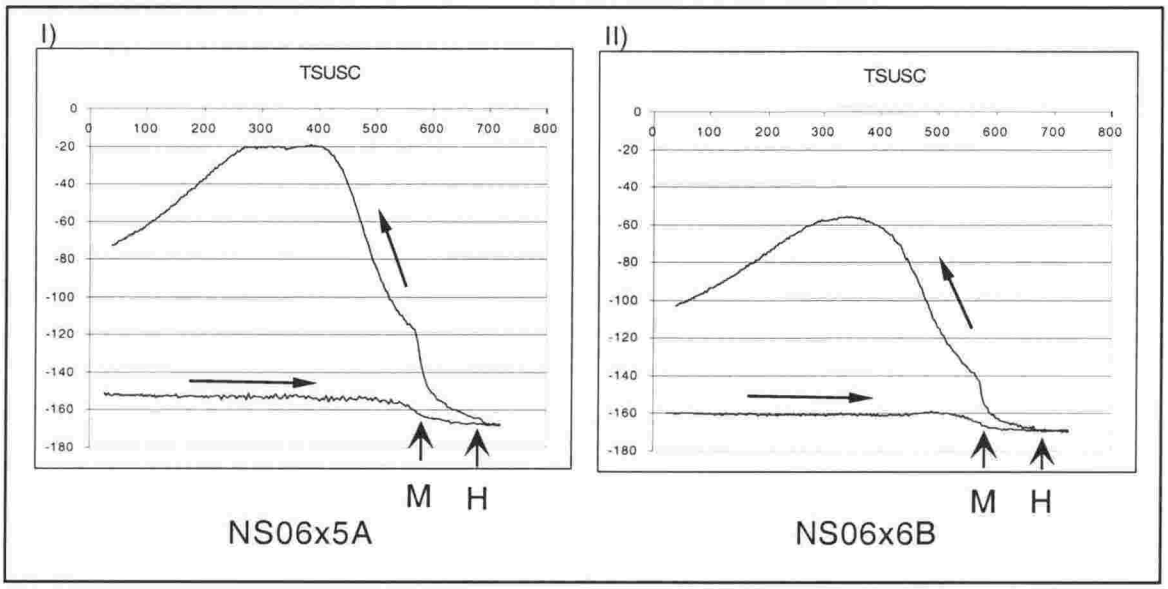

Figure A2.5.C. Temperature dependent susceptibility behaviour of samples NS06X5A (I) and NS06X6B (II) of Waima Formation siltstone from Waterfall Creek. Arrows on plots mark the Curie temperatures of magnetite (M; ~580°C) and haematite (H; ~680°C). Inflection points at ~580°C on heating suggest that magnetite is the magnetic remanence carrier, with no measurable haematite.

The structurally corrected inclinations of the inferred primary components of both normal and reverse polarity samples, where determined, are generally around 10-30°. This is much shallower than the expected ~65° for Early Miocene rocks of the Pacific Plate. Samples that underwent AF demagnetisation, where a primary vector was obtained, also yielded shallow inclinations. Samples from the same site are generally internally consistent, but most have considerably different mean directions from sites only a few metres above or below. The bedding orientation varies by only a few degrees between all sampled sites at Waterfall Creek, therefore structural correction cannot reduce the scatter.

Two sampled horizons at NS1 yielded inclinations close to the reference GAD field (sites N01 & N05). Site N01 consists of 4 samples (7 specimens), which all give reverse polarity magnetisation directions (Fig. A2.5.D.I), and site N05 consists of one stable normal sample, which is approximately antipodal to N01 (Fig. A2.5.D.II). The mean directions of the intervening sites, N02 - N04, mostly record shallow inclinations (Figs. A2.5.E & F), or directions that can be interpreted as recording a transitional field or a magnetic reversal (as do other sites at NS1). This justifies the rejection of other sites at NS1 that yield shallow inclinations and the tentative acceptance of sites N01 and N05 as recording a GAD field direction. The *in situ* magnetisation direction of these two sites is 272°, 27° and the structurally corrected vector is 302°, 54°. These data suggest a clockwise rotation of ~122°, which probably does not average out secular variation.

Appendix 2.5. -continued

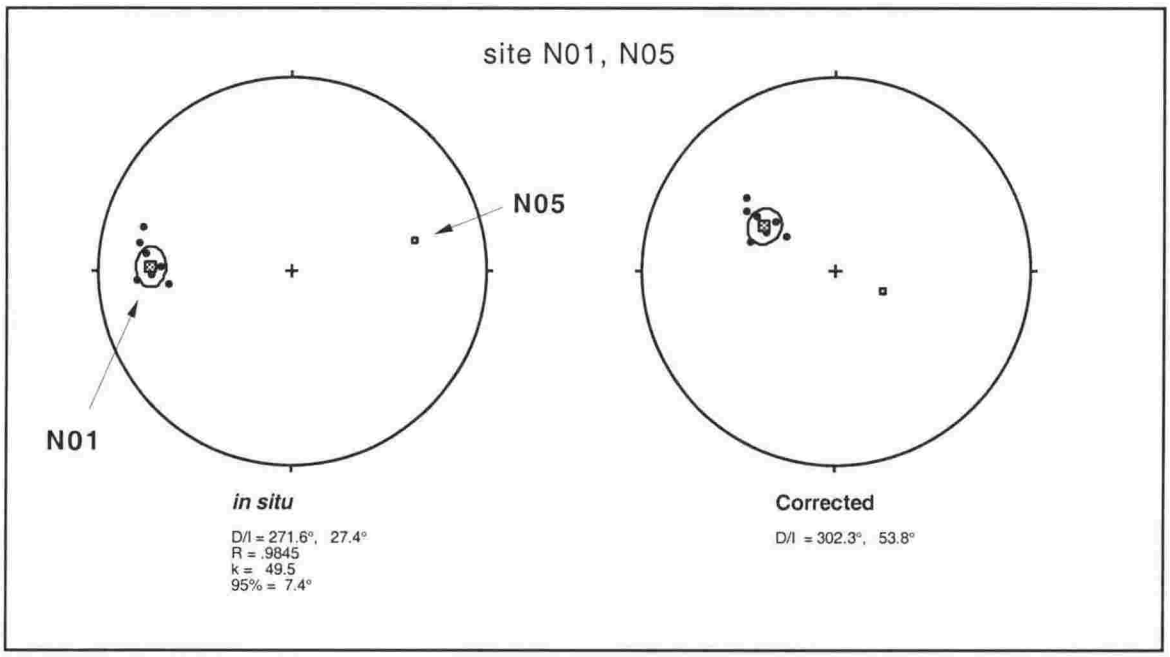

Figure A2.5.D. The only two sites (out of 12 that had stable demagnetisation characteristics) at Waterfall Stream that were not rejected on the grounds of shallow inclinations. The site vector from the 8 reverse polarity cores is 302°, 54°, but this average probably does not account for secular variation. The declination anomaly in these ~22 Ma rocks is 122°.

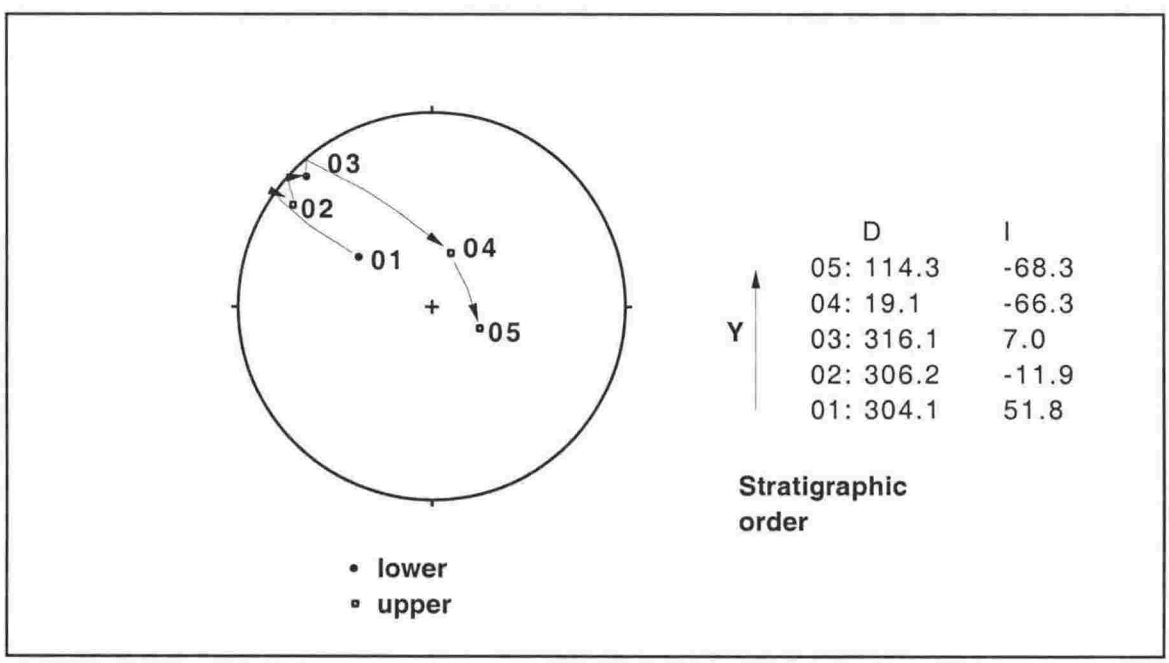

Figure A2.5.E. Declination and inclination of sites N201 - N205, downstream from the road at locality NS1. Sites 01 and 05 have inferred primary magnetisation directions that are nearly antipodal and which resemble the reference direction inclination (I = 65°), but intermediate sites do not. Most of the intermediate sites are shallow or can be interpreted as recording a transitional period during a magnetic field reversal.

Appendix 2.5. -continued

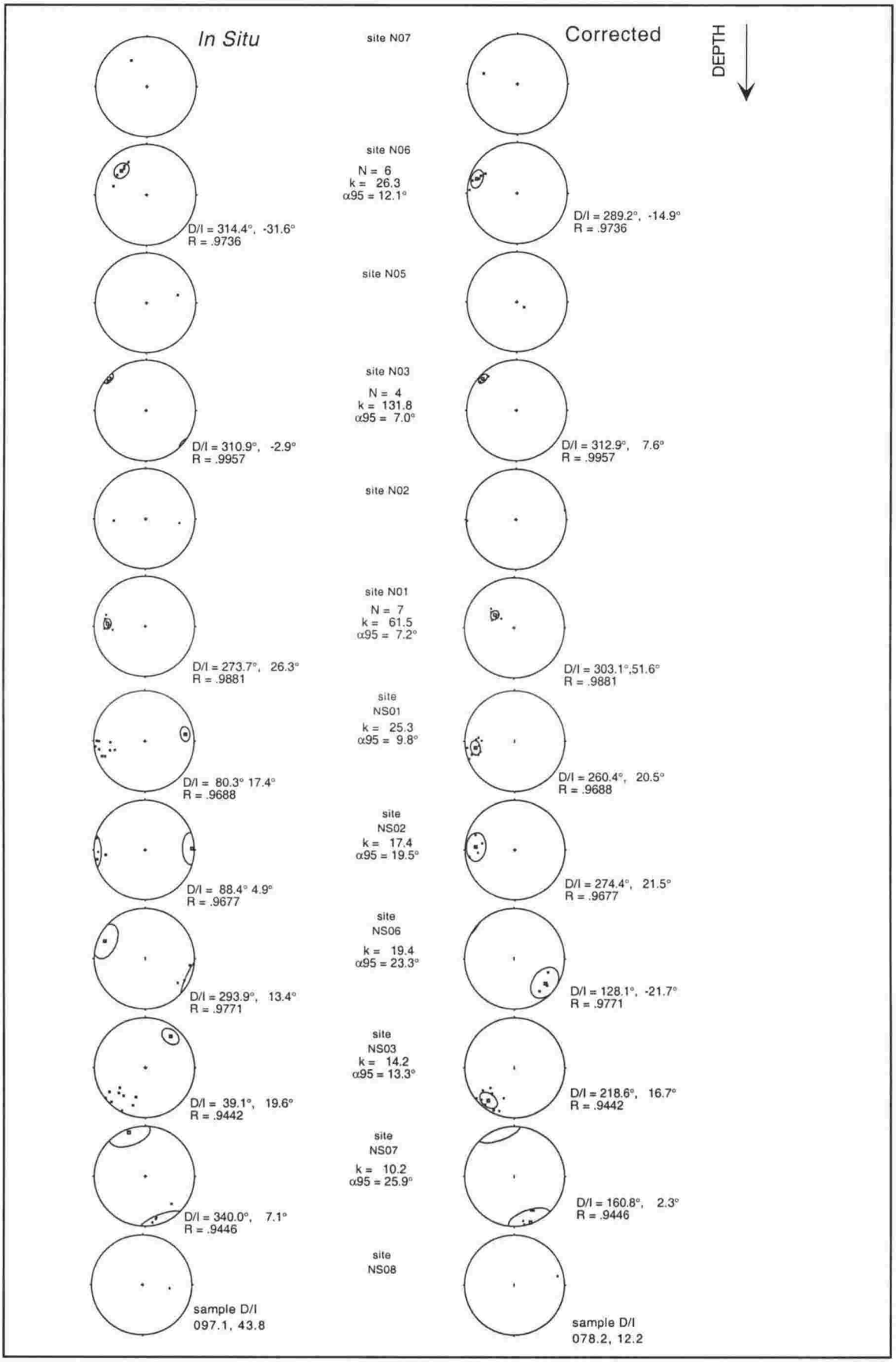

Figure A2.5.F. Mean directions of each site at Waterfall Creek are fairly well-grouped, but different from neighbouring horizons. Most of the data are shallow compared with the expected inclination of -65°.

Appendix 2.6.

Laings Nut (LN)

Laings Nut is a prominent hill formed by a structural culmination of Amuri Formation limestone at the southern end of the same NW-SE -trending erosion-resistant ridge on which the WH and WW palaeomagnetic sites lie. This site in Amuri Formation occupies a similar stratigraphic position as the Waima Hills limestone site (WH) and also the Woodside Creek sites WC1 [Vickery, 1994] and WC3 [this study], but is separated from the latter two locations by the Black Hill Fault. The Black Hill Fault is interpreted as part of the Early Miocene Flags Creek Fault System (FCFS) [see Chapter 3].

Five cores were sampled as part of an initial pilot study on the pink Amuri Formation limestone member which yielded 11 specimens. Demagnetisation results of limestone from Laings Nut showed similar characteristics to those outlined at the Waima Hills limestone site, with the exception of an additional, low temperature, modern overprint that is removed by ~200° C. NRM values are around 2-4 mA/m. However, only four specimens exhibited an underlying component that can be regarded as a true primary direction (Fig. A2.6.A), whereas others have shallow inclinations and are interpreted as "transitional" vectors that may represent major excursions of secular variation or periods during magnetic reversals. The 4 data points from this site are statistically unquantifiable, because the mean vector is steep and the 95% confidence cone includes the vertical. It can be seen, though, that the mean direction of the 4 data points with reasonable inclinations lies within the 95% confidence cone of the Waima Hills limestone site (WH locality; main text), located only 2 km to the north. It is therefore probable that these two sites have undergone a similar amount of vertical-axis rotation, but the LN site is not used due to the low sample density.

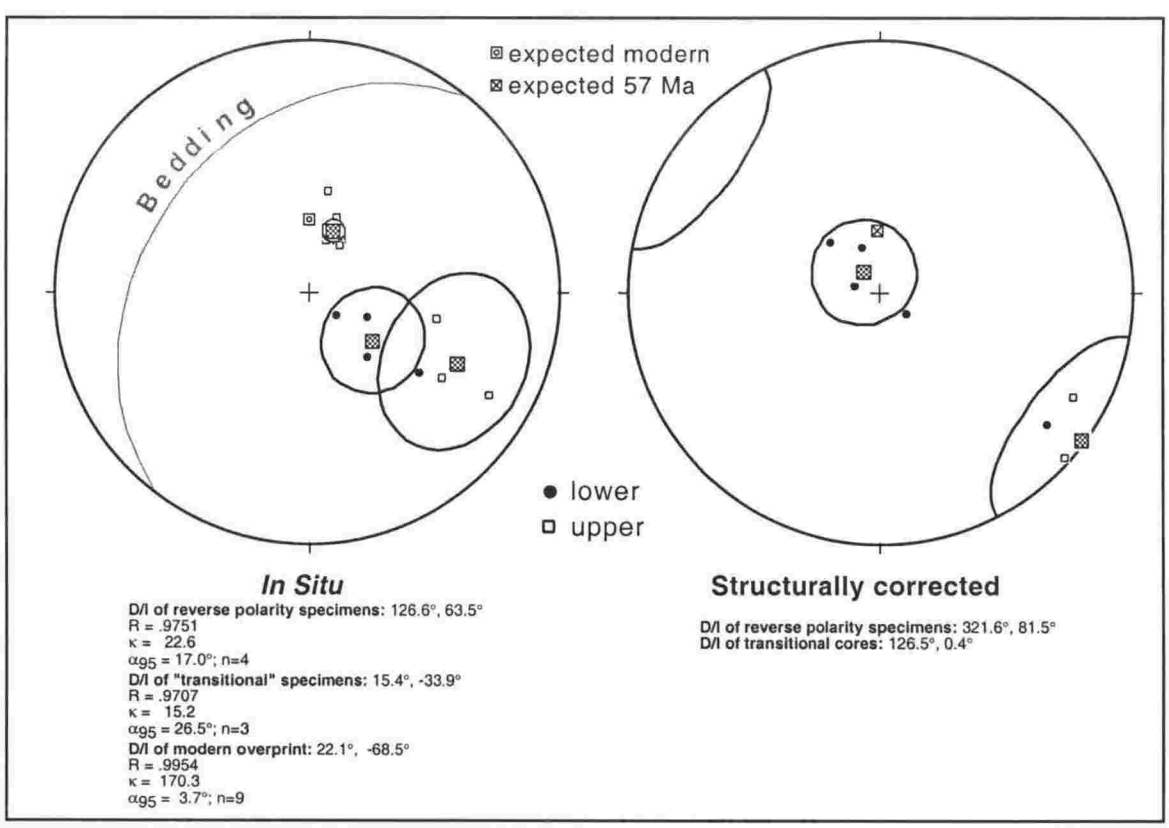

Figure A2.6.A. Plot of components from pink limestone at Laings Nut. Removal of a slightly rotated(?) modern overprint to temperatures of ~250°C leaves an underlying component that, when structurally corrected, is either steep and reverse polarity or shallow and in both hemispheres. This suggests the possibility of a systematic bias in the data, such as a third component of magnetisation that was not removed.

Appendix 2.7.

Woodside Member of Amuri Formation at Woodside Creek (WF)

The Woodside Member ("Woodside Formation" [Prebble, 1976]) of the Amuri Formation lies above "lower marl" [Strong et al., 1995] at the lower Woodside Gorge and consists of graded sandstone and mudstone beds on the order of 30-cm to 2-m-thick, often with flute casts on sandstone bases that indicate a NE flow direction. The lower contact is not satisfactorily exposed to deduce its relationship with underlying members of the Amuri Formation, but in the north of the study area, turbidites are interbedded with Amuri–type marl and limestone. The Woodside member includes gabbroic units up to 60-m-thick that are generally parallel to sedimentary strata and interpreted as either sills or flows. The stratigraphic top of the Woodside Formation is not seen anywhere in the study area, due to its truncation by the Flags Creek Fault.

Five cores were drilled from turbidite beds at stream level over a stratigraphic distance of 2.1 m. Grading of sandstone/mudstone couplets indicate that these strata are upright. This location is probably similar in age to the Waima Hills site of the same lithology (WW) as it occupies a similar stratigraphic position.

NRM of the siltstone from Woodside Gorge was weak, being around 4-7 mAm^{-1}. Demagnetisation of samples was relatively stable to approximately 450°C, where an increase in bulk magnetic susceptibility accompanied by a distinct change in colour, indicated thermal alteration. A modern-day geomagnetic field overprint (001°, -64° for n=11; α_{95} = 2.1°) is dominant until about 250°C (Fig. A2.7.A, A2.7.B).

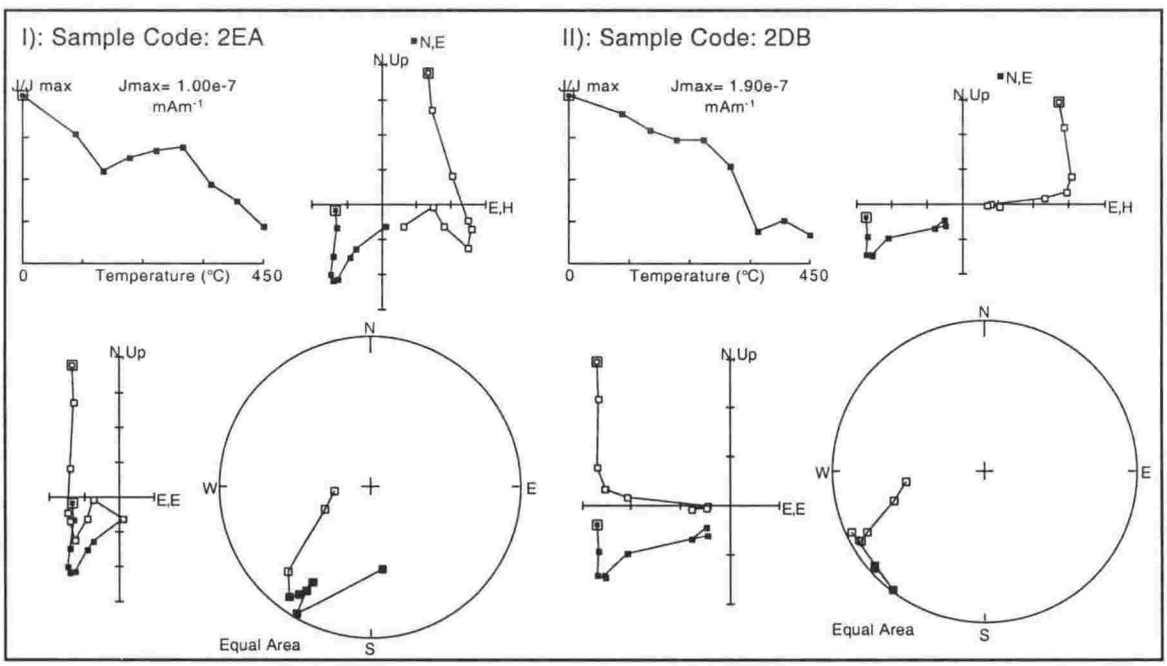

Figure A2.7.A. Examples of thermal demagnetisation of the siltstone/sandstone cores from the Woodside Formation at Woodside Creek. A modern-field component is clearly removed up to ~250°C, where an underlying component is revealed. It is unclear whether this component is a detrital remanence or a later thermal overprint that has been clockwise-rotated by ~35°. All plots are *in situ* coordinates. Conventions are the same as in Figure 2.8.2.

Appendix 2.7. -continued.

Demagnetisation of the underlying component was erratic, but a general clustering of data is mostly constrained by a few trustworthy points. All samples but one exhibited reverse polarity magnetisation; the exception is shallow and is interpreted as transitional. The structurally corrected mean vector implies a clockwise rotation of these Eocene rocks of 32° (Fig. A2.7.B). As Palaeocene Amuri Formation only ~50 m stratigraphically below exhibits statistically well constrained clockwise rotations of 120° – 140°, the ~90° less rotation at WF is interpreted as a remagnetisation direction and is therefore not used for tectonic interpretations. This overprinting may have occurred as a result of contact metamorphism from emplacement of a nearby gabbro unit, which is highly crystalline and probably a sill. The age of emplacement is not known.

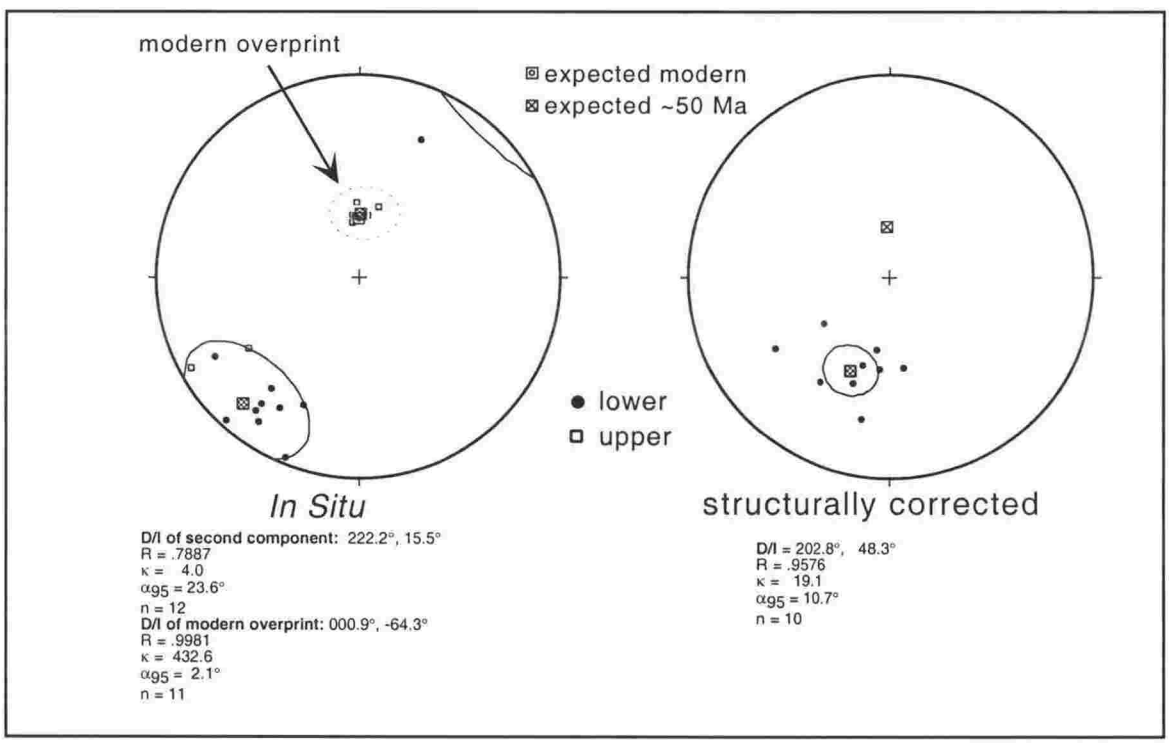

Figure A2.7.B. Uncorrected (above left) and corrected (above right; two cores rejected) site mean vector for WF samples. An extremely well clustered secondary component ($\alpha_{95} = 2.1°$) is indistinguishable from a modern geomagnetic field and attests to the magnetic softness of this lithology. This suggests that the underlying component may also be an overprint.

Appendix 3

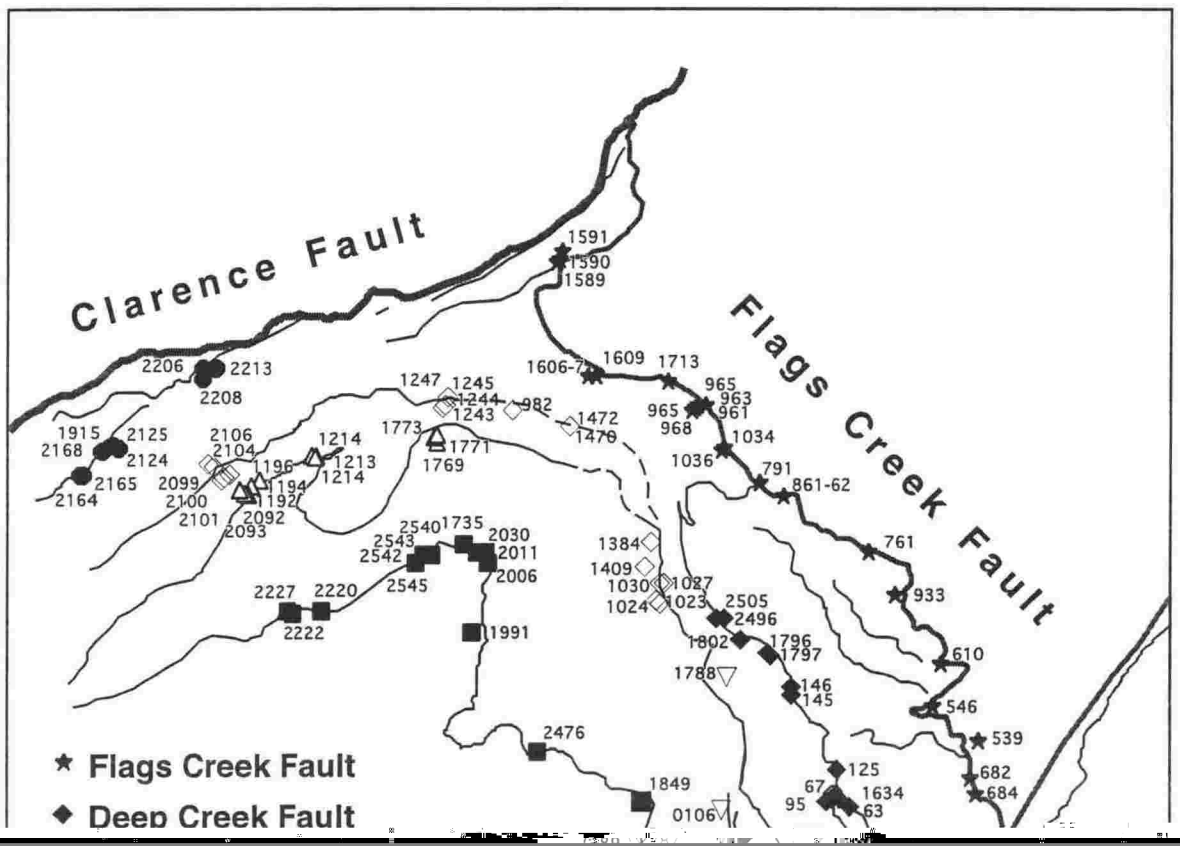
Clarence Fault
Flags Creek Fault
★ Flags Creek Fault
◆ Deep Creek Fault
1591
1590
1589
1609
1713
965
963
961
968
1034
1036
791
861-62
761
933
610
546
539
682
684
1606-7
1247
1245
1244
1243
982
1472
1470
1773
1771
1769
1214
1213
1214
1196
1194
1192
2106
2104
2125
2124
2168
1915
2165
2164
2099
2100
2101
2092
2093
2206
2213
2208
2540
1735
2543
2542
2030
2011
2006
2545
2227
2220
2222
1991
1384
1409
1030
1027
1024
1023
2505
2496
1802
1796
1797
1788
146
145
2476
1849
0106
125
67
1634
95
63

Box Stream Fault

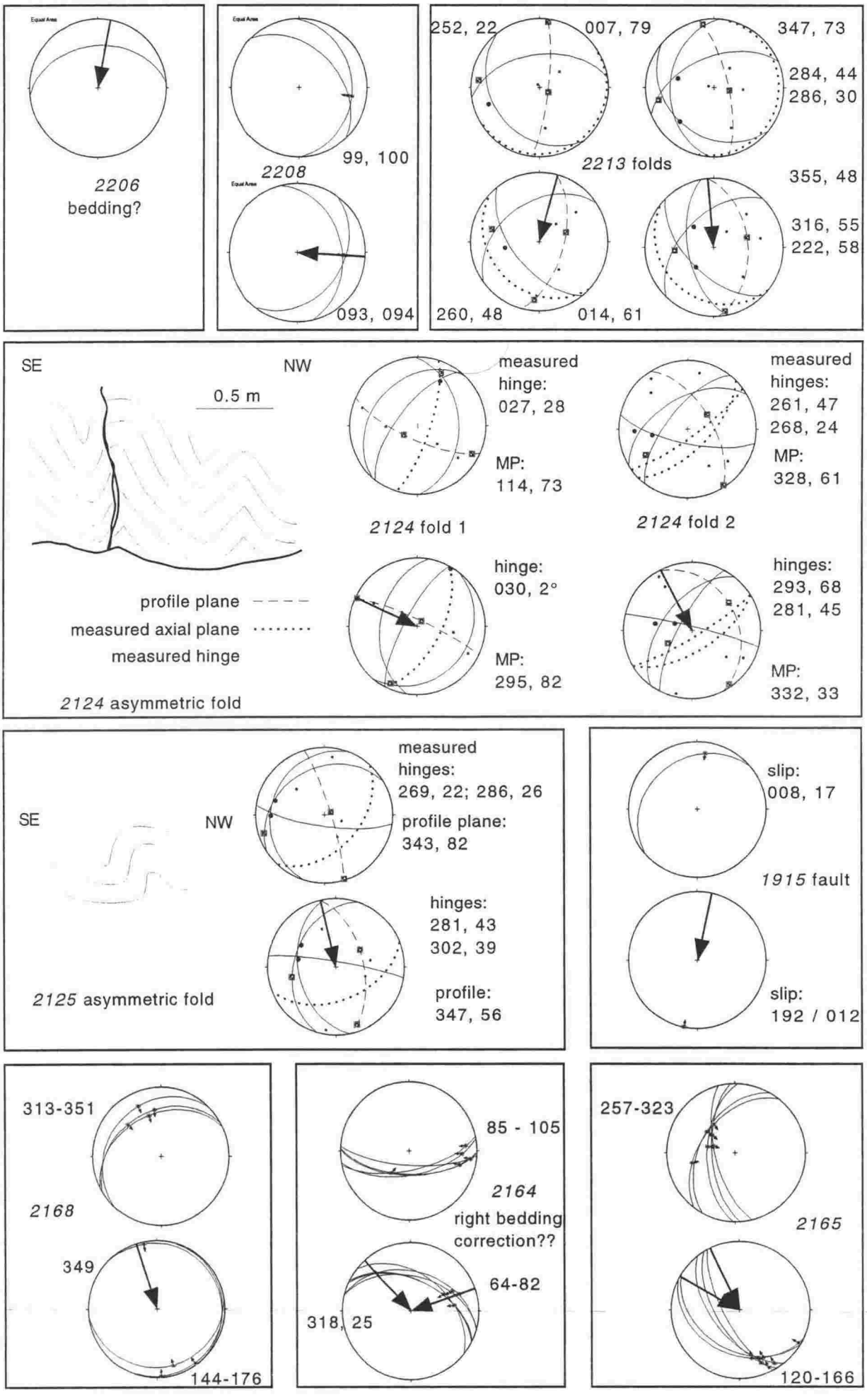

Waima Fault -southwest

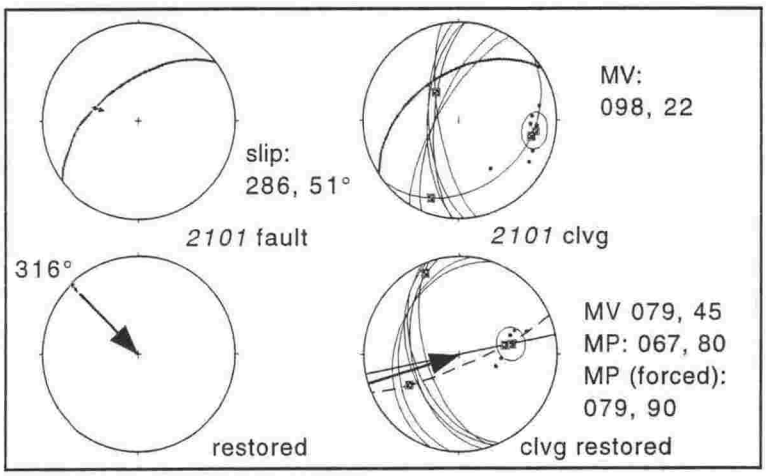

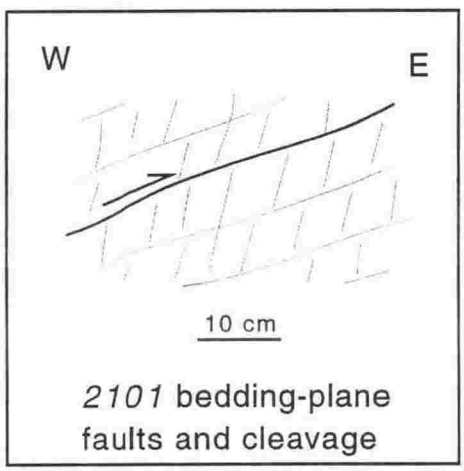

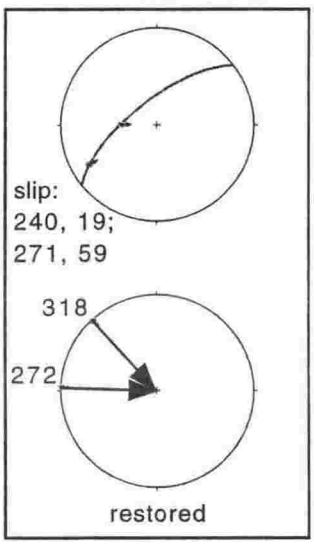

2100 two faults

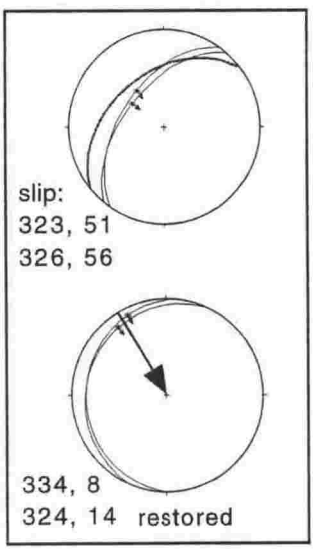

2104 faults

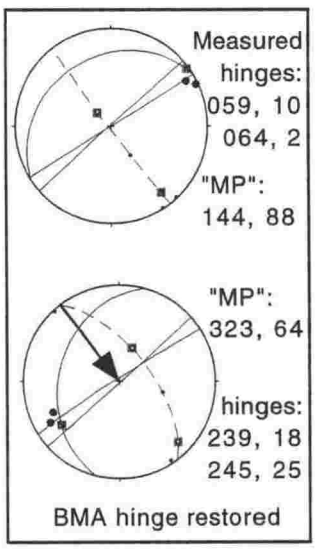

2106 fold

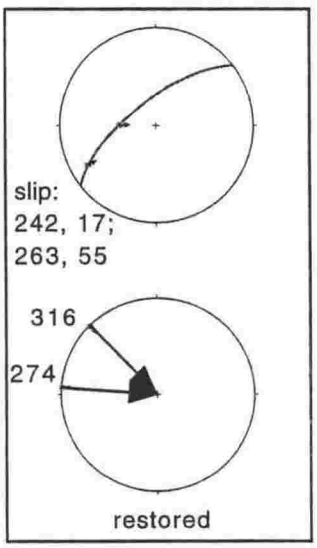

2099 two faults

Waima Fault -northern

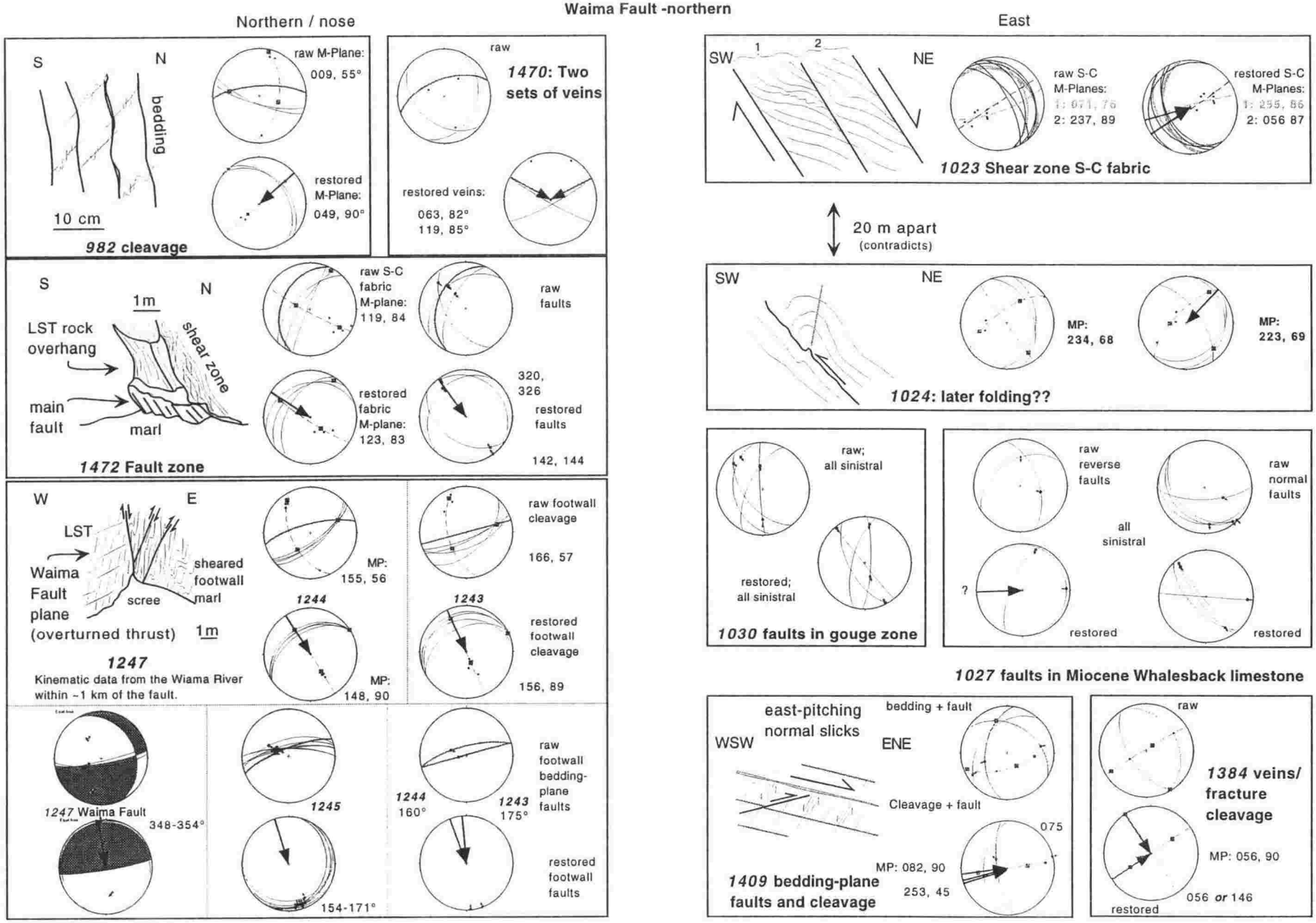

Brian Boru
-Waima Faults

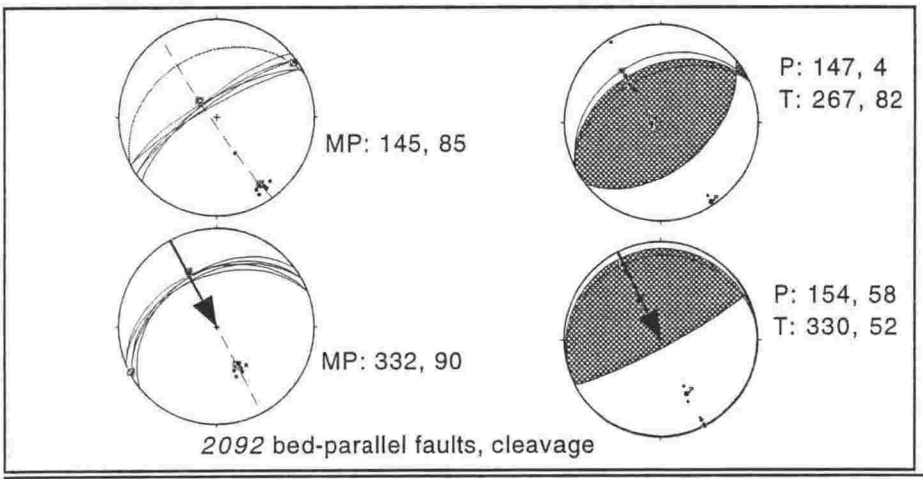

2092 bed-parallel faults, cleavage

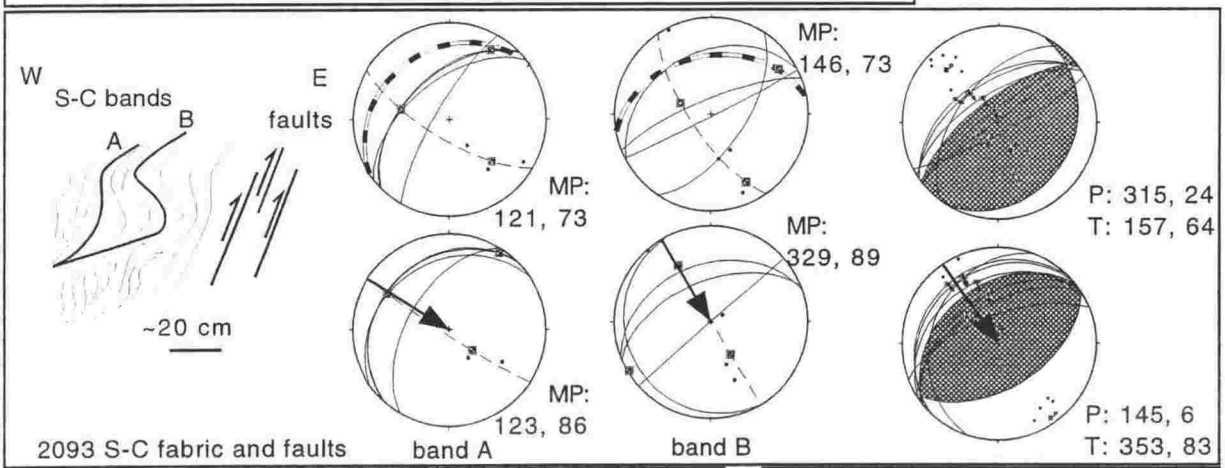

2093 S-C fabric and faults band A band B

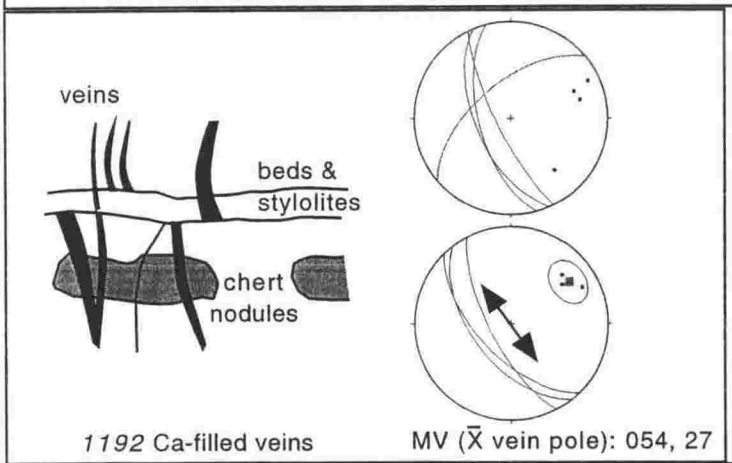

1192 Ca-filled veins MV ($\bar{X}$ vein pole): 054, 27

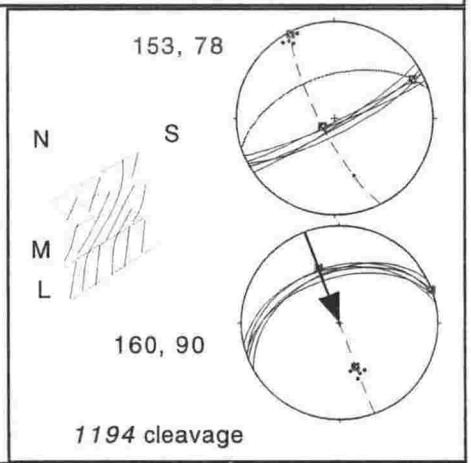

1194 cleavage

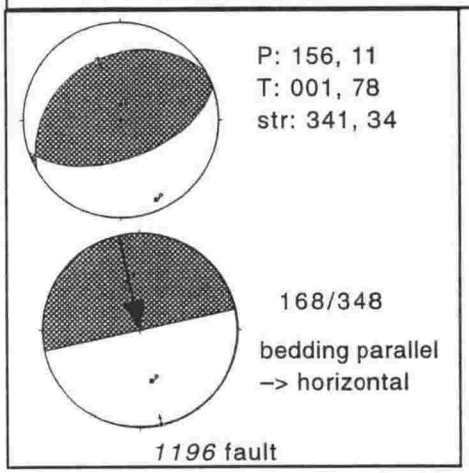

1196 fault

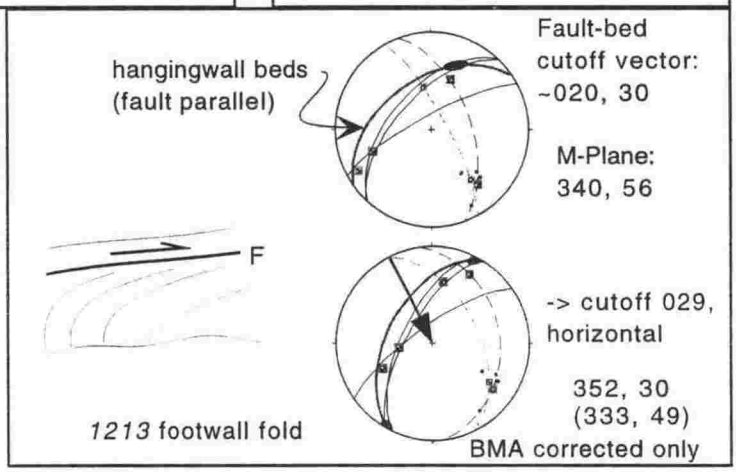

1213 footwall fold

Brian Boru Fault -2

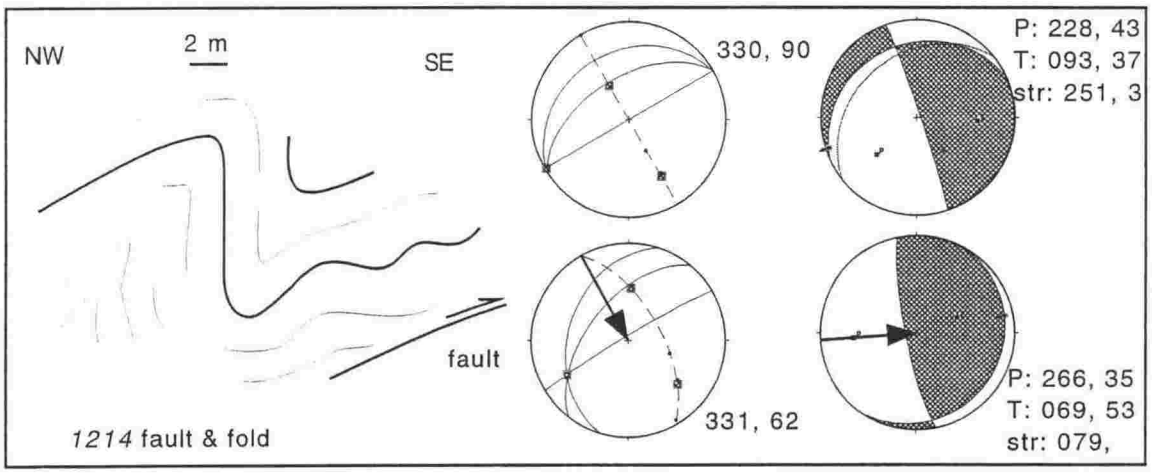

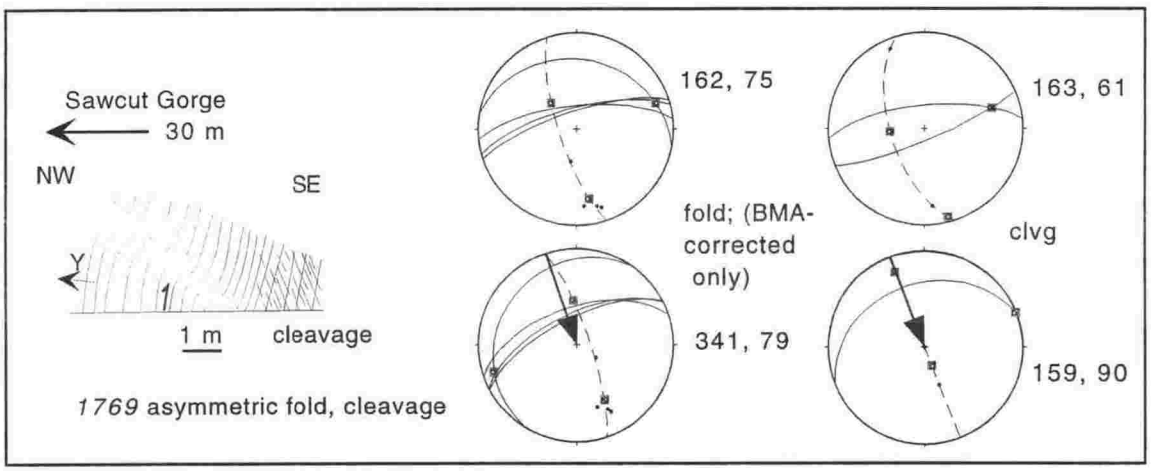

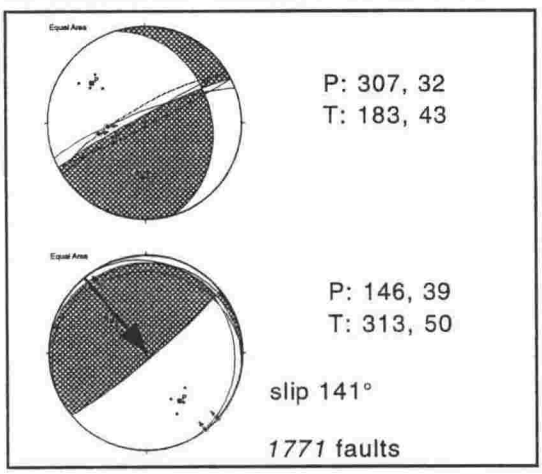

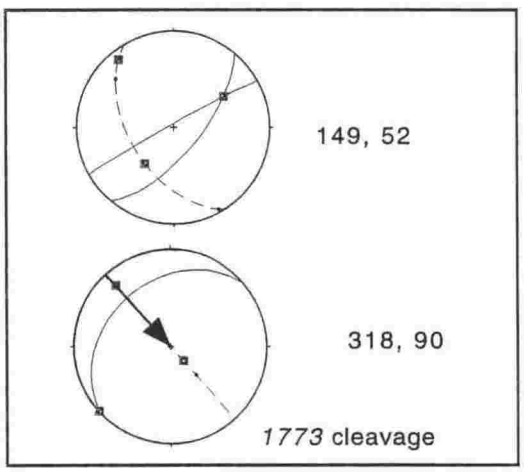

Ben More Fault

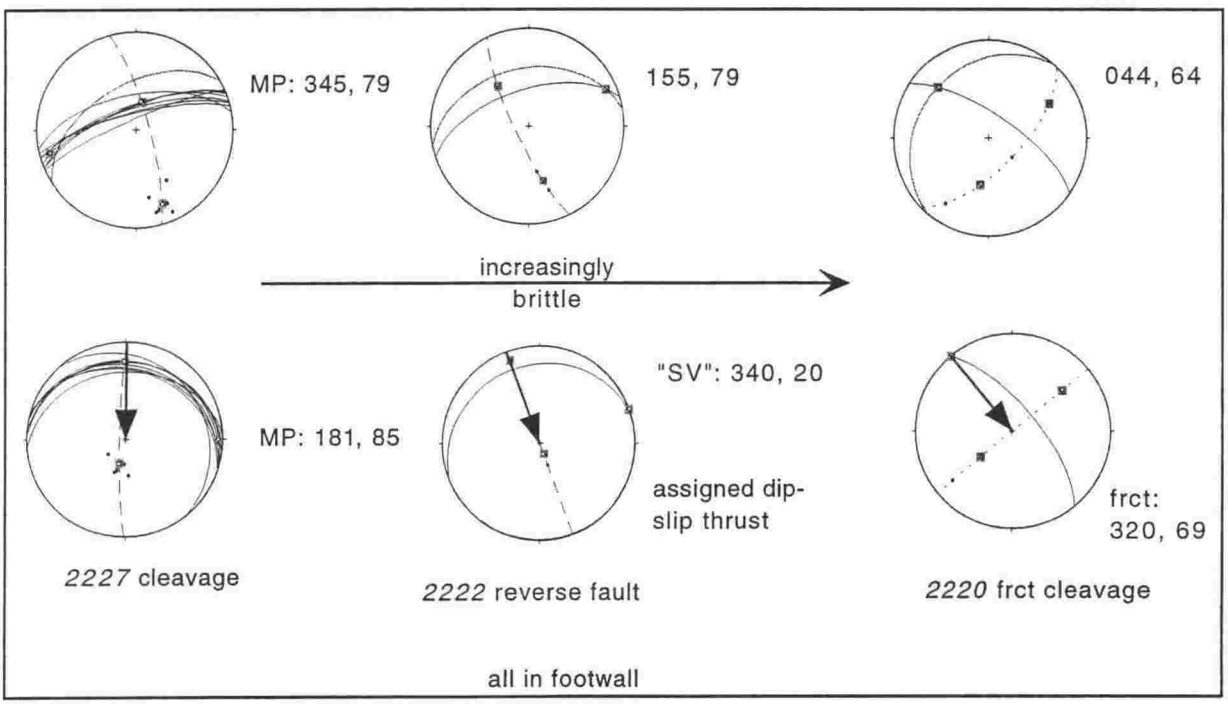

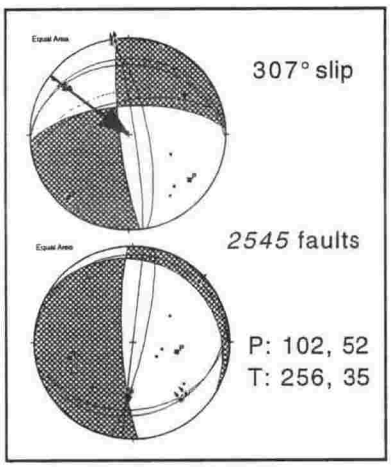

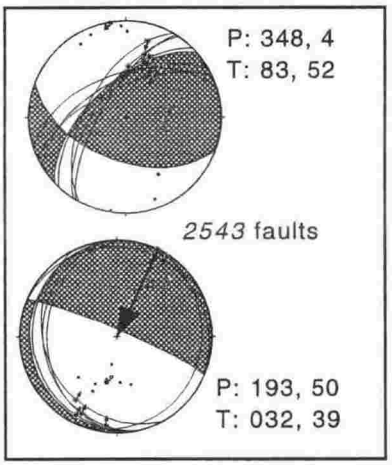

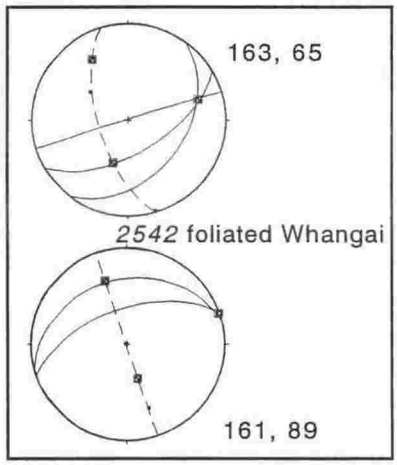

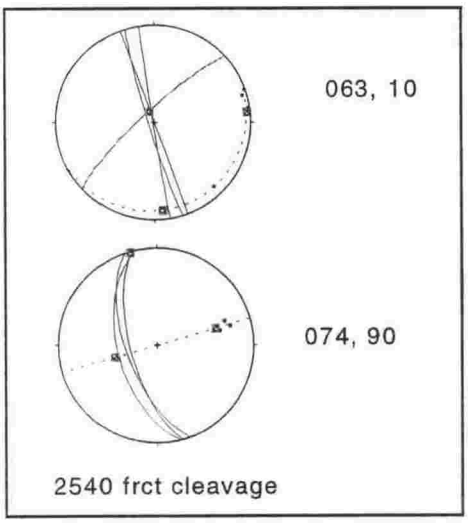

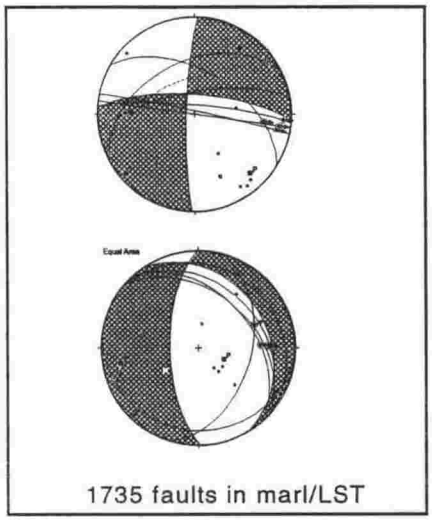

Ben More Fault -2

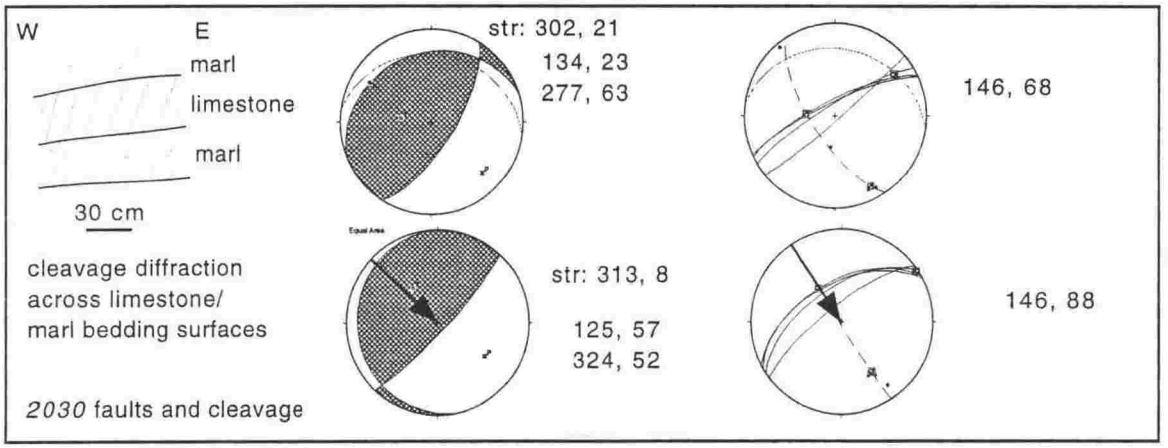

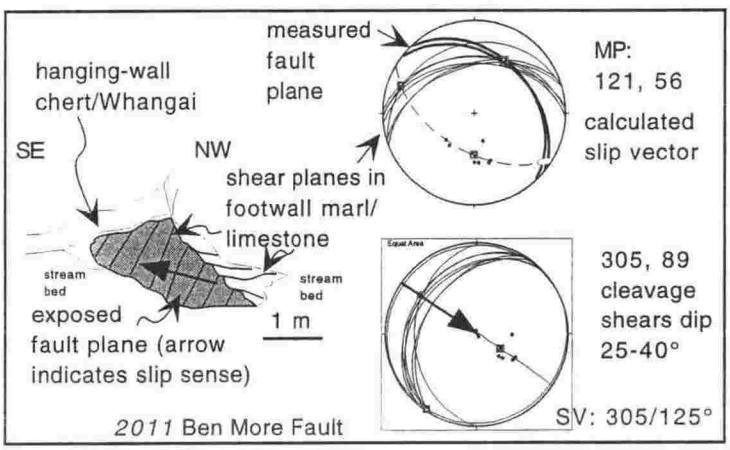

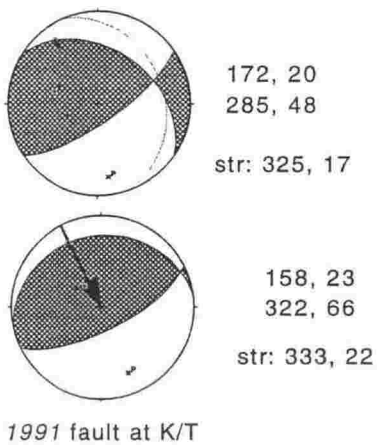

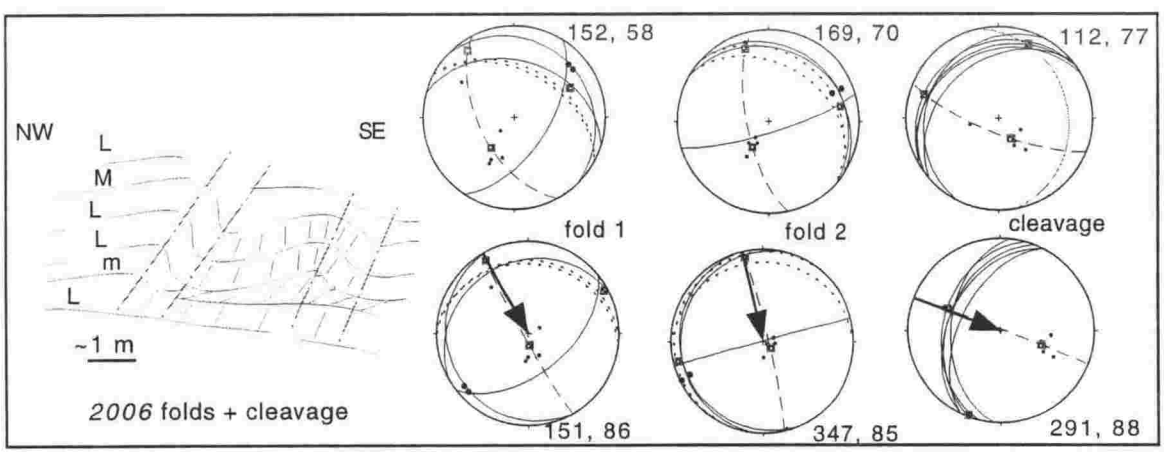

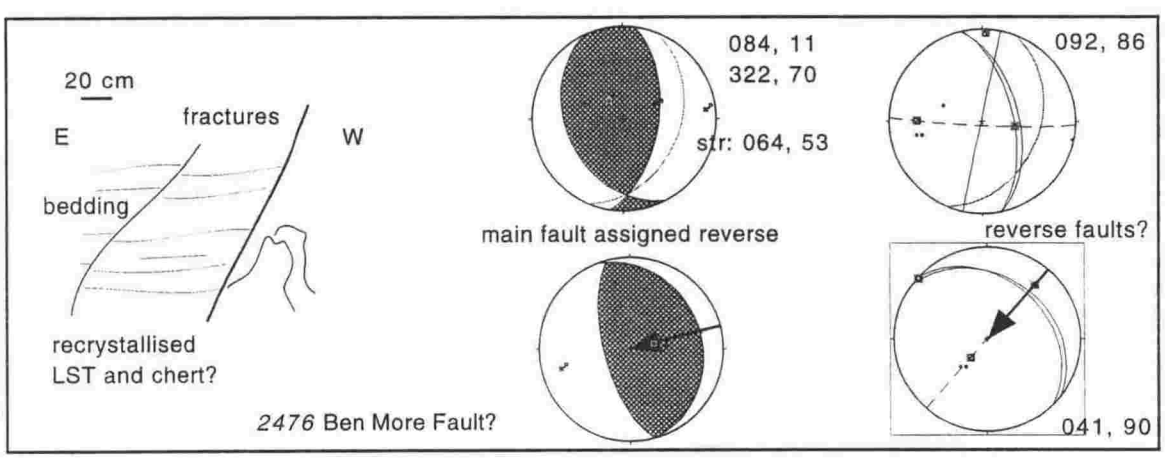

Ben More Fault -3

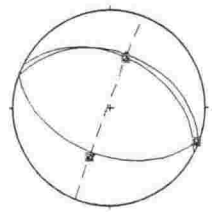

201, 88

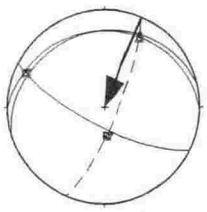

023, 78

BMA corrected only

1849 medium-scale fold

NE

SW

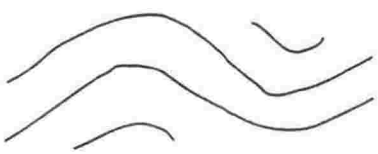

2.5 m

192 macro-fold

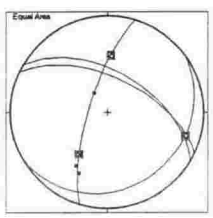

197, 74

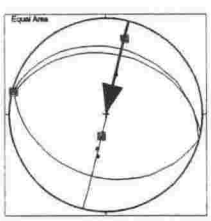

014, 89

BMA corrected only

Tirohanga Fault

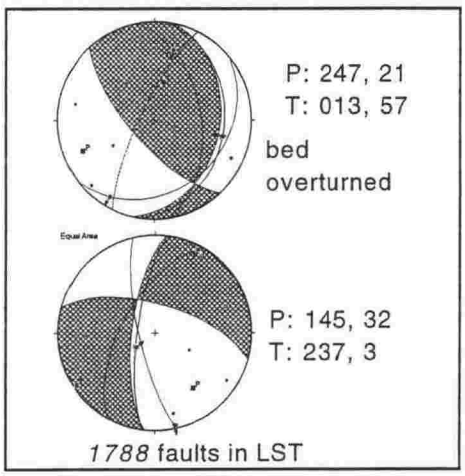

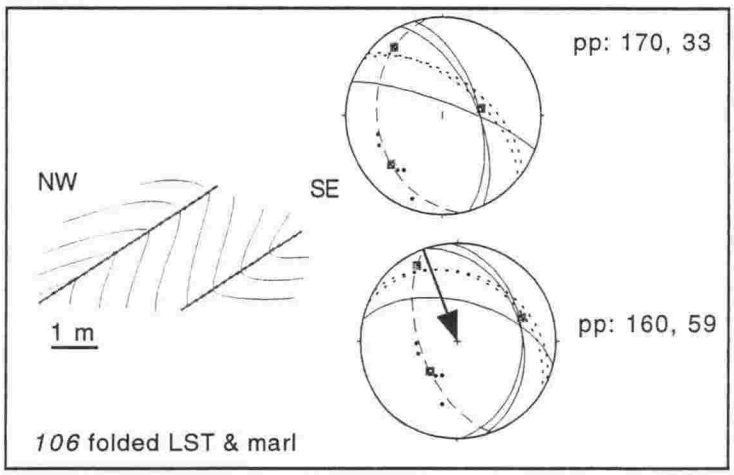

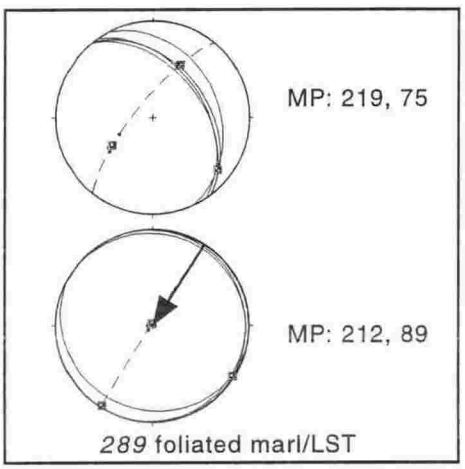

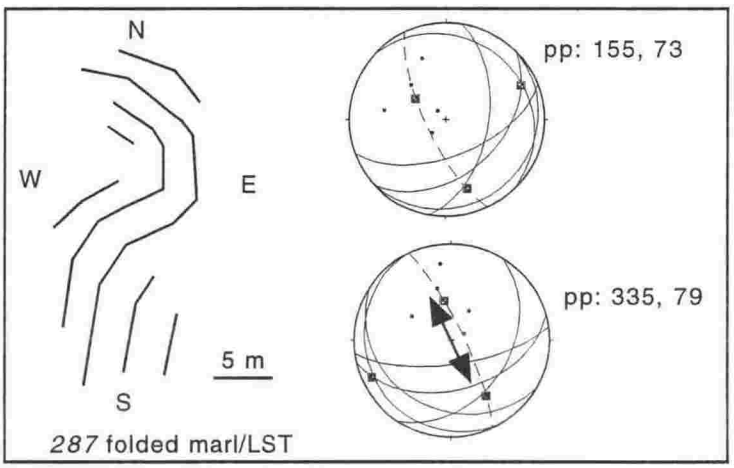

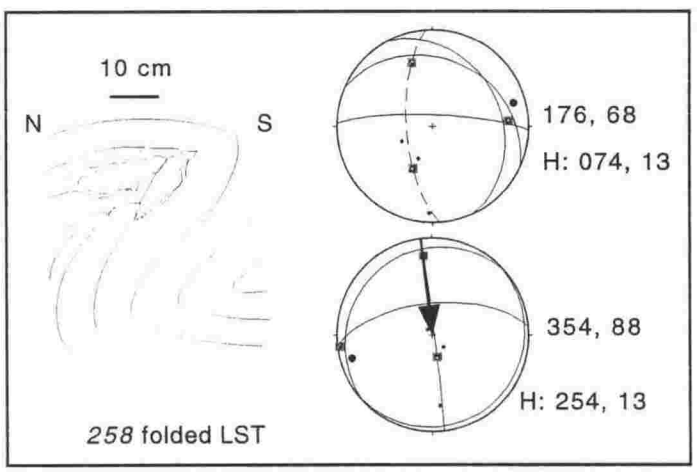

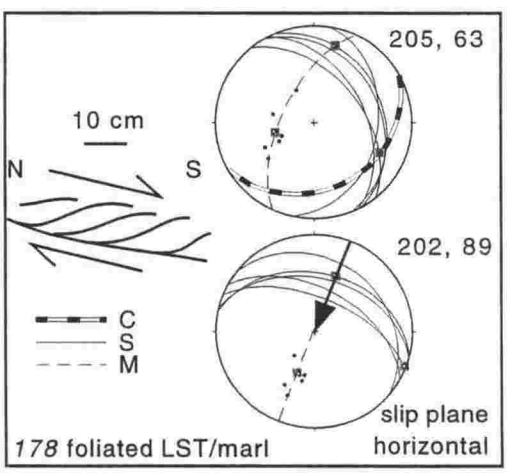

Deep Creek Fault

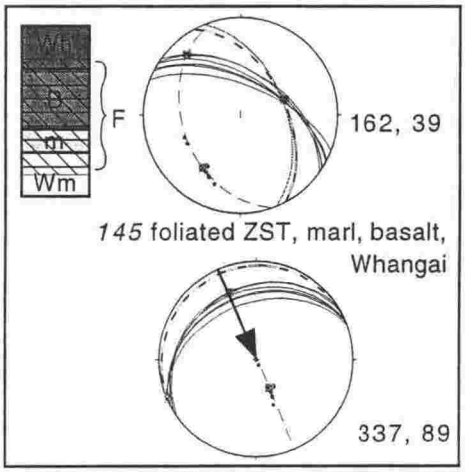

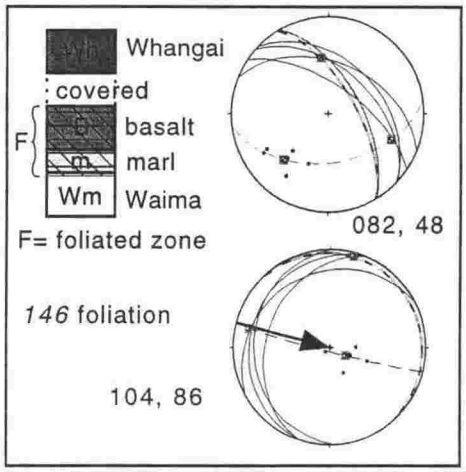

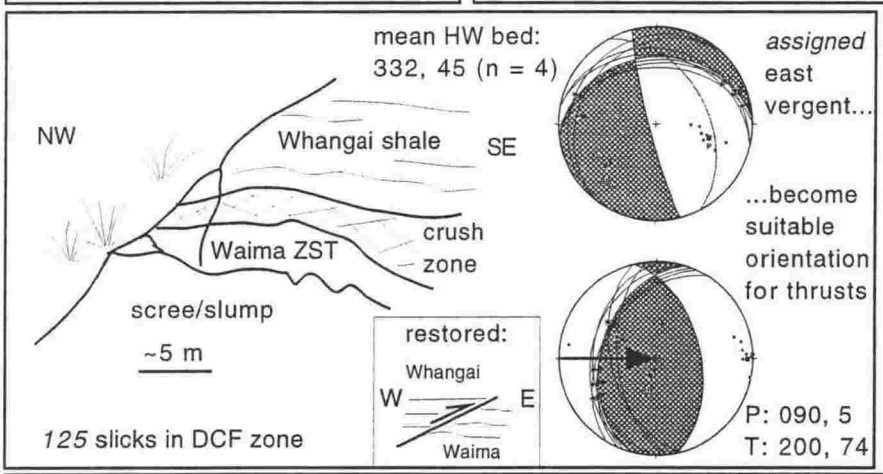

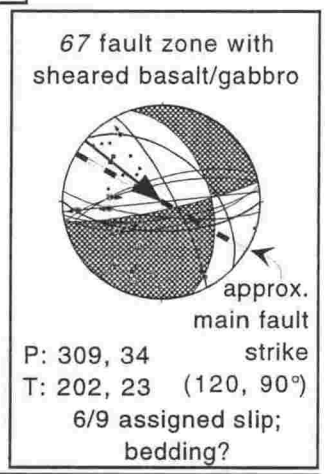

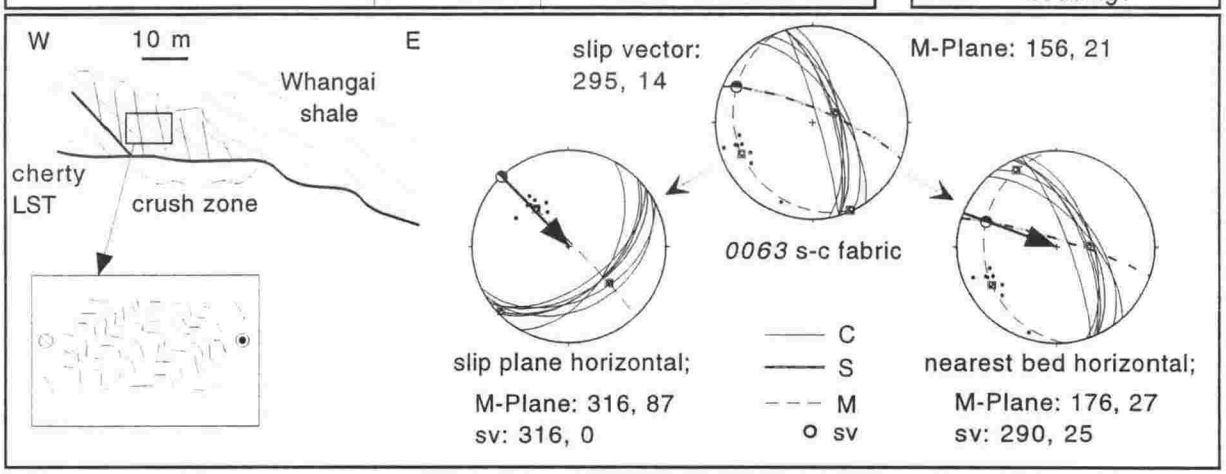

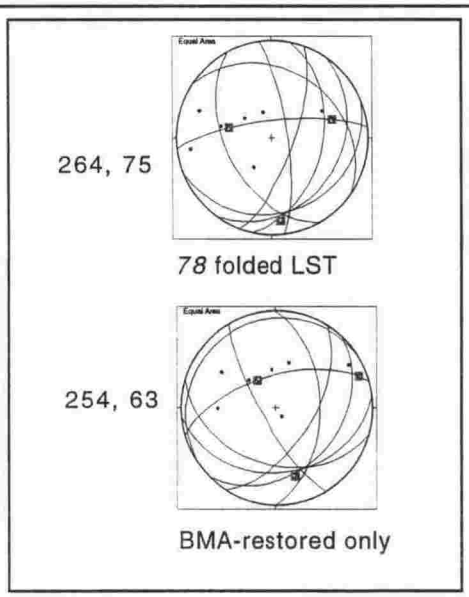

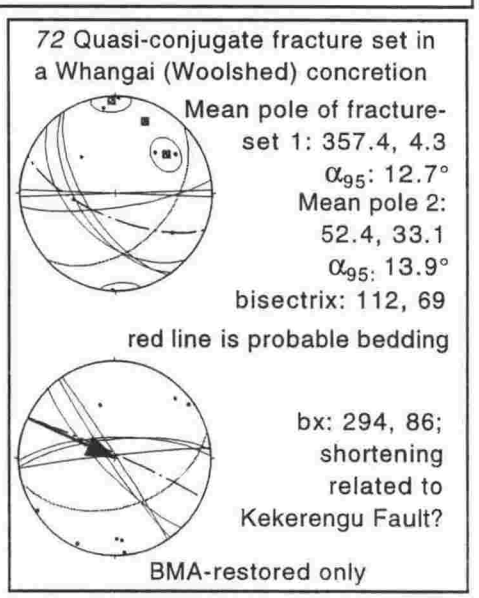

Deep Creek Fault -2

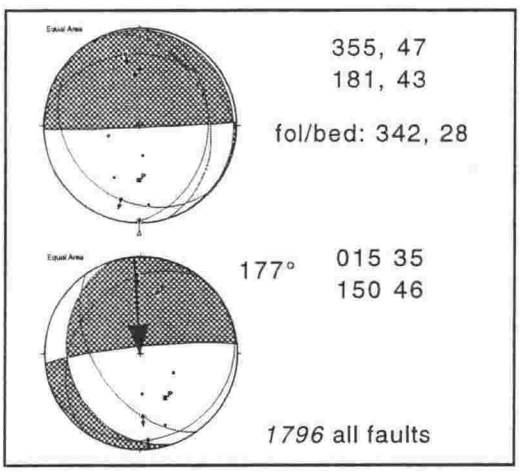

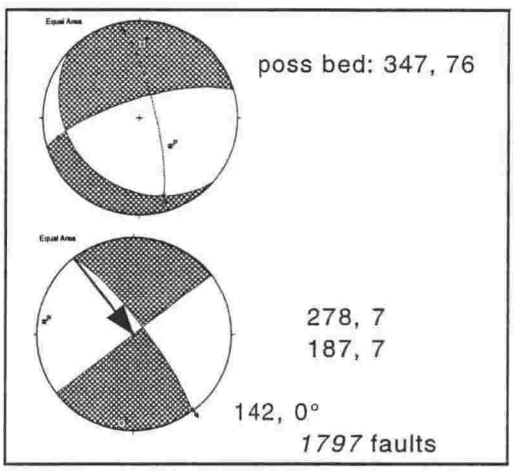

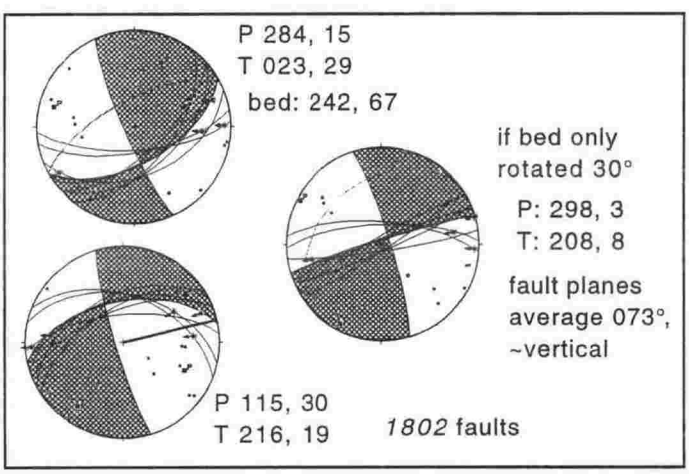

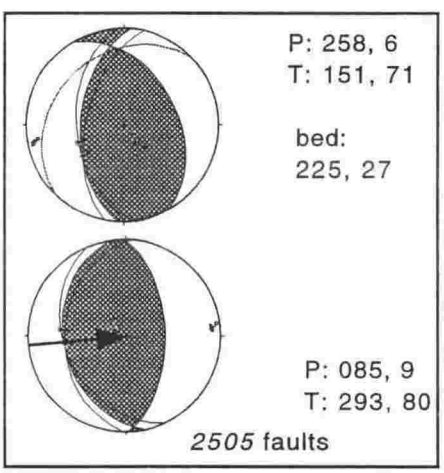

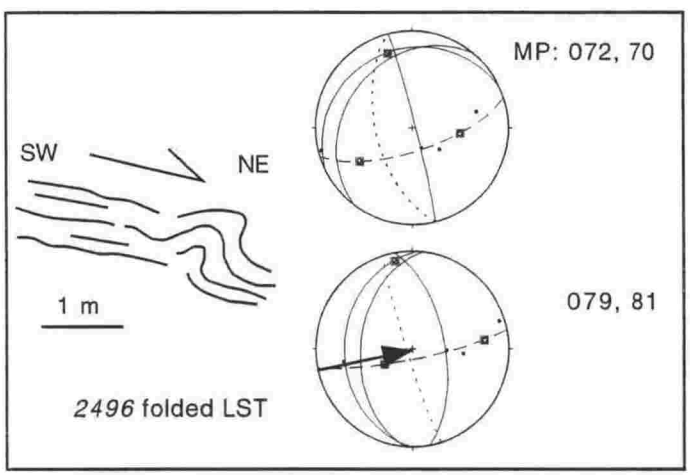

Deep Creek Fault -3

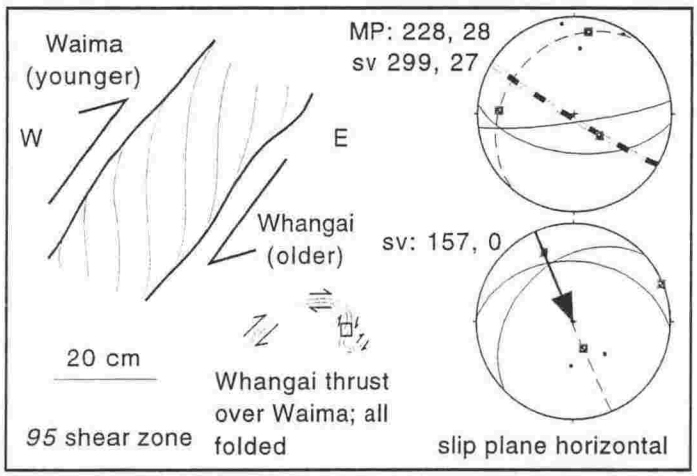

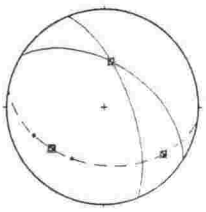
MP: 009, 51

0445 folded Waima

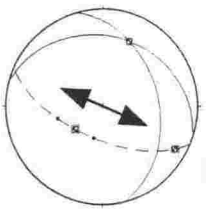
MP: 113, 62

BMA restored only

075, 74

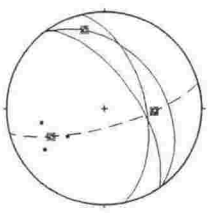

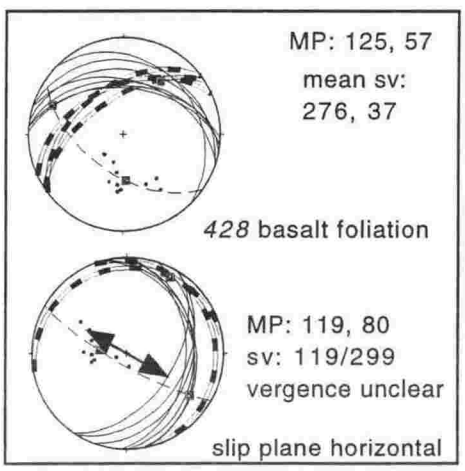

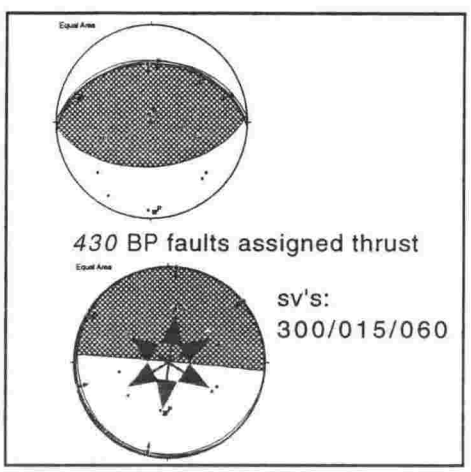

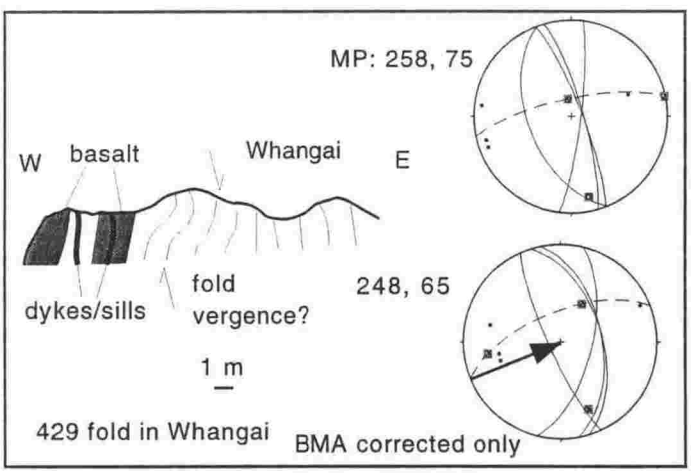

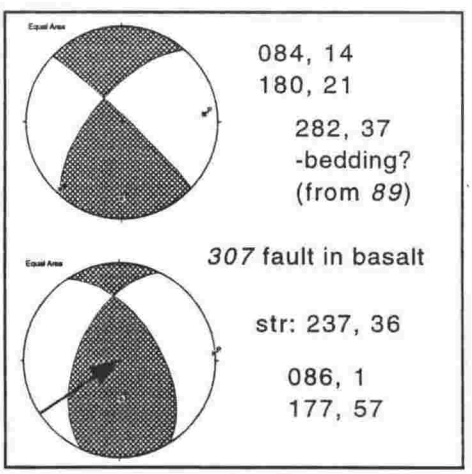

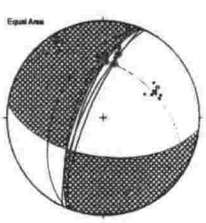
P: 064, 41
T: 327, 7

1373 -north end

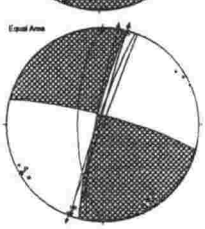
P: 240, 1
T: 150, 10

Flags Creek Fault

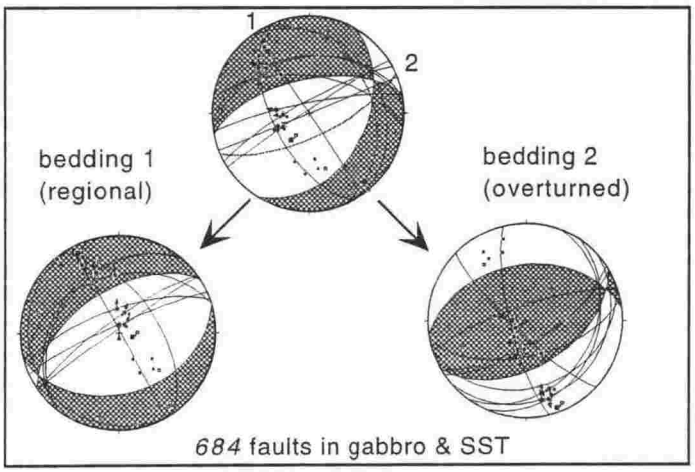

684 faults in gabbro & SST

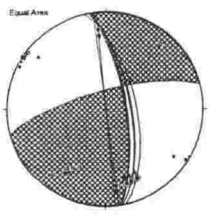

539 faults in Torlesse

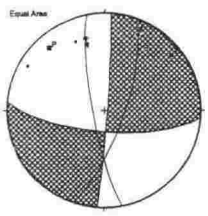

546 faults in Torlesse

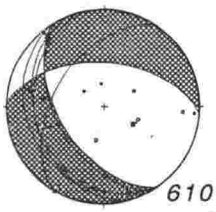

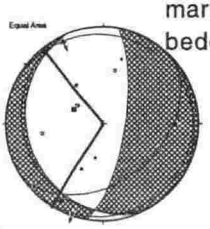

610 faults in Torlesse/ marl shear zone; if GW bedding overturned...

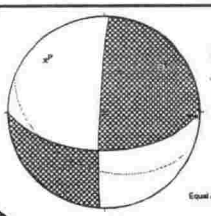

P: 312, 20
T: 052, 26

bed upright

if bed overturned

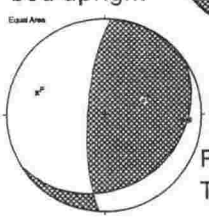

P: 298, 28
T: 070, 56

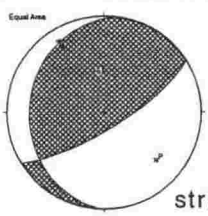

133, 28
352, 56

str: 328, 14

933 fault in basalt CGL
bedding borrowed from *932* WDSD SST

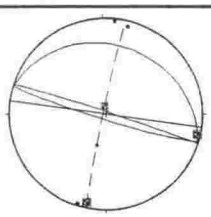

PP: 193, 87

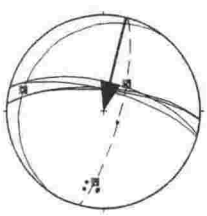

pp: 015, 75

BMA corrected

860 - 863 folded WDSD SST

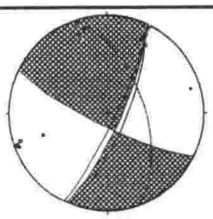

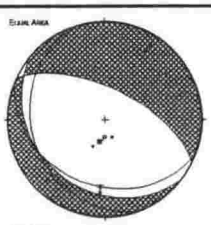

P: 246, 59
T: 350, 9

str: 186-204

761 ss faults in basalt

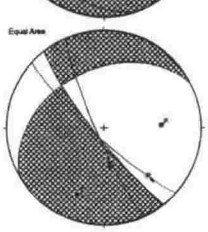

088, 41
203, 26

nml faults?

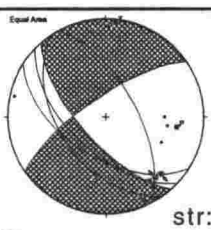

098, 27
006, 3

str: 137-156

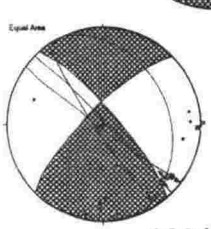

bedding correction as for 684 (1)

682 faults in gabbro

Flags Creek Fault -2

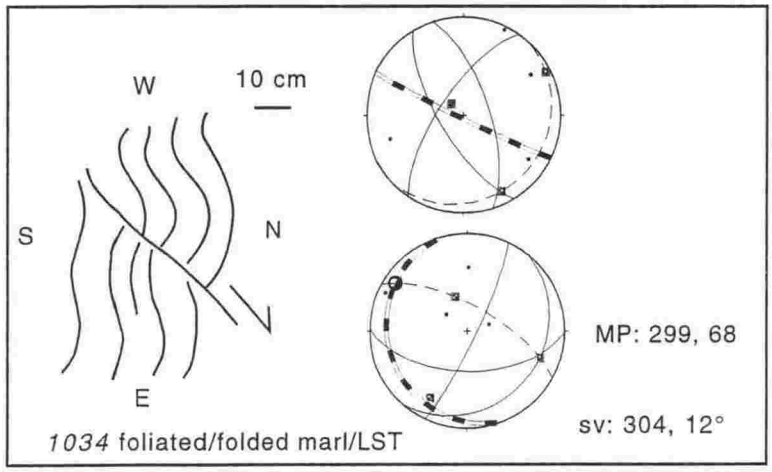

1034 foliated/folded marl/LST

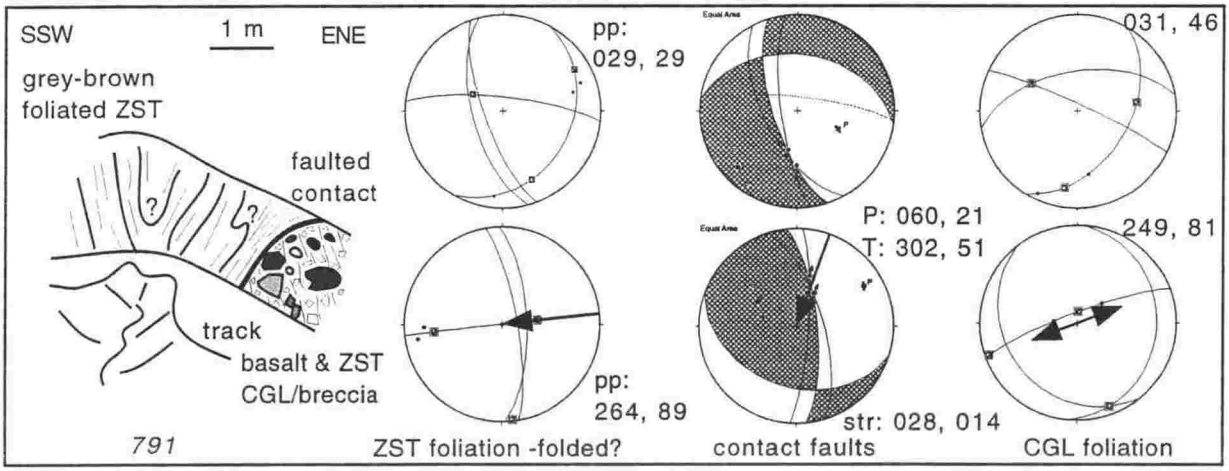

791

ZST foliation -folded?

contact faults

CGL foliation

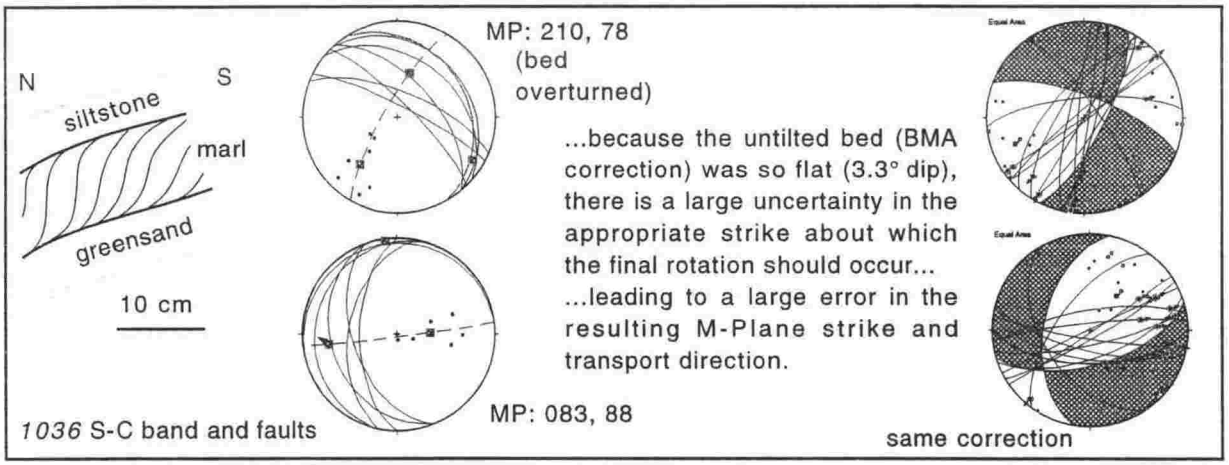

1036 S-C band and faults

same correction

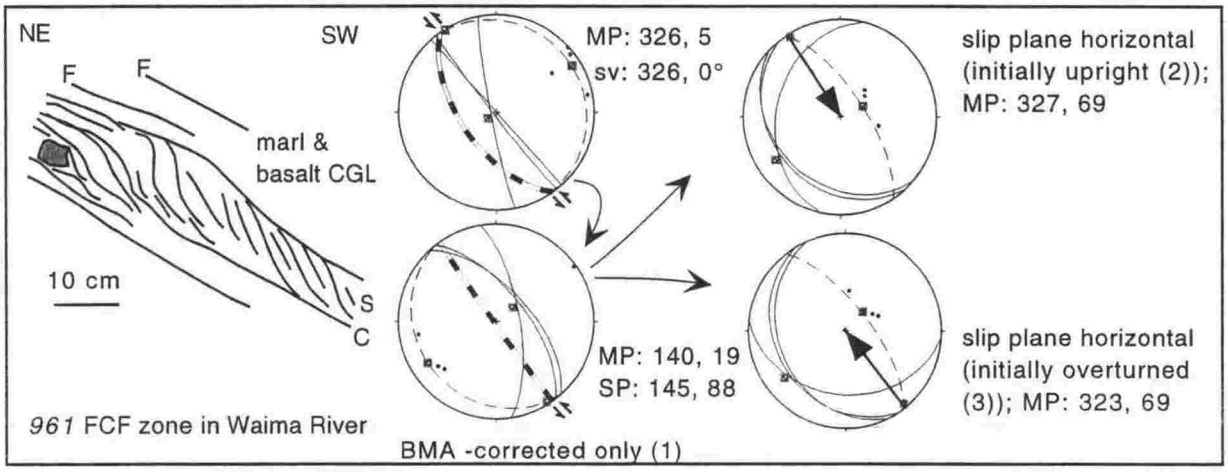

961 FCF zone in Waima River

BMA -corrected only (1)

Flags Creek Fault -3

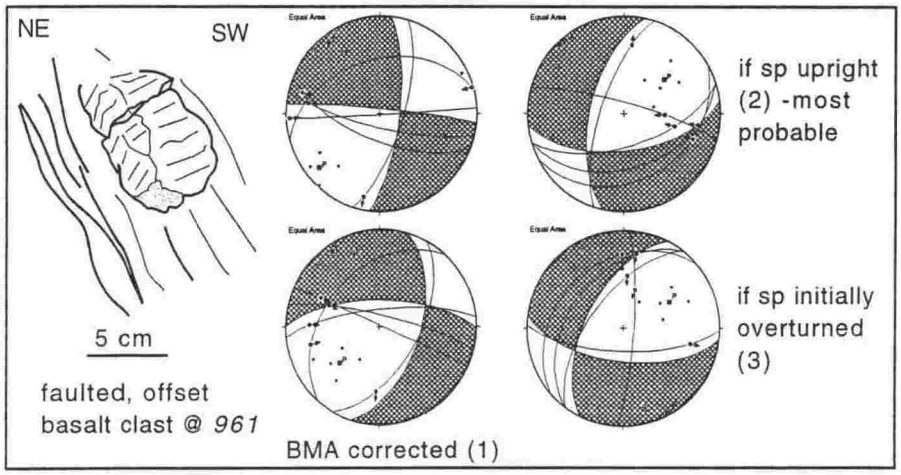

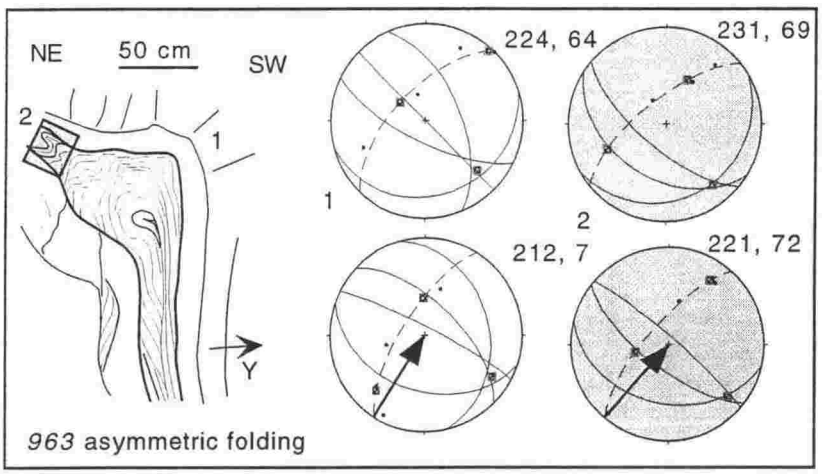

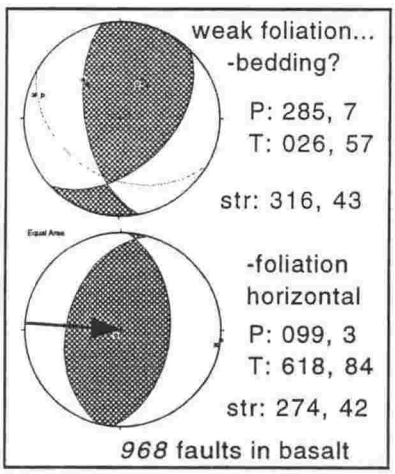

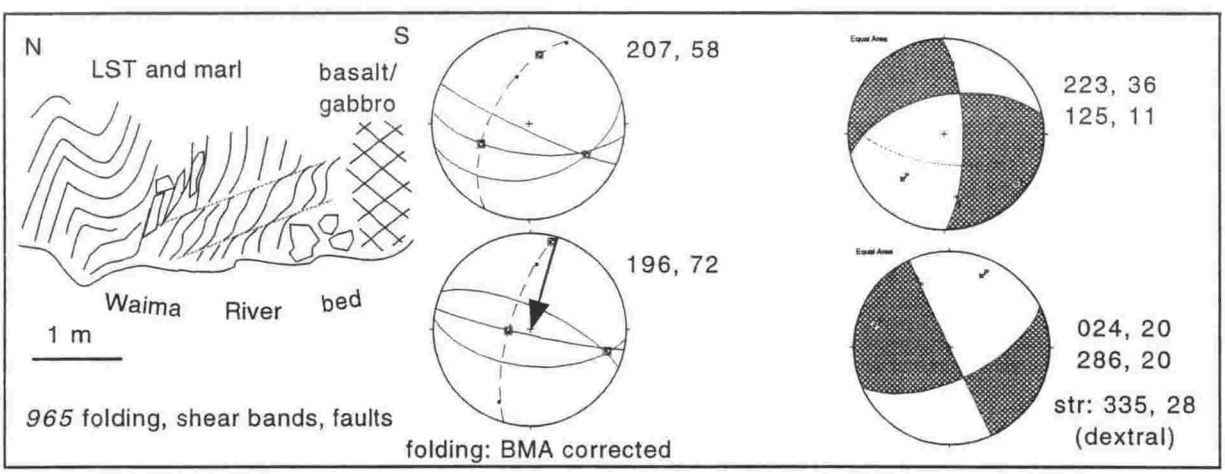

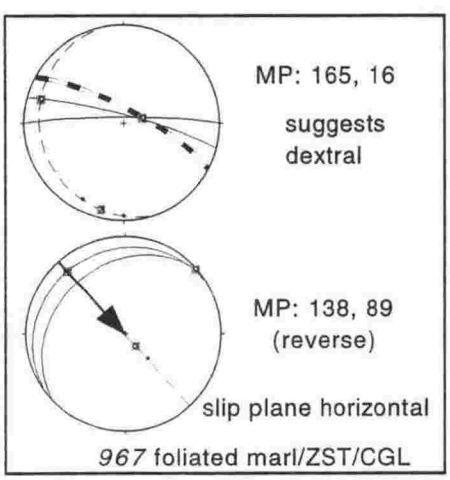

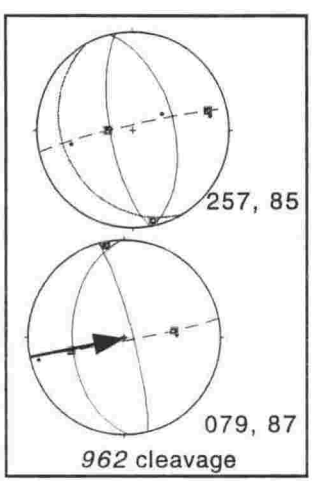

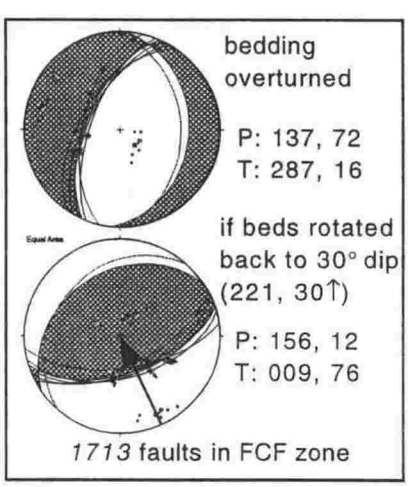

Flags Creek Fault -4

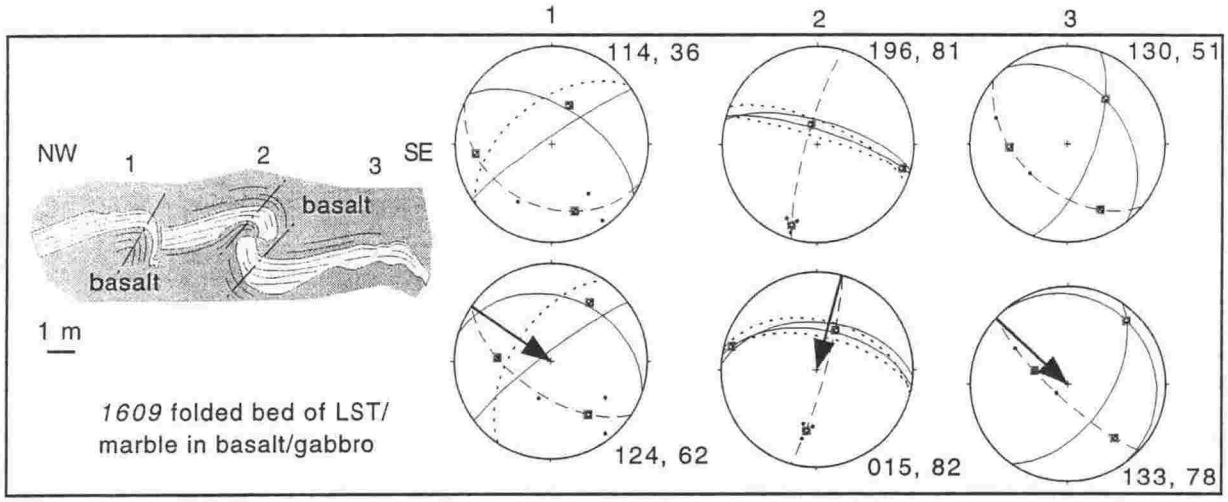

1609 folded bed of LST/ marble in basalt/gabbro

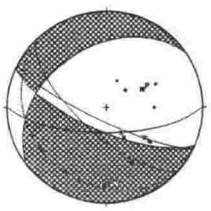

P: 063, 55
T: 182, 19

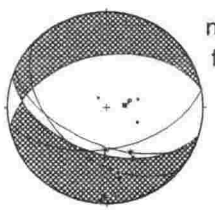

normal faults!

P: 084, 75
T: 184, 3

1606 faults in WBLST

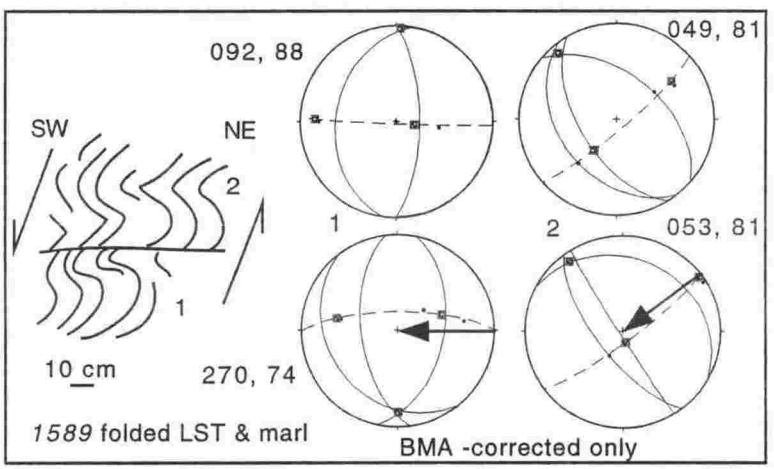

1589 folded LST & marl

BMA -corrected only

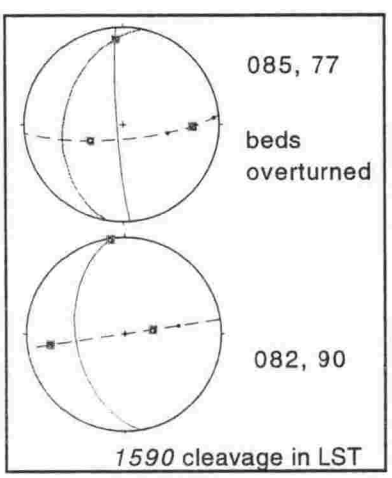

1590 cleavage in LST

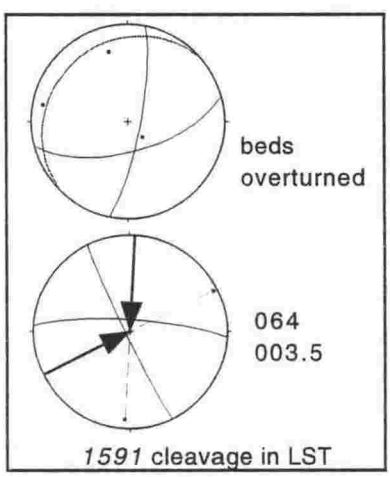

1591 cleavage in LST

Good Creek Fault

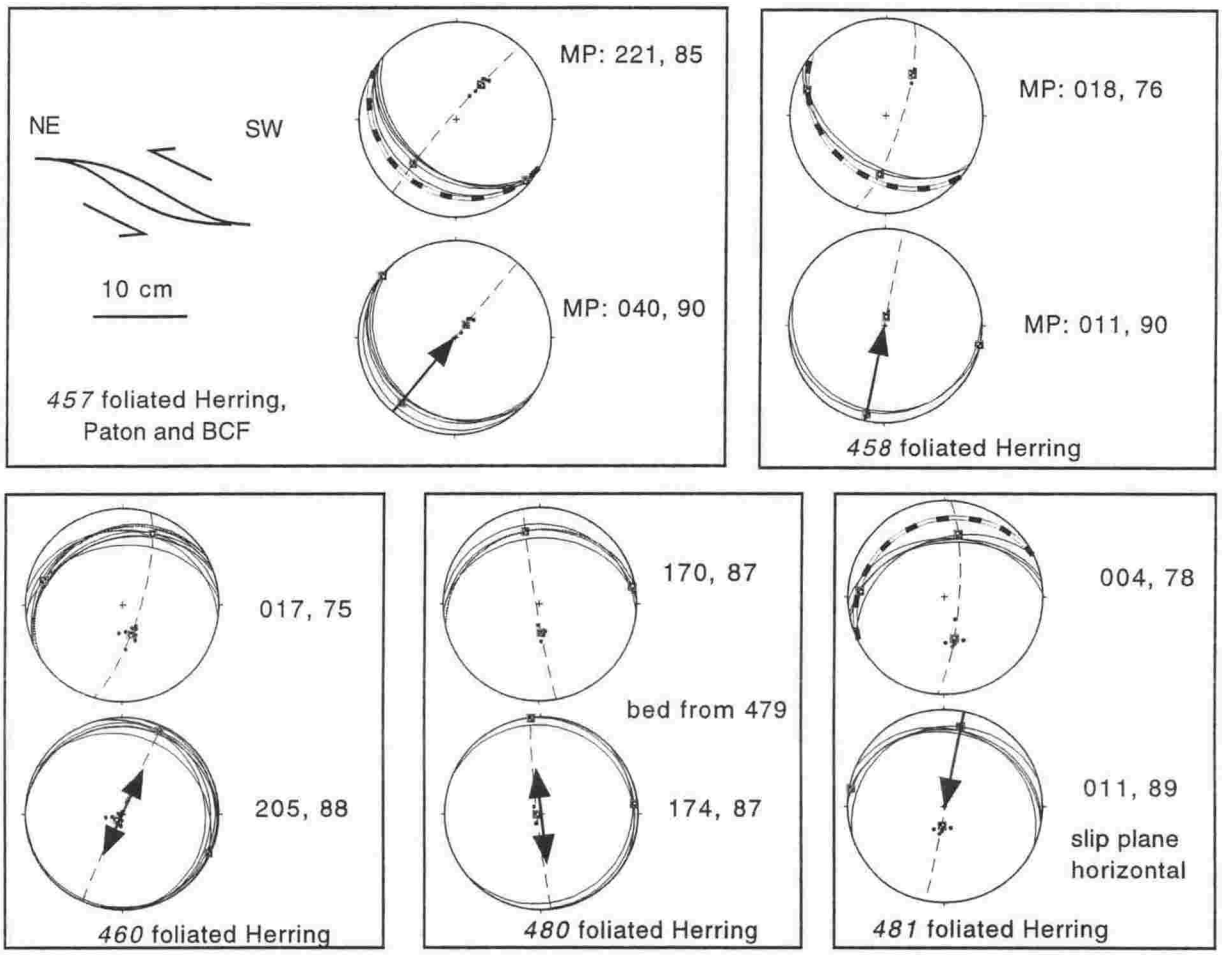

Appendix 4.1

Characteristics of terrace surfaces that are useful distinguishing them both from the air and from the ground are presented below. Morphological traits are derived from analysis of aerial photographs covering well-correlated surface outcrops, whereas gravel thickness and the degree of weathering of Tapuae-O-Uenuku plutonic complex (TPC) igneous clasts are from Eden [1983].

STARBOROUGH 3 - 9:

Usually distinctively well preserved with sharp edges, these surfaces are generally underlain by 1 – 2 m of gravel. The youngest terraces often do not have grass or are not farmed because of lack of soil development. Generally vegetated with scrub. St –9 is the youngest surface recognised by Eden [1989] and is analogous to the modern floodplain. Very little -to no -loess cover.

STARBOROUGH-2:

Well-preserved, sharp-edged terraces with little or no modern stream incision, sometimes apparent as longitudinal strip beside Starborough-1. Starborough-2 terraces are generally underlain by <3 m of gravel and often have many remnant (abandoned) braided channels visible on aerial photos due to lack of loess cover; sometimes boulders are visible at the surface. These terraces are seldom overlain by fans of lateral valleys. Tapuae-O-Uenuku plutonic complex (TPC) igneous clasts show no visible signs of weathering.

STARBOROUGH-1:

The Starborough-1 terrace tread is extensively preserved; broad surfaces with sharp-edged scarps are underlain by up to 6 m of gravel. This terrace represents the last major aggradational phase of the Awatere River. It is often dissected by streams in deep gorges (on softer mudstone bedrock) rather than open valleys. Many of these gorges have a knick-point some way between the front and the back edge of the terrace, upstream from which the modern stream lies in a shallow, trough-like channel. St-1 is usually extensively farmed with good soil development and a loess cover of around 2 - 3 m. Sometimes overlain by lateral fans shedding from gullies and steep hill country

(undifferentiated or mapped as "fan" by Eden [1989]), especially at the periphery of the main Awatere River terraces and along the Awatere Fault. These overlying fans are not characteristic of surfaces younger than St-1. TPC clasts may break after several hammer blows.

DOWNS-1:

Often only small remnants with rounded scarps are preserved. The surface is characterised as undulating or rolling, underlain by 5 - 7 m of gravel. It is commonly covered with moderately thick loess, which contains the Kawakawa Tephra, and is dissected by shallow streams, forming open, rounded valleys. Downs-1 is seldom cut by steep-sided gorges. TPC clasts crumbly and/or break after a few hammer blows.

DOWNS-2:

Downs-2 appears not to be associated with aggradation from the Awatere River, rather it commonly forms broad fan surfaces shedding from tributaries (such as Stafford Creek and Kennel Brook valleys). The thickness of gravel associated with these fans, where they are truncated by younger terrace risers or by the modern Awatere River, is typically around 3 m. Clast lithologies generally always consist of (locally derived) Torlesse Terrane cobbles.

UPTON-1, 2 & 3:

Characteristically only preserved as flat-topped remnant ridges, this series of terraces are hard to distinguish by using aerial photographs alone. They are frequently exposed only as interfluves with an accordant height and common slope, fingering down the northern flanks of the Haldon Hills into the Awatere River. One broad remnant of Ut-3 is preserved along the drainage divide between the Awatere River and Deep Creek (of the Blind River catchment) and may have become stranded by dip-slip displacement on the nearby Hog Swamp Fault. It is from this remnant that the most robust correlation with other exposures of this surface are made. The thickness of gravel cover is typically about 5 m. TPC clasts are generally fractured and break with gentle tapping. All TPC clasts show some degree of weathering or exfoliation.

CLIFFORD:

This terrace is generally not widely preserved. The largest remnant is near Seaview, at the coast between Awatere and Blind rivers. The surface is gently to moderately undulating due to uneven deposition/erosion of loess cover and dissection by Station Creek, with gravel thickness of 4 – 5 m.

MURITAI:

This surface was subdivided by Eden [1983] into Muritai-1, -2 and -3 on the basis of loess units. It is morphologically very similar to the Clifford surface; slightly higher in elevation but less extensively preserved as a surface. Mu terraces are difficult to map from aerial photos. Gravel thicknesses are generally 2 – 3 m. TPC clasts are covered or cemented by reddish oxides; most are rotten and collapse when touched.

SHERBOURNE:

This terrace is not recognised as a distinctive surface from aerial photos due to its more-extensive erosion. Gravel deposits only, as mapped by Eden [1989], indicate presence of this terrace.

Appendix 4.2. Site means of electron microprobe analyses of tephra from Marlborough.

OXIDE	SiO2	TiO2	Al2O3	FeO	MgO	CaO	Na2O	K2O	H20
Elterwater (15)	78.83	0.18	12.82	1.22	0.15	1.11	2.66	3.04	7.04
STDEV	0.28	0.05	0.17	0.08	0.04	0.08	0.37	0.15	1.27
BRL (12)	78.89	0.18	12.97	1.22	0.13	1.12	2.43	3.07	7.58
STDEV	0.24	0.04	0.14	0.12	0.03	0.06	0.19	0.13	0.77
BRQ (10)	78.75	0.18	13.01	1.23	0.15	1.14	2.68	2.86	7.07
STDEV	0.80	0.06	0.21	0.10	0.03	0.09	0.92	0.10	0.95
Dun. Ck. (12)	79.03	0.15	12.79	1.20	0.15	1.06	2.64	2.97	7.36
STDEV	0.57	0.04	0.14	0.08	0.02	0.05	0.50	0.11	0.87
F1QT2 (10)	78.04	0.16	12.76	1.30	0.14	1.05	3.48	3.07	5.42
STDEV	0.35	0.04	0.14	0.08	0.02	0.07	0.36	0.09	0.96
FS1T (10)	79.11	0.20	12.75	1.25	0.15	1.10	2.51	2.93	6.58
STDEV	0.62	0.05	0.08	0.12	0.04	0.08	0.65	0.15	1.07
FT2 (15)	78.12	0.16	12.69	1.23	0.13	1.10	3.49	3.08	6.83
STDEV	0.43	0.04	0.19	0.10	0.03	0.08	0.38	0.19	0.80
WARD (20)	79.19	0.10	12.28	1.16	0.12	1.00	3.04	3.11	4.33
STDEV	0.60	0.04	0.15	0.21	0.04	0.12	0.44	0.11	0.74
QT1T1 (10)	77.66	0.15	12.93	1.26	0.15	1.19	3.69	2.97	6.46
STDEV	0.20	0.06	0.11	0.07	0.02	0.06	0.15	0.14	1.03

BRL: Blind River loop Road, BRQ: Blind River Quarry, Dun. Ck.: Dunsandel Creek, F1QT2: Tachalls Creek,
FS1T: Flaxbourne terrace T4, FT2: Flaxbourne terrace T3, QT1T1: Flaxbourne River upper.
WARD data courtesy of Dr. Paul Froggatt. Number of analyses per site given in brackets.

Appendix 4.2 -contd. Electron microprobe analyses of Kawakawa Tephra from previous workers.

OXIDE	SiO2	TiO2	Al2O3	FeO	MgO	CaO	Na2O	K2O	H20
sample 1	78.11	0.15	12.3	1.25	0.14	1.11	3.79	3.09	5.88
STDEV	0.77	0.03	0.23	0.12	0.02	0.12	0.62	0.19	1.36
sample 2	78.79	0.2	11.97	1.29	0.15	1.05	3.83	3.21	5.96
STDEV	0.55	0.04	0.18	0.2	0.04	0.07	0.2	0.19	1.22
sample 3	78.4	0.14	12.2	1.17	0.12	1.08	3.62	3.09	5.27
STDEV	0.31	0.04	0.11	0.11	0.03	0.08	0.18	0.16	1.07
sample 4	77.94	0.18	12.54	1.22	0.25	1.06	3.81	2.99	4.49
STDEV	0.37	0.04	0.23	0.11	0.11	0.08	0.24	0.18	0.82
sample 5	78.1	0.17	12.52	1.31	0.14	1.13	3.97	2.97	4.62
STDEV	0.45	0.04	0.19	0.09	0.03	0.09	0.11	0.18	0.93

sample:
1: reworked in loess overlying Moa site (n=15)
2: tephra-rich layer 200m SE of Moa site (n=12)
3: mean analysis of Kawakawa Tephra from 14 NI locations (n=14)
4: NINA BROOK (n=15) [Little et al., 1998]
5: WHITE BLUFFS (n=11) [Little et al., 1998]

Appendix 4.2 –continued. Backscattered SEM images of tephra shards from Marlborough, chemically identified as the Kawakawa Tephra. These grains exhibit classic tephra morhpology.

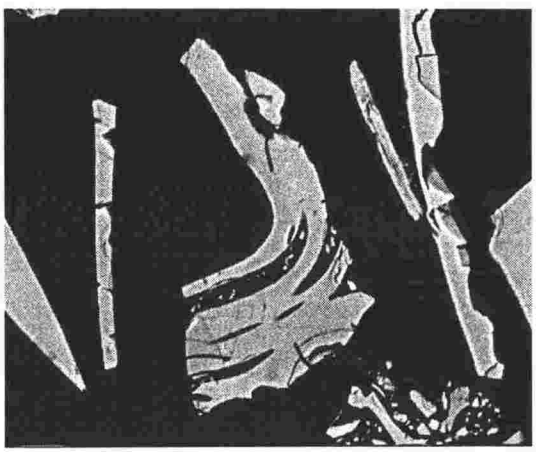

Northern Lake Elterwater

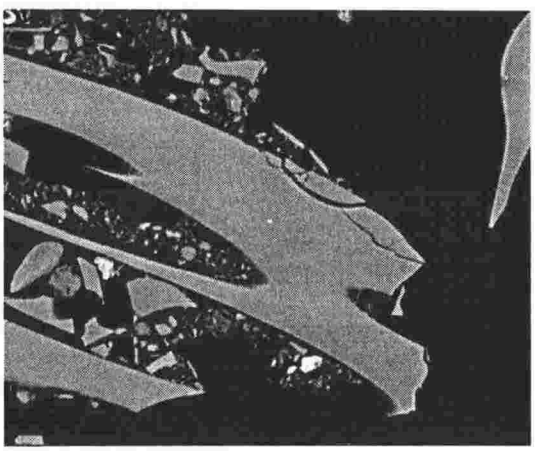

Dunsandel Creek

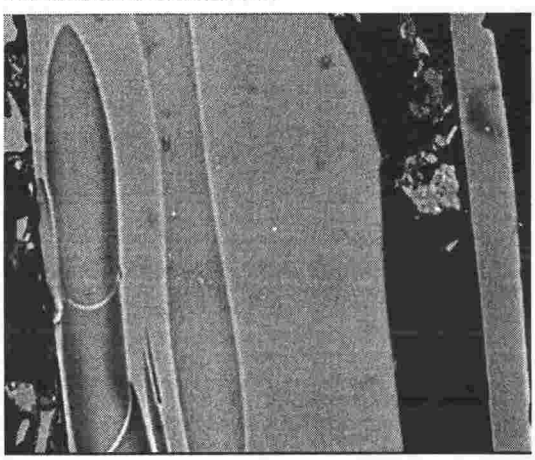

Dunsandel Creek

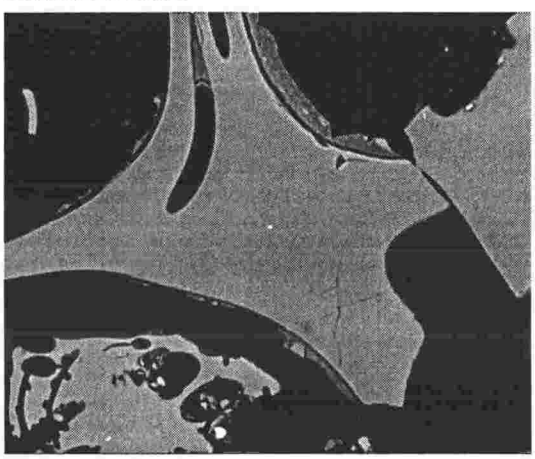

Dunsandel Creek

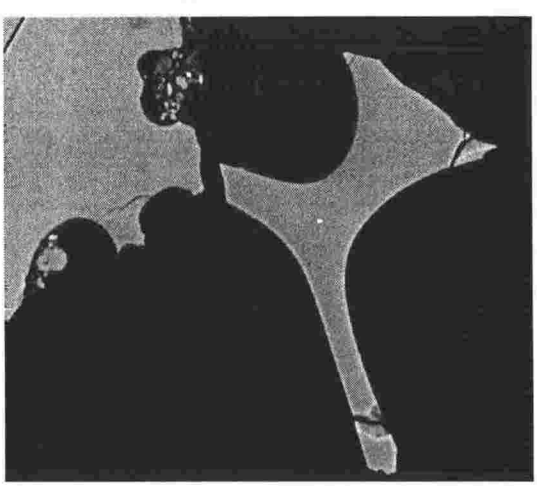

Dunsandel Creek

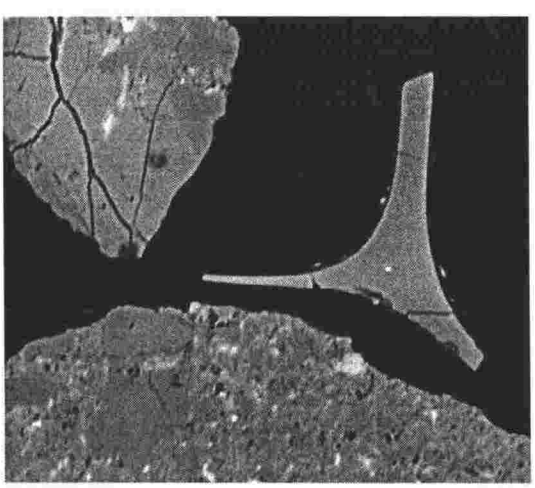

FS1T -The Plateau -T3

Appendix 4.3 –notes on Optically Stimulated Luminescence technique

IRSL: Infrared Stimulated Luminescence, using the single aliquot regenerative (SAR) process [modified by Dr. Uwe Rieser, after Murray & Wintle, 2000] on fine grained feldspars.

Stimulation: LED; 880 nm, half width of 80 nm

Detector filters: Schott BG3g
Kopp 5-58

Which give ~410 nm (blue) –thought to be stable

Luminescence measured at room temperature

Sample preheated to 220°C for 5 minutes to remove unstable components

Sample protocol:

Preheat
Measure natural dose
Irradiate D_T (test dose)
Preheat
Measure D_T
Irradiate $D_\#$ (dose)
Preheat
Measure $D_\#$

Repeat with:

Irradiation dose first at 0.5 D_E (equivalent dose)
Then 1 D_E
Then 1.5 D_E
Then 0 D_E
Then 0.5 D_E to measure repeatability of first step and test correction factor

Source: ^{90}Sr / ^{90}Y (β-source –calibrated)

Appendix 5.1

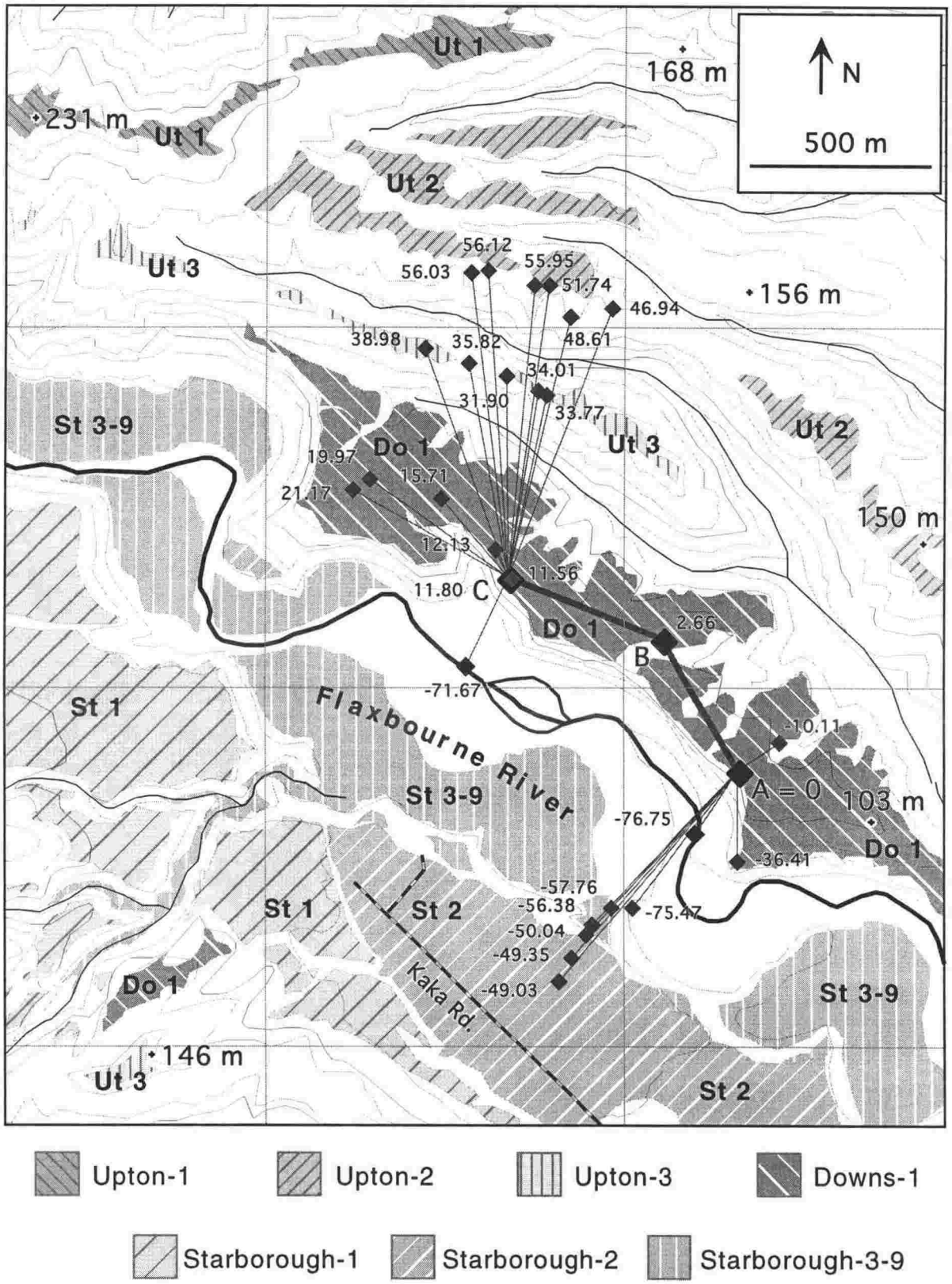

Appendix 5.1. EDM survey of fluvial terraces at "The Plateau", along the Flaxbourne River, NW of Ward. Numbers by survey points are elevation in metres, relative to station "A". See Fig. 5.2 for location.

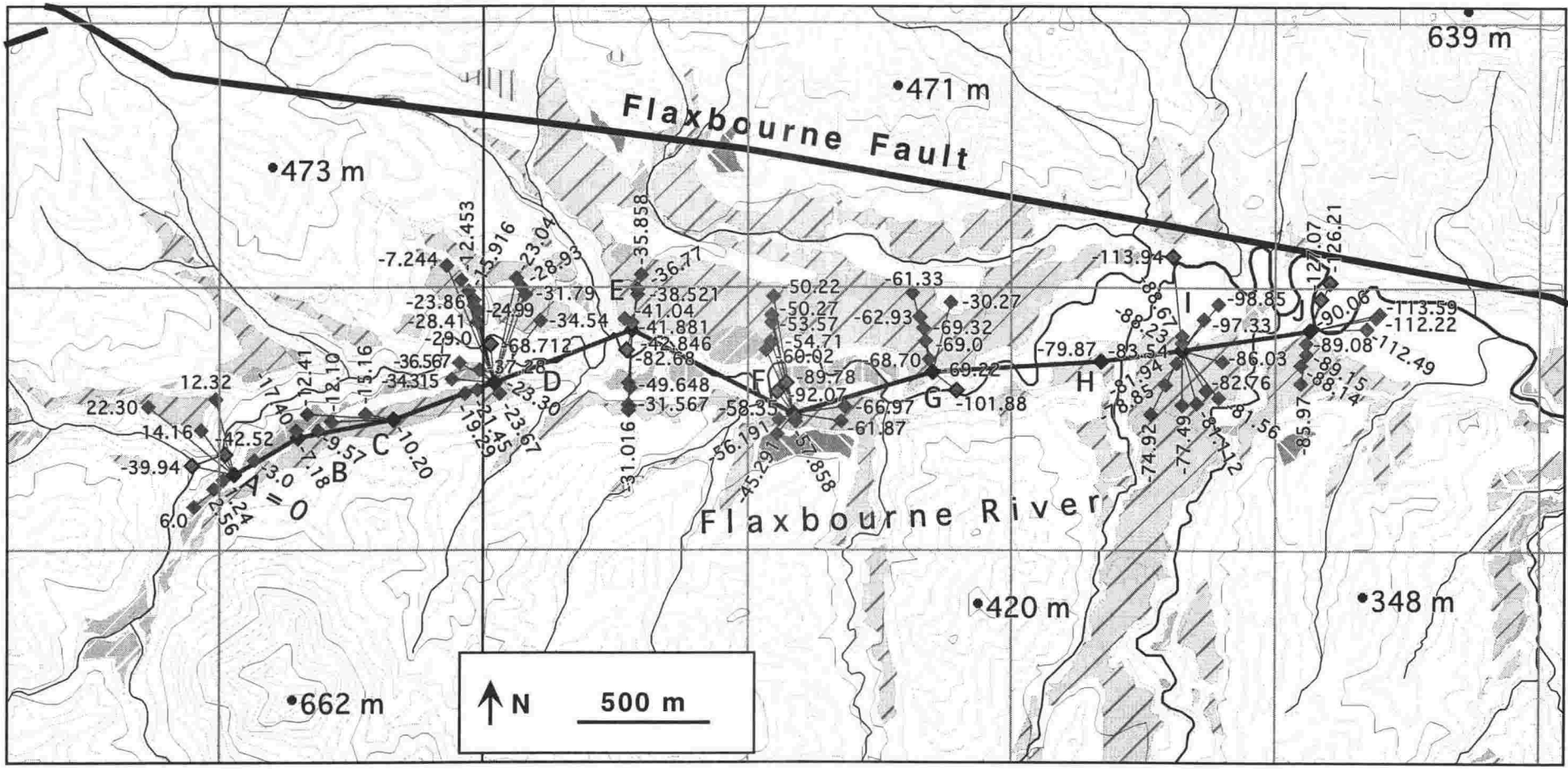

Appendix 5.2

Appendix 5.2. EDM survey of the upper Flaxbourne Valley, along strike from the termination of the Clarence Fault. Values are in metres, relative to station "A". See Fig. 5.2 of main text for location.

Appendix 5.3

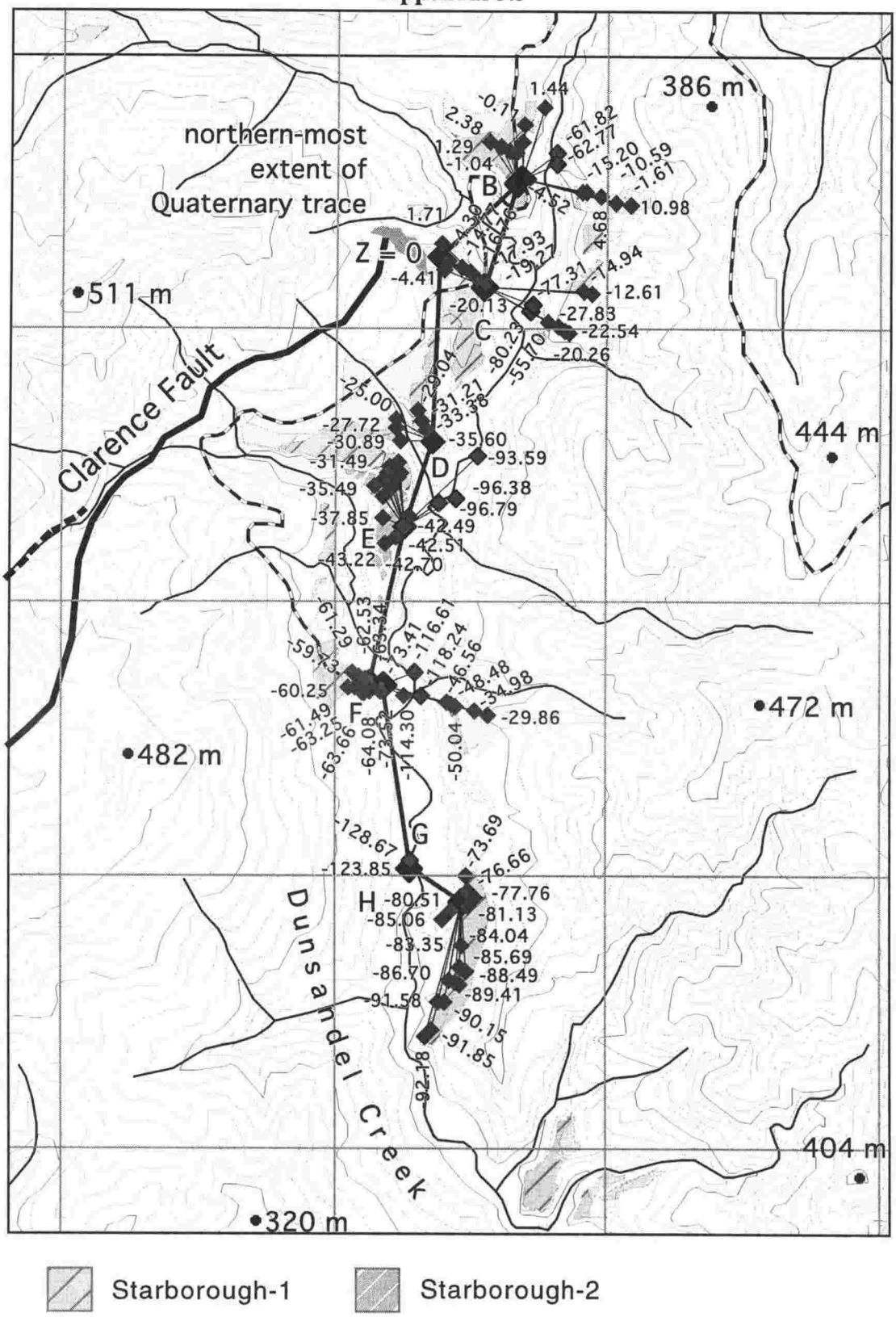

Appendix 5.3. EDM survey of fluvial terraces along Dunsandel Creek, near the termination of the Clarence Fault. Values are in metres, relative to station "Z". See Fig. 5.2 of main text for location.

New Zealand Journal of Geology & Geophysics, 1998, Vol. 41: 401–417
0028–8306/98/4104–0401 $7.00/0

Chapter 6:

Pliocene–Quaternary deformation and mechanisms of near-surface strain close to the eastern tip of the Clarence Fault, northeast Marlborough, New Zealand

D. B. TOWNSEND
T. A. LITTLE
Geology Department
Victoria University of Wellington
P.O. Box 600
Wellington, New Zealand

Abstract In coastal northeast Marlborough, New Zealand, the termination of the dextral strike-slip Clarence Fault requires a mechanism for the accommodation of strain about its tip. The Awatere Block, to the northeast of the tip, is inferred to be undergoing a clockwise vertical-axis rotation as mid-lower crustal simple shear is transmitted upward into an upper crustal rigid-body rotation. Clockwise vertical-axis rotation of the Awatere Block of up to 44° has previously been constrained by paleomagnetic data in Pliocene rocks, and the deflection of near-vertical bedding in Torlesse Terrane basement rocks suggests a rotation of up to c. 55°. The attitude and slip direction of mesoscopic faults in coastal exposures of late Miocene–Pliocene rocks allow directions of faulting-related maximum instantaneous strain to be deduced. These directions swing from east–west in the north of the Awatere Block to southeast–northwest in the south of the block as the style of faulting changes from oblique-normal to strike-slip to thrust. This changing pattern of strain is inferred to be due to a clockwise rotation of the Awatere Block.

The London Hill Fault forms an eastern boundary to the rotating Awatere Block. Gouge-zone foliation and stratigraphic data reveal that the London Hill Fault is currently a reverse fault that reactivates an Eocene(?) normal fault. Post-Pliocene dip-slip on the London Hill Fault is in the order of 2 km. New radiocarbon dating of a marine terrace to the southwest of Cape Campbell requires a rate of uplift of 1.7–2.5 mm/yr over the last 5500 yr, much faster than other rates nearby. This difference in rate is inferred to be due to active folding of the adjacent Cape Campbell Syncline. Regional Holocene northeast tilting of the Awatere Block is inferred from stream piracy patterns and tilted fluvial and coastal marine terraces. Local tilting patterns are more complex and indicate surface deformation near currently active fault and fold structures.

Keywords Awatere Block; block rotation; Clarence Fault; London Hill Fault; Marlborough; mesoscopic faults; Miocene; Pliocene; Quaternary; uplift; tectonics

G98017
Received 28 May 1998; accepted 9 September 1998

INTRODUCTION

In northeastern Marlborough, New Zealand, the Marlborough Fault System (MFS) is a transition zone in continental crust that links subduction beneath the Hikurangi margin to oblique dextral strike-slip on the Alpine Fault (Fig. 1). The MFS is a series of northeast striking, dextral strike-slip faults which, together with the Alpine Fault and the Hikurangi subduction zone, accommodate c. 39 mm/yr of convergence between the Pacific and Australian plates in the northern part of the South Island (DeMets et al. 1994). This paper is concerned with late Cenozoic deformation at the northeastern end of the MFS (Fig. 1).

One of the principal strike-slip faults of the MFS, the Clarence Fault, terminates in the southwestern part of the study region (Browne 1992b). This termination requires that slip on the Clarence Fault must be accommodated at the surface by structures to the northeast of the tip, such as the Ward Syncline and the London Hill Fault (Fig. 2), or by processes of distributed deformation. To the northwest of the Clarence Fault in the central Awatere Valley, the Haldon Hills and Flaxbourne Faults are part of the Medway Fault System of reverse faults that are late Miocene in age (Melhuish 1988; Maxwell 1990; Little & Jones 1998). On the basis of paleomagnetic and structural data, Little & Roberts (1997) interpreted the Cape Campbell – Lake Grassmere region as lying on a crustal block that has rotated 30–60° clockwise about a vertical axis since the early Pliocene. This magnitude of clockwise rotation is much greater than the 20–25° of post-Pliocene rotation that the rest of northeast Marlborough has experienced on either side of the Awatere Block to the north of the Awatere Fault (Roberts 1992) and to the east of the London Hill Fault (Walcott et al. 1981; Roberts 1995). Thus, the Awatere and London Hill Faults form the northern and eastern boundaries between surface crustal domains that have rotated differentially in the last c. 8 m.y. in the region to the east of the Clarence Fault tip. The western boundary of the strongly rotated Awatere Block has been located in the Awatere Valley as a northwest-trending discontinuity (Fig. 1, "R.B.") across which there is a c. 56 ± 18° clockwise change in bedding strike of mostly vertical Torlesse Terrane. To the west of this boundary, late Miocene rocks of the Awatere Valley are paleomagnetically unrotated (Little & Roberts 1997). The Haldon Hills and Flaxbourne Faults undergo a clockwise change in strike of c. 40° across this boundary: their east–west strike to the east is anomalous with respect to the rest of the Medway faults farther to the west that strike northeast–southwest (Fig. 1).

In this paper, the roles of faulting, folding, and block rotation are investigated as mechanisms of strain accommodation. We present fault-kinematic data from within the Awatere Block and from the adjacent areas to the north across the Awatere Fault, and to the east across the London Hill Fault.

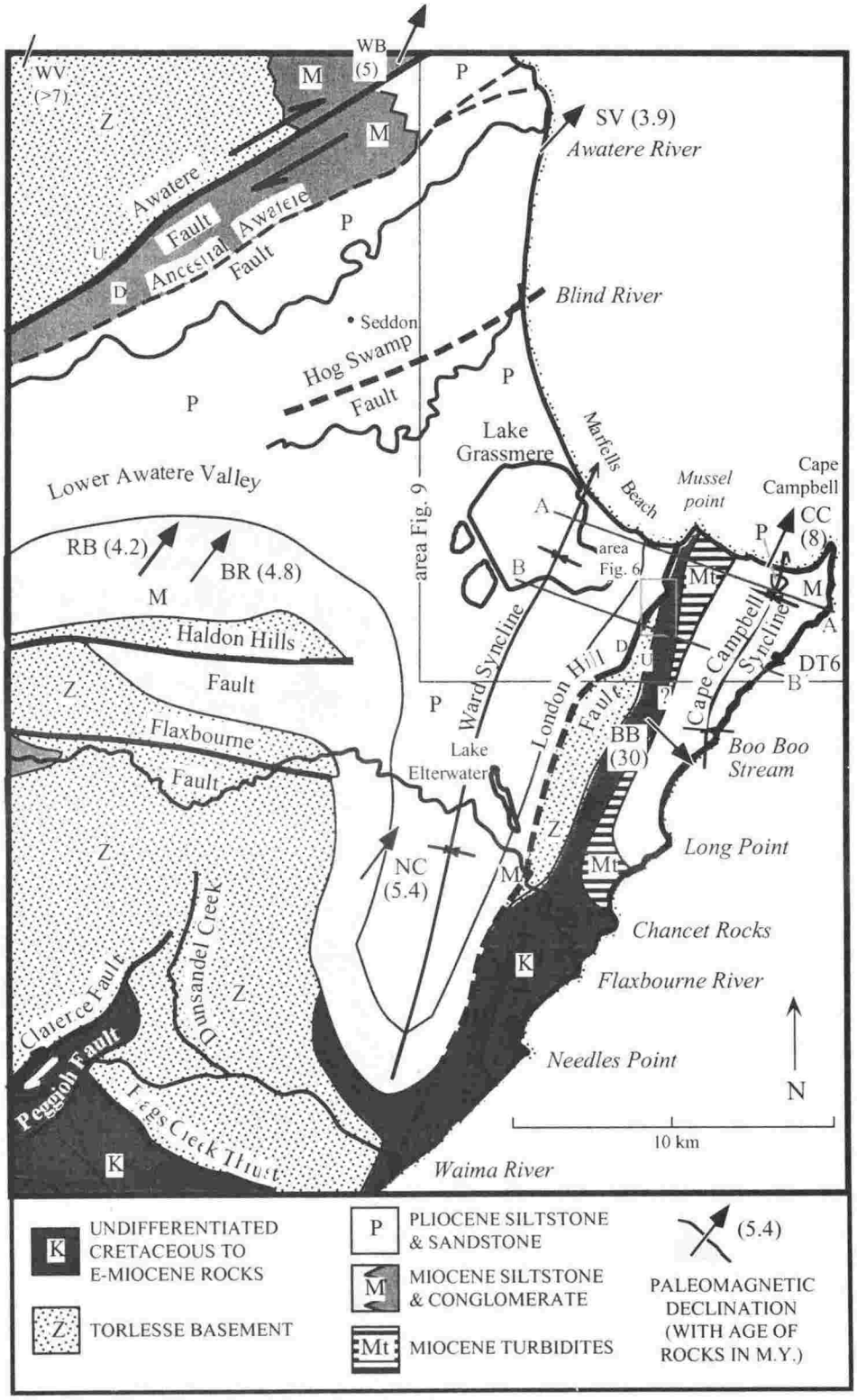

Fig. 2 Simplified geologic and tectonic map of the Awatere to Lake Grassmere region. Black arrows are available paleomagnetic declination anomalies (relative to the Pacific plate), with the age of rocks sampled shown in parentheses. Inland slip of 7–10 mm/yr on the Clarence Fault dies out in the southwest of the region. Data compiled from Browne (1992a), Roberts & Wilson (1992), Vickery & Lamb (1995), and Little (1995).

rhyolites erupting in the Coromandel region during the late Miocene (Townsend 1996).

Pliocene rocks in the Awatere–Grassmere region consist of a thick sequence of marine sandstones, siltstones, and mudstones (the Starborough Formation) that are lithologically monotonous and regionally extensive on the western side of the London Hill Fault (Roberts & Wilson 1992). The only exposure of Pliocene rocks east of the London Hill Fault is a small down-folded inlier of Starborough Formation-equivalent mudstone in the hinge of the Cape Campbell Syncline (Fig. 2) (Russell 1959).

REGIONAL FOLDING OF BEDROCK UNITS

Pliocene Starborough Formation between the Awatere River mouth and Cape Campbell is folded on a kilometre scale (see Fig. 2). The hinge lines of the post-Pliocene Ward and Cape Campbell Syncline trend NNE and plunge gently north

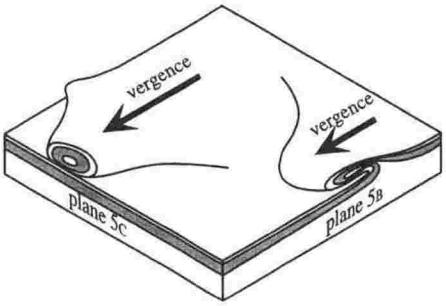

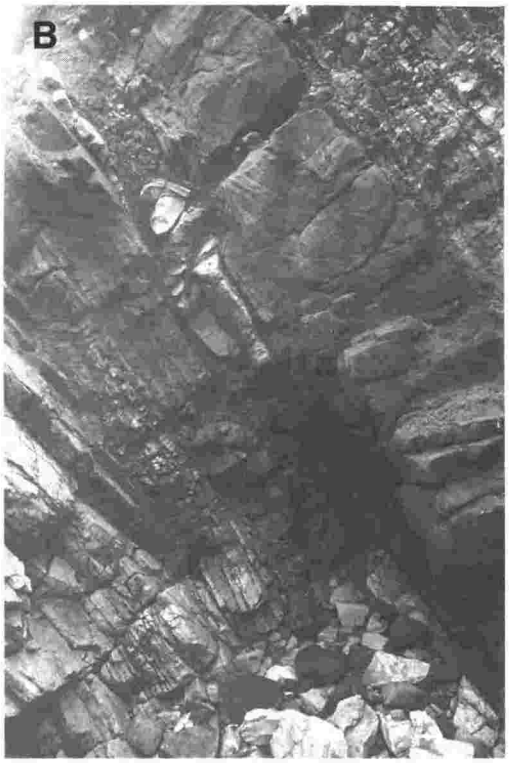

Fig. 5 Mesoscopic structures near the London Hill Fault at Marfells Beach. **A**, The foliated cataclasite that anastomoses to define an s-c foliation within the fault zone; this view is to the south showing a northwest vergent, reverse shear sense. **B**, View parallel to hinge of isoclinal fold in a thin limestone bed in the Amuri Limestone hanging wall in the shore platform. The isocline verges to the northwest and lies on the surface of a bedding-parallel decollement in the Amuri Limestone. **C**, View in cross-section of the tongue-like fold revealing complete stratigraphic closure. *Inset*: Orientation of views B and C relative to folding.

Eocene–Oligocene on this east-dipping, high-angle fault may have caused subsidence and preservation of Cretaceous and Paleogene rocks on its eastern side, whereas correlative strata may have been eroded on its uplifted footwall to the west, thus explaining the difference in stratigraphic preservation across the London Hill Fault (Fig. 3). Timing of breccia deposition and, by inference, normal slip on the paleo-London Hill Fault, is loosely constrained (stratigraphically) to the middle Eocene on the basis of lithological correlation with the Fells Greensand member of the Amuri Limestone.

Today the fault clearly has a net reverse separation and exposes Torlesse Terrane in its hanging wall to the south of the study area (Fig. 2). A foliated cataclasite (Fig. 5A) outcropping at Marfells Beach is the only exposure of the London Hill Fault in bedrock within the study area. There, Paleogene Amuri Limestone of the hanging wall sequence is thrust over Miocene siltstone of the footwall, and the resulting foliated cataclasite deforms both blocks over a width of c. 50 m.

In a seismic study of the Clarence Basin—a marine basin offshore from Cape Campbell inferred to contain Cretaceous rocks—Uruski (1992) suggested a similar slip history for a western boundary fault that, in part, controlled the basin's sedimentation patterns. Inferred Late Cretaceous normal faults, forming half-graben, were reactivated in the early Miocene as contractional structures with sedimentary wedges thickening away from the fault. Shortening on these structures continued into the Pleistocene.

The London Hill Fault generally strikes NNE and dips between 45 and 55° to the east. This dip was measured in three ways: (1) the map-scale trace of the fault on topography

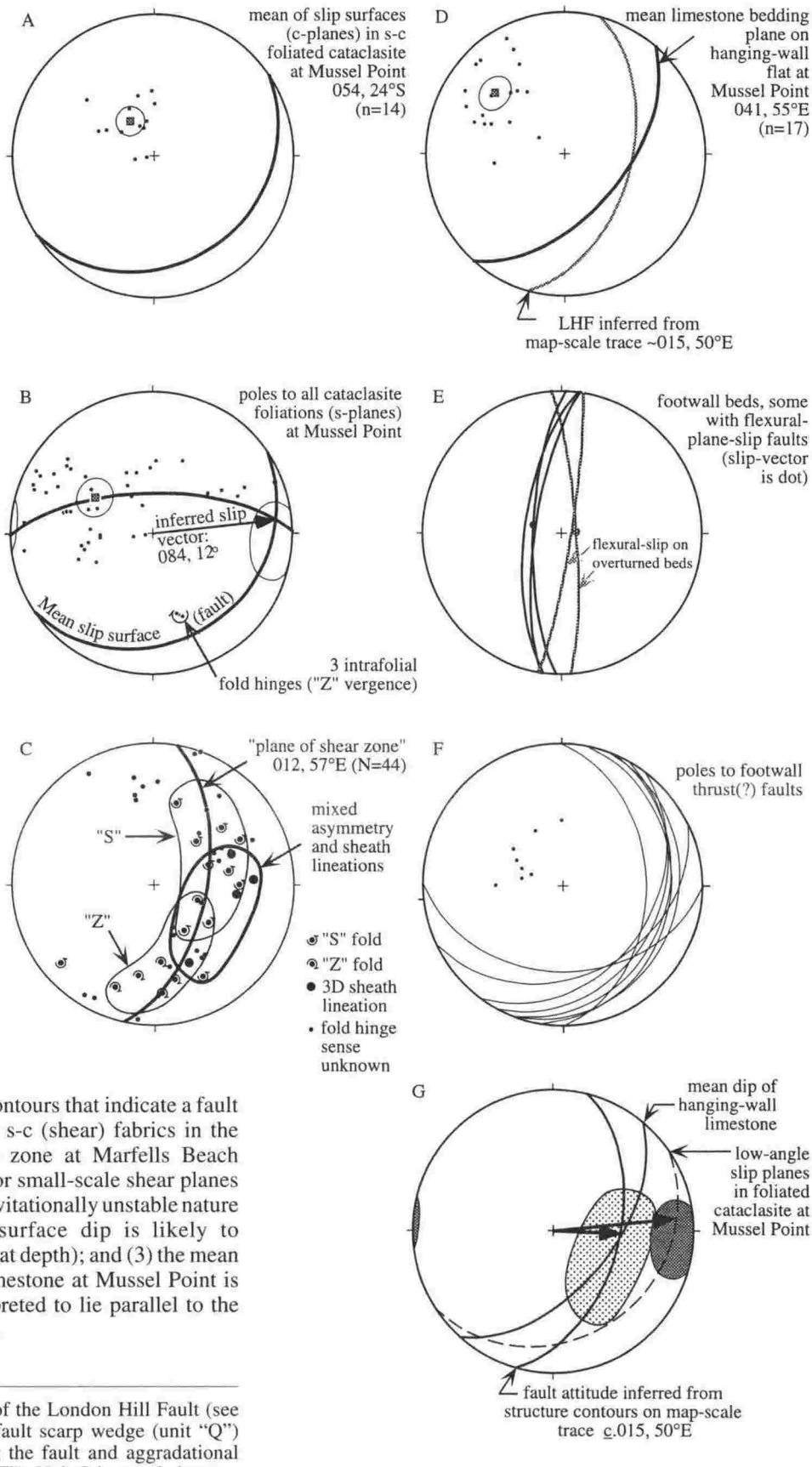

Fig. 7 Structural data for the shear zone fabrics adjacent to the London Hill Fault at Marfells Beach; grey squares and ellipses are Fisher means and 95% confidence cones of poles to foliation planes. **A**, Mean c-plane inferred from low-angle slip planes in foliated cataclasite. **B**, Poles to foliation with best fit m-plane (great circle) defining slip vector for the cataclasite zone. **C**, Isoclinal fold hinges in hanging wall Amuri Limestone at Mussel Point, with "S" and "Z" fold asymmetries defining the planar girdle. Enclosed fold noses (large dots) plot within and close to the zone of mixed asymmetries. **D**, Estimates of the attitude of the London Hill Fault based on the mean attitude of hanging wall beds at Mussel Point (poles to bedding) and by construction of structure contours of the fault. **E**, Steep bedding in the footwall siltstone with flexural slip faults. **F**, Local thrust faults in the footwall subparallel to the London Hill Fault. **G**, Summary of the fault kinematic data for the London Hill Fault.

was used to construct structure contours that indicate a fault dip of c. 50°; (2) the composite s-c (shear) fabrics in the foliated gouge within the fault zone at Marfells Beach suggest an eastward dip of 45° for small-scale shear planes at this outcrop (because of the gravitationally unstable nature of reverse fault scarps, this surface dip is likely to underestimate the dip of the fault at depth); and (3) the mean dip of bedding in the Amuri Limestone at Mussel Point is c. 55°E, where bedding is interpreted to lie parallel to the fault (e.g., Fig. 6, section Y–Y′).

◀ **Fig. 6** Detail of part of the trace of the London Hill Fault (see Fig. 2 for location) with localised fault scarp wedge (unit "Q") infilling incised paleocanyon along the fault and aggradational alluvial terrace west of the fault ("HT"). Unit Q is mantled across the fault and does not appear to be offset by it. Section Y–Y′ shows overturned bedding immediately to west of the London Hill Fault. Flexural slip, including the Quaternary fault, accommodates folding in this region as do contractional faults in the footwall of the London Hill Fault observed near the coast.

A mean slip-vector for the London Hill Fault cataclasite zone at Marfells Beach was obtained by determining the mean attitude for the slip planes (c-planes) within the foliated cataclasite zone (Fig. 5A, 7A). In addition, the mean

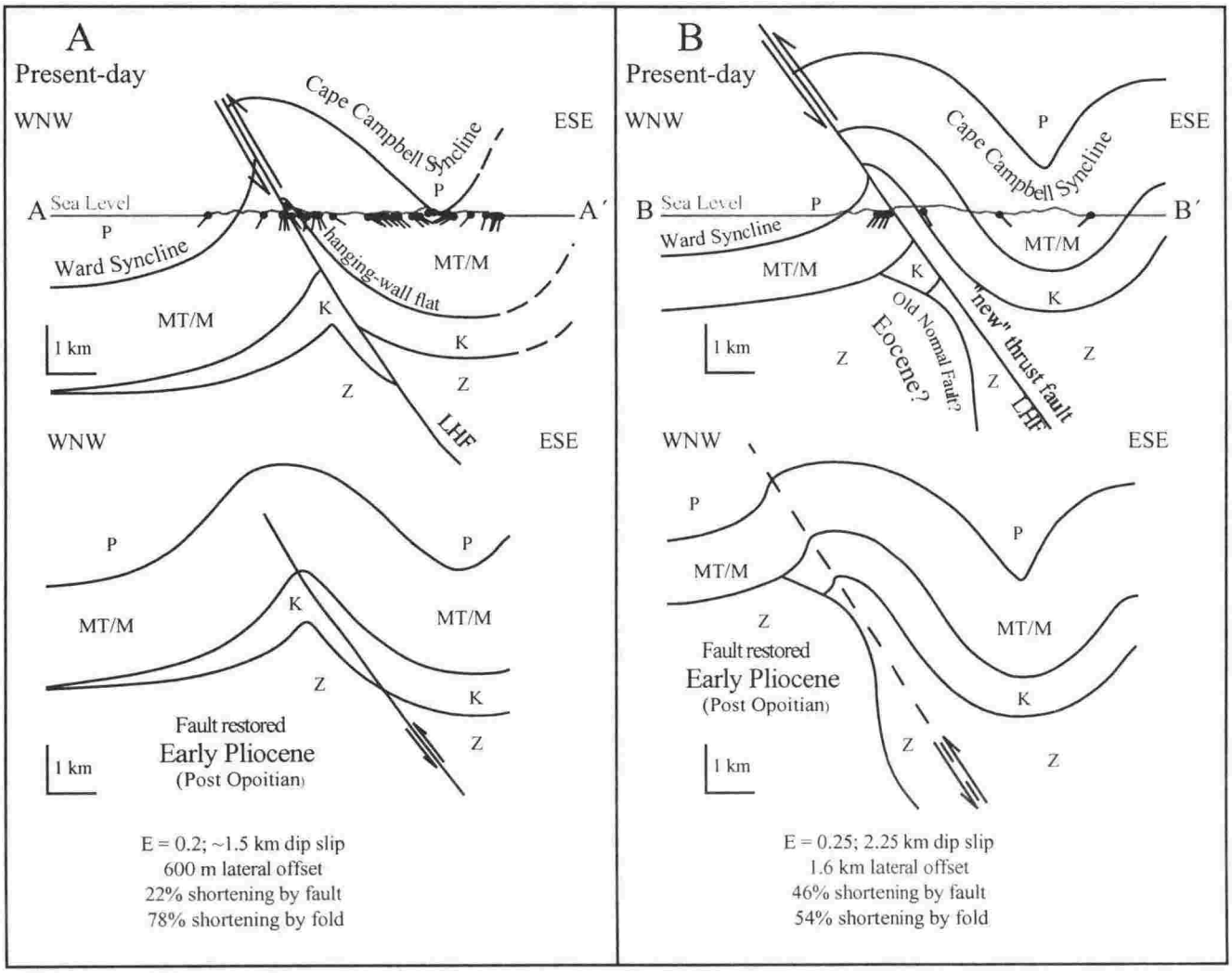

Fig. 8A, B Two cross-sections across the Ward Syncline, London Hill Fault, and Cape Campbell Syncline (locations on Fig. 2, symbols as for Fig. 2). Note the post early-Pliocene dip-slip of 1.5–2.2 km on the London Hill Fault. Regional shortening today is accommodated by continued folding of the synclines.

west of the London Hill Fault to explain their lack of outcrop there. The second possibility invokes a folded (Eocene?) normal fault truncating the Cretaceous–Paleogene rocks west of the London Hill Fault. The total amount of post-early Pliocene reverse slip is not changed by the use of either model.

If the London Hill Fault is considered to be a rigid footwall ramp near the surface above which hanging wall beds have been deformed by fault-bend folding, then the 2–3 km dip-slip offset is equivalent to the horizontal shortening accomplished by the fault. Stratigraphically, this slip must be post-early Pliocene in age (<5 Ma). A dip-slip rate of >0.4 mm/yr is suggested by the two sections. This is a minimum value because the slip may have occurred at any time <5 m.y. ago.

Quaternary activity of the London Hill Fault

Mapping of Quaternary features adjacent to the London Hill Fault implies that the main trace of the fault is presently inactive. To the south of Marfells Beach, overlying the trace of the London Hill Fault, an extensive body of Quaternary gravel crops out (Fig. 6; "unit Q"). The gravel is poorly consolidated, yet it is self-supporting and consists of river-rounded to subrounded clasts up to c. 1 m in diameter of chert, limestone, greywacke, and sandstone, derived locally from the Amuri Limestone and other units of the hanging wall of the London Hill Fault. The thickness of unit Q is estimated to be c. 50+ m (Townsend 1996). The gravel crops out in a series of deeply incised streams transverse to the London Hill Fault trace and is also exposed on the intervening steep ridges. Based on its mapped geometry, the deposit is interpreted to infill a c. 300 m wide paleocanyon incised into the late Miocene footwall siltstone (Fig. 6, section Y–Y′). These gravels straddle and overlap the London Hill Fault and do not appear to be cut by it. Due to its local derivation and proximity to the London Hill Fault, this poorly sorted deposit is interpreted as being a fault-scarp wedge derived from erosion of the immediately adjacent hanging wall of the London Hill Fault. This eroded material may have initiated as scree, but was eventually deposited as alluvium by a stream, possibly flowing longitudinally along the trace of the London Hill Fault.

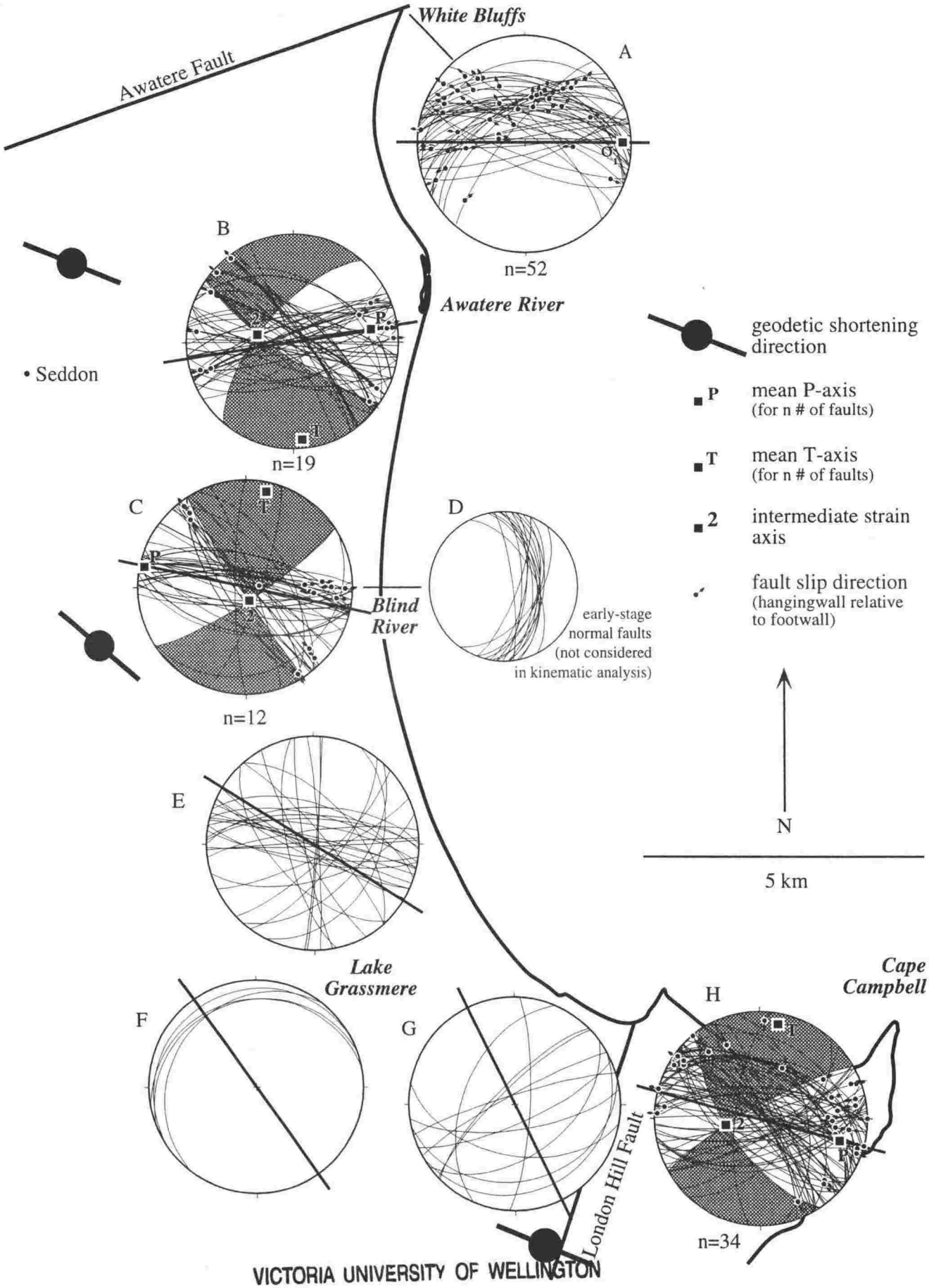

This northeast regional tilting is also expressed in the Awatere Valley, where Little et al. (1998) measured a 2.5°/m.y. northeastward tilt in the Lower Awatere Valley, based on the present tilt of a deformed c. 300 000 yr old terrace surface near the Awatere Fault. Eden (1989) measured an uplift rate of c. 1 mm/yr near the Awatere River mouth, and Wellman (1979) measured c. 2 mm/yr, 35 km upstream in the middle Awatere Valley. Using differential uplift of these fluvial terraces of the Awatere River, a tilt rate of c. 1.6°/m.y. in a northeast direction is obtained. Northeastward tilting of the block on the northern side of the Haldon Hills Fault (Fig. 10) is expressed as a northeastward deflection of otherwise north-flowing stream channels. The tilting has caused "capture" of these streams by Blind River, which flows at a high angle to the streams shedding from the Haldon Hills. This pattern is consistent with the NNE dip of a Holocene marine terrace surrounding Cape Campbell, as revealed by levelling with a theodolite (Townsend 1996; Fig. 10). The terrace occurs at c. 4.5 m above the current shore platform 1.5 km south of Cape Campbell, whereas at Cape Campbell the same terrace stands at c. 1.5 m above the shore platform. This elevation gradient indicates a tilt of 0.08° in a NNE direction over a distance of 2.25 km and suggests a tilting rate of c. 8°/m.y.

Local growth of structures such as the Ward and Cape Campbell Synclines, the London Hill Fault, and the eastern extensions of the Haldon Hills and Flaxbourne Faults superimpose second-order tilt patterns that deviate from the regional pattern of northeast tilting. Active blind structures (thrust faults?) extending eastward from the surface traces of the Haldon Hills Fault and Flaxbourne Fault can be inferred from complex drainage patterns within the Ward Syncline. The ponding of Lake Elterwater occurs between tectonically raised bulges to the north and south that have interrupted a once-continuous drainage basin (Fig. 10). This drainage probably originally flowed northwards to Lake Grassmere but has been tectonically dammed by a bulge along-strike from the trace of the Haldon Hills Fault.

Cattle Creek (Fig. 10, inset A) is another example of stream piracy that has probably resulted from localised uplift/bulging. This stream once flowed to the northeast through Kainui, forming a broad terrace in the valley bottom. It has since been deflected to the south by active uplift to the northeast of the mapped trace of the Haldon Hills Fault, leaving a stranded paleosurface and air gap to the north (Kainui Homestead). Downstream from its deflection, Cattle Creek has incised deeply into the relatively soft siltstone. Farther to the south, swampy drainage occurs immediately south of the inferred blind trace of the Haldon Hills Fault, which is perhaps propagating eastward as an active fault. Inset B (Fig. 10) shows how a small unnamed stream in the Cape Campbell region has been progressively deflected westward from its original north-bound course, producing a dog-leg in the channel just upstream from the air gap.

The Hog Swamp Fault (Fig. 10) was last known to have been active in 1966 during the Seddon earthquake, when it caused deformation of the main trunk railway line (Adams & Lensen 1970). No surface rupture or slip sense was documented, but given the northeast strike of the Hog Swamp Fault, it is most likely to be a dextral strike-slip fault, similar to the neighbouring Awatere Fault and its paleostrands (Little & Jones 1998).

New uplift data for a marine terrace c. 3 km southwest of Cape Campbell lighthouse (Fig. 10, "DT6"; grid ref. 147383; NZMS 260 P29 & Q29; Townsend 1996) are presented here. Accelerator mass spectrometry dating of an avian bone found within uplifted beach gravel on the terrace tread yielded an age of 5746 ± 78 yr BP (calibrated; IGNS, Gracefield, Lower Hutt). The position of the bone was levelled by theodolite to a height of 13.76 ± 0.1 m above the present shore platform (Townsend 1996), requiring an uplift rate of between 1.73 and 2.52 mm/yr. This is much faster than rates obtained previously (Ota et al. 1995, 1996) for two terrace remnants 4 and 7 km to the SSW of DT6, with rates of 0.4 and 0.6 mm/yr, respectively (see Fig. 10). This difference in rate is inferred to be due to active folding and westward tilting of the eastern limb of the Cape Campbell Syncline, which has given rise to locally higher uplift rates farther away from the fold hinge.

A study of raised beach ridges surrounding Lake Grassmere (Ota et al. 1995) yielded Quaternary uplift rates of c. 0.15 mm/yr, much lower than the 1.7–2.5 mm/yr of Townsend (1996) to the south of Cape Campbell. This difference in uplift rate reflects active westward tilting of surface topography at c. 28 ± 15°/m.y., an effect which is most likely due to localised deformation associated with past activity of the London Hill Fault and present folding of the Cape Campbell and Ward Synclines.

DISCUSSION

The termination of shear dislocation in an elastic medium produces an inhomogeneity in the stress field which is intensified at the tip of the discontinuity (Scholz 1990). If the termination of the Clarence Fault is the tip of a mode II shear dislocation (Scholz 1990), elastic accommodation of dextral slip produces an increase of mean compressive stress relative to the remote stress near the northwestern side of the tip (Fig. 11 "+" sign). Conversely, on the southeastern side of the tip, relatively lower amounts of mean compressive stress are expected (Fig. 11 "–" sign). We might expect this relationship to be reflected in structures observed near the tip of the Clarence Fault.

Slip on an elastic dislocation will also cause deflection of surface principal stress trajectories in the vicinity of the tip. Figure 11 shows part of the stress distribution field around the tip of a discontinuity in a homogeneous elastic medium using a 2-D distinct element numerical modelling approach (adapted from Homberg et al. 1997). The pictured model assumes very small (infinitesimal) increments of strain, a dextral fault with a friction coefficient (μ) of 0.01, a differential stress (σ_1–σ_3) of 50 MPa, and a remote maximum principal compressive stress orientation (σ_1) of 110°. There is a clockwise swing in the trend of σ_1 across the eastern tip of the discontinuity. The magnitude of this deflection in stress trajectory depends on the coefficient of friction, differential stress, the elastic constants, and the orientation of the remote stress (Homberg et al. 1997). The boxed area in Fig. 11 approximates an area comparable with that of the study region. The modelled rotation of stress trajectories mirrors the observed pattern of faulting-related PHS between the Awatere Valley and Lake Grassmere, suggesting that elastic tip deformation is responsible for the observed distribution of structures. A linear, elastic fracture model cannot, however, explain large amounts of finite deformation implied by

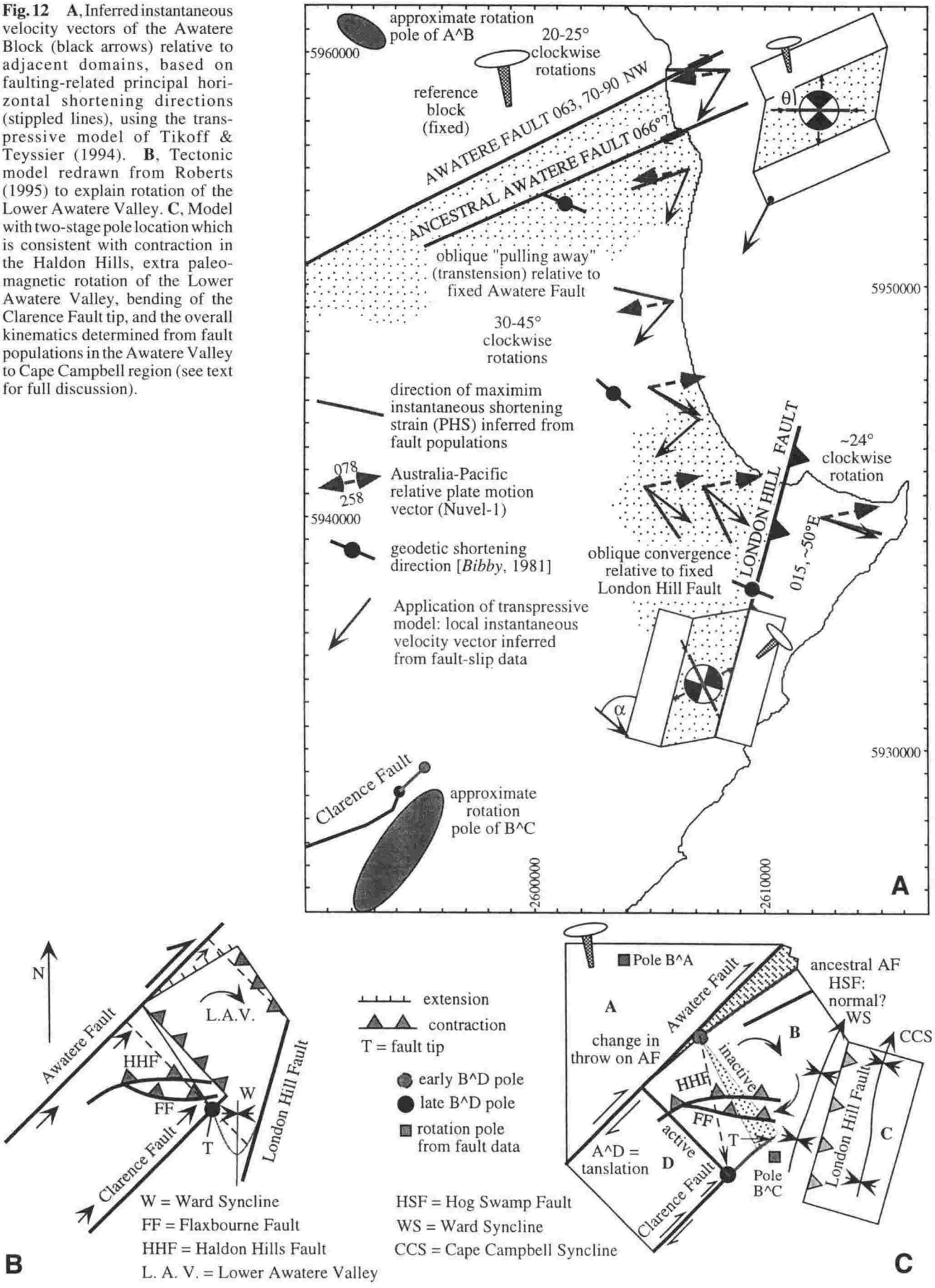

Fig. 12 **A**, Inferred instantaneous velocity vectors of the Awatere Block (black arrows) relative to adjacent domains, based on faulting-related principal horizontal shortening directions (stippled lines), using the transpressive model of Tikoff & Teyssier (1994). **B**, Tectonic model redrawn from Roberts (1995) to explain rotation of the Lower Awatere Valley. **C**, Model with two-stage pole location which is consistent with contraction in the Haldon Hills, extra paleomagnetic rotation of the Lower Awatere Valley, bending of the Clarence Fault tip, and the overall kinematics determined from fault populations in the Awatere Valley to Cape Campbell region (see text for full discussion).

from Mike Hannah was instrumental in identification of forams, and Roger Sparks and Nancy Beavan at IGNS (Gracefield) allowed a "hands-on", learning approach with radiocarbon dating. Russell Van Dissen loaned us unpublished material on the London Hill Fault. We are grateful to R. Almendinger, R. Marrett, and T. Cladouhos for the fault-kinematic analysis program "FaultKin". We would also like to thank Sue Cashman and Geoff Rait for reviewing this manuscript.

REFERENCES

Adams, R. D.; Lensen, G. J. 1970: Seddon earthquake, New Zealand, April 1966. *DSIR bulletin 199*. Wellington, New Zealand. Department of Scientific and Industrial Research.

Bibby, H. M. 1981: Geodetically determined strain across the southern end of the Tonga-Kermadec-Hikurangi subduction zone. *Geophysical journal of the Royal Astronomical Society 66*: 513–533.

Browne, G. H. 1992a: The northeastern portion of the Clarence Fault: tectonic implications for the late Neogene evolution of Marlborough. *New Zealand journal of geology and geophysics 35*: 437–445.

Browne, G. H. 1992b: A late Miocene flysch sequence near Ward, Marlborough. *New Zealand Geological Survey record 44*: 9–14.

Cobbold, P. R.; Quinquis, H. 1980: Development of sheath folds in shear regimes. *Journal of structural geology 2*: 119–126.

DeMets, C.; Gordon, R. G.; Argus, D. F.; Stein, S. 1990: Current plate motions. *Geophysical journal international 101*: 425–478.

DeMets, C.; Gordon, R. G.; Argus, D. F.; Stein, S. 1994: Effect of recent revisions to the geomagnetic reversal timescale on estimates of current plate motions. *Geophysical research letters 21 (20)*: 2191–2194.

Eden, D. 1989: River terraces and their loessial cover beds, Awatere River Valley, South Island, New Zealand. *New Zealand journal of geology and geophysics 32*: 487–497.

Groshong, R. H. 1988: Low-temperature deformation mechanisms and their interpretation. *Geological Society of America bulletin 100*: 1329–1360.

Hansen, E. 1971: Strain facies. New York, Springer-Verlag.

Homberg, C.; Hu, J. C.; Angelier, J.; Bergerat, F.; Lacombe, O. 1997: Characterisation of stress perturbations near major fault zones: insights from 2-D distinct-element modelling and field studies (Jura Mountains). *Journal of structural geology 19 (5)*: 703–718.

Knuepfer, P. L. K. 1992: Temporal variations in the latest Quaternary slip across the Australian-Pacific plate boundary, northeastern South Island, New Zealand. *Tectonics 11 (3)*: 449–464.

Little, T. A. 1995: Brittle deformation adjacent to the Awatere strike slip fault in New Zealand: Faulting patterns, scaling relationships, and displacement partitioning. *Geological Society of America bulletin 107 (11)*: 1255–1271.

Little, T. A. 1996: Faulting-related displacement gradients and strain adjacent to the Awatere strike-slip fault in New Zealand. *Journal of structural geology 18 (2/3)*: 321–340.

Little, T. A.; Jones, A. 1998: Seven million years of strike-slip and related off-fault deformation, northeastern Marlborough fault system, South Island, New Zealand. *Tectonics 17 (2)*: 285–302.

Little, T. A.; Roberts, A. P. 1997: Distribution and mechanism of Neogene to present-day vertical-axis rotations, Pacific-Australia plate boundary zone, South Island, New Zealand. *Journal of geophysical research 102 (B9)*: 20447–20468.

Little, T. A.; Grapes, R.; Berger, G. W. 1998: Late Quaternary strike-slip on the eastern part of the Awatere Fault, South Island, New Zealand. *Geological Society of America bulletin 110 (2)*: 127–148.

Marrett, R.; Almendinger, R. 1990: Kinematic analysis of fault-slip data. *Journal of structural geology 12 (8)*: 973–986.

Maxwell, F. A. 1990: Late Miocene to Recent evolution of the Awatere Basin, Medway and Middle Awatere Valleys, Marlborough. Unpublished MSc thesis, lodged in the Library, Victoria University of Wellington, Wellington, New Zealand. 133 p.

Melhuish, A. 1988: Synsedimentary faulting in the Lower Medway River area, Awatere Valley, Marlborough. Unpublished BSc (Hons) thesis, lodged in the Library, Victoria University of Wellington, Wellington, New Zealand. 72 p.

Ota, Y.; Brown, L. J.; Berryman, K. R.; Fujimori, T.; Miyauchi, T. 1995: Vertical tectonic movement in northeastern Marlborough: stratigraphic, radiocarbon, and paleoecological data from Holocene estuaries. *New Zealand journal of geology and geophysics 38*: 269–282.

Ota, Y.; Pillans, B.; Berryman, K.; Beu, A.; Fujimori, T.; Miyauchi, T.; Berger, G. 1996: Pleistocene marine terraces of Kaikoura Peninsula and the Marlborough coast, South Island, New Zealand. *New Zealand journal of geology and geophysics 39*: 51–73.

Prebble, W. M. 1976: Geology of the Kekerengu-Waima River district, north-east Marlborough. Unpublished MSc thesis, lodged in the Library, Victoria University of Wellington, Wellington, New Zealand. 103 p.

Reay, M. B. 1993: Geology of the Middle Clarence Valley. *Institute of Geological & Nuclear Sciences geological map 10*.

Roberts, A. P. 1992: Paleomagnetic constraints on the tectonic rotation of the southern Hikurangi margin, New Zealand. *New Zealand journal of geology and geophysics 35*: 311–323.

Roberts, A. P. 1995: Tectonic rotation about the termination of a major strike-slip fault, Marlborough fault system, New Zealand. *Geophysical research letters 22 (3)*: 187–190.

Roberts, A. P.; Wilson, G. S. 1992: Stratigraphy of the Awatere Group, New Zealand. *Journal of the Royal Society of New Zealand 22*: 187–204.

Roberts, A. P.; Turner, G. M.; Vella, P. P. 1994: Magnetostratigraphic chronology of late Miocene to early Pliocene biostratigraphic and oceanographic events in New Zealand. *Geological Society of America bulletin 106*: 665–683.

Russell, W. A. C. 1959: A geological reconnaissance of Northeast Marlborough (Geological report no. 1). *Petroleum report series 279*.

Scholz, C. H. 1990: The mechanics of earthquakes and faulting. New York, Cambridge University Press.

Tikoff, B.; Teyssier, C. 1994: Strain modelling of displacement-field partitioning in transpressional orogens. *Journal of structural geology 16 (11)*: 1575–1588.

Townsend, D. B. 1996: Cenozoic to Quaternary tectonics of the Awatere/Cape Campbell area, Marlborough, New Zealand. Unpublished BSc (Hons) thesis, lodged in the Library, Victoria University of Wellington, Wellington, New Zealand. 122 p.

Uruski, C. 1992: Sedimentary basins and structure of Cook Strait. Hydrocarbon resources & basin studies. Lower Hutt, Institute of Geological & Nuclear Sciences.

Van Dissen, R. 1995: Immediate report: London Hill Fault. EDS File 831/49, London Hill Fault: November. 9 p, incl. photos.

Vickery, S.; Lamb, S. H. 1995: Large tectonic rotations since the Early Miocene in a convergent plate boundary zone, South Island, New Zealand. *Earth and Planetary Science letters 136*: 44–59.

Walcott, R. I. 1984: The kinematics of the plate boundary zone through New Zealand: a comparison of short-and long-term deformations. *Geophysical journal of the Royal Astronomical Society 79*: 613–633.

Walcott, R. I.; Christoffel, D. A.; Mumme, T. C. 1981: Bending within the Axial Tectonic belt of New Zealand in the last 9 Myr from paleomagnetic data. *Earth and planetary science letters 52*: 427–434.

Wellman, H. W. W. 1979: An uplift map for the South Island of New Zealand and a model for the uplift of the Southern Alps. *In*: Walcott, R. I.; Cresswell, M. M. *ed.* Origin of the Southern Alps. *The Royal Society of New Zealand bulletin 18*.